

ORNL/M-6068

CONF-9705290--PROC.

**Proceedings of the Ninth IEA Workshop
on Radiation Effects in Ceramic Insulators**

Cincinnati, Ohio

May 8-9, 1997

RECEIVED

JAN 08 1998

OSTI

S. J. Zinkle, E. R. Hodgson, and T. Shikama, Co-Chairs

Compiled by S. J. Zinkle and G. L. Burn

Oak Ridge National Laboratory
Oak Ridge, Tennessee, USA

MASTER
DISTRIBUTION OF THIS DOCUMENT IS UNLIMITED

DISCLAIMER

This report was prepared as an account of work sponsored by an agency of the United States Government. Neither the United States Government nor any agency thereof, nor any of their employees, makes any warranty, express or implied, or assumes any legal liability or responsibility for the accuracy, completeness, or usefulness of any information, apparatus, product, or process disclosed, or represents that its use would not infringe privately owned rights. Reference herein to any specific commercial product, process, or service by trade name, trademark, manufacturer, or otherwise does not necessarily constitute or imply its endorsement, recommendation, or favoring by the United States Government or any agency thereof. The views and opinions of authors expressed herein do not necessarily state or reflect those of the United States Government or any agency thereof.

DISCLAIMER

Portions of this document may be illegible in electronic image products. Images are produced from the best available original document.

ORNL/M-6068

**Proceedings of the Ninth IEA Workshop
on Radiation Effects in Ceramic Insulators***

Cincinnati, Ohio

May 8-9, 1997

S. J. Zinkle, E. R. Hodgson, and T. Shikama, Co-Chairs

Compiled by S. J. Zinkle and G. L. Burn

*Research sponsored by the Office of Fusion Energy Sciences, U.S. Department of Energy, under contract DE-AC05-96OR22464 with Lockheed Martin Energy Research Corp.

Table of Contents

Workshop summary.....	1
E.R. Hodgson, Evidence for bulk RIED.....	13
T. Shikama, Long-term increase of electrical conductivity under fission reactor irradiation...	31
C. Kinoshita, Electrical conductivity of alumina under irradiation with fast electrons in a high voltage electron microscope.....	77
Y. Chen, Radiation induced electrical degradation of α - Al_2O_3 crystals by electron irradiation.....	93
W. Kesternich, On the electrical conductivity of Al_2O_3 under irradiation	109
A. Möslang, Electrical conductivity measurements on alumina during α -particle irradiation.....	125
S.J. Zinkle, In-situ measurement of the electrical conductivity of aluminum oxide in HFIR: summary of the TRIST-ER1 experiment.....	139
K. Noda, In-situ measurement of electrical conductivity of Al_2O_3 and MgO in JRR-3.....	193
E.R. Hodgson, Neutron RIED experiment at Mol.....	202
E.R. Hodgson, Possible explanations for conflicting RIED results.....	205
A. Möslang, 1.8 MeV electron irradiations in alumina: Transport calculations and implanted charge effects.....	219
S.J. Zinkle, Comments on electron beam straggling and charge deposition in dielectrics.....	223
S.J. Zinkle, Possible role of irradiation spectrum effects on the RIED phenomenon.....	230
S.J. Zinkle, Comments on existing models for RIED.....	238
E.R. Hodgson, Recent ceramics work.....	241
R. Vila, Outside RIED effect work.....	251
K. Noda, Effects of triple beam irradiation with H, He and O-ions on damage structures in Al_2O_3	261
T. Shikama, In-situ measurement of optical properties in a fission reactor.....	271
S.J. Zinkle, Recent ORNL research on ceramic insulators.....	273
Distribution list.....	275

Introduction

Several IEA workshops have been held over the past few years to discuss the growing number of experimental studies on the intriguing phenomenon of radiation induced electrical degradation (RIED). The experimental evidence for RIED is primarily based on electron irradiation studies performed by Eric Hodgson and coworkers on single and polycrystal forms of Al_2O_3 [1-6]. Additional evidence for RIED has been reported by several research groups for electron-, light ion- and neutron-irradiated Al_2O_3 [7-11]. These studies suggest that the electrical conductivity of Al_2O_3 may exceed 10^{-5} S/m after doses as low as $\sim 10^{-3}$ displacements per atom (dpa) if an electric field >100 V/mm is applied during irradiation in the temperature range of ~ 200 to 550°C . On the other hand several other research groups have failed to observe catastrophic RIED in Al_2O_3 following electron [12,13], light ion [14-16], or neutron irradiation [17-20]. Some published results for electron [3,5,21] and light ion [22] irradiation have suggested that the initiation of RIED may be influenced by the purity or quality of the insulator.

Due to the difficulties associated with performing in-situ electrical conductivity measurements on irradiated insulators, considerable attention has recently been focused on measurement methods. The essential experimental techniques for accurate in-situ measurement of the electrical conductivity of ceramic insulators were discussed in detail at an IEA workshop held in Stresa, Italy in September, 1993. It was concluded that the experimental techniques used by the investigators which had observed RIED were generally appropriate, but additional recommendations for future experimental studies were formulated. A round robin RIED experiment on Wesgo AL995 alumina (the IEA reference insulator) was initiated following the Stresa workshop, and the results were reported at an IEA workshop held in Obninsk, Russia in September, 1995. No evidence for bulk RIED in this material was observed by 5 different research groups using electron, light ion, and neutron irradiation sources [23].

In the past year, several new RIED irradiation experiments have been performed which have a significant impact on the understanding of the RIED phenomenon. These experiments include a HFIR neutron irradiation experiment on 12 different grades of single- and poly-crystal alumina (450 C, ~ 3 dpa, 200 V/mm) and several additional neutron, electron and light ion irradiation experiments. The primary objective of the IEA workshop was to review the available RIED studies on ceramic insulators. Some discussion of recent work in other areas such as loss tangent measurements, mechanical strength, etc. occurred on the final afternoon of the workshop. The workshop was held immediately after a related symposium on "Fabrication and Properties of Ceramics for Fusion Energy and Other High Radiation Environments", which was convened on May 5-7, 1997 as part of the American Ceramic Society annual meeting in Cincinnati, Ohio. Copies of the viewgraphs presented at the IEA workshop and abstracts of the presentations are contained in this report. The IEA workshop was held in conjunction with a US-Japan JUPITER program experimenter's workshop on dynamic radiation effects in ceramic insulators.

Workshop Presentations

The agenda for the workshop is given in Table 1, and the list of attendees is given in Table 2. In the opening talk, Eric Hodgson summarized the experimental evidence generated in his laboratory for bulk RIED in ceramic insulators. A clear increase in the volume current was measured using guard ring techniques in several specimens irradiated with electrons. Small surface currents were observed in sapphire and Vitox alumina, whereas large surface and bulk currents were measured in MgO and spinel. Optically visible features could be observed in the bulk of electrically degraded sapphire specimens, which are apparently clusters of gamma alumina precipitates according to TEM analysis. He presented results which support the importance of point defect production in the degradation process, and then outlined a theoretical model which may explain the RIED process. The model assumes that the degradation is due to the formation and clustering of oxygen vacancies via the following sequence: F (oxygen vacancy with two trapped electrons) \rightarrow F⁺ (one trapped electron, enhanced mobility compared to F center) \rightarrow F₂ \rightarrow colloids (Al metal precipitate due to deficiency of oxygen). The colloids are assumed to promote gamma alumina precipitation in neighboring regions, since the gamma alumina (spinel) structure can be formed by introducing cation vacancies on octahedral sites [24].

Tatsuo Shikama summarized evidence for long-term increases in the electrical conductivity of ceramic insulators irradiated in fission reactors. The presence of an offset current which has been attributed to "radiation induced electro-motive forces" (RIEMFs) was observed in essentially all cases, although the physical mechanism responsible for this offset current remains unclear. He proposed that the premature failure (electrical shorting) observed in several of the specimens irradiated in the HFIR-TRIST-ER1 experiment may be correlated with specimen type, although there was no evidence for an increase in electrical conductivity prior to the shorting. A pronounced increase in the electrical conductivity of a 0.05%Cr-doped sapphire (ruby) specimen was observed in the HFIR experiment at low doses (~0.1 dpa). The conductivity slowly decreased with increasing dose for the remainder of the irradiation.

Chiken Kinoshita presented in-situ electrical conductivity data obtained on sapphire specimens with thicknesses of 0.27 and 0.75 mm irradiated with 1 MeV electrons in an HVEM. The temperature dependence of the bulk radiation induced conductivity was found to be dependent on the specimen electrode type (vacuum deposited Ti or Au versus sputter deposited Pt). Permanent RIED was not detected for irradiation up to $\sim 9 \times 10^{-5}$ dpa at 420°C with an applied electric field of 93 V/mm. It was proposed that previous reports of RIED may be due to the effect of electrode materials and/or the measuring system.

Yok Chen summarized electron irradiation RIED results on unguarded sapphire specimens reported in two recent publications [10,11]. He concluded that the mechanisms leading to RIED in Al₂O₃ appear to be similar to those for thermal dielectric breakdown. In particular, a moderately high dislocation density ($\sim 10^{12}/\text{m}^2$) was present in both irradiated and thermally degraded oxide specimens. Precipitates were not observed in the irradiated specimens. A theoretical model based on carrier injection from the electrodes was outlined which appeared to describe the main features

of the RIED process in his experimental studies. RIED was observed to be inhibited when the electric field was reversed, in contrast to an earlier study by Hodgson [3]. According to the carrier injection model, the electrical conductivity should decrease immediately after the electric field is reversed.

Eric Hodgson reported his recent work on Wesgo AL995 surface/bulk conductivity. He observed that irradiation in vacuum causes severe surface degradation, but irradiation in air or He does not. In further irradiations it was observed that collimation of the electron beam to irradiate only the central electrode drastically reduces the surface degradation (i.e. the surface degradation is radiation induced or enhanced) He noted that this observation helps to explain the conflicting results of Kesternich and Möslang. Further experiments were carried out with a collimated beam to study the volume degradation in vacuum. Up to 500 kV/m no volume degradation was observed (> 200 h irradiation). However at 1 MV/m a clear volume degradation was observed. The process is complicated by radiation enhanced impurity segregation (electrolysis) at the negative electrode, which caused saturation in the observed RIED. However polishing off < 0.1 mm indicated severe volume degradation. At 1.5 MV/m (AC 50 Hz) a clear volume degradation was observed with no saturation.

Wilto Kesternich summarized RIED data obtained on several different grades of alumina, including Rubalit, Wesgo AL995 and Deranox (Vitox) irradiated with energetic protons or alpha particles. Bulk RIED was not observed in any of these specimens. In one case, specimen microcracking produced an increase in the current measured by the center electrode. After an initial increase in the measured current, the crack appeared to slowly heal (or else the surface conducting layer oxidized and became poorly conducting) with further increases in dose. He reiterated the importance of adhering to all of the measurement techniques approved at the Stresa IEA workshop in 1993, and added that the possibility of surface microcracking must be investigated (using SEM) in all specimens which show an apparent increase in bulk conductivity.

Anton Möslang presented the results of RIED studies on 104 MeV He⁺ ion irradiated Al₂O₃ (Vitox/Deranox, Wesgo AL995) and AlN specimens. A previously reported [22] observation of pronounced RIED in a Vitox alumina specimen was attributed to specimen cracking effects in his presentation; a nominally identical grade of alumina (Deranox) produced by the same manufacturer did not exhibit any permanent electrical degradation following irradiation to similar conditions as the Vitox specimen. In addition, RIED was not observed in Wesgo AL995 alumina or AlN specimens. He concurred with Kesternich's conclusion that specimen cracking must be investigated in specimens which exhibit apparent bulk RIED.

Vyacheslav Chernov reported that neither RIC nor RIED was observed in alumina irradiated with 10 MeV protons at room temperature or with fission neutrons at ~580°C, 70 Gy/s. These irradiation conditions are outside of the temperature range where previous studies have reported RIED (~250-530°C). The lack of observable RIC in the neutron irradiated specimen may be attributable to the relatively high temperature and low ionizing dose rate. On the other hand, the absence of observable RIC in the proton-irradiated specimen is unexpected based on previous RIC studies near room temperature by other research groups. He also reported observation of dielectric

breakdown and cracking within ~0.8 mm of the incident surface of a 2.7 mm thick sapphire specimen irradiated with 1 MeV electrons.

Steve Zinkle summarized the results of a recently completed DOE/Monbuscho in-situ electrical conductivity experiment on several different grades of alumina that was performed at 450-500°C in the HFIR fission reactor. A total of 15 specimens (3 without dc bias) were irradiated to a maximum dose of ~3 dpa. The bulk conductivity measured during full-power irradiation (10-16 kGy/s) remained below 1×10^{-6} S/m in all of the pure alumina specimens. The only specimen which exhibited an apparent bulk conductivity higher than 1×10^{-6} S/m was a 0.05% Cr-doped sapphire specimen, which showed a rapid initial increase in conductivity to $\sim 2 \times 1 \times 10^{-4}$ S/m after ~0.1 dpa, followed by a gradual decrease to $< 1 \times 10^{-6}$ S/m after 2 dpa. Nonohmic electrical behavior was observed in all of the specimens, and was attributed to preferential attraction of ionized electrons in the capsule gas to the unshielded low-side bare electrical leads emanating from the subcapsules. The electrical conductivity was determined from the slope of the specimen current vs. voltage curve at negative voltages, where the gas ionization effect was minimized. More than half of the coaxial cables shorted during the 3 month irradiation. Dielectric breakdown tests performed on nonirradiated coaxial cables indicated that the shorting was associated with breakdown in the glass used to seal the ends of the cables. Postirradiation measurements of the temperature-dependent electrical conductivity of all specimens is planned, along with examination of the shorted coaxial cables. Measurements made on two high purity sapphire specimens which were irradiated for the full 3 reactor cycles indicate that the electrical conductivity did not exceed the normal RIC value of $\sim 1 \times 10^{-6}$ S/m at any point during the irradiation.

Tatsuo Shikama reported results of a JMTR fission neutron experiment carried out under the US/Japan collaboration in conjunction with the recent HFIR experiment (performed under the same collaboration framework, and reported at the workshop by Steve Zinkle). He pointed out some interesting but mysterious phenomena obtained in fission reactor experiments. These results were first recognized in JMTR and clearly and confidently confirmed in HFIR. These results may infer problems associated with fusion reactor developments. He implied that they may have some correlation with a long term degradation of electrical insulation of ceramics. He proposed to continue international collaborations which focus on studying the fundamental nature of these phenomena in inexpensive and easily accessible reactors such as JMTR.

Kenji Noda described a recently completed in-situ electrical conductivity experiment on MgO and Al₂O₃ performed at 300 to 450°C in the JRR-3 reactor. The RIC values appeared to be in good agreement with previous studies. It was concluded that RIED did not occur to any significant degree up to the maximum damage level of 0.2 dpa. The session was concluded by Eric Hodgson with a brief description of a neutron irradiation experiment in the Mol reactor that is scheduled to begin in the summer of 1997.

On the second day of the workshop, the morning session was devoted to discussion of possible reasons for the apparent conflicting results regarding the presence of RIED in irradiated specimens. Eric Hodgson noted that most of the observations of RIED were obtained using electrons at low dose rates ($< 10^9$ dpa/s), whereas most of the ion and neutron irradiation

experiments were performed at 3 orders of magnitude higher dose rate. Assuming that the incubation dose for RIED is proportional to the square root of dose rate (in analogy with void swelling and colloid processes), then RIED for typical ion and neutron conditions would become evident at doses ~10 to 100 times higher than that for the electron irradiations. However, the reported absence of RIED at doses above 0.01 to 0.1 dpa in several ion and neutron irradiation studies cannot be explained by dose rate effects. Hodgson also noted that several experiments which reported the absence of RIED were performed at temperatures outside the RIED temperature regime of ~250-530°C. The electric field threshold for initiation of RIED is expected to be material dependent, and it is possible that low-purity materials may have higher threshold electric fields than the ~50 kV/m threshold reported for high-purity sapphire. Similarly, impurities may increase the incubation dose for initiation of RIED. Hodgson also suggested that additional work is needed to understand the role of test environment (air vs. vacuum, etc.) on the electrical degradation process.

Anton Möslang and Steve Zinkle discussed aspects associated with electron irradiation which might promote the RIED process in electron-irradiated specimens compared to neutron-irradiated specimens. Both presentations pointed out that, due to the large range straggling for electrons, greater than 20% of the charge from a 1.8 MeV electron beam incident on a 1 mm-thick Al₂O₃ specimen would be deposited in the specimen. This implanted charge might produce high localized electric fields under certain circumstances, which could lead to internal dielectric breakdown (similar to the well-known Lichtenberg avalanche breakdown patterns in electron-implanted insulators). A further consideration for near-threshold irradiation sources such as electron beams is the nonstoichiometric defect production rate on the anion and cation sublattices, which may contribute to localized polarization effects. It was noted that the internal electric field is generally not related to the applied electric field in a simple manner; however, it was interesting to note that the macroscopic electric field due to the injected charge from the electron beam in a 1 mm-thick specimen was comparable to the threshold electric field for rapid RIED obtained in electron irradiation studies. Another effect worth considering is that the relatively high ionization/displacement ratio for electron irradiation may enhance the F⁺/F center ratio compared to neutron irradiations, which could have an impact on the microstructural evolution of irradiated specimens (particularly if colloid formation is responsible for the initiation of RIED).

Several additional details associated with RIED were brought up in the ensuing general discussion. Yok Chen expressed concern about F⁺ center identification and recommended cathodoluminescence instead of radioluminescence/ photoluminescence. However Hodgson insisted that the optical characteristics of the F, F⁺ and F₂ reported were in excellent agreement with literature values and could be adequately identified by absorption and radioluminescence.

Two preliminary models were proposed to describe the RIED process, based on charge injection from the electrodes and colloid/gamma alumina precipitation, respectively. Both models appear to successfully explain some aspects of the electrical degradation observed in electron irradiated specimens, but do not explain other aspects. For example, pronounced electrical degradation would have been predicted by the charge injection model for the long-term (2 days to 3 months) ion and neutron irradiation experiments where RIED was not detected. There also appeared to be a

discrepancy between the results of two research groups [3,11] on whether RIED is suppressed when the electric field is periodically reversed during electron irradiation. Further work is clearly required to address this discrepancy.

There was general agreement by the workshop participants that, with the possible exception of ion irradiation results by Pells [7] (which might be attributable to specimen cracking similar to that observed by Möslang and Kesternich), definitive levels of bulk RIED have not been observed for ion or neutron irradiations. This raises the possibility that perhaps some aspect of electron irradiation promotes RIED more vigorously than ion or neutron irradiation sources. Even for the case of electron irradiation, several studies have failed to detect RIED under conditions where pronounced electrical degradation was found by Hodgson and coworkers and Zong et al. Therefore, the workshop participants concluded that the most fruitful research area for future RIED studies would be to develop an improved understanding of the electron irradiation conditions which enhance RIED (e.g., effect of specimen thickness, reversed electric fields, etc.). Eric Hodgson agreed to distribute virgin specimens of the Union Carbide sapphire used in his electron irradiation studies to W. Kesternich and T. Terai for a round-robin electron irradiation study.

Concerning fission reactor experiments, there was a general consensus that the recent HFIR experiment gave conclusive results in a helium environment. To confirm the results, postirradiation examination of irradiated specimens, including the temperature dependence of the conductivity of irradiated specimens and examination of the mineral insulated cables, and if possible microstructure (TEM) examination, was recommended. Eric Hodgson's planned reactor experiment in Mol will be a useful complement to the HFIR experiment, since it will provide information on the effect of environment (inert gas vs. vacuum) and dose rate dependence. Tatsuo Shikama's proposal of a JMTR experiment will enlighten fundamental aspects of electrical conductivity of ceramic insulators under fission reactor irradiation (which is the closest high-intensity approximation to the fusion irradiation environment presently available).

Brief summaries of recent non-RIED work on ceramic insulators were presented by the workshop participants in the final afternoon session. Copies of the presented viewgraphs are contained in the bound volume (ORNL/M-6068) to be distributed to the workshop participants.

Workshop Summary Statement

Volumetric defects (gamma-alumina and/or dislocations) and evidence for bulk RIED-like behavior have been observed in sapphire by two research groups during electron irradiation near 450°C with applied E fields >100 V/mm [5,10,11,24]. However, 2 other research groups did not observe pronounced RIED in sapphire after electron irradiation [12,13]. Evidence for bulk RIED has been found in only one new experiment [24] since the Stresa IEA workshop in September 1993, where revised standard experimental conditions were defined. However, very few electron irradiations have been performed on sapphire since that time.

Definitive levels of bulk RIED have not been observed in high purity Al₂O₃ by several research groups during energetic ion or fission neutron irradiation. All ion and neutron irradiation

experiments performed since the Stresa workshop have not observed bulk RIED. Some previous reports of RIED in ion and neutron irradiated specimens are due to surface leakage currents or specimen cracking. Postirradiation examination of the HFIR-TRIST-ER1 specimens should be performed to determine if any low-level RIED (i.e., below $\sim 5 \times 10^{-7}$ S/m at 450°C) exists in the irradiated specimens. To aid in the interpretation of the HFIR and other reactor experimental results, some radiation-induced phenomena such as RIEMF and non-ohmic behavior should be studied using smaller reactors. The planned BR-1 and BR-10 reactor experiments (with vacuum environment) will provide additional important information concerning RIED under fission reactor irradiation.

Two models have been proposed to explain the RIED phenomenon under electron irradiation, based on Al colloid/gamma alumina formation and electrode charge injection, respectively. Neither model fully explains all of the available electron irradiation data on RIED.

RIED does not appear to be of immediate concern for near-term fusion devices such as ITER. However, continued research on the RIED phenomenon with particular emphasis on electron irradiations of single crystal alumina is warranted in order to determine the underlying physical mechanisms. This will allow a better determination of whether RIED might occur under any of the widely varying experimental conditions in a fusion energy device. Future studies on RIED should continue to follow the Stresa IEA workshop recommendations regarding essential features of the experimental technique [23], including careful measurement of surface and contact resistances. In addition, detailed postirradiation microstructural examination (SEM for cracks and TEM for bulk defects) should be performed and reported on all specimens exhibiting apparent RIED. Research is particularly recommended in two areas: 1) effects of AC or periodically reversed DC electric fields on the RIED process, and 2) vacuum/gas environmental effects (strong effects have been reported for the surface conductivity, but it is uncertain whether any effect on the bulk conductivity may occur).

Although RIED does not appear to be an issue for near-term fusion devices such as ITER, numerous experiments have highlighted technological problems which need to be considered in the reactor design. These issues include enhanced surface conductivity, crack propagation, and issues associated with the best way to terminate mineral insulated cables. Additional work is needed to determine if acceptable engineering designs can be made to accommodate these problem areas.

Critical Issues and Recommended Future Work

- The priority for future RIED studies should be on electron irradiation experiments on UV-grade sapphire
 - air vs. vacuum
 - field reversal effects (flipped sample and ac electric field)

(Eric Hodgson agreed to supply unirradiated Union Carbide sapphire specimens to W. Kesternich and T. Terai for electron irradiation studies)

- Attention should be given to the various experimental problems which have been identified in recent RIED studies (specimen cracking, surface conductivity, MI cable terminations, etc.)
 - any relation to bulk RIED?
 - significance of these problems for ITER and future devices?
- Concerning the increase in electrical conductivity due to RIC, the most recent results have a tendency to give lower values of RIC. This could be interpreted that the more improved techniques will give more appropriate and lower values of RIC. Considering that the accumulated values of RIC do not always satisfy the ITER magnetic coil criteria for ceramic insulators, namely conductivity lower than 10^{-6} S/m at 10 kGy/s, confident evaluation of RIC values by the most accurate experimental technique is recommended.
- Standardized dpa calculations for ceramics are urgently needed
- R&D on blanket insulator coatings is needed (not discussed in workshop)
- The value of IFMIF was recognized, but details regarding effective utilization of such an irradiation source were not discussed in the workshop

References

- [1] E.R. Hodgson, *Cryst. Latt. Def. Amorph. Mater.* 18 (1989) 169.
- [2] E.R. Hodgson, *J. Nucl. Mater.* 179-181 (1991) 383.
- [3] E.R. Hodgson, *J. Nucl. Mater.* 191-194 (1992) 552.
- [4] E.R. Hodgson, in *Int. Conf. on Defects in Insulating Materials* vol. 2, eds. O. Kanert and J.-M. Spaeth (World Scientific, 1993) p. 332.
- [5] E.R. Hodgson, *J. Nucl. Mater.* 212-215 (1994) 1123.
- [6] A. Morono and E.R. Hodgson, *J. Nucl. Mater.* 212-215 (1994) 1119.
- [7] G.P. Pells, *J. Nucl. Mater.* 184 (1991) 177.
- [8] T. Shikama et al., *J. Nucl. Mater.* 191-194 (1992) 575.
- [9] T. Shikama, M. Narui, H. Kayano and T. Sagawa, *J. Nucl. Mater.* 212-215 (1994) 1133.
- [10] X.-F. Zong et al., *Phys. Rev. B* 49 (1994) 15514.
- [11] X.-F. Zong et al., *Phys. Rev. B* 54 (1996) 139.
- [12] T. Terai, T. Kobayashi and S. Tanaka, *Nucl. Instr. Meth. B* 116 (1996) 294.
- [13] K. Shiiyama, T. Izu, C. Kinoshita and M. Kutsuwada, *J. Nucl. Mater.* 233-237 (1996) 1332.
- [14] W. Kesternich, F. Scheuermann and S.J. Zinkle, *J. Nucl. Mater.* 219 (1995) 190.
- [15] C. Patuwathavithane, W.Y. Wu and R.H. Zee, *J. Nucl. Mater.* 225 (1995) 328.
- [16] P. Jung, Z. Zhu and H. Klein, *J. Nucl. Mater.* 206 (1993) 72.
- [17] L.L. Snead, D.P. White and S.J. Zinkle, *J. Nucl. Mater.* 226 (1995) 58.

- [18] L.L. Snead, D.P. White, W.S. Eatherly and S.J. Zinkle, in Fusion Materials Semiannual Progress Report for Period ending December 31, 1995, DOE/ER-0313/19 (Oak Ridge National Lab, 1995) p. 249.
- [19] E.H. Farnum and F.W. Clinard, Jr., J. Nucl. Mater. 219 (1995) 161.
- [20] E.H. Farnum et al., J. Nucl. Mater. 228 (1996) 117.
- [21] A. Morono and E.R. Hodgson, J. Nucl. Mater. 233-237 (1996) 1299.
- [22] A. Möslang, E. Daum and R. Lindau, in Proc. 18th Symp. on Fusion Technology, eds. K. Herschbach, W. Naurer and J.E. Vetter (North-Holland, Amsterdam, 1994) p. 1313.
- [23] S.J. Zinkle, in Fusion Materials Semiannual Progress Report for Period ending December 31, 1995, DOE/ER-0313/19 (Oak Ridge National Lab, 1995) p. 258.
- [24] G.P. Pells and E.R. Hodgson, J. Nucl. Mater. 226 (1995) 286.



Table 1. Agenda for IEA Workshop on Radiation Effects in Ceramic Insulators.

Wednesday afternoon (May 7):

1:00 pm Introductory Comments--Workshop organizers

1:10 pm Evidence for bulk RIED in ceramics

E.R. Hodgson (CIEMAT)
T. Shikama (Tohoku Univ.)

1:50 pm Recent RIED experiments

1:50 pm Electron irradiations
C. Kinoshita (Kyushu Univ.)
T. Terai (U. Tokyo)
Y. Chen (DOE)
E.R. Hodgson (CIEMAT)

2:50 pm Ion irradiations

W. Kesternich (KFA-Jülich)
A. Möslang (Forschungszentrum Karlsruhe)
V.M. Chernov (IPPE-Obninsk)

3:50 pm Neutron irradiations

S.J. Zinkle/HFIR-TRIST-ER1 (ORNL)
T. Shikama/JMTR (Tohoku Univ.)
K. Noda/JRR (JAERI)
V.M. Chernov (IPPE-Obninsk)
E.R. Hodgson/Mol (CIEMAT)

Thursday (May 8):

8:30 am Possible explanations for conflicting results on bulk RIED

Effects of dose rate, temperature, electric field, material, and test environment
E.R. Hodgson (CIEMAT)

Electron beam straggling and implanted charge effects

A. Möslang (Forschungszentrum Karlsruhe)
S.J. Zinkle (ORNL)

Irradiation spectrum effects on F/F⁺/colloid formation

S.J. Zinkle (ORNL)

1:00 pm Overview of recent work on ceramic insulators (non-RIED)

E.R. Hodgson (CIEMAT)
R. Vila (CIEMAT)
V.M. Chernov (IPPE-Obninsk)
K. Noda (JAERI)
C. Kinoshita (Kyushu Univ.)
T. Shikama (Tohoku Univ.)
S.J. Zinkle (ORNL)

3:00 pm Discussion of critical issues, workshop statement on RIED, recommendations for future work (including proposed collaborations/round-robin experiments)

Table 2. Attendees at IEA Fusion Ceramics Workshop

Anton Möslang, Forschungszentrum Karlsruhe, Germany

Wilto Kesternich, Forschungszentrum Jülich, Germany

Rafael Vila, CIEMAT, Spain

Eric Hodgson, CIEMAT, Spain

Tatyana Bazilevskaya, Kharkov State University, Ukraine

Vyacheslav M. Chernov, SSC RF-IPPE, Obninsk, Russia

Chusei Namba, National Institute for Fusion Science, Japan

Akira Kohyama, Kyoto University, Japan

Tatsuo Shikama, Tohoku University, Japan

Akira Hasegawa, Tohoku University, Japan

Kenichi Shiiyama, Kyushu University, Japan

Chiken Kinoshita, Kyushu University, Japan

Toyohiko Yano, Tokyo Institute of Technology, Japan

Takayuki Terai, University of Tokyo, Japan

Kenji Noda, Japan Atomic Energy Research Institute, Japan

Lance Snead, Oak Ridge National Laboratory, USA

Steve Zinkle, Oak Ridge National Laboratory, USA

Kenneth Young, Princeton Plasma Physics Laboratory, USA

Yok Chen, U.S. Department of Energy, USA

F. W. Wiffen, Office of Fusion Energy Sciences, U.S. Department of Energy, USA

J. Y. Park, Korean Atomic Energy Research Institute, Korea

Evidence for bulk RIED

E.R.Hodgson and A. Morono

Euratom/CIEMAT Fusion Association, Madrid, Spain

1. Electrical measurements

The electrical conductivity in the critical experiments was measured with a guard ring system which permitted the voltage between centre and guard electrodes to be varied from zero by approximately ± 1 V (fig. 1). The resistance between the electrical leads and the platinum electrodes was always $< 1 \Omega$, and normally about 0.5Ω .

In the cases reported as RIED, a clear increase in the volume current was observed. For UV grade sapphire and Vitox alumina (high purity small grain size) surface currents were very small.

For MgO (Spicers 4N), UC MgAl₂O₄, Wesgo AL995 alumina (low purity large grain size) volume and surface currents were observed.

2. Optical microscope measurements

RIED samples show clear visible features in optical microscope in the volume - but only in the electric field region.

(Samples sent to Pells, Kinoshita and Zinkle. Pells and Zinkle confirm observation)

These features, believed to be related to the internal stress caused by gamma alumina, appear as disc shapes in the c-plane (figs. 2 & 3)

3. Internal stress

Problems were experienced in preparing the TEM samples (Pells), consistent with internal stresses.

Initial mechanical tests show lowering of UBS in comb samples (Heidinger fig. 4))

These effects are again believed to be related to gamma alumina.

Could explain microcracking reported by Zinkle.

4. TEM observations

Gamma alumina clusters have been observed in the bulk of RIED sample (figs.5 & 6)
The volume difference (14%) explains the observed stress effects.

5. Point defects

It has been argued that point defects do not play a role in RIED

It has been claimed contrary to much evidence in the literature that;

i) the effective cross section for O displacement at RT is ~ 5 mb

This was based on the fact that following 10^{19} e⁻ no F centres were observed

Numerous authors with $< 10^{17}$ e⁻ have seen F centres (fig. 7)

The theoretical cross section is ~ 10 b, and experimental values are in the range 1 - 4 b

One expects $\sigma_{th} > \sigma_{exp}$ as σ_{exp} only takes into account stable single oxygen vacancies
and it has been further claimed that;

ii) oxygen interstitials are unstable at 300 C

But oxygen interstitials only begin to become unstable by about 300 C, and the
corresponding F centres are observed even above 800 C (fig. 8)

It is important to note that low numbers of anion vacancies **observed** is not an indication
that colloids cannot be formed.

Case for alkali halides is well documented, where the ratio of observed vacancies at RT to
those observed at 150 to 200 C (peak temperature for colloid production) is ≥ 35 (fig. 9)

Using in-situ techniques the following observations have been made;

The applied electric field has a marked effect on the point defect (oxygen vacancy)
behaviour. These are well documented volume defects.

Under RIED conditions observe F \rightarrow F⁺ (enhanced mobility) \rightarrow F₂ \rightarrow colloids

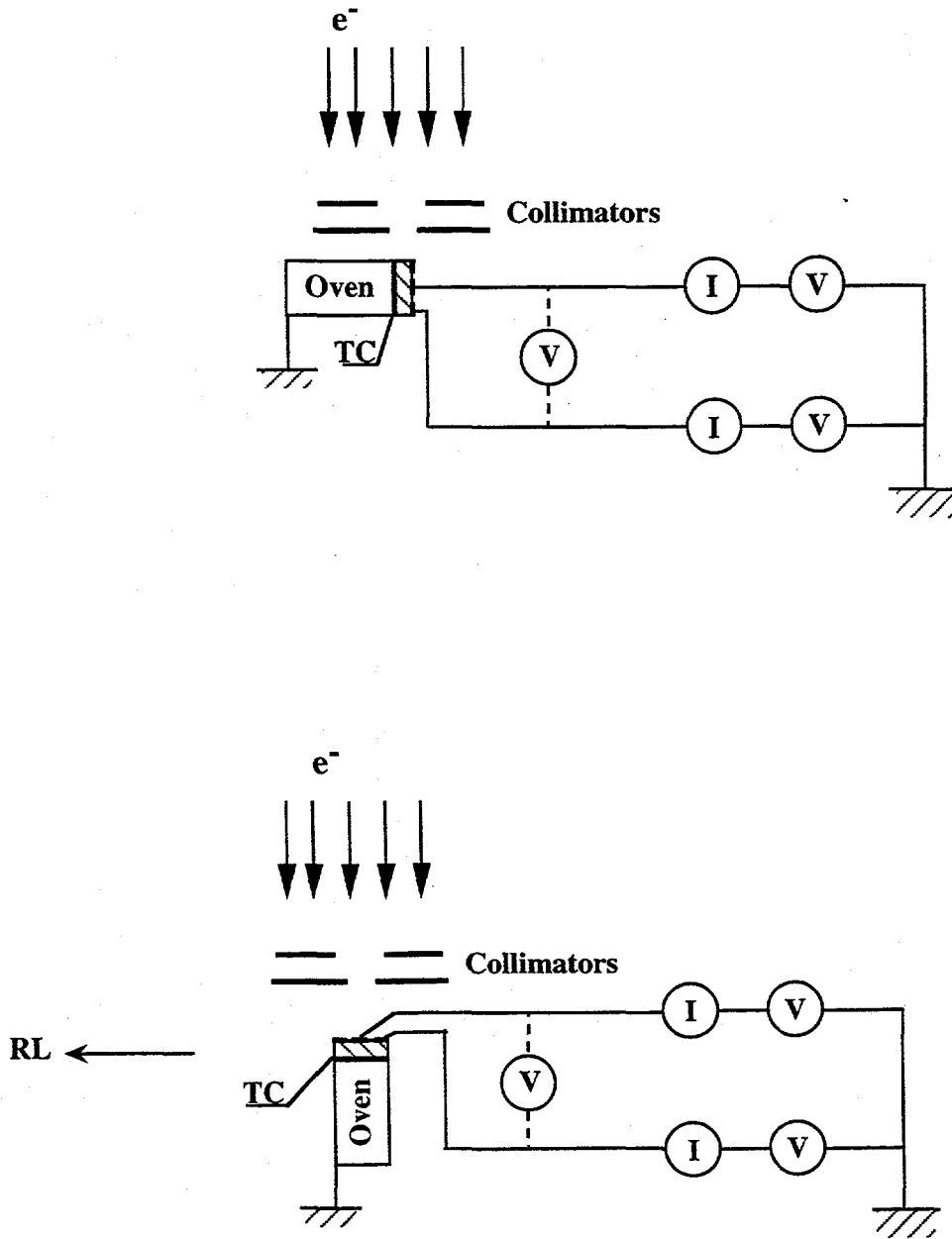
Colloids explain gamma alumina formation (remove aluminium and increase oxygen)
(figs. 10 to 13)

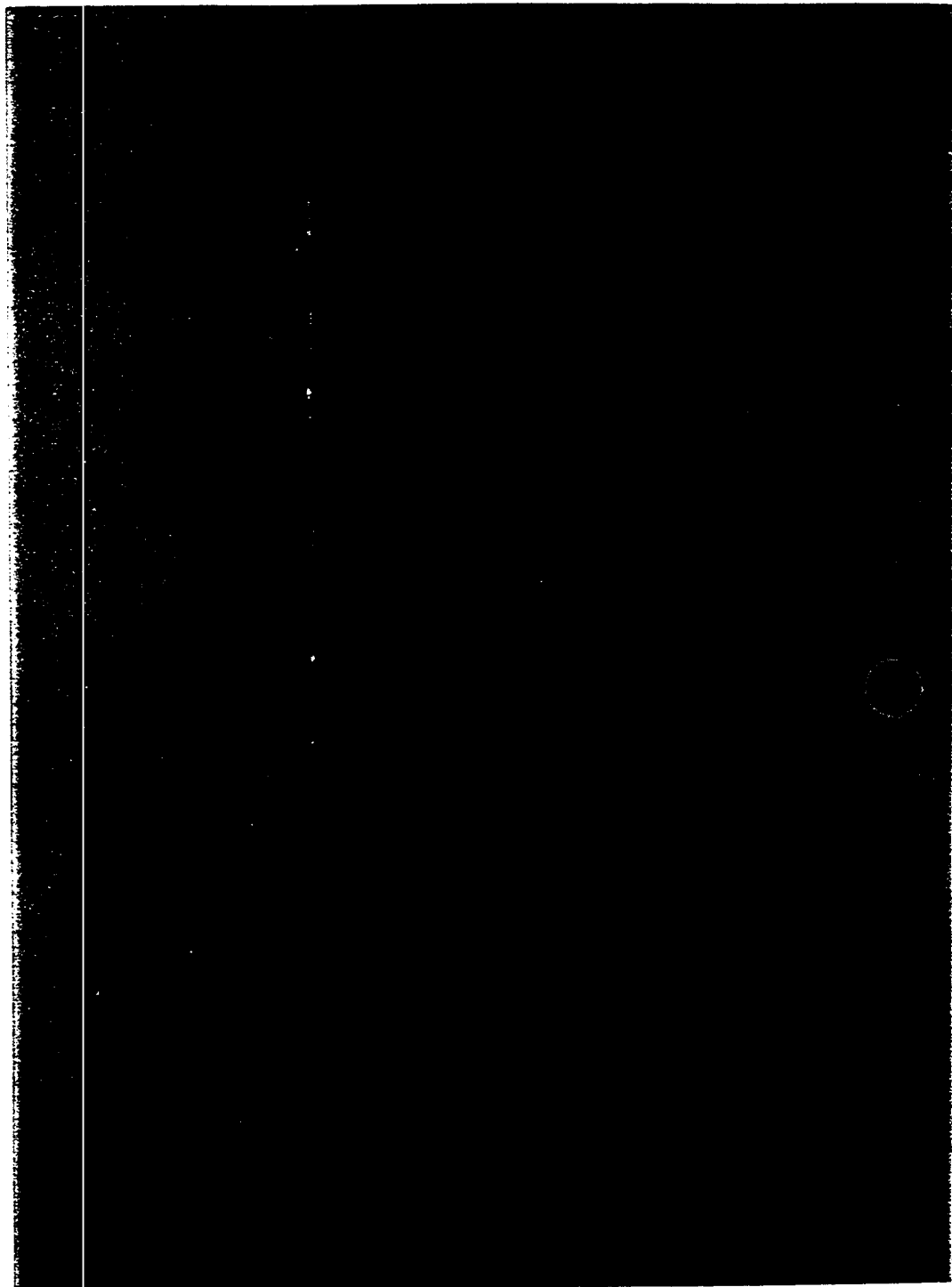
Theoretical model predictions \rightarrow F⁺ lifetime increase with field \rightarrow voltage threshold

The model predicts both DC and AC degradation (fig. 13)

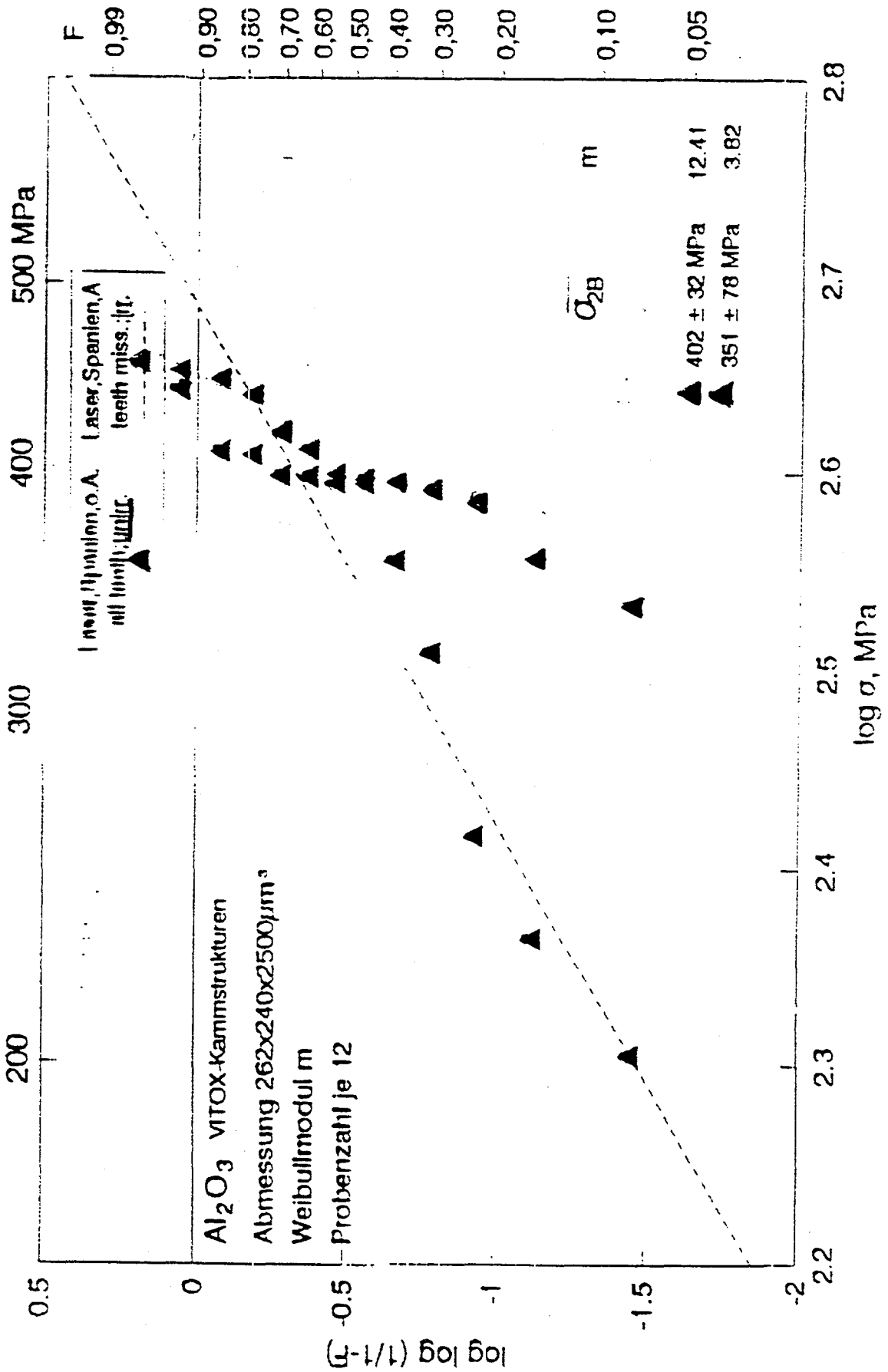
Colloids + γ alumina + α alumina explain conductivity increase and activation energy
(fig.15)

Schematic Electrical Conductivity System





← disc in
c-plane



(Handwritten signature)

Fig. 4

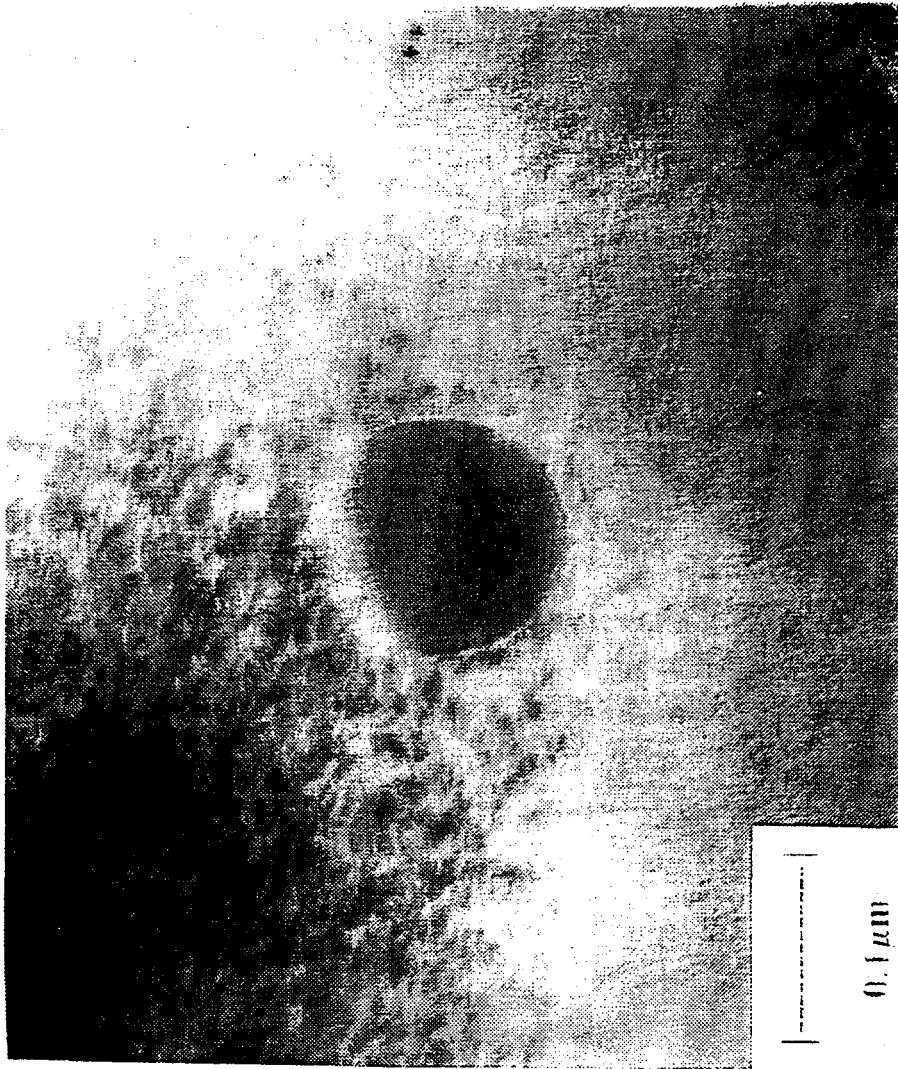


Fig. 3 Bright field TEM photomicrograph of a defect produced in sapphire by 1.8 MeV electron irradiation at 450°C with an applied electric field of 1.30 kV/cm to a damage dose of 8×10^{17} dpa.

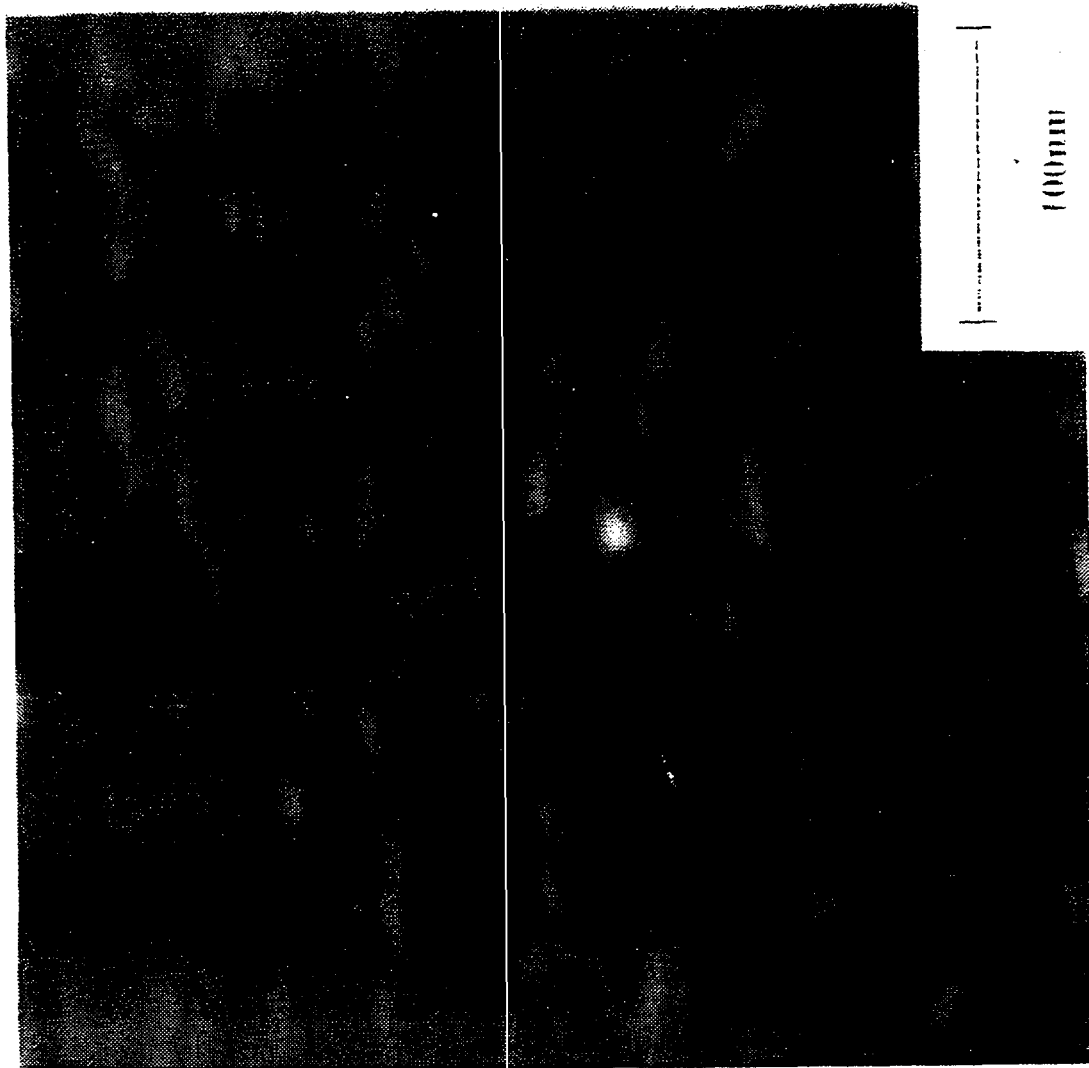
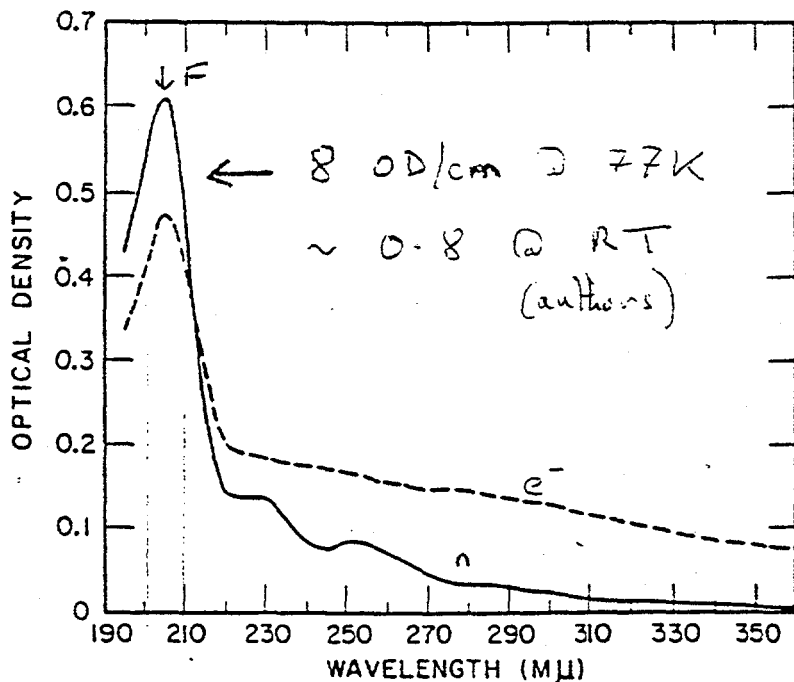
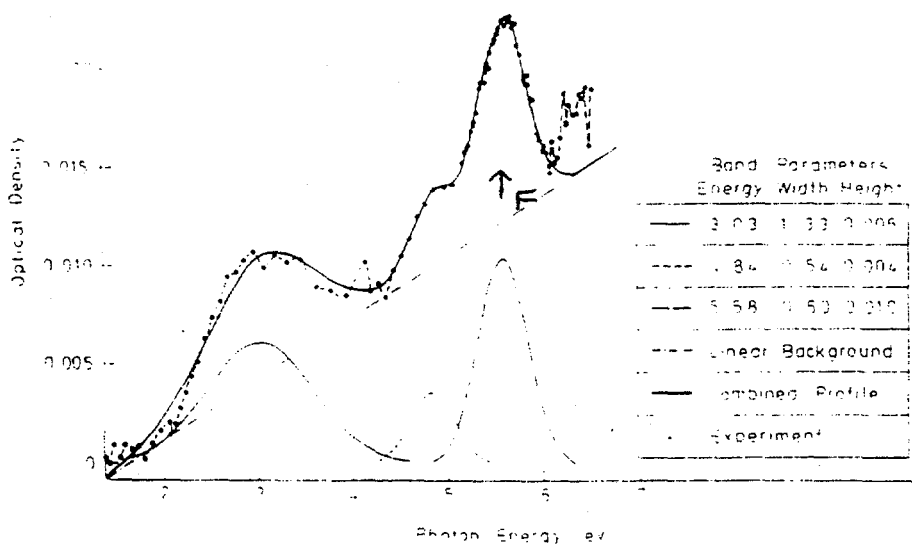


Fig. 6. Dark field image from a 'superlattice' reflection observed close to the $[10\bar{1}0]$ pole



Arnold & Compton
 $\leq 10^{17} e/cm^2$



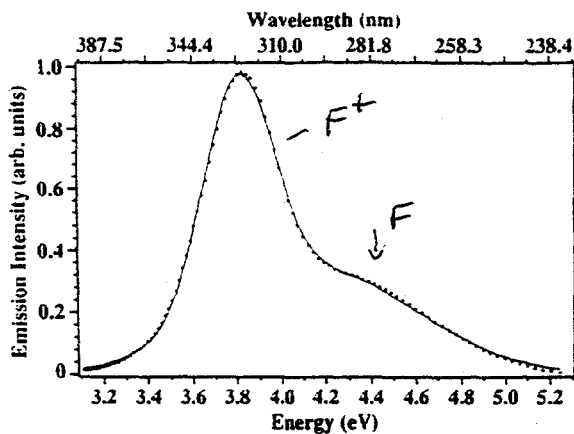
Agnew

R.T.

$\sim 10^{16} e/cm^2$

450 keV

Resolution of absorption bands induced by 450 keV electron irradiation.



Caulfield et al
 RT and 83K
 $\sim 12 J (\sim 10^{14} e)$
 $0.48 \rightarrow 3 MeV$

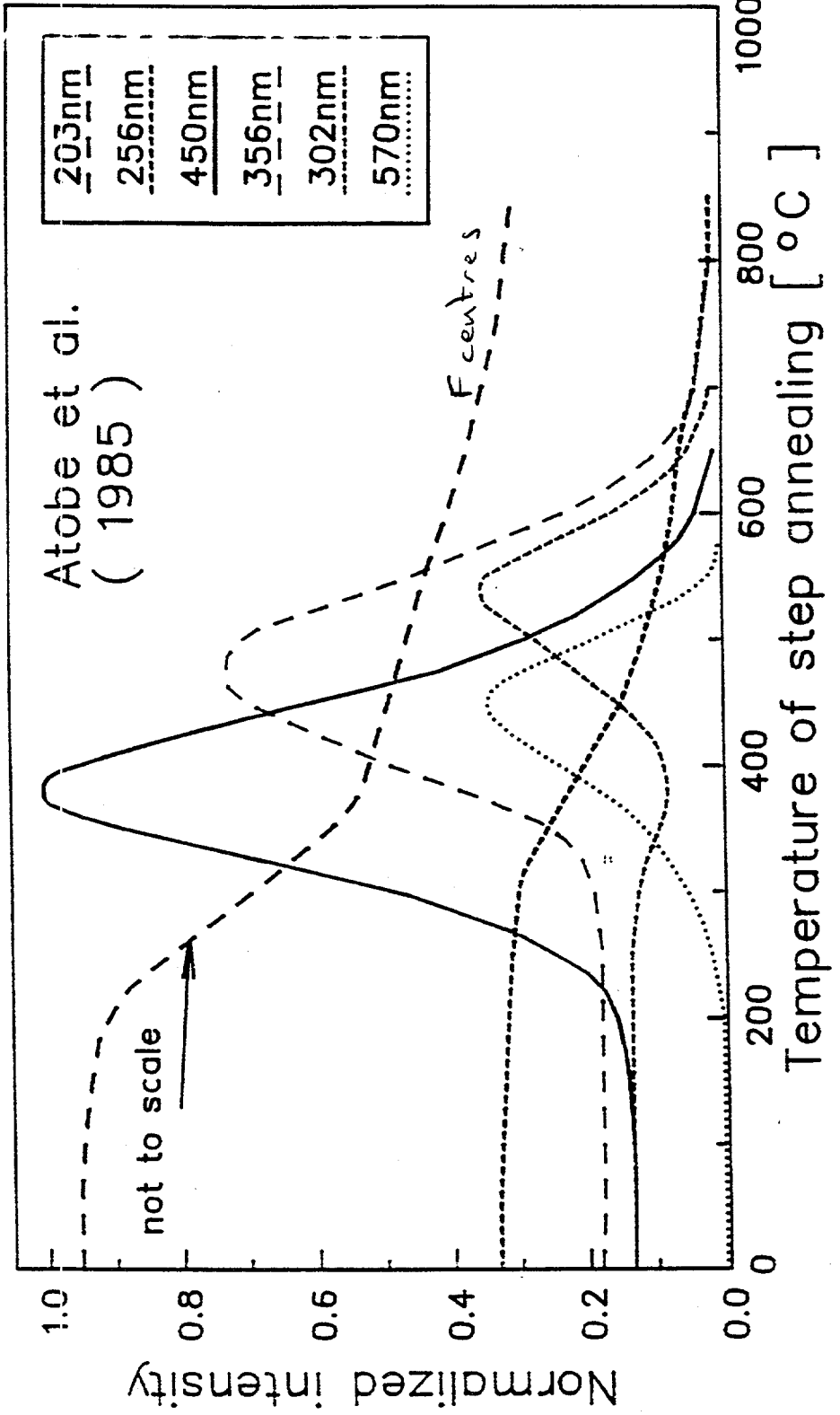
FIG. 6. Luminescence spectrum of the Union Carbide sap-

Optical spectra of neutron - irradiated sapphire

F - centres with strong electron - lattice coupling (203 / 256 / 450 nm)

F - centres with weak electron - lattice coupling (302 / 356 nm)

F - centre with unknown electron - lattice coupling (570 nm)



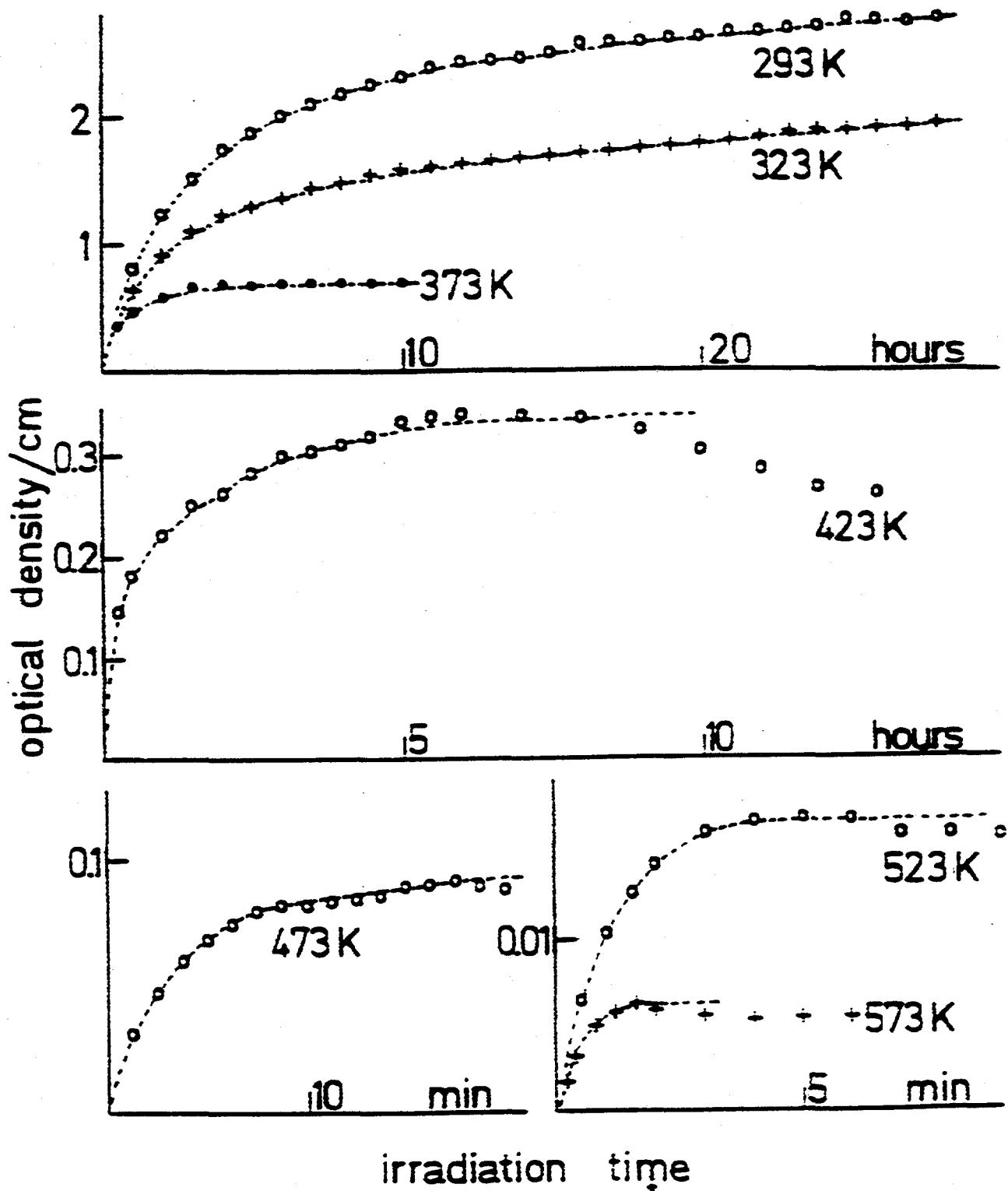
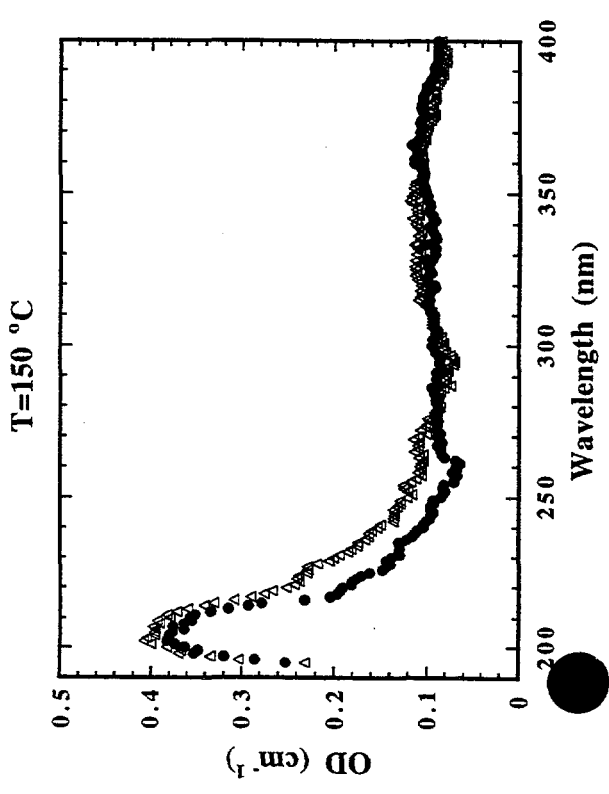
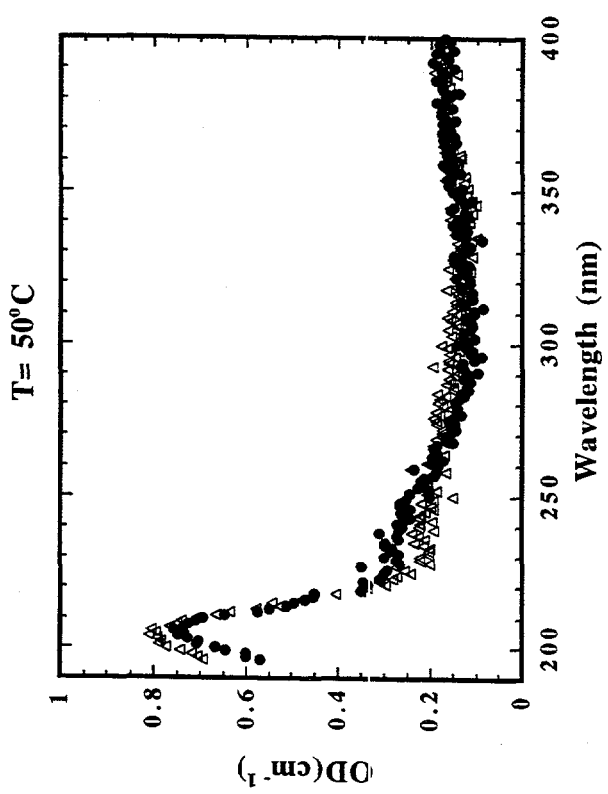
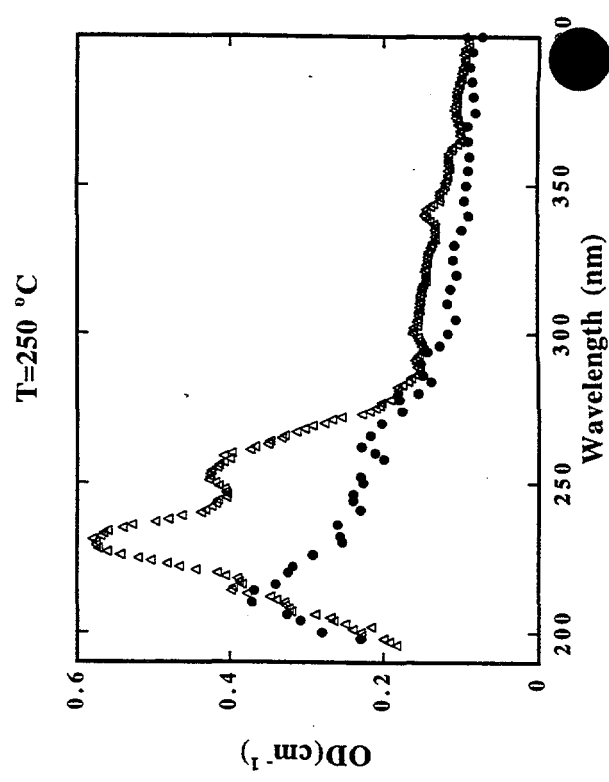
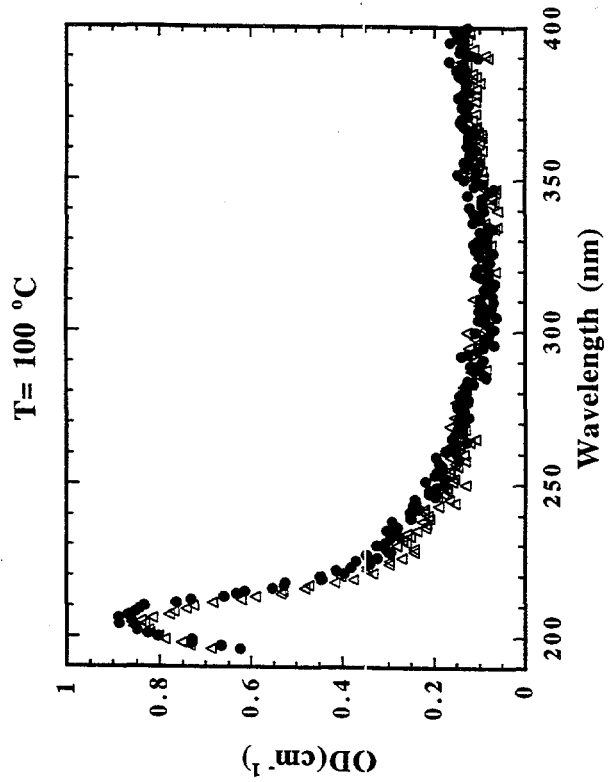
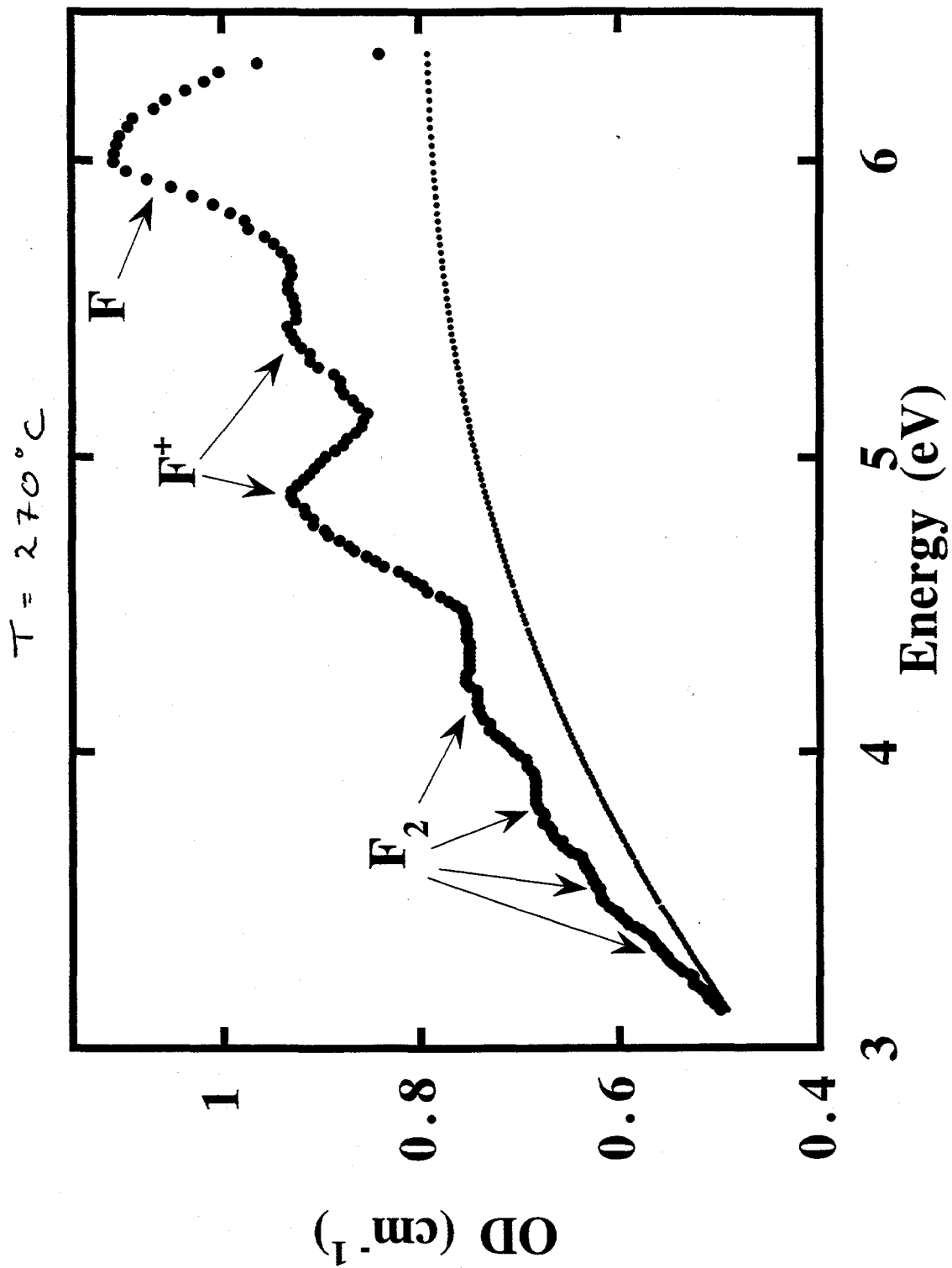


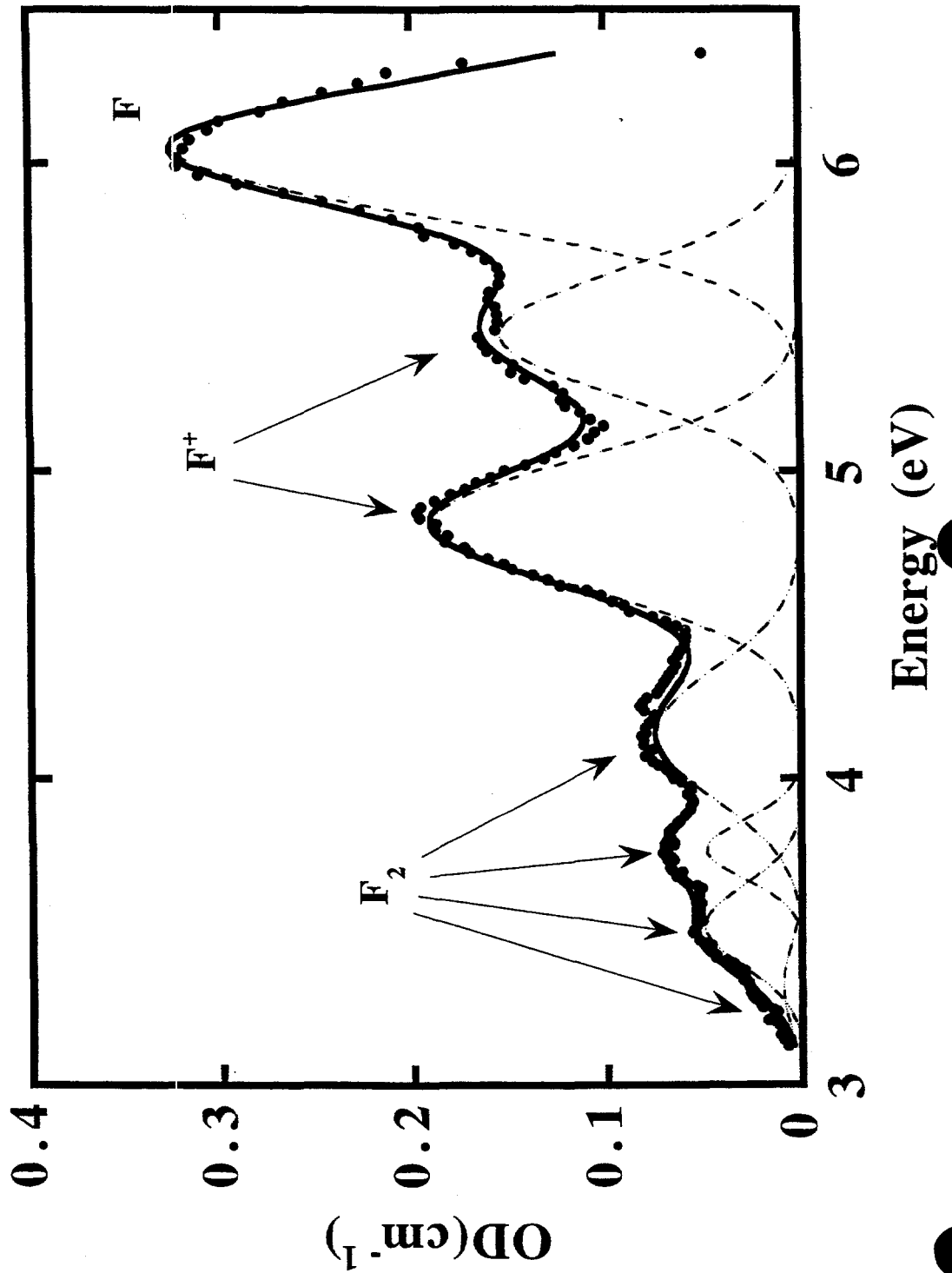
FIG. 2. *F* centre colour curves obtained for NaCl at temperatures between 20 and 300°C at a dose rate approximately 350 R/min.

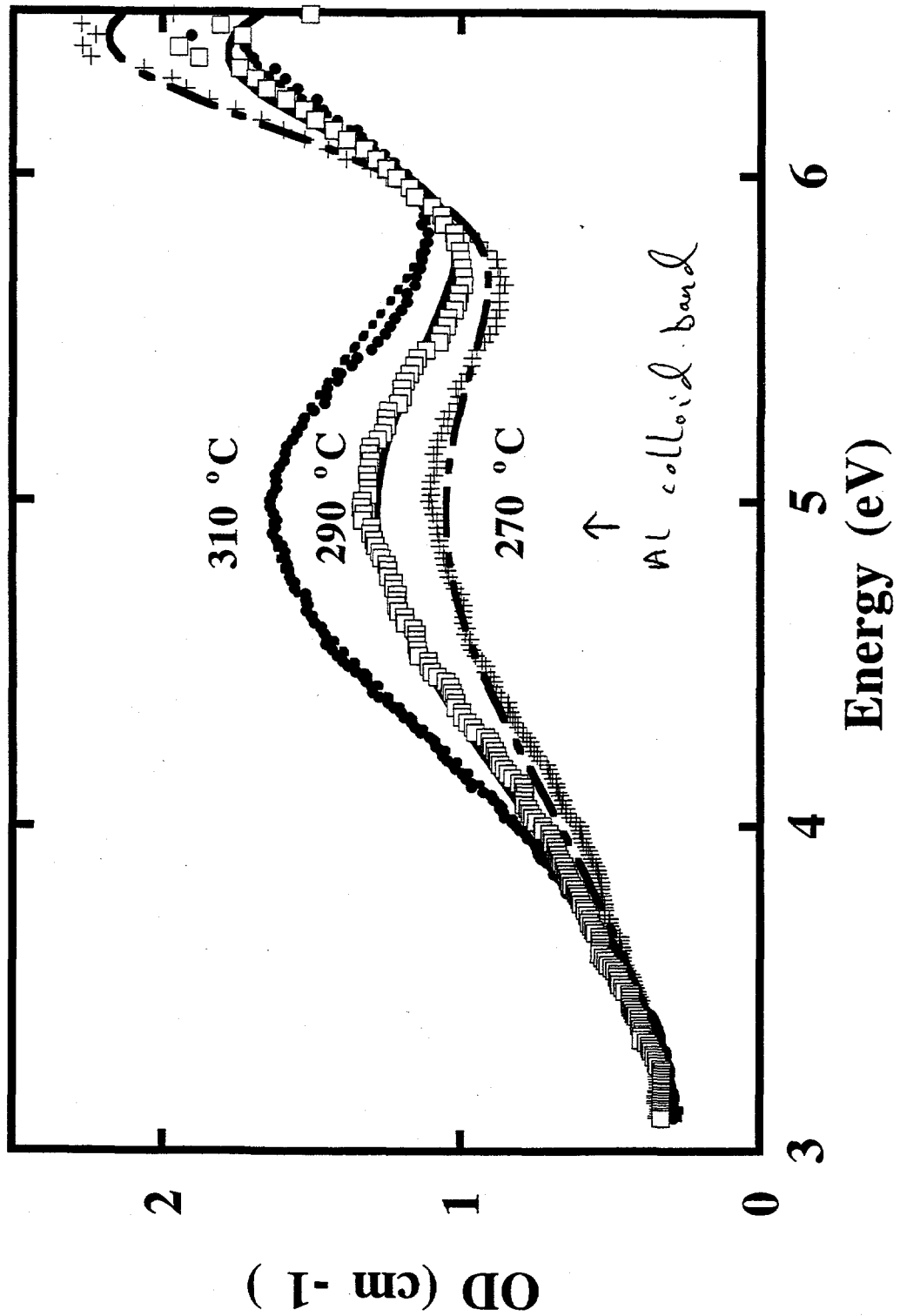
At 150°C the curves have been Fig. 2

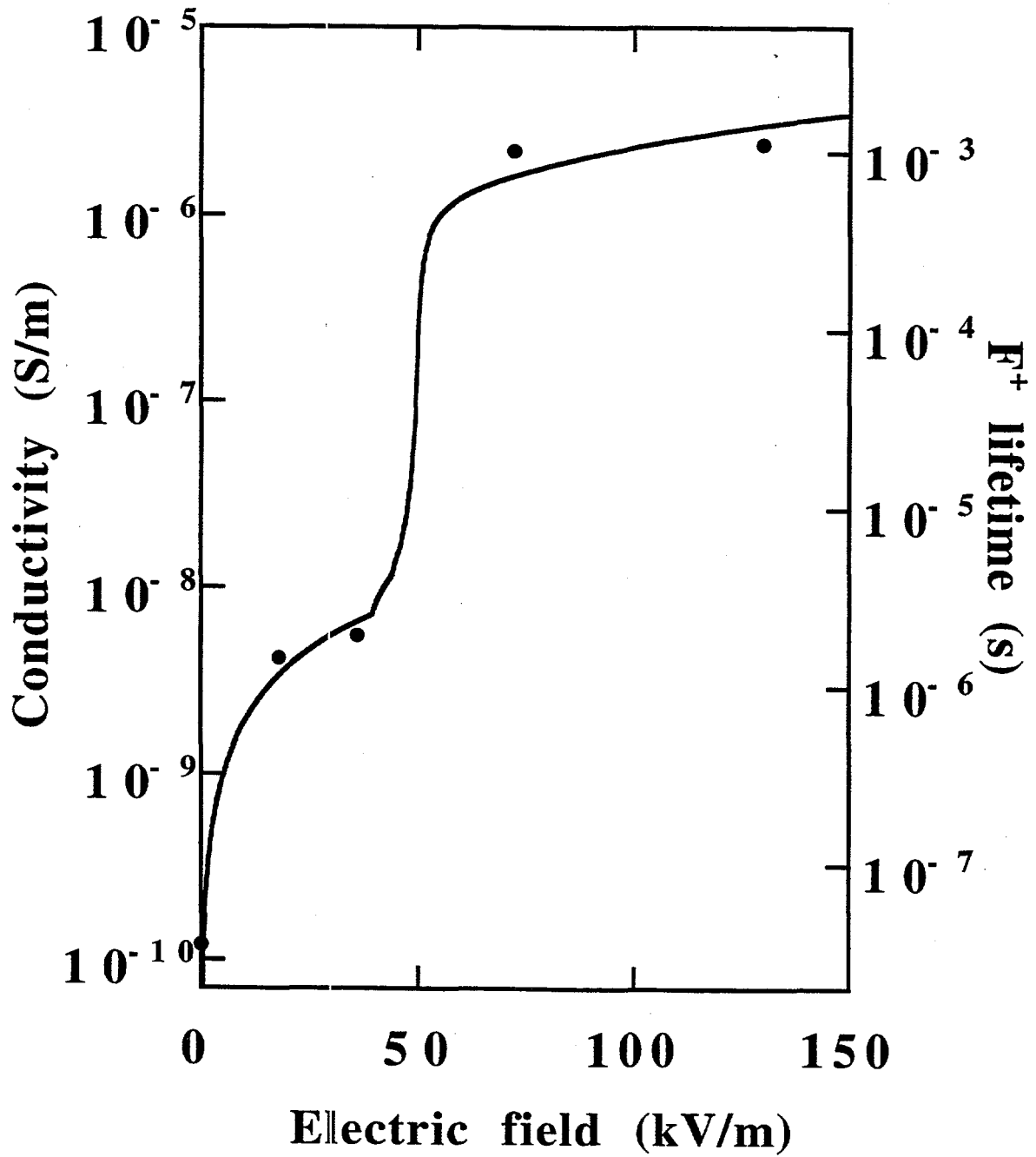




As Fig. 11 with colloid background subtracted







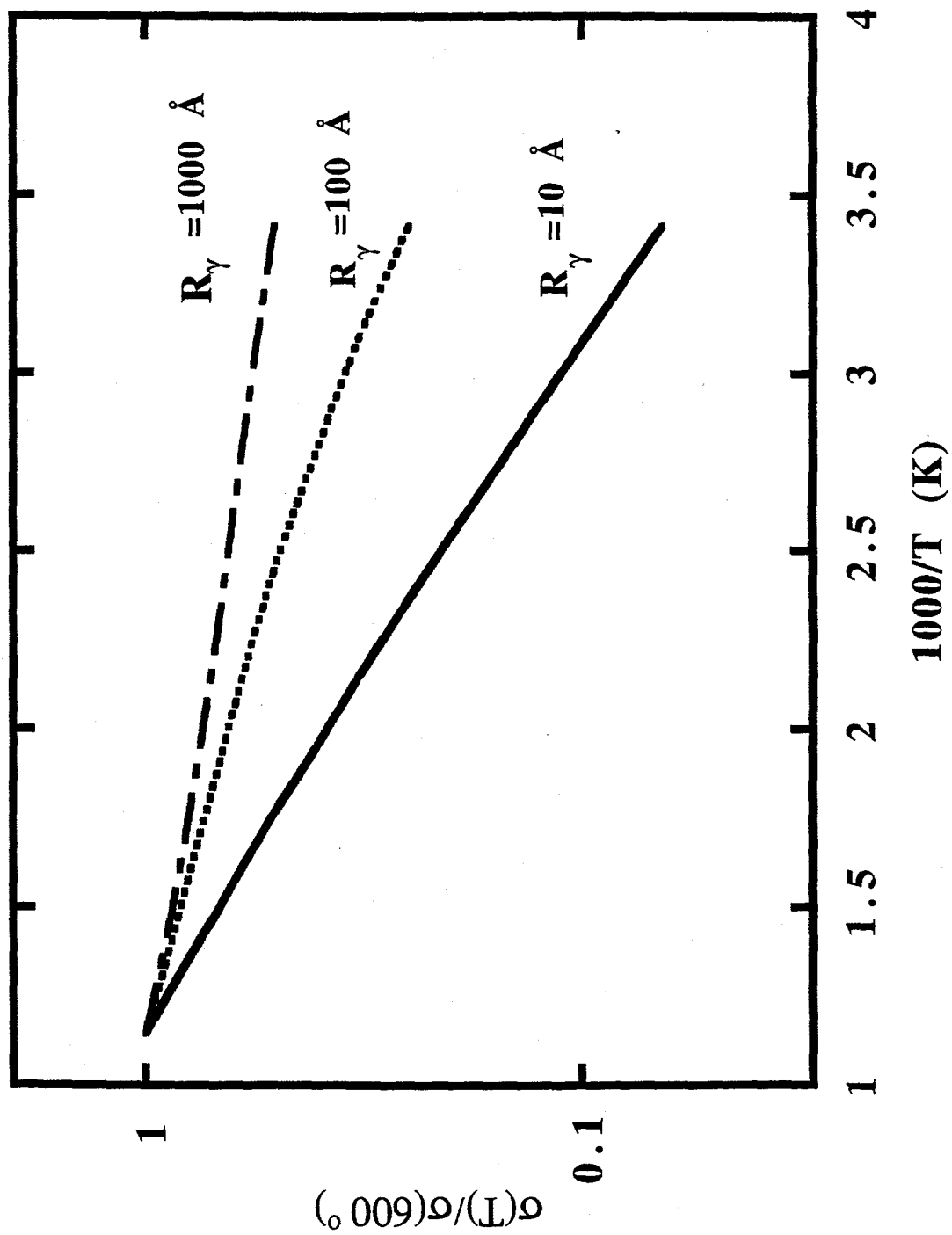


Fig. 15



Long-term increase of electrical conductivity under fission reactor irradiation

Tatsuo Shikama

the Oarai Branch, Institute for Materials Research

Oarai, Higashiibarakigun, Ibaraki, 311-13

Ceramic electrical insulators are expected to play important roles in various components under irradiation in fusion reactors. Irradiation dose rates in the most severe case will be in the range of 10^4 Gy/s for electronic excitation and of 10^{-6} dpa/s for atomic displacement. At present, only high flux fission reactors will realize these irradiation conditions in a specimen large enough to measure its bulk electrical properties. For a while, it can be said that a fission-reactor-irradiation will be only an irradiation relevant to fusion irradiation environment namely having an appropriate ratio of electronic excitation to atomic displacement for evaluation of bulk electrical properties of ceramic insulators.

There will be irradiation-related-phenomena which will increase electrical conductivity such as a radiation induced conductivity(RIC). The RIC has been well studied in a variety of irradiation sources including 14MeV neutron sources and increase of the electrical conductivity due to it has been evaluated well qualitatively as well as quantitatively. Results are showing that the ceramic insulators will have an electrical conductivity smaller than 10^{-6} S/m even in the severest irradiation environments expected in fusion reactors.

In the meantime, recent studies have evoked worries about long-term increase of the electrical conductivity or long-term degradation of an electrical insulating ability of ceramic materials. It is known that insulating silicon carbide (SiC) showed increase of an electrical conductivity after heavy irradiation in a fission reactor, while semiconducting silicon carbide showed decrease of an electrical conductivity. Some ceramic insulators have been reported to show catastrophic increase of an electrical conductivity under specific irradiation conditions.

Measurements of electrical properties in-situ under a fission reactor irradiation need elaborate techniques, because there will be many disturbances such as radiation induced parasitic electrical currents and not-well-specified grounded potential. Up to now, several

attempts have been made to measure electrical conductivity of ceramic insulators under fission reactor irradiations. Some results showed increase of the electrical conductivity along irradiation but some did not. The discrepancies may be explained by differences of irradiation environment, such as vacuum or helium, by difference of irradiation temperatures, or by difference of measuring techniques. Some results may be explained by a kind of artifacts caused by parasitic currents.

The round-robin tests were proposed in the previous IEA meeting at Stresa In Italy in 1993. The Japan/USA collaborative efforts, so-called JUPITER project, took this research field as one of its important task and it carried out in-situ experiment in the world-highest flux experimental reactor at present, the HFIR(High Flux Isotope Reactor) in Oak Ridge national Laboratory.

The experiment was successfully carried out and electrical conductance of 12 different alumina specimens including highly pure single crystal sapphires, were measured under irradiation of 10KGy/s of electronic excitation and of 10^{14} n/cm²s of fast($E>0.1$ MeV) neutrons at about 670K up to a total dose of 3dpa.

Major part of specimens showed premature breakdown. The cause of the breakdown is under study, but, it can be assumed that the glass-seal at high side MI-cable made normal electrical breakdown. Electrical test at elevated temperatures without irradiation confirmed that the glass-seal used in the present experiment was susceptible to the electrical breakdown.

In the meantime, the data can be interpreted that the observed breakdown had some correlation with kinds of specimens. For example, c-axis sapphire survived longer than a-axis ones. Purer polycrystal alumina showed shorter earlier breakdown than normal grade polycrystal alumina. Also, the two specimen which were applied voltage showed earlier breakdown with one reverse case.

However, it should be noted that there were no evidence of increase of electrical conductance before the observed premature breakdown. Every specimen showed nearly constant electrical conductance up to the observed breakdown or up to the end of irradiation.

The Crystal System c-axis sapphire did not showed any increase of electrical conductivity up to the end of irradiation. In the previous papers, it was reported that the single crystal sapphire would be more susceptible to the electrical degradation under irradiation.

Thus, in general, it can be concluded that there are alumina insulators which keep their good electrical insulating ability up to 3dpa under fusion relevant irradiation. For design of experimental fusion reactor, there will be choices of electrical insulators which can be used up to a few dpa near burning plasma.

Along with the premature breakdown, a large set-off current was observed. The measured current was a few micron to a few tens micron ampere. The cause of this large set-off current was not clear yet. However, some specimens looked like showing some electrical charge-up before they showed the premature breakdown. The observed set-off current may be speculated to reveal some redistribution of ions under electrical field in irradiation environments. So-called radiation enhanced ionic conduction may promote the redistribution and may cause electrical current when an electric field is took off.

Increase of electrical conduction through alumina specimen and through magnesia powder in MI-cables was observed in the JMTR(Japan Materials Testing Reactor in Oarai Research Establishment in Japan Atomic Energy Research Institute) irradiation. The increase was only observable under the irradiation. So, the observed increase may be due to dynamic irradiation effects. Increase of contribution of ionic conduction along with increase of the irradiation may be one interpretation.

In the HFIR irradiation, chromium doped sapphire, namely ruby, showed substantial increase of its electrical conductivity. Some surface contamination may caused this increase but at present, no evidence of distinct surface contamination was confirmed.

These results will suggest that there will be mechanisms which will increase the electrical conductivity under fusion relevant irradiation. Further and detailed study using a high flux fission reactor will be strongly recommended, which should be focused on the fundamental aspects of electrical conducting mechanisms in ceramic insulators.

The detailed study of kinetics of the observed set-off current is an urgent task and a joint US/Japan venture is proposed in the JMTR.



**Long-term increase of
electrical conductivity
under fission reactor irradiation**

Tatsuo Shikama

the Oarai Branch, Institute for Materials Research
Oarai, Higashiibarakigun, Ibaraki, 311-13

Reactor Irradiation

- **In JMTR**
 - **1st experiment**
 - **AC measurement : small increase of conductivity in long run**
 - **2nd experiment**
 - **DC application effect was observed**
 - **Increase of conductivity in specimen applied voltage**
 - **3rd experiment**
 - **Increase of conductivity during irradiation but not without irradiation**
 - **4th experiment**
 - **similar results on MgO MI-cable, but no increase of conductivity was observed on alumina**

Observation

- Existence of large contribution of gas conduction
 - it can be minimized by measuring electrical conductivity at negative voltage
- Large radiation-induced current(RIEMF?)

Even under these disturbance, large increase of electrical conductivity was not observed

cf: premature breakdown at high side degradation in Ruby

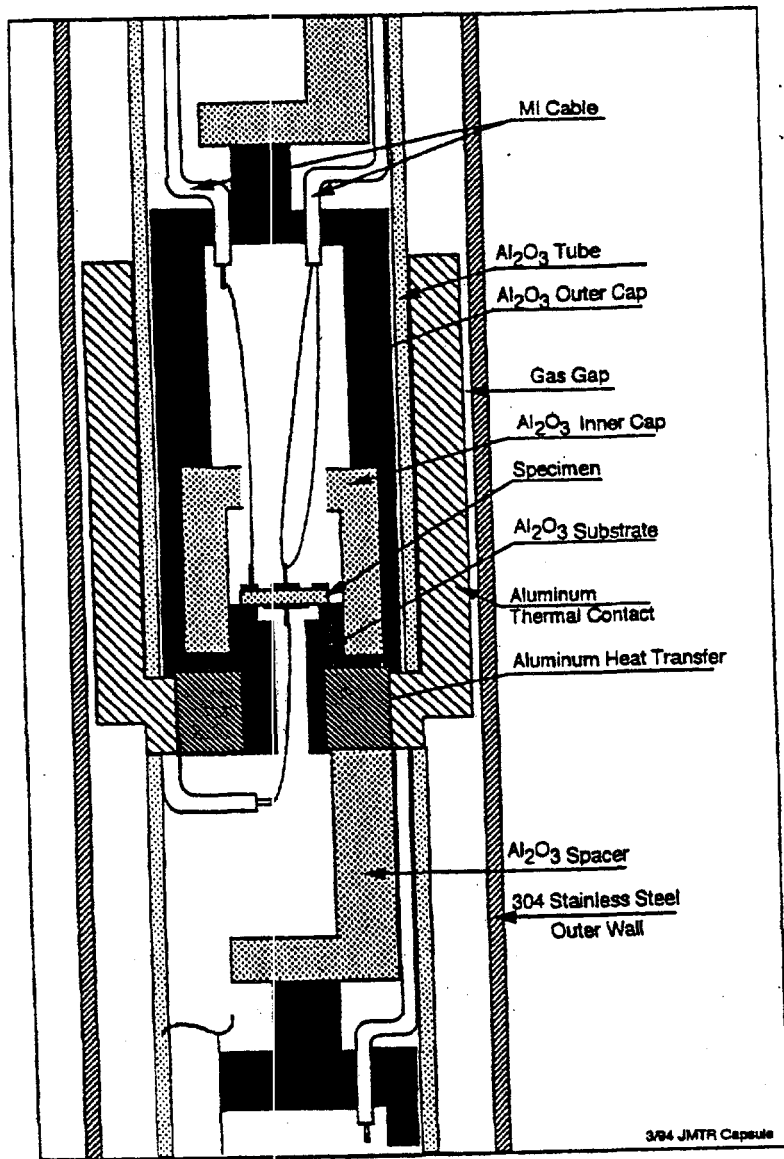


Fig. 1. Drawing of the capsule used for the sapphire sample (number 1).

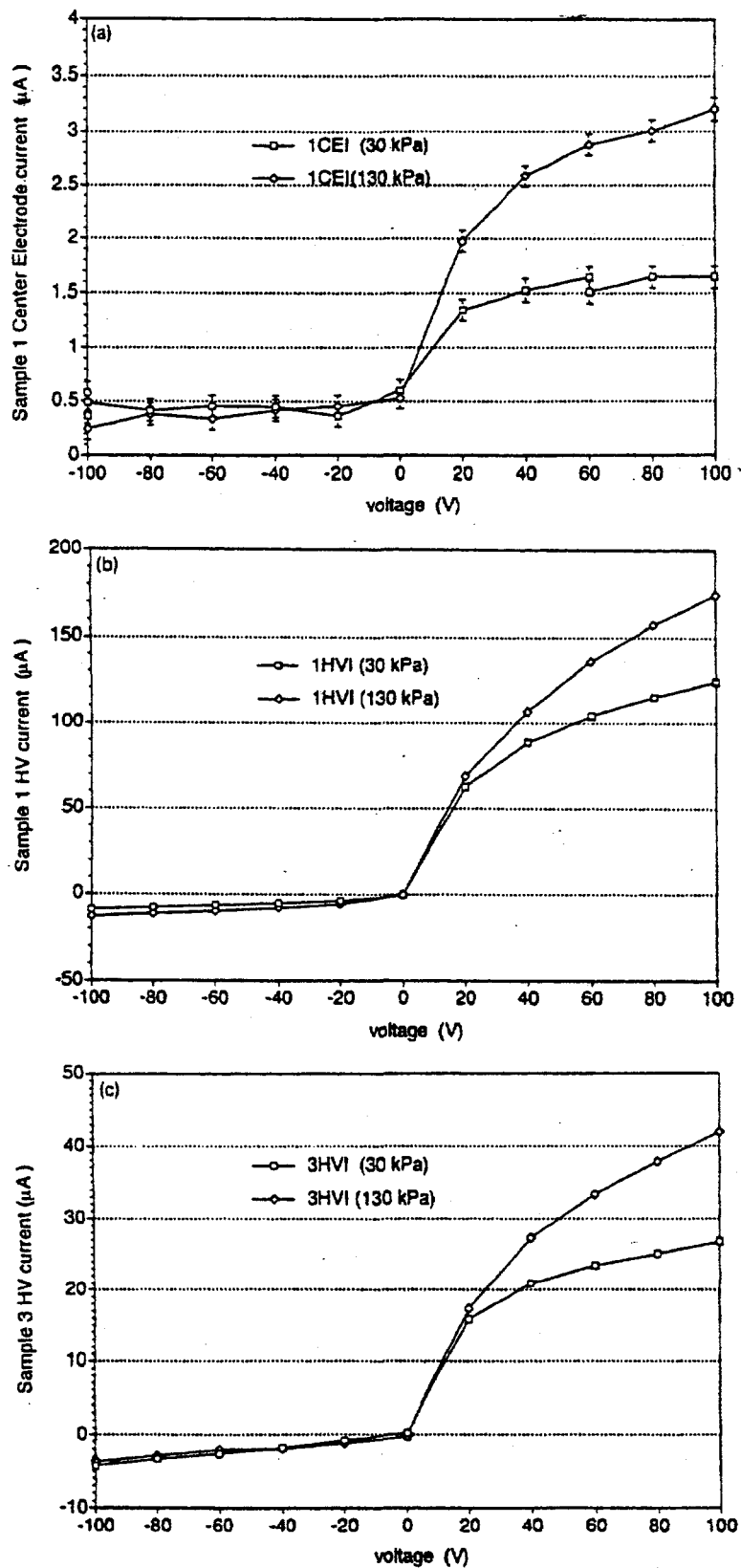


Fig. 7. Plot of current versus voltage in various samples with the reactor at 50 MW power. The temperature was $285 \pm 5^\circ\text{C}$ and the fast neutron flux was $7.9 \times 10^{17} \text{ n/m}^2\text{s}$ at a fluence of about $1.5 \times 10^{24} \text{ n/m}^2$. Measurements were taken first at 30 kPa and then at 130 kPa. (a) Sample 1 center electrode current. (b) Sample 1 high voltage electrode current. (c) Sample 3, coaxial MI cable high voltage current.

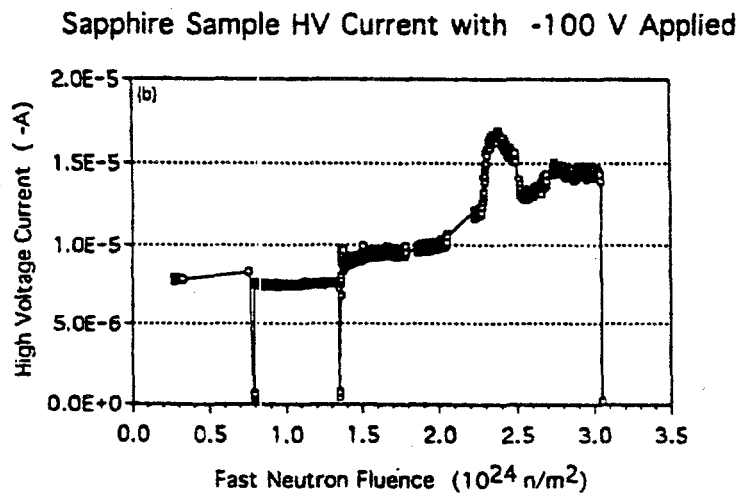
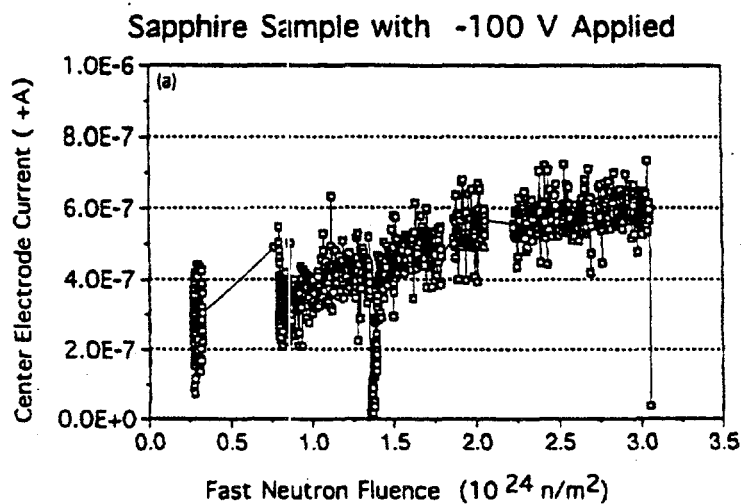
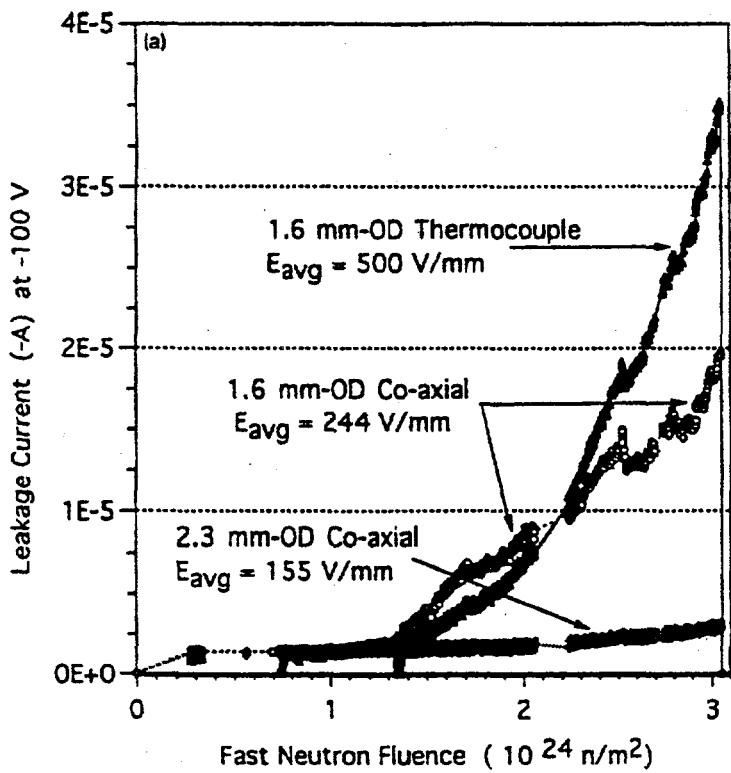


Fig. 9. Current versus fluence for the sapphire sample with the reactor at full power and an applied electric field of -100 kV/m . The data at a fluence of 0.7 , 1.35 and $3.05 \times 10^{24} \text{ n/m}^2$ are with the reactor off. (a) Center electrode current. (b) High-side electrode current.



MI Thermocouple Cable Recovery During Second Cycle

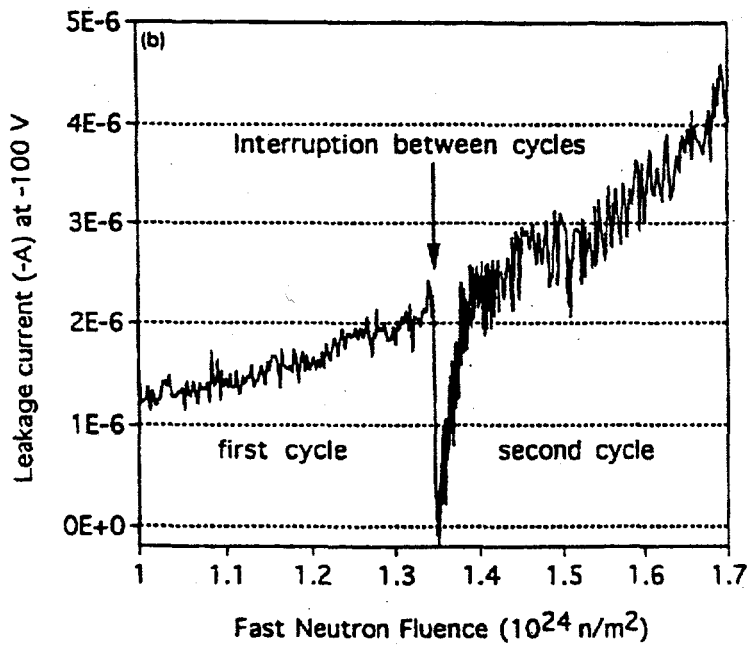
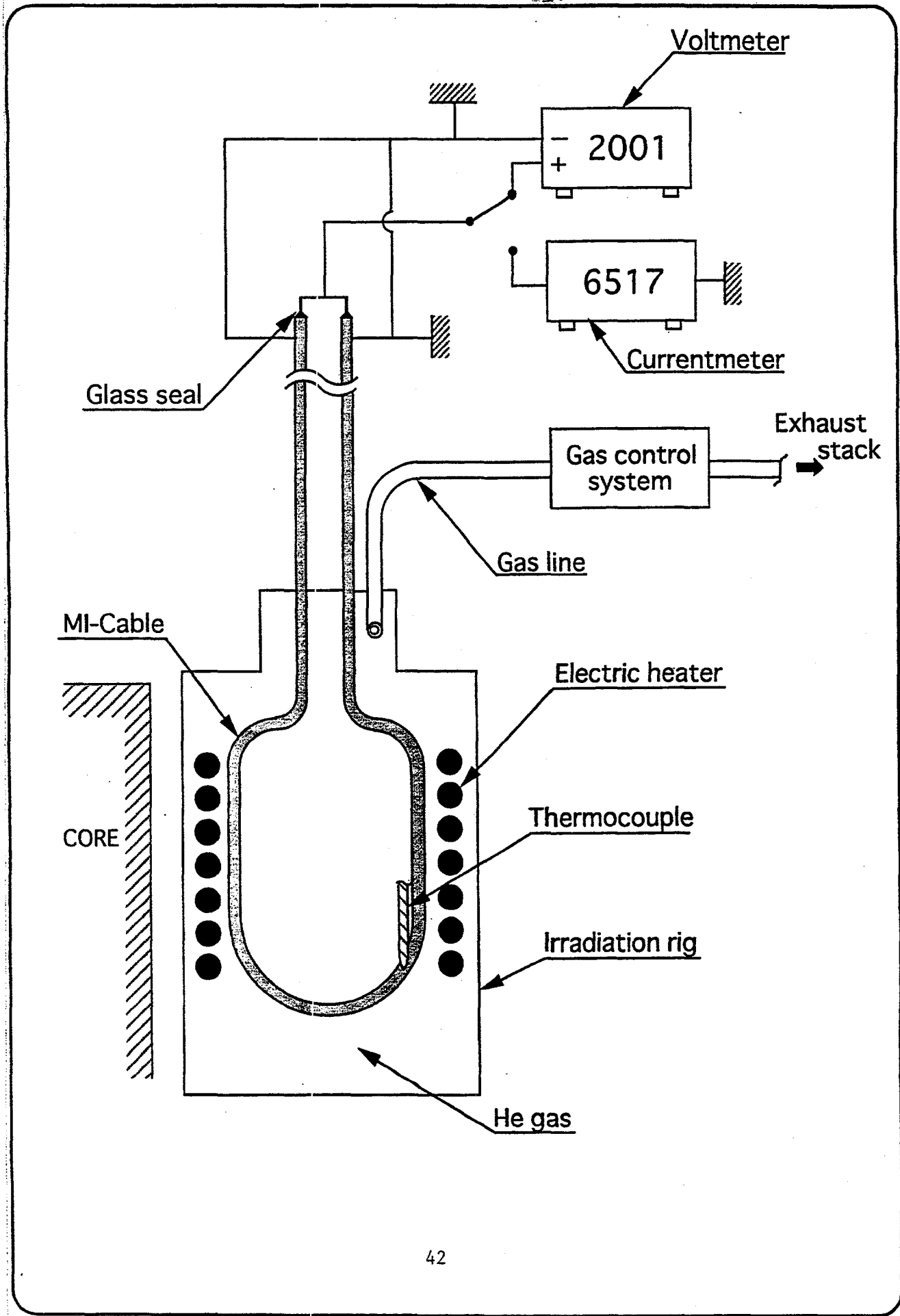
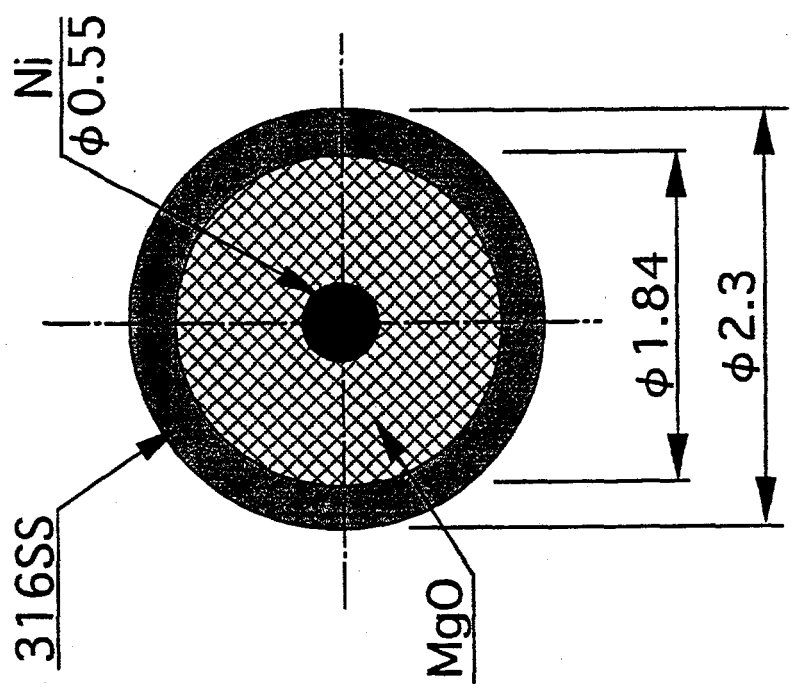
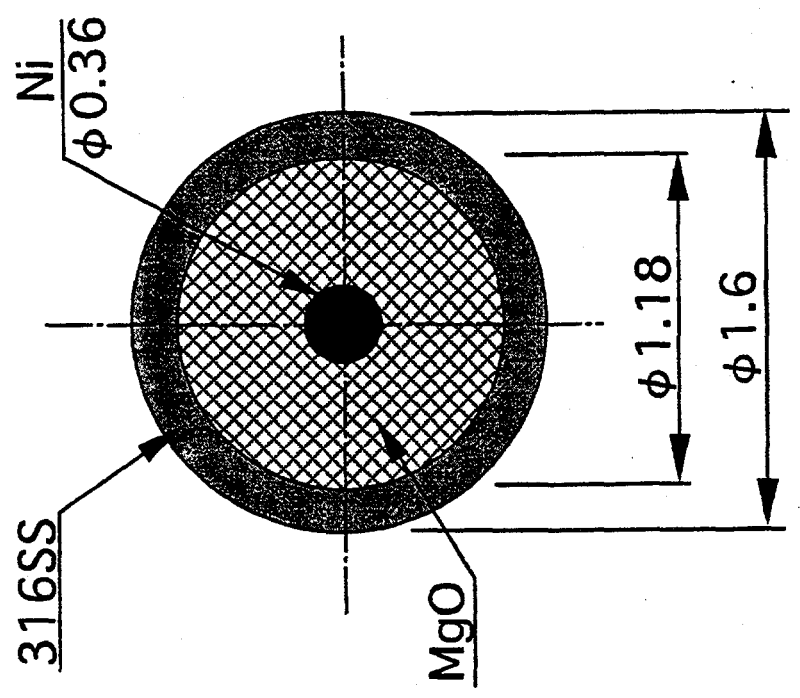


Fig. 10. Leakage current in the three MgO-insulated MI cables versus fluence: with -100 V applied, at reactor full power and at $\sim 260^\circ\text{C}$. (b) Leakage current in the MI thermocouple cable (sample 2) before and after the inter-cycle break.

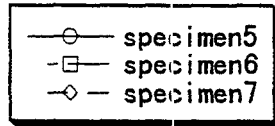




Specimen B & C



Specimen A



Sheet1

Keithley 6517, at 1000V

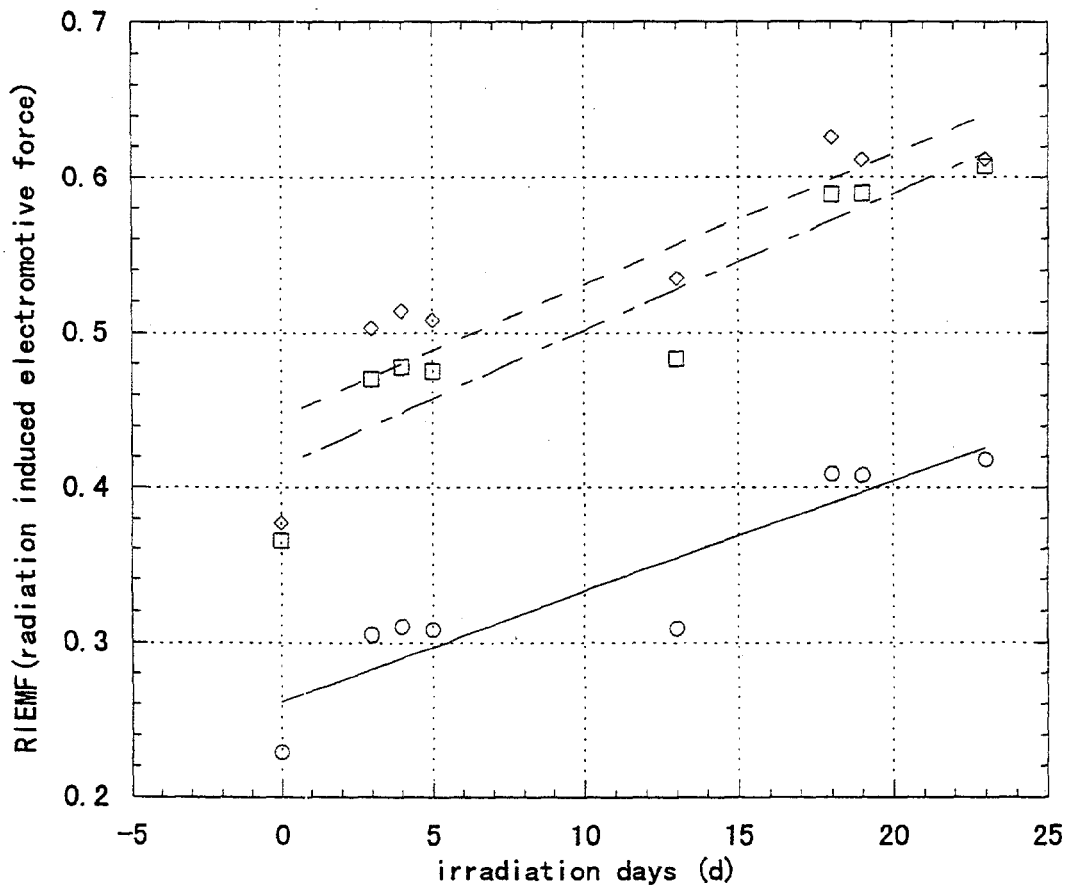
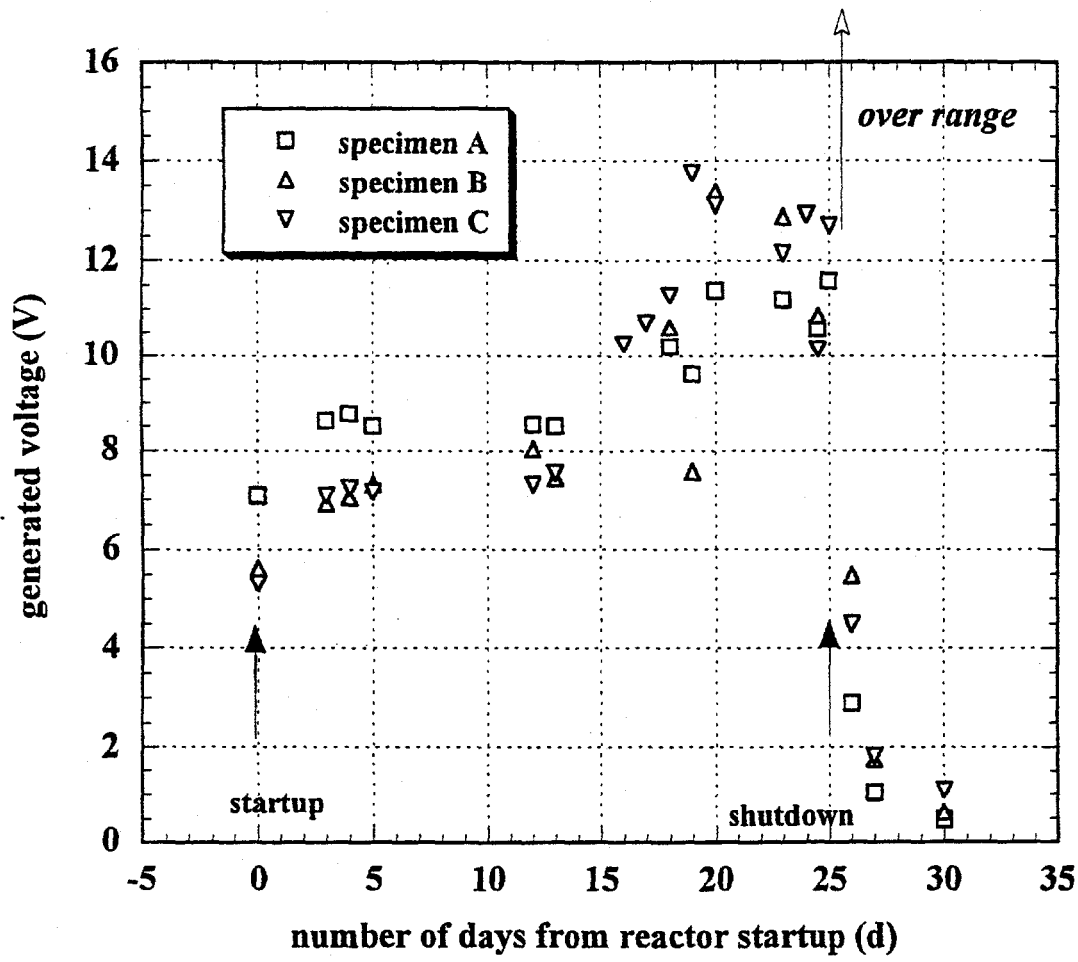


Fig. 4



$$V_{\text{RIEMF}} = -28.069 + 23.022(1000/T),$$

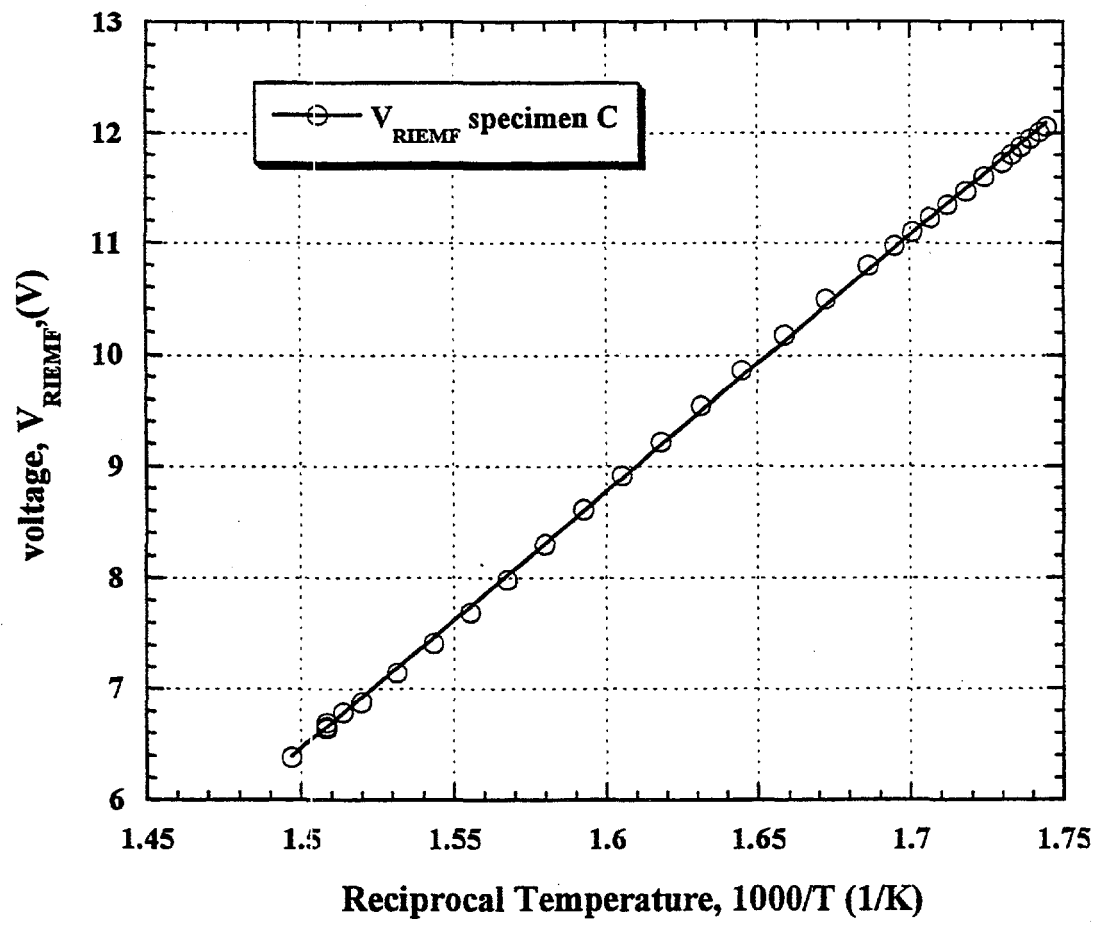


Fig. 6

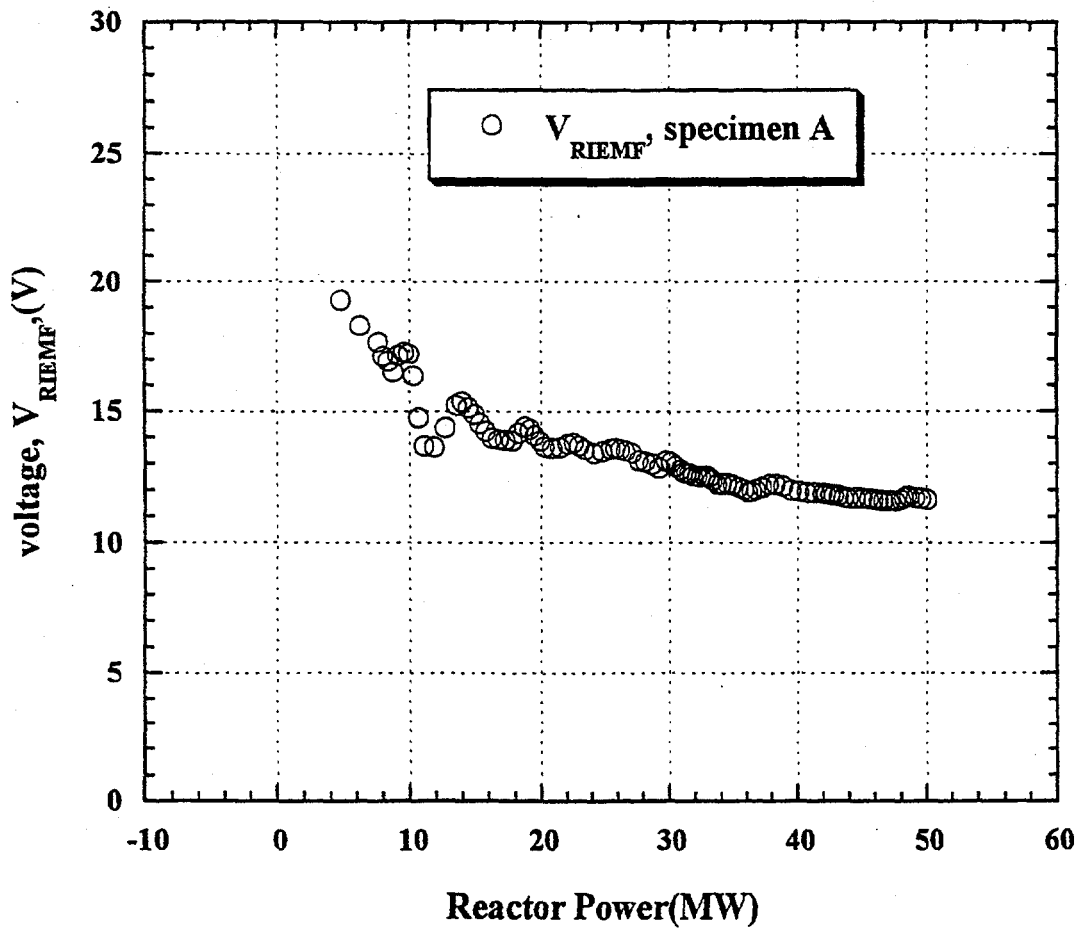
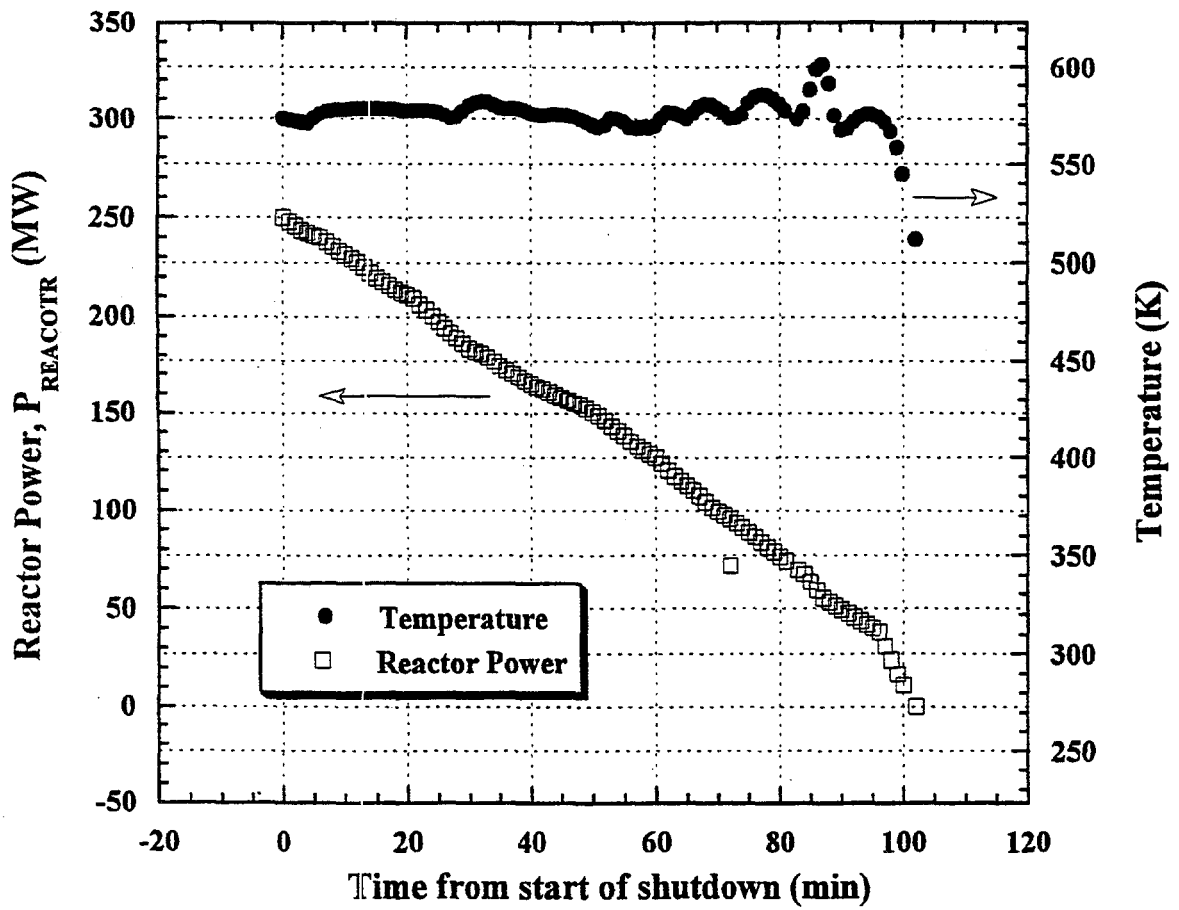


Fig. 7



○ resistance (Mohm)

Resistance of MI cables

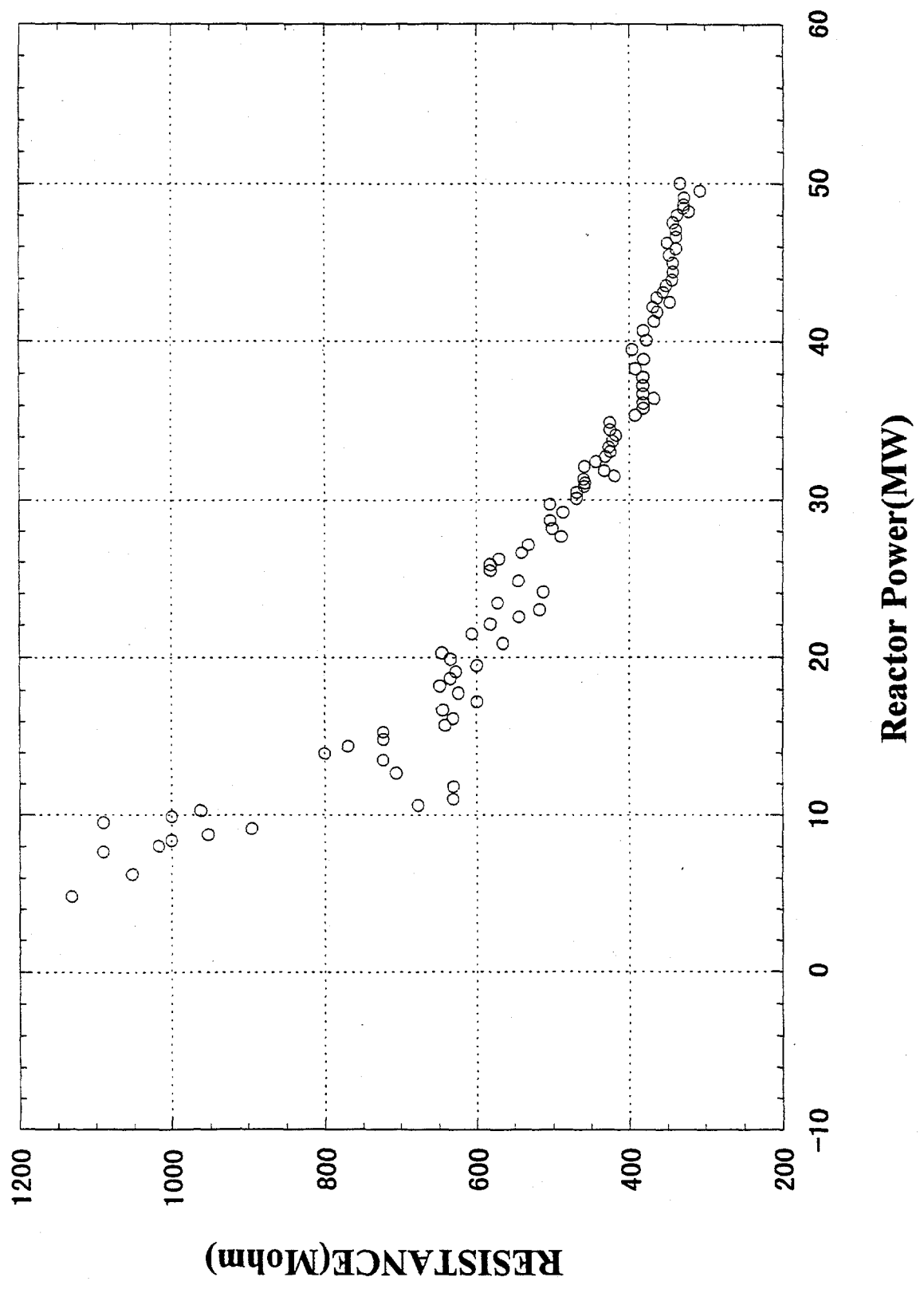
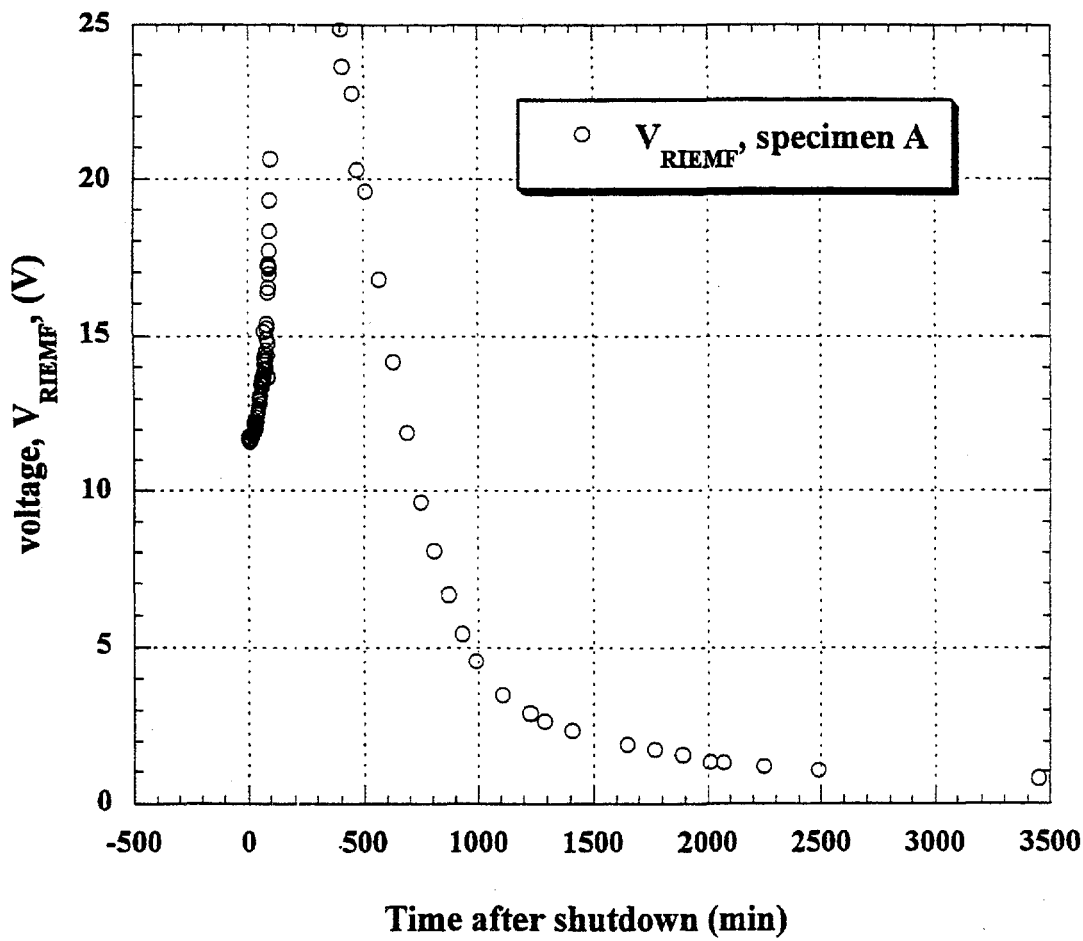


Fig. 8



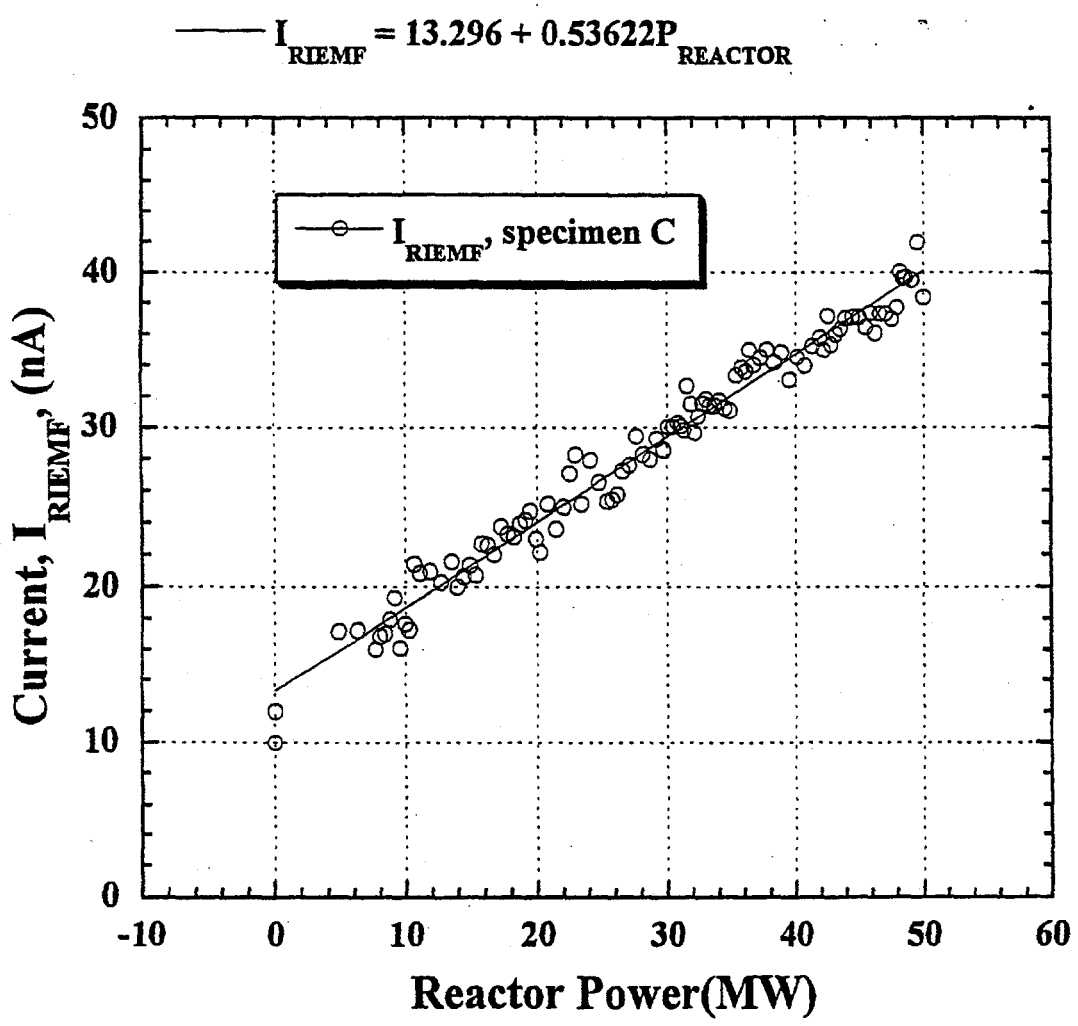


Table 1 current induced by RIEMF in nano A

	50MW, 16rfpd	50MW, 22rfpd	after shutdown
Temperature	573K	573K	321K
SPECIMEN A	24.731	25.245	0.067
SPECIMEN B	44.432	45.708	0.081
SPECIMEN C	45.167	45.221	0.1

Proposal of HFIR Irradiation

- More reliable experimental techniques
 - Joint development of subcapsule
 - elimination of possible current leakage
 - reliable temperature control
 - etc.
- More detailed measurements
 - ohmic check, resistance between electrodes
- High dose rate and high fluence
 - JMTR and HFBR : beginning of degradation even if there exists degradation

HFIR irradiation

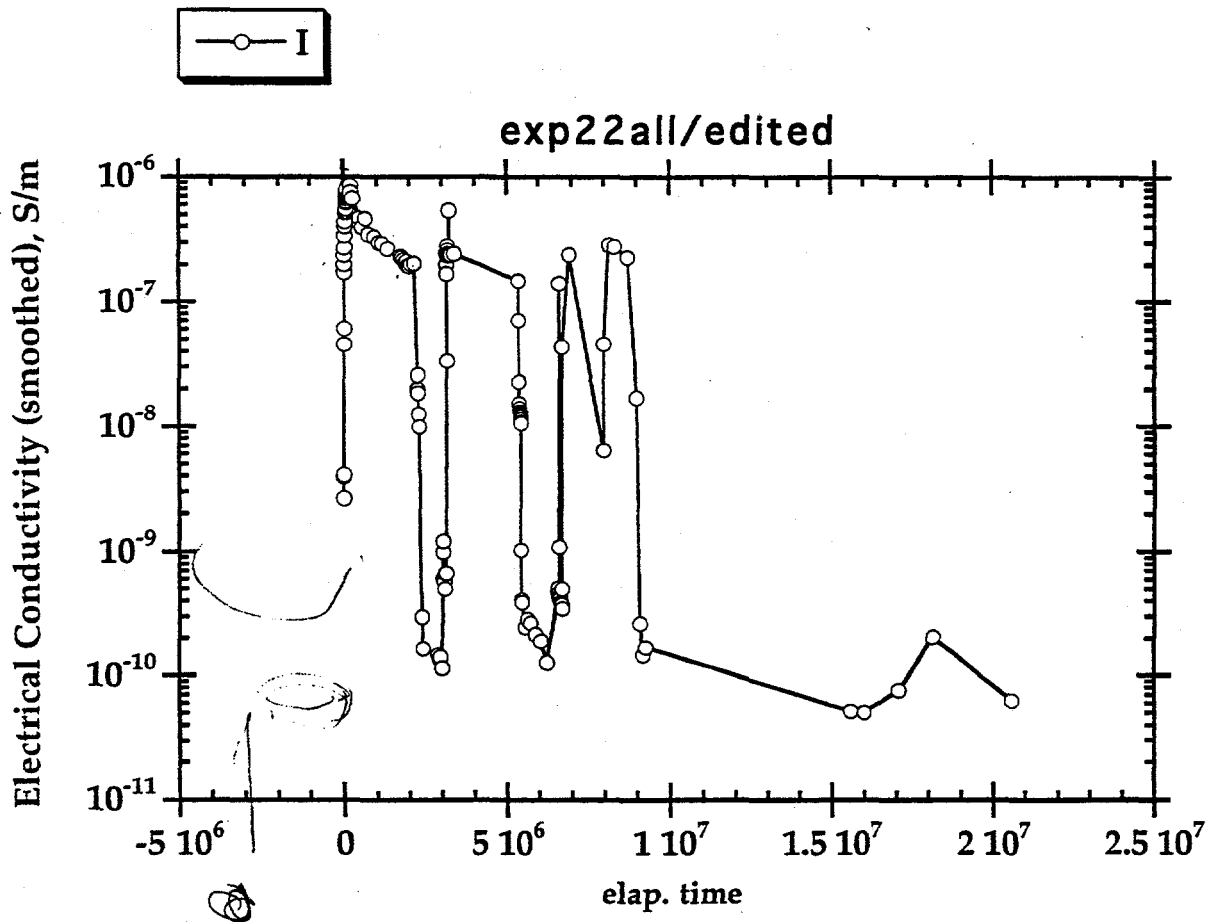
- 500C irradiation up to 3dpa
 - in the most probable region for the RIED
- Detailed measurements of electrical conduction
 - non-ohmic behavior, radiation-induced current
 - surface resistance, etc.

The first thorough measurements and analysis of electrical conduction under high flux irradiation

conductivity estimate from dI/dV at negative voltage application

estimate of contribution of gas conduction

estimate of contribution of radiation-induced current(RIEMF)



History of Irradiation (Specimens and their premature failure)

specimen No.	manufacturer	name	type	grade	voltage	failure
1	crystal system	UV sphire	single, a	UV	applied	290h
2	crystal system	UV sphire	single, c	UV	applied	3 cycles
3	crystal system	regular	single, c	regular	applied	3 cycles
4	crystal system	regular	single, a	regular	applied	340h
5	Vitox	regular	poly	regular	applied	270h
6	Kyocera	A-480	poly	highly pure	applied	220h
7	Wesgo	AL300	poly	regular	applied	1093h
8	Kyocera	A-479	poly	regular	applied	1125h
9	Coors	AD998	poly	highly pure	applied	230h
10	Wesgo	AL995	poly	highly pure	applied	240h
11	Wesgo	AL995	poly	highly pure	no bias	1850h
12	crystal system	regular	single, c	regular	no bias	540h
13	Union carbide	ruby	single	doped	applied	3 cycles
14	Kyocera	SA100	single, t	regular	applied	240h
15	Kyocera	SA100	single, t	regular	no bias	1700h

About the Premature Failure

- Hypothesis 1
 - There is no correlation; random failures
- Hypothesis 2
 - Upper position survived longer.
 - If the failure related the gamma heating rate, the centers should have the shortest lives. No!
- Hypothesis 3
 - There is some correlation. Likely

About an effect of voltage application

- Kyocera single crystal sapphire SA100 applied(14)<no bias(15)
- Wesgo polycrystal AL995 applied(10)<no bias(11)
- But, Crystal System sapphire, regular-grade c-axis showed
- no bias(12)<applied(3)

Crystal-orientation Dependence

- *Comparing crystal systems single crystal*

- C-axis specimens have longer life-time.(1,2,3,4) than A-axis.

- But, no-bias has a shorter life(12).

Dependence on Purity of Polycrystal

• *Comparing polycrystals,*

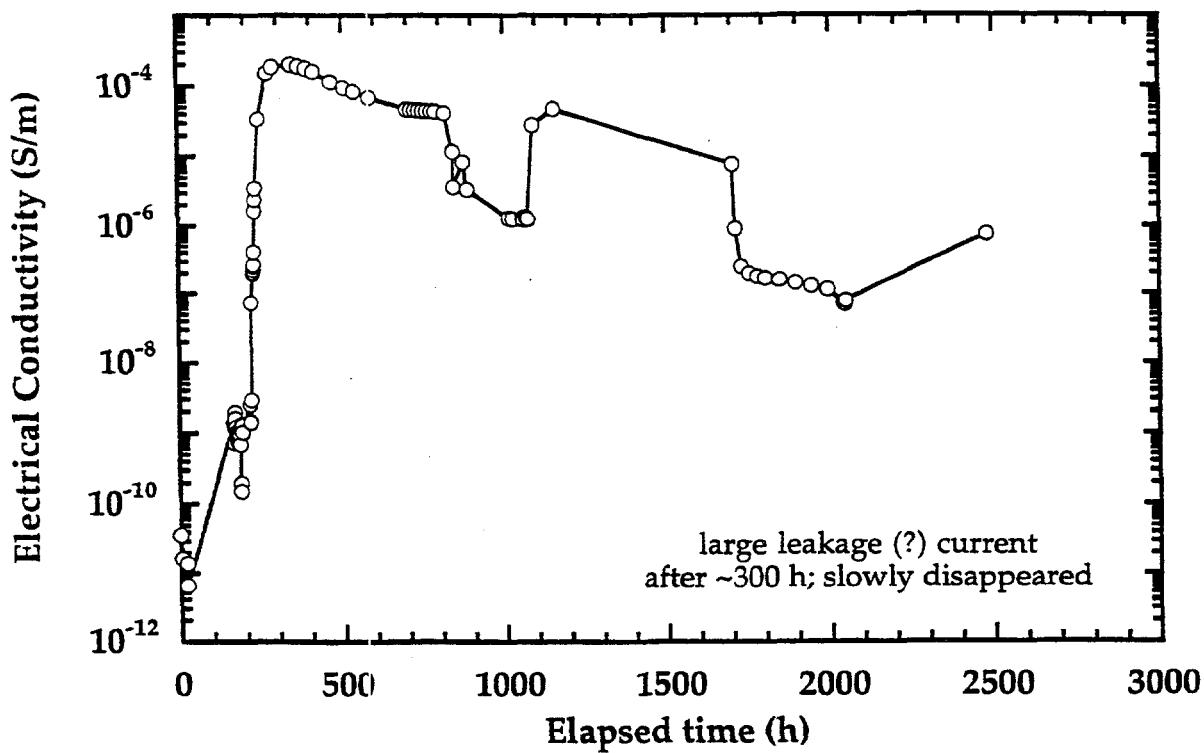
- Low grade(impure) specimens have longer life-time.
 - Kyocera; 480(6)<479(8)
 - Wesgo; AL995(10)<AL300(7)
- If it is assumed that Vitox has high-purity,
 - All the highly pure polycrystals, Vitox(5), KyoceraA-480(6), WesgoAL995(10), and Coors(9) had very short lives, only about a few tens hours(220-240 elapsed hour)
- Low grade polycrystals survived the first cycle.
 - WesgoAL300(7) and KyoceraA479(8)

Ruby

- Ruby showed degradation. Its leads (coaxial, center and guard) behaved well. So, it looked that the degradation would be genuine.
- The guard current did not show strong increase.
- The surface resistance did not degrade substantially.

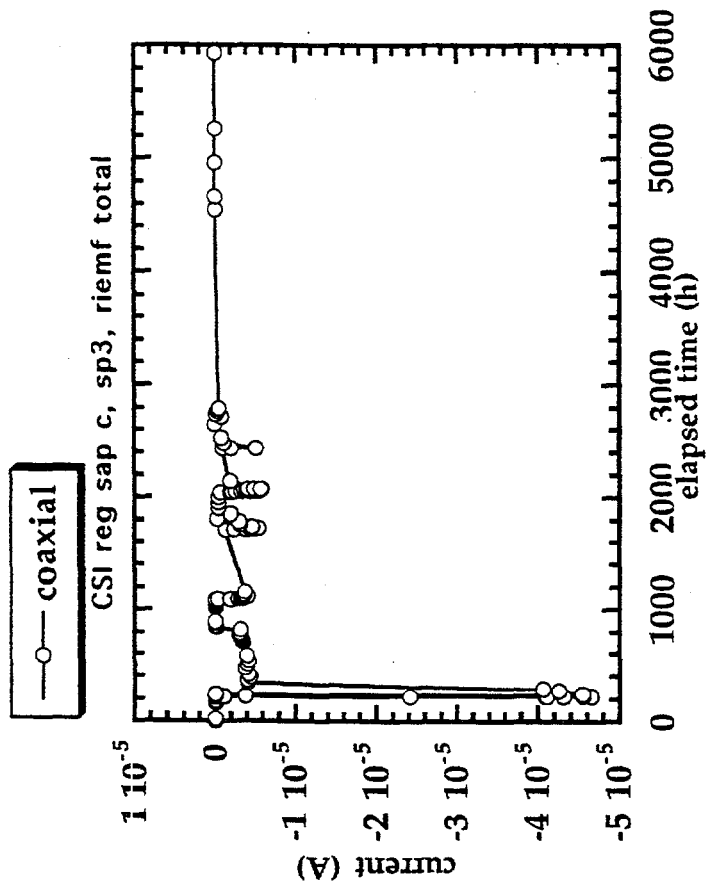
exp 213 / master / all

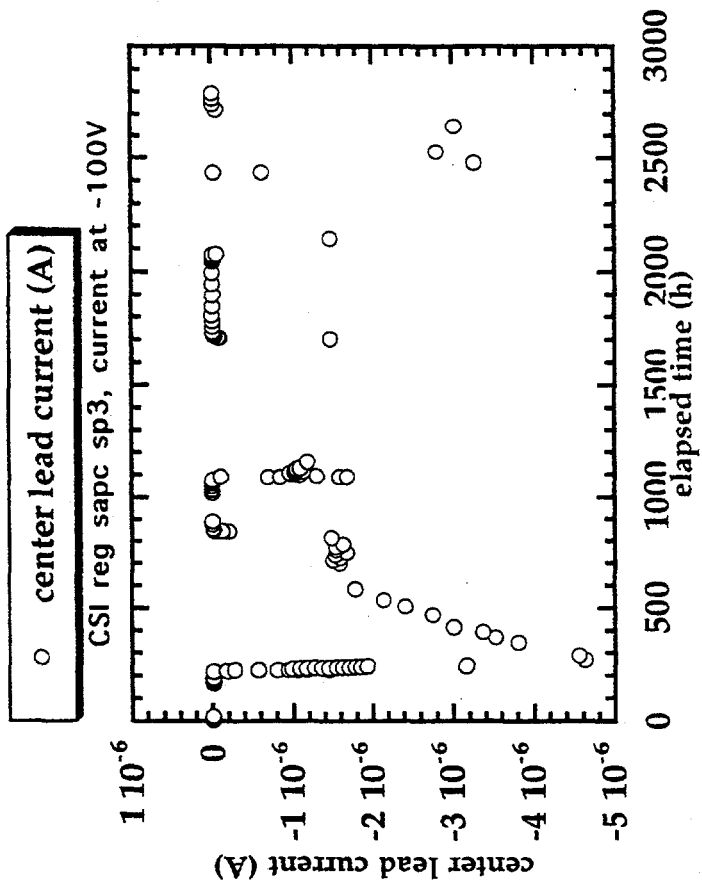
exp213/all (Union Carbide ruby)



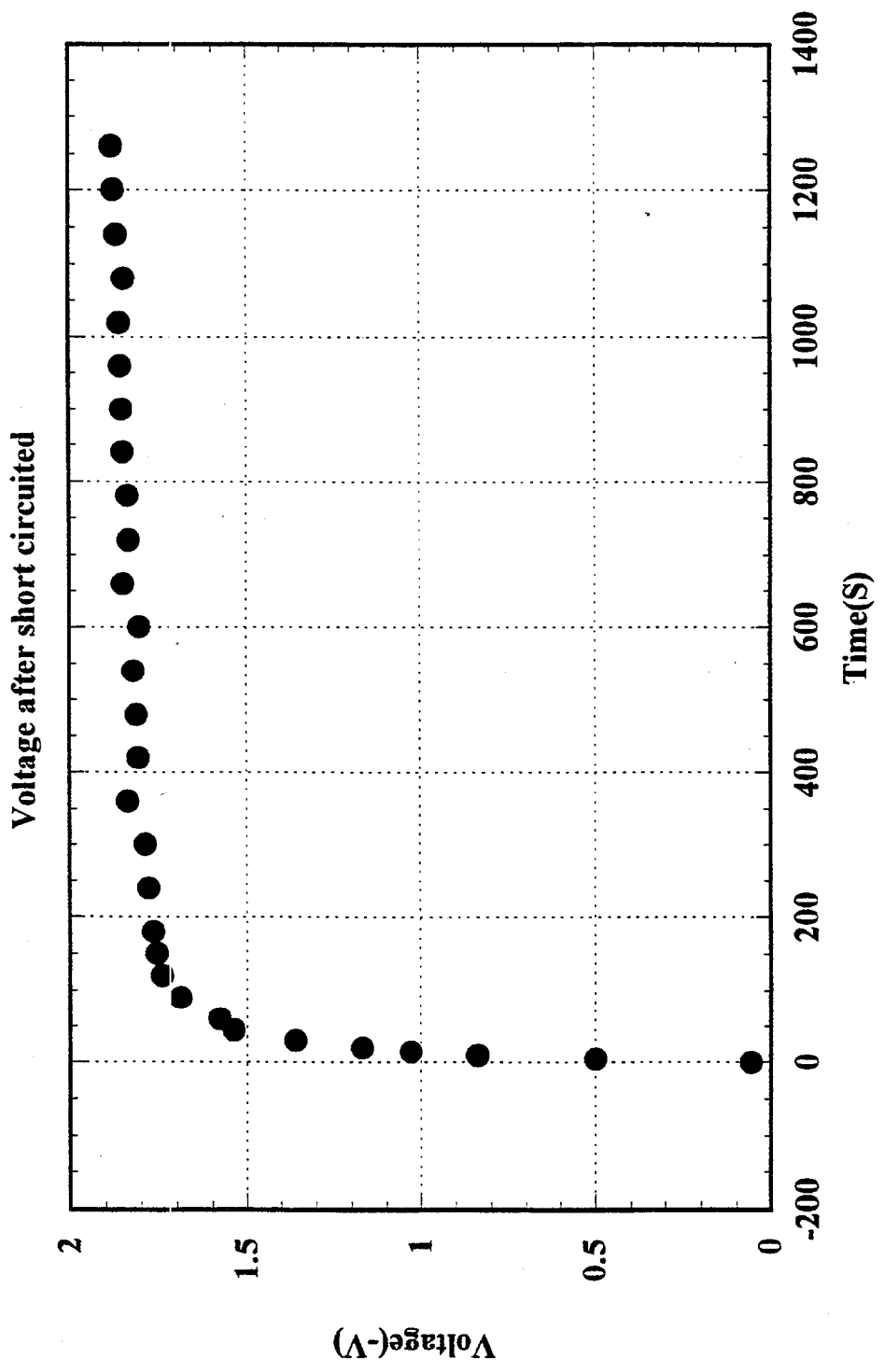
Observed Large RIEMF

- The cause of the RIEMF is not clear yet.
- It may suggest charge drift and redistribution along electric field(ionic conduction).
- It may suggest existence of electrical barrier near interface between insulator and electrodes.





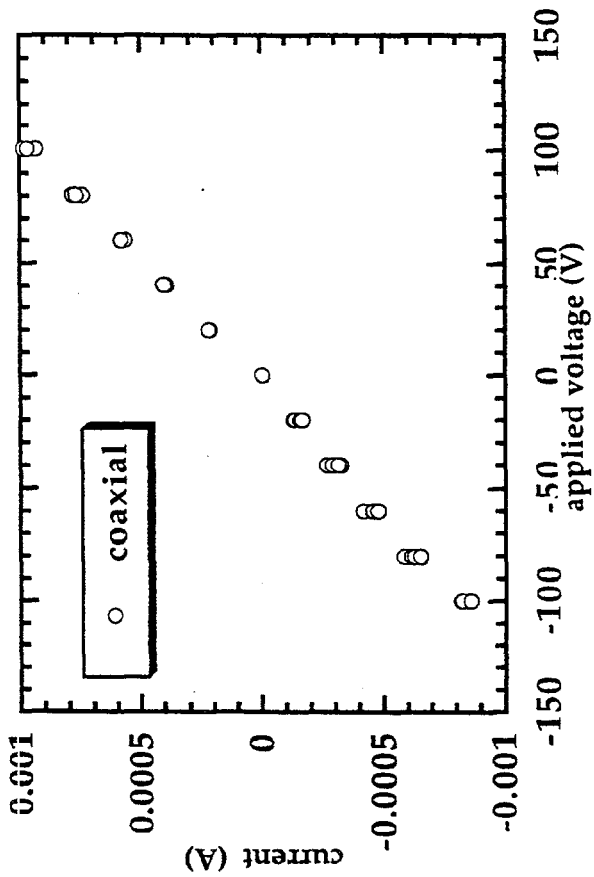
● Specimen 6



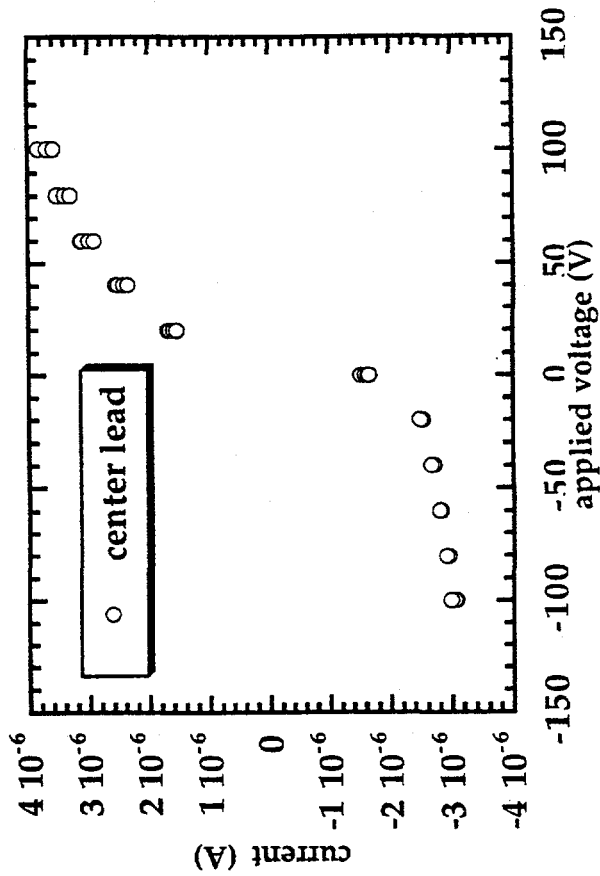
RIC(Radiation Induced Conductivity)

- Materials dependence at low dose rate
 - Ruby < low grade alumina < high grade alumina < normal sapphire < high grade sapphire
- However, at high dose rate
 - materials dependence becomes weak and rather high grade alumina and sapphire would have lower RIC
- Saturation behavior at the beginning of irradiation, but in the second startup it showed nearly linear dependence on the dose rate.
 - Effects of atomic displacement on the RIC

CSI sapphire UV c-axis 697-735, sp.2
at the end of 1st cycle



CSI sapphire UV c-axis 697-735 sp.2
at the end of 1st cycle

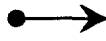


Important items left for further studies

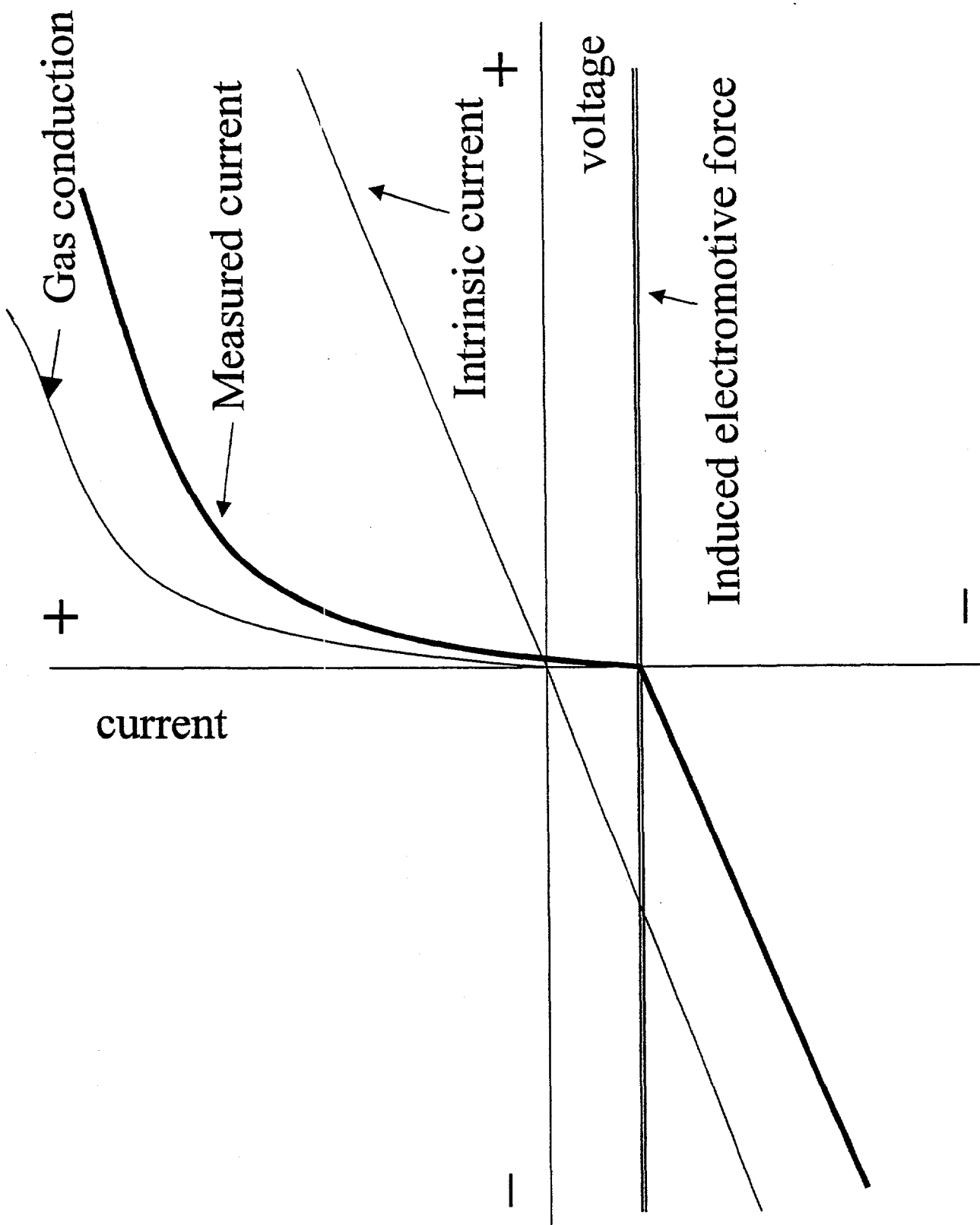
- Effects of gas environments
 - vacuum or reductive environment is essential for the RIED?
- Effects of radiation-induced current
 - it will affect the measurements and estimate of electrical conductivity
 - it may suggest ionic conduction and charge redistribution?

Proposal

- The RIEMF may have correlation with degradation.
- Observed RIEMF would be different from that in MI-cables.



- Measurements of kinetics of RIEMF in JMTR



1-3 μA



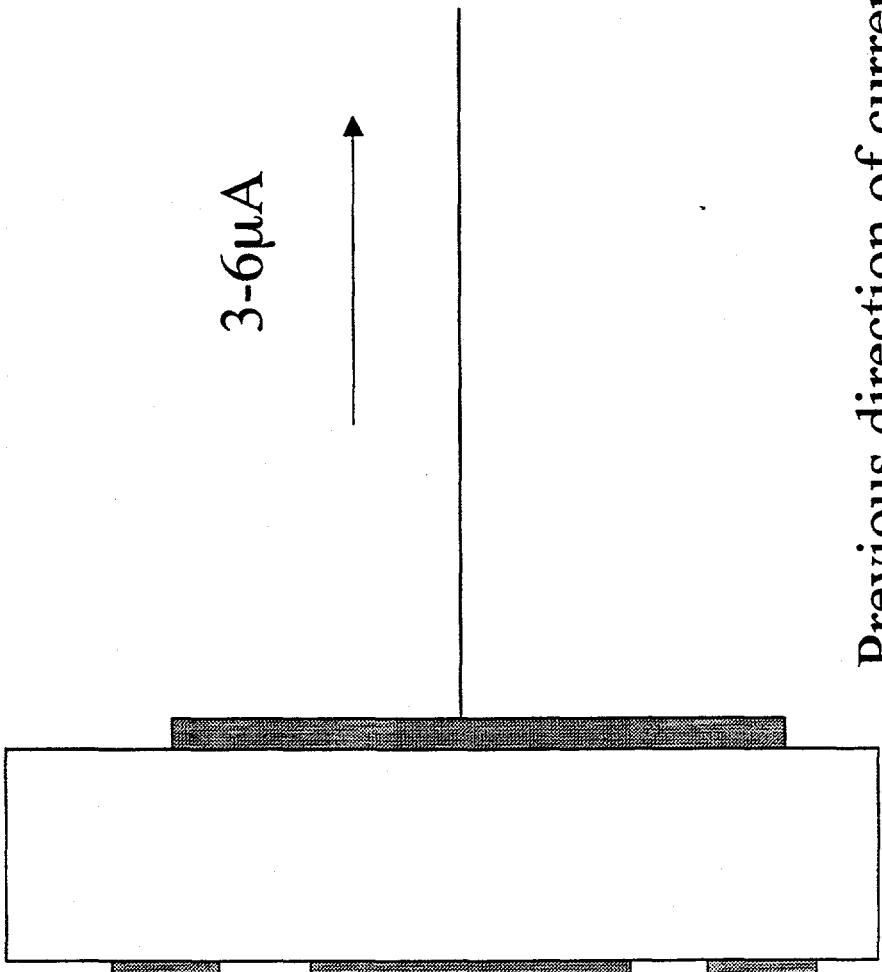
2-3 μA

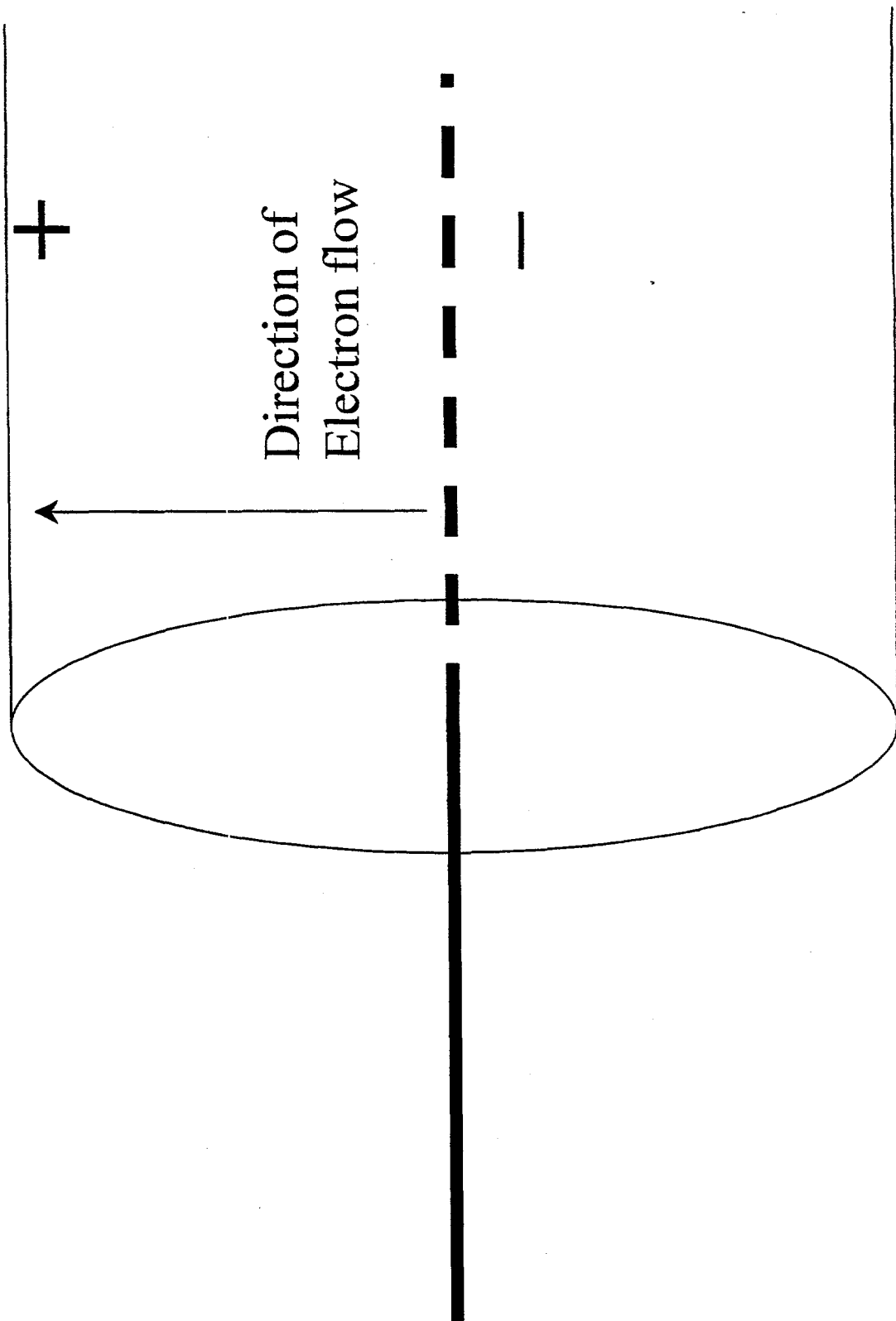


3-6 μA



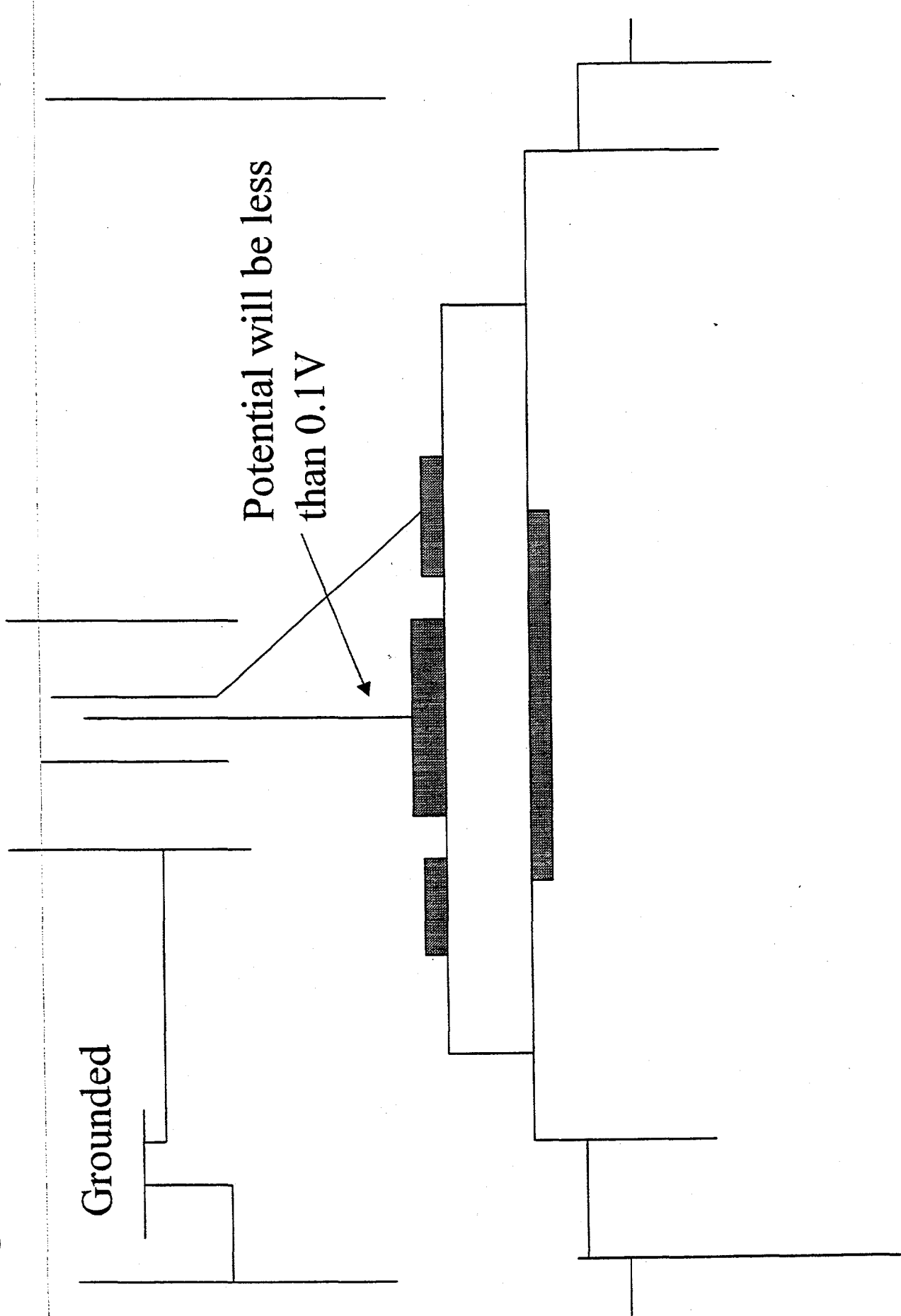
Previous direction of current





Grounded

Potential will be less
than 0.1V





Electrical Conductivity of Alumina under Irradiation with Fast Electrons in a High Voltage Electron Microscope

M.M.R. Howlader, C. Kinoshita, K. Shiiyama and M. Kutsuwada

Department of Nuclear Engineering, Kyushu University 36,
Fukuoka 812-81, Japan

The electrical conductivity of 750 μm thick sapphire ($\alpha\text{-Al}_2\text{O}_3$, Kyocera) specimens with vacuum deposited titanium and gold electrodes has been measured before and during irradiation with 1 MeV electrons in a high voltage electron microscope. Similar experimental conditions to our previous study¹, namely temperatures of 290-690 K and applied voltage of 93 kV/m are used in this study, except that the previous study used a sample thickness of 230 μm and platinum paste electrodes. The voltage-current measurements before and during irradiation show non-ohmic behavior at different temperatures. The radiation induced conductivity (RIC) results show that the bulk RIC of alumina increases and decreases with increasing irradiation flux and temperature, respectively, while the bulk RIC with platinum paste in the previous study increased with increasing irradiation flux and temperature. On the other hand, the surface RIC increases with increasing irradiation flux and temperature in both cases. Although the conductivity reaches at a certain level which is much greater than that of the unirradiation value when the beam is turned on and the large part of the conductivity abruptly disappears when the beam is turned off is found in both studies, a transient peak at 623 K with beam off condition which is higher than that of the relevant irradiation value was found only in the previous study. Simultaneous measurements of the bulk and the surface conductivity with 1 MeV electrons irradiation to a total dose of 9.1×10^{-5} dpa (7.1×10^{22} e/m²) at 690 K show that no bulk or surface degradation are present in the specimen. Instead, both of the conductivities appeared to decrease with increasing dpa, in contrast to the abrupt increase in the surface conductivity at 3.3×10^{-5} dpa observed in our previous study. The post irradiation conductivity after this total damage is the same as the unirradiated conductivity at the respective temperature. Even though there was not any degradation, the irradiated specimen was examined with a Scanning Electron Microscope (SEM) X-ray microprobe to detect the possibility of impurity segregation on the surface that might have a role on causing surface degradation. Based on the present results as well as our previous study, it is argued that the degradation of ceramic insulators may be due to the effect of electrode materials and/or the measuring system.

¹K. Shiiyama, T. Izu, C. Kinoshita and M. Kutsuwada, J. Nucl. Mater. 233-237 (1996) 1332.

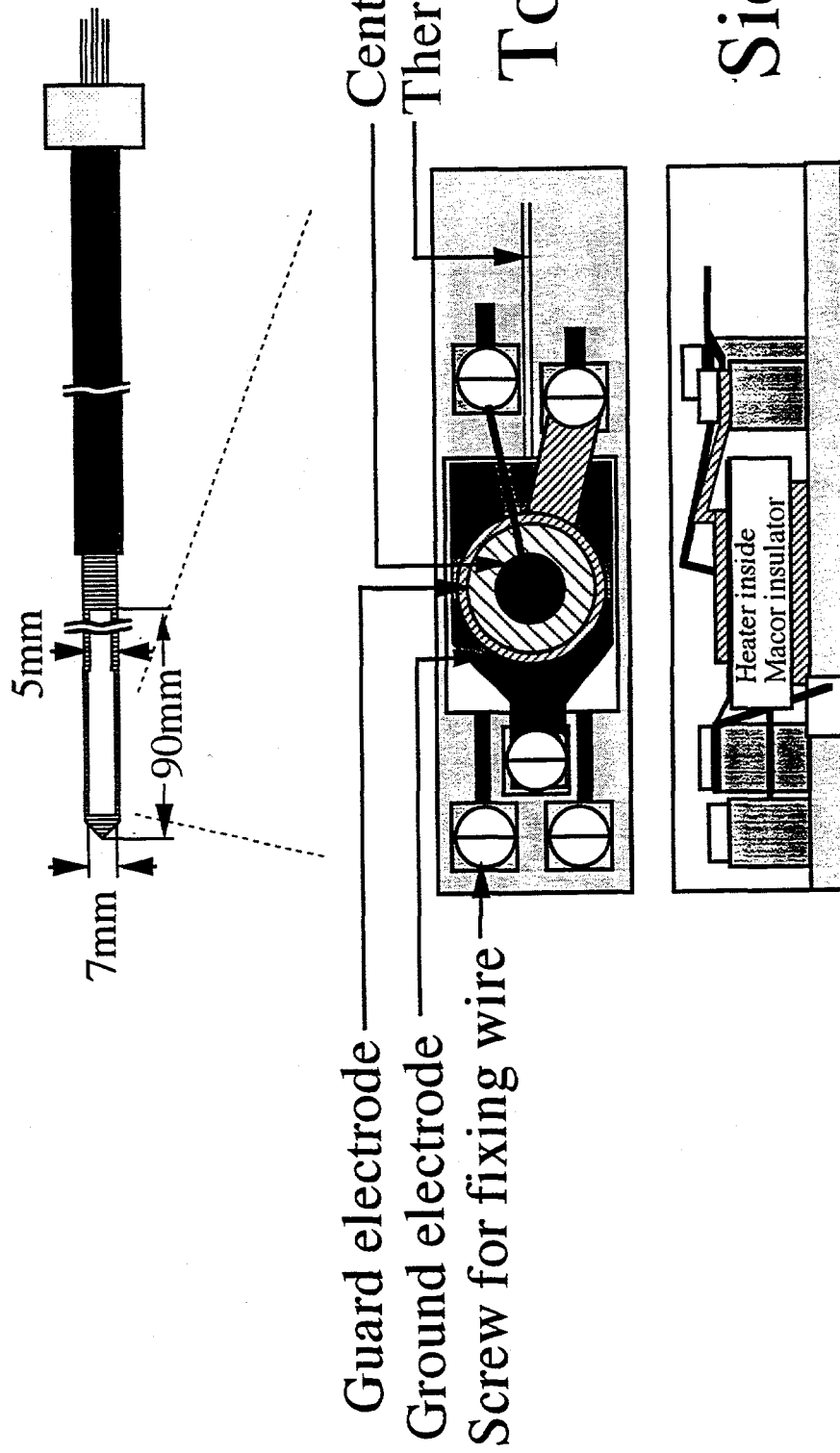
— RECENT RIED EXPERIMENTS —

Electrical Conductivity of Alumina under Irradiation with Fast Electrons in a High Voltage Electron Microscope

M.M.R. Howlader, C. Kinoshita, K. Shiyyama
and M. Kutsuwada

Department of Nuclear Engineering, Kyushu University 36,
Fukuoka 812-81, Japan

Specimen holder:



Schematic diagram of specimen holder.

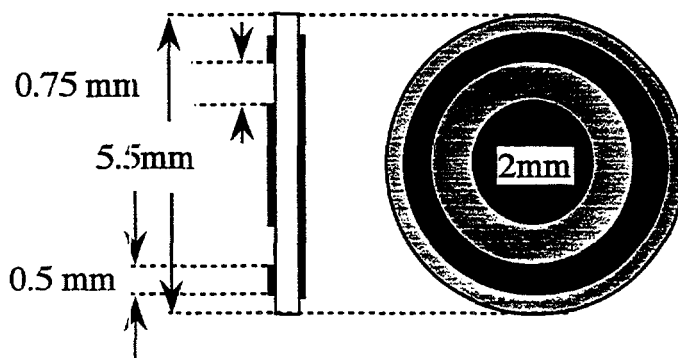
Experiment:

Specimen:

α -Al₂O₃ [Kyocera SA 100
with 99.99% purity and 1102
orientation]

Electrode:

Platinum paste
Titanium and gold



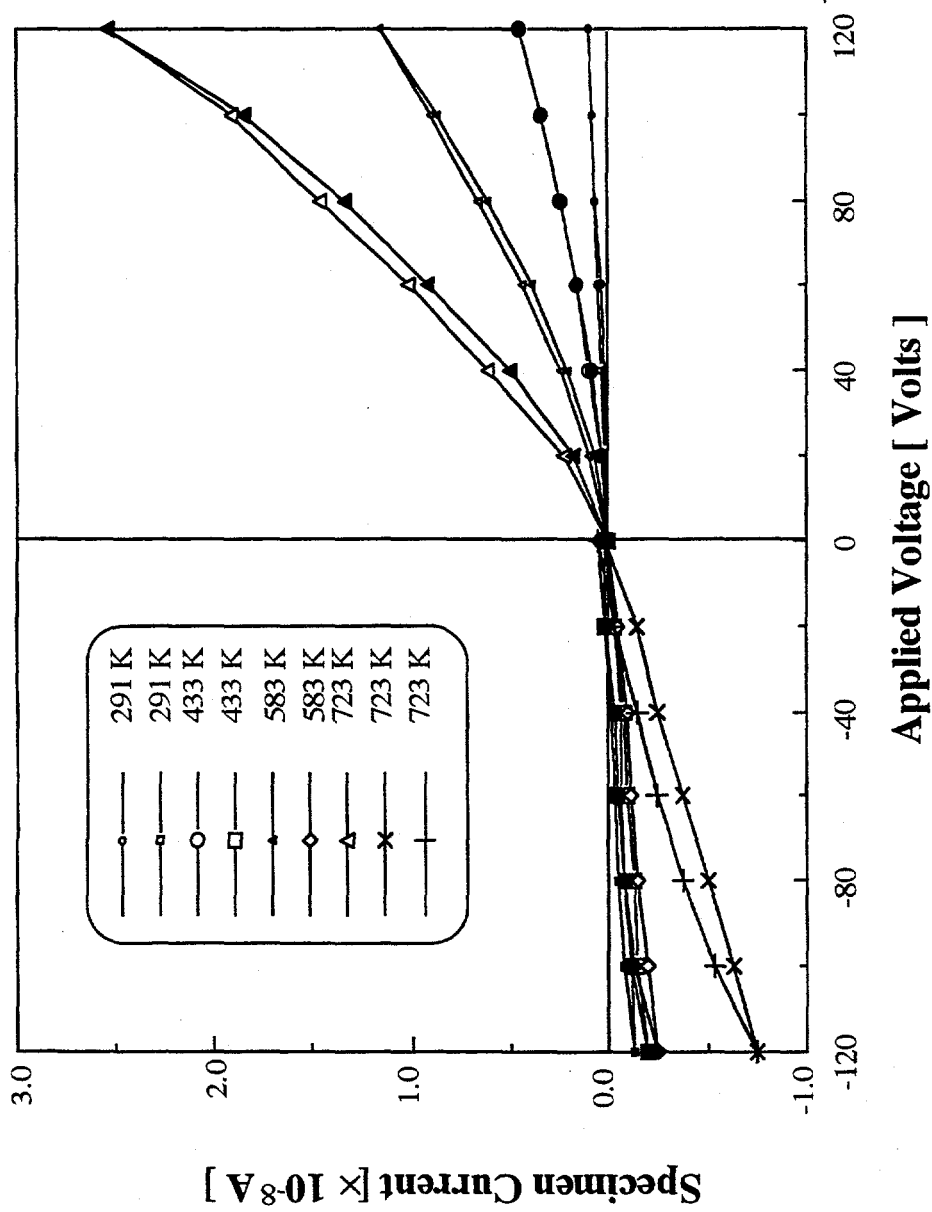
Schematic diagram of three electrode system

Measurement of current:

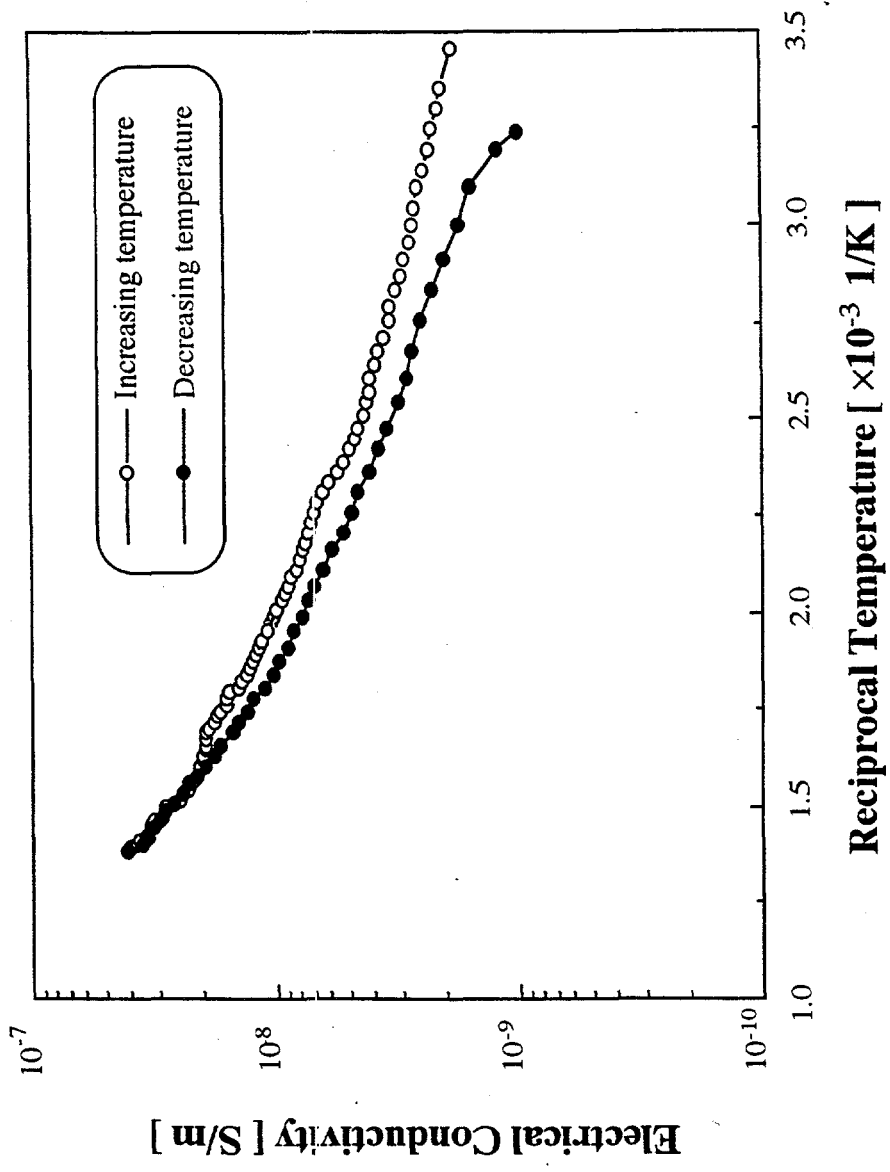
HP4339A high resistance meter
with use of three electrode system

Other conditions:

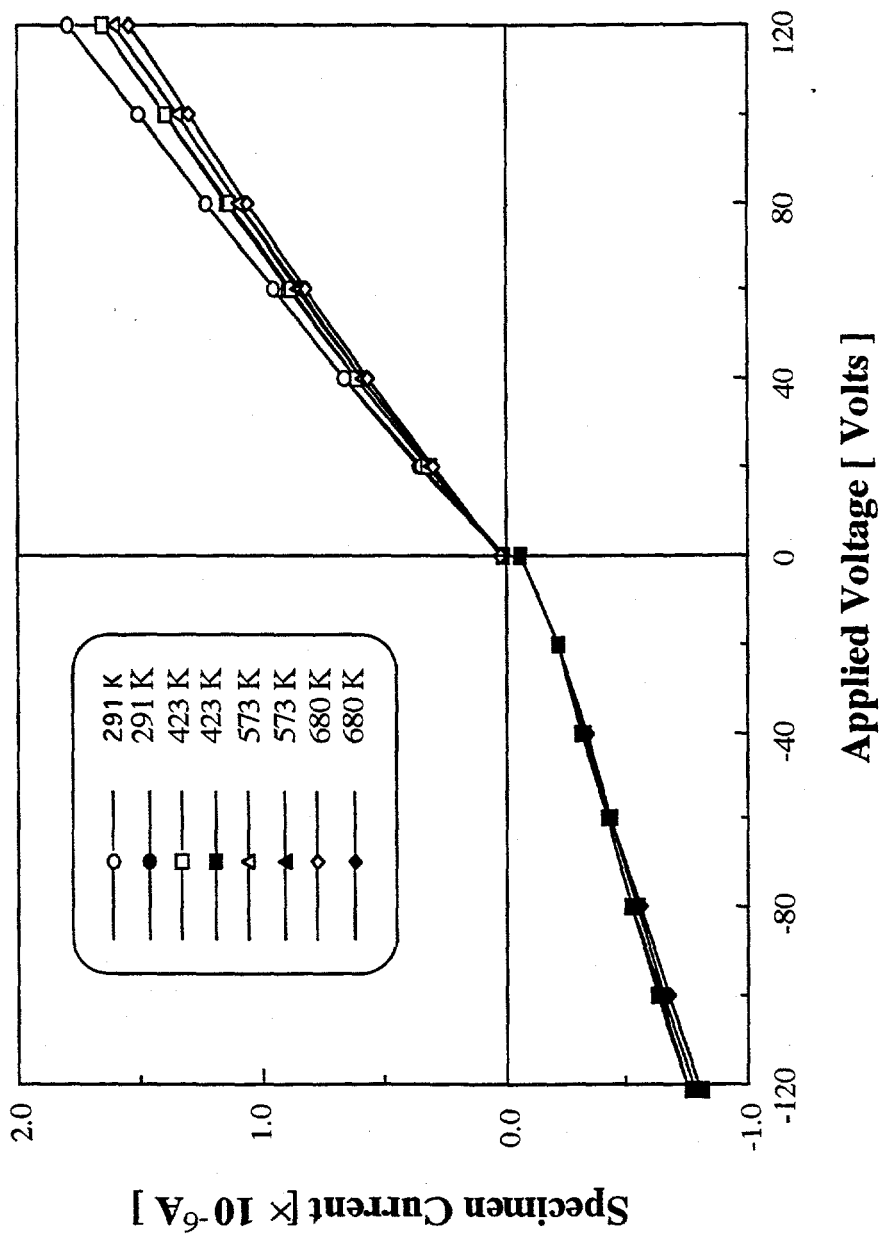
Temperature: 296 K-723 K
Vacuum pressure: 10^{-4} - 10^{-5} Pa



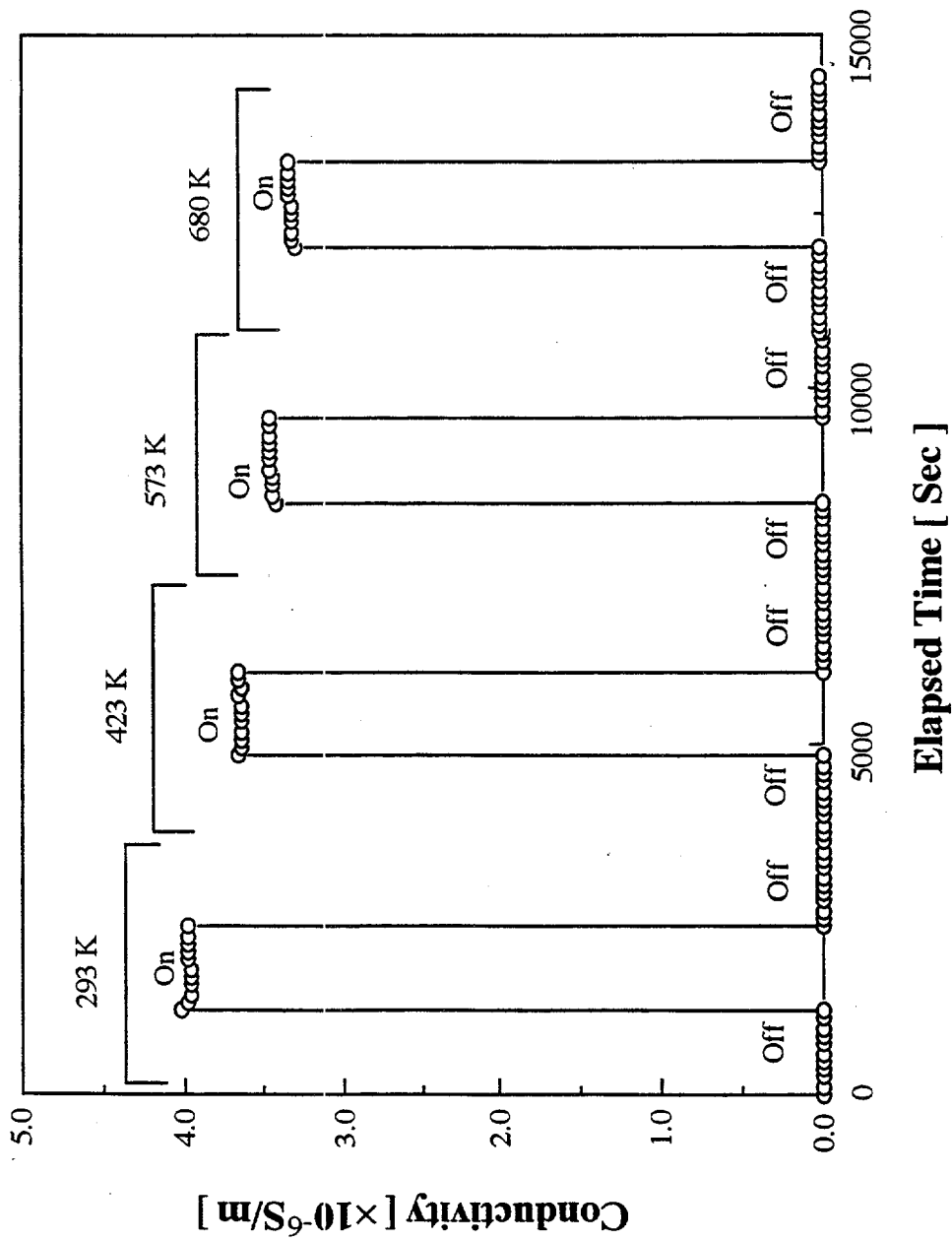
Current-Voltage behavior of a 750 μm thick α -alumina with titanium and gold electrode before irradiation.



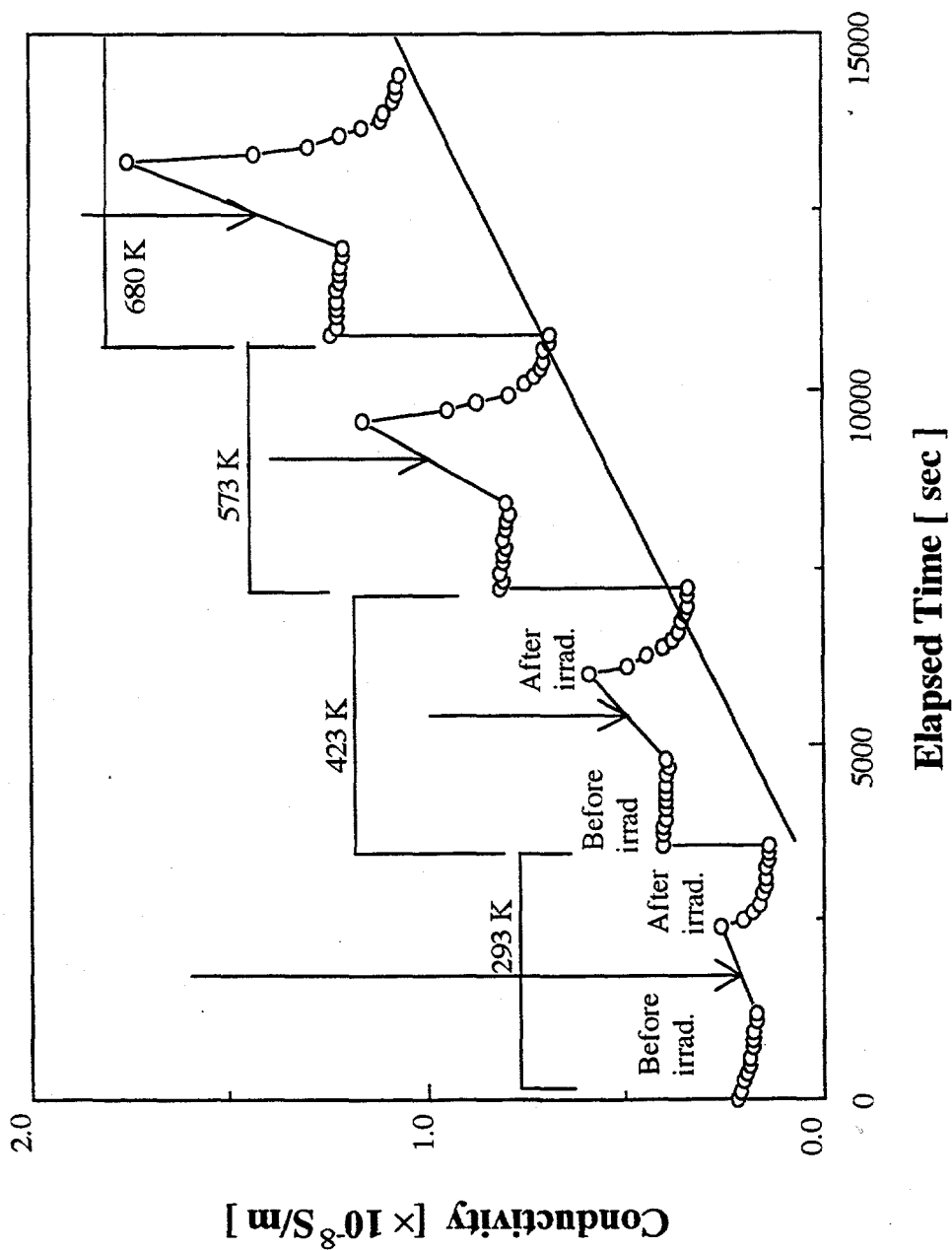
Temperature dependence of electrical conductivity of a 750 μm thick α -alumina with titanium and gold electrode in an applied electric field of 93 kV/m.



Current-voltage behavior of a 750 μm thick α -alumina having titanium and gold electrode under irradiation with a 1 MeV electron flux of 1.5×10^{18} $\text{e}/\text{m}^2 \cdot \text{s}$.

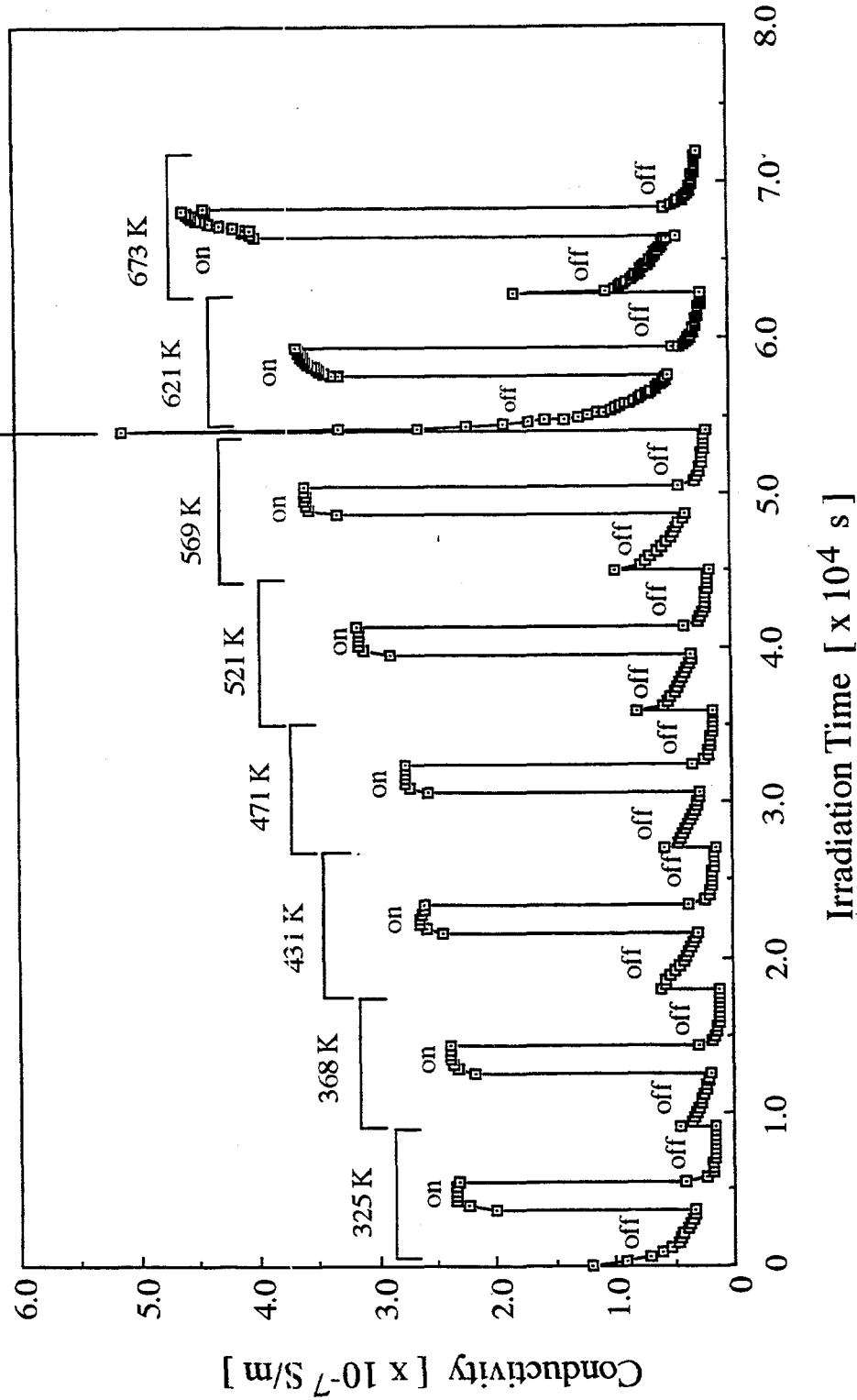


Temperature dependence of bulk conductivity of a 750 μm thick α -alumina having titanium and gold electrode with a 1 MeV electron irradiation flux of 1.5×10^{18} $\text{e}/\text{m}^2 \cdot \text{s}$ at beam-on and -off.

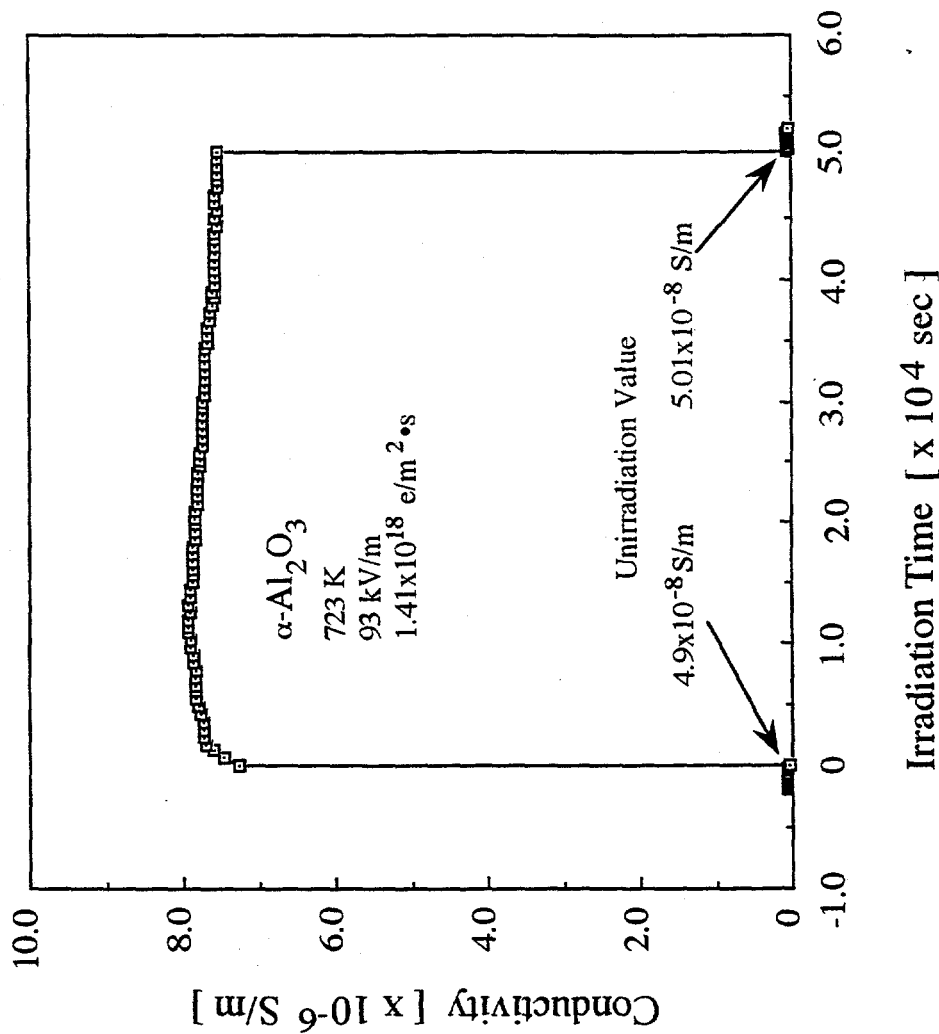


Bulk conductivity of a 750 μm thick α -alumina with titanium and gold electrode prior and later to irradiation in the electric field of 93 kV/m. Arrow lines show the span where irradiation has been done.

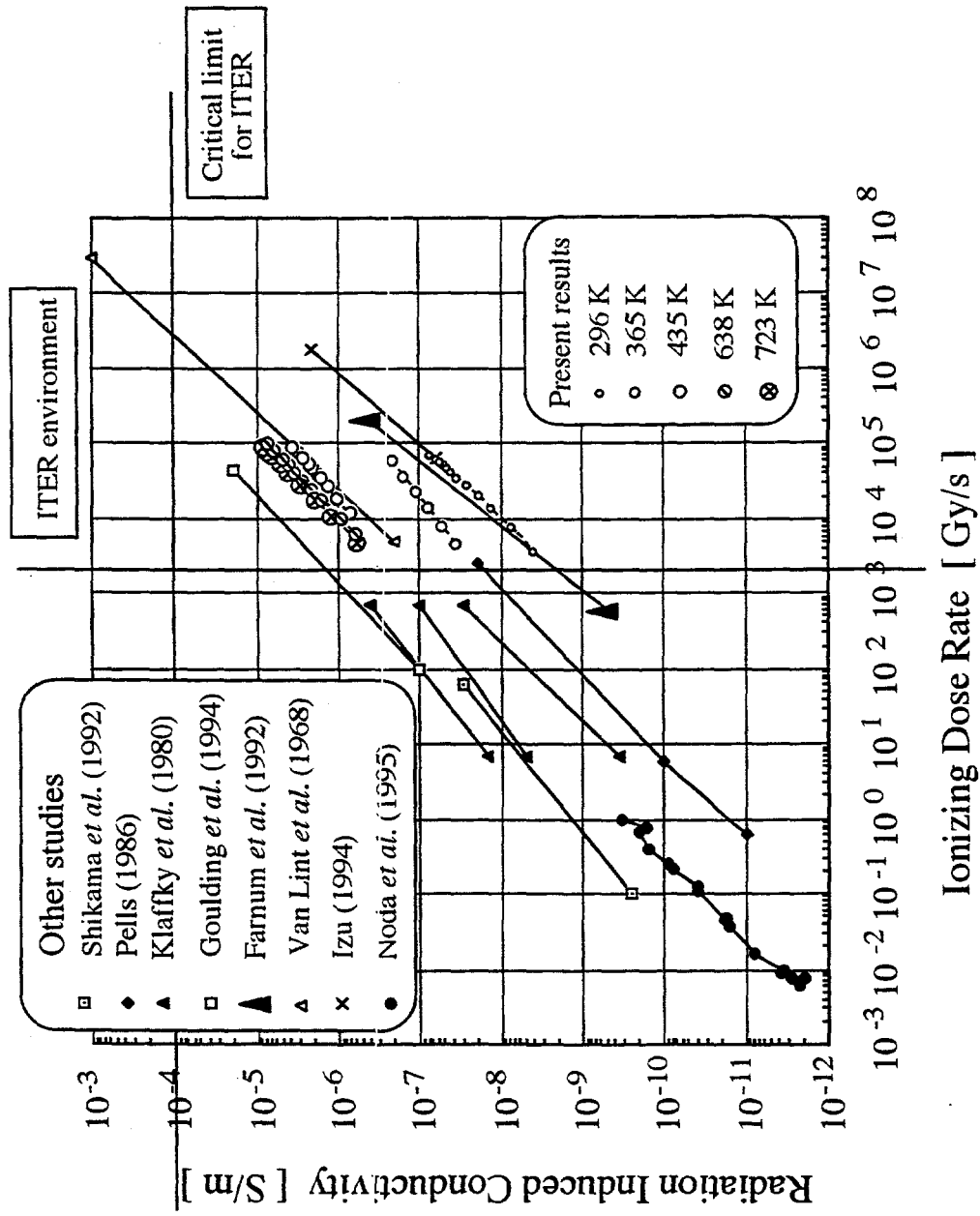
Transient peak = 6×10^{-6} S/m



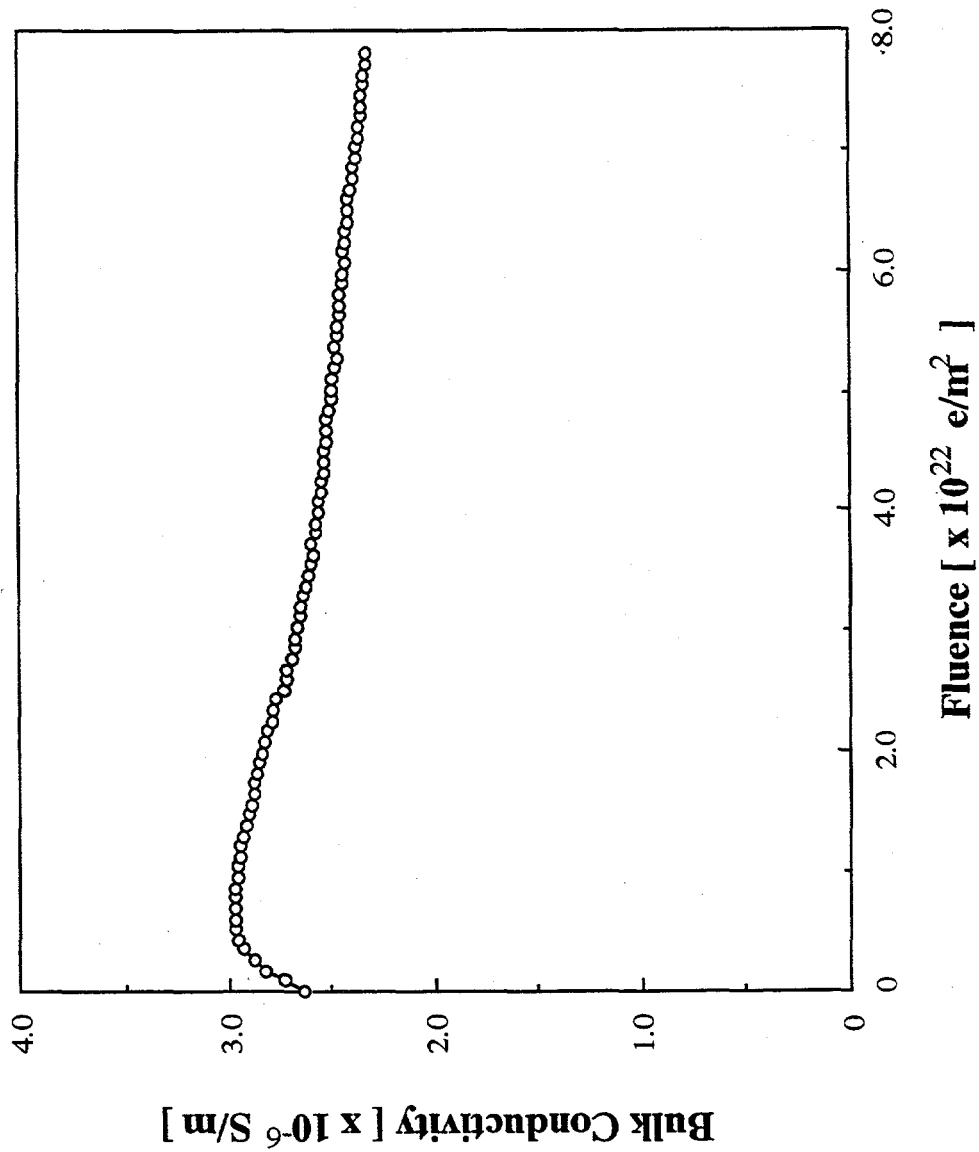
The temperature dependence of electrical conductivity for a 288 μm thick $\alpha\text{-Al}_2\text{O}_3$ under a 1 MeV electron flux of 1.5×10^{18} $\text{e}/\text{m}^2 \cdot \text{s}$ with beam on and off conditions in a dc electric field of 93 kV/m (platinum paste electrode).
(after Howlader and Kinoshita)



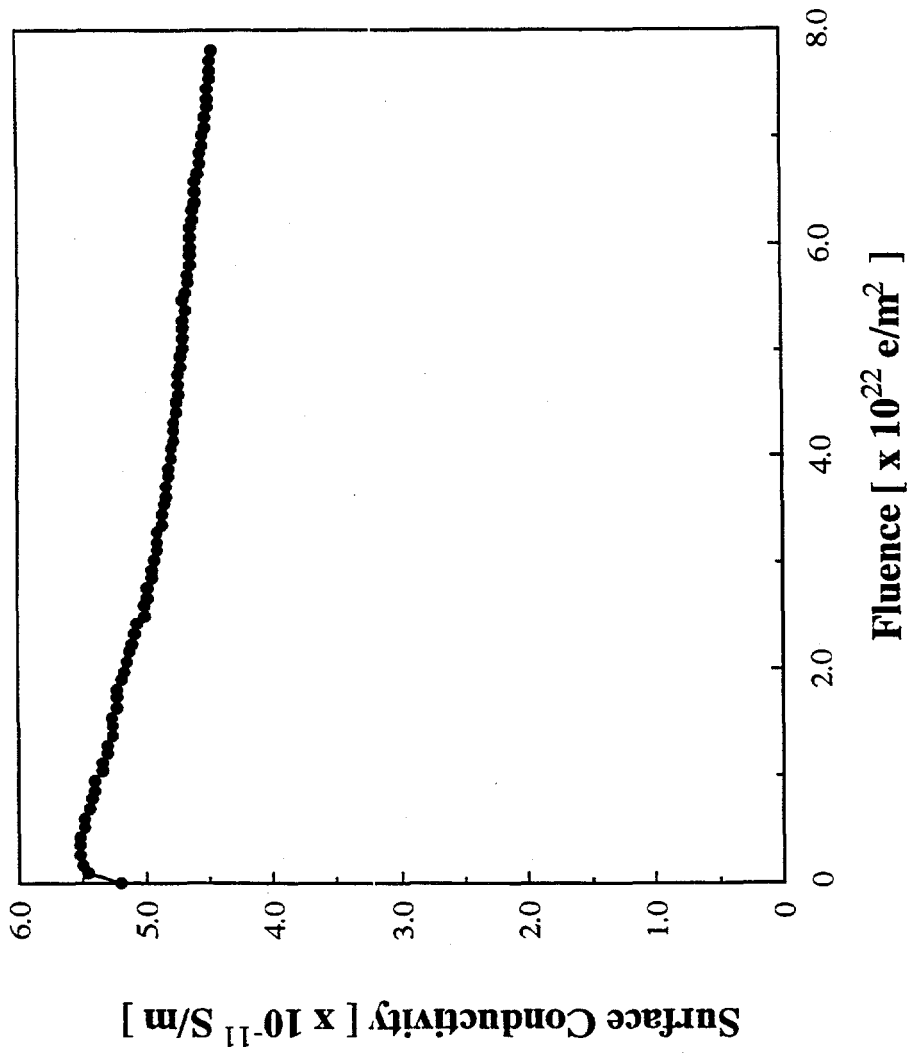
Variation of conductivity of a 270 μm thick $\alpha\text{-Al}_2\text{O}_3$ under irradiation with platinum paste electrode at 723 K with a 1 MeV electron flux of $1.4 \times 10^{18} \text{ e/m}^2 \cdot \text{s}$ under an applied voltage of 93 kV/m and that after cutting the electron beam.
 (after Howlader and Kinoshita)



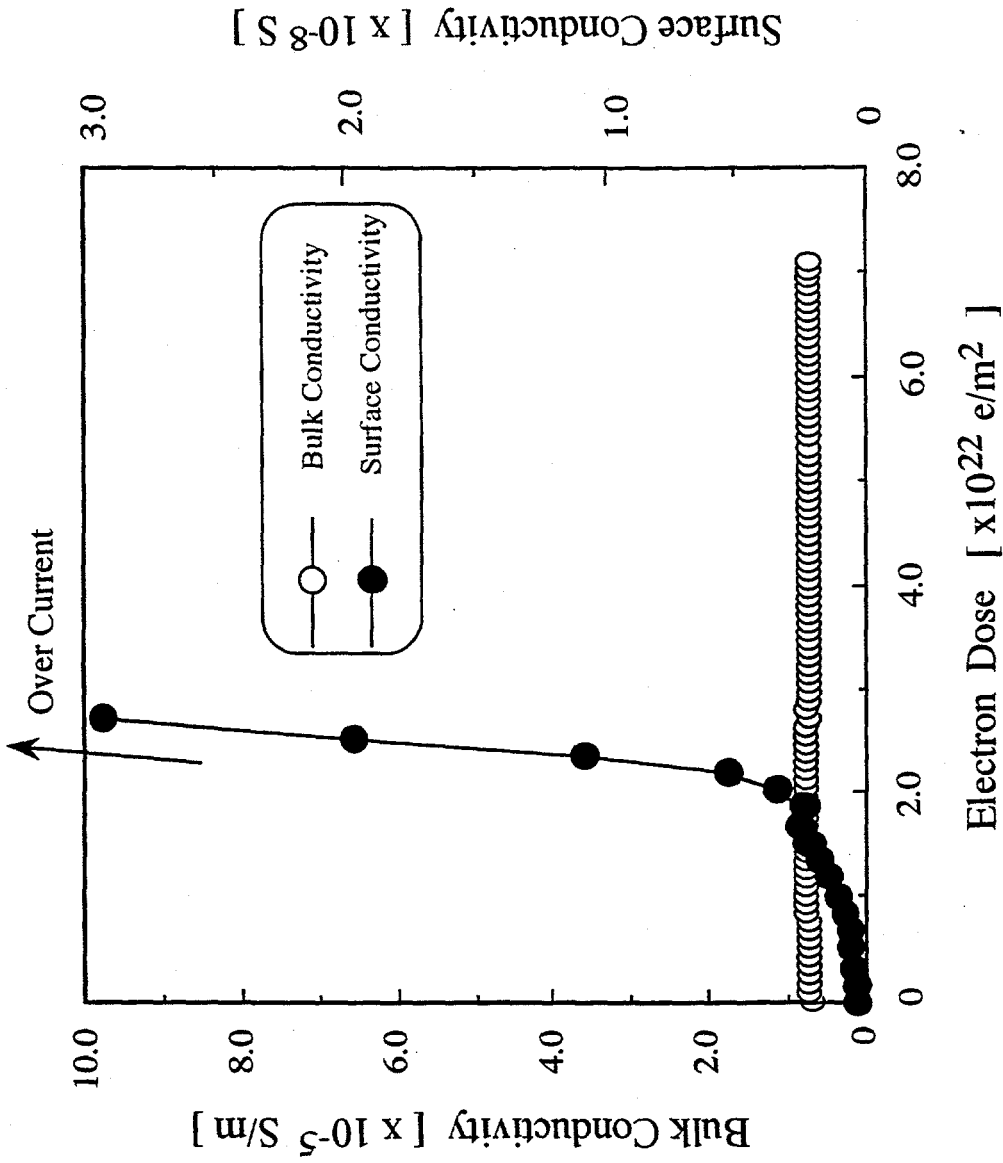
Radiation induced conductivity in $\alpha\text{-Al}_2\text{O}_3$
 (after Howlader and Kinoshita)



Bulk conductivity of a 750 μm thick α -alumina with titanium and gold electrode under 1 MeV electron irradiation flux of $1.4 \times 10^{18} \text{ e/m}^2 \cdot \text{s}$ in the electric field of 93kV/m at 680 K.



Surface conductivity of a 750 μm thick α -alumina with titanium and gold electrode under 1 MeV electron irradiation flux of $1.4 \times 10^{18} \text{ e/m}^2 \cdot \text{s}$ in the electric field of 93kV/m at 680 K.



The bulk and surface electrical conductivity of a 270 μm thick $\alpha\text{-Al}_2\text{O}_3$ versus electron fluence under a 1 MeV electron flux of $1.4 \times 10^{18} \text{ e/m}^2 \cdot \text{s}$ with a dc electric field of 93 kV/m at 723 K (platinum paste electrode).
(after Howlader and Kinoshita)



Radiation Induced Electrical Degradation
of α -Al₂O₃ Crystals by Electron Irradiation

Xiang-Fu Zong, Cheng-Fu Shen, Song Liu, Yi Chen,
Renjun Zhang
Fudan University, Shanghai, China

Y. Chen
Office of Basic Energy Sciences
U.S. Department of Energy

Jane G. Zhu
Oak Ridge National Laboratory

B.D. Evans
Edtek, Inc.

R. Gonzalez
Universidad Carlos III, Madrid, Spain

The mechanisms leading to RIED in Al_2O_3 appear to be similar to those for electrical breakdown of oxide crystals at high temperatures (without irradiation)

Chronology & Synergism

ELECTRICAL BREAKDOWN

($E = 1500 \text{ V/cm}$; $T = 1473 \text{ K}$)

RIED

($E=1500 \text{ V/cm}$; 773 K ; e-irrad)

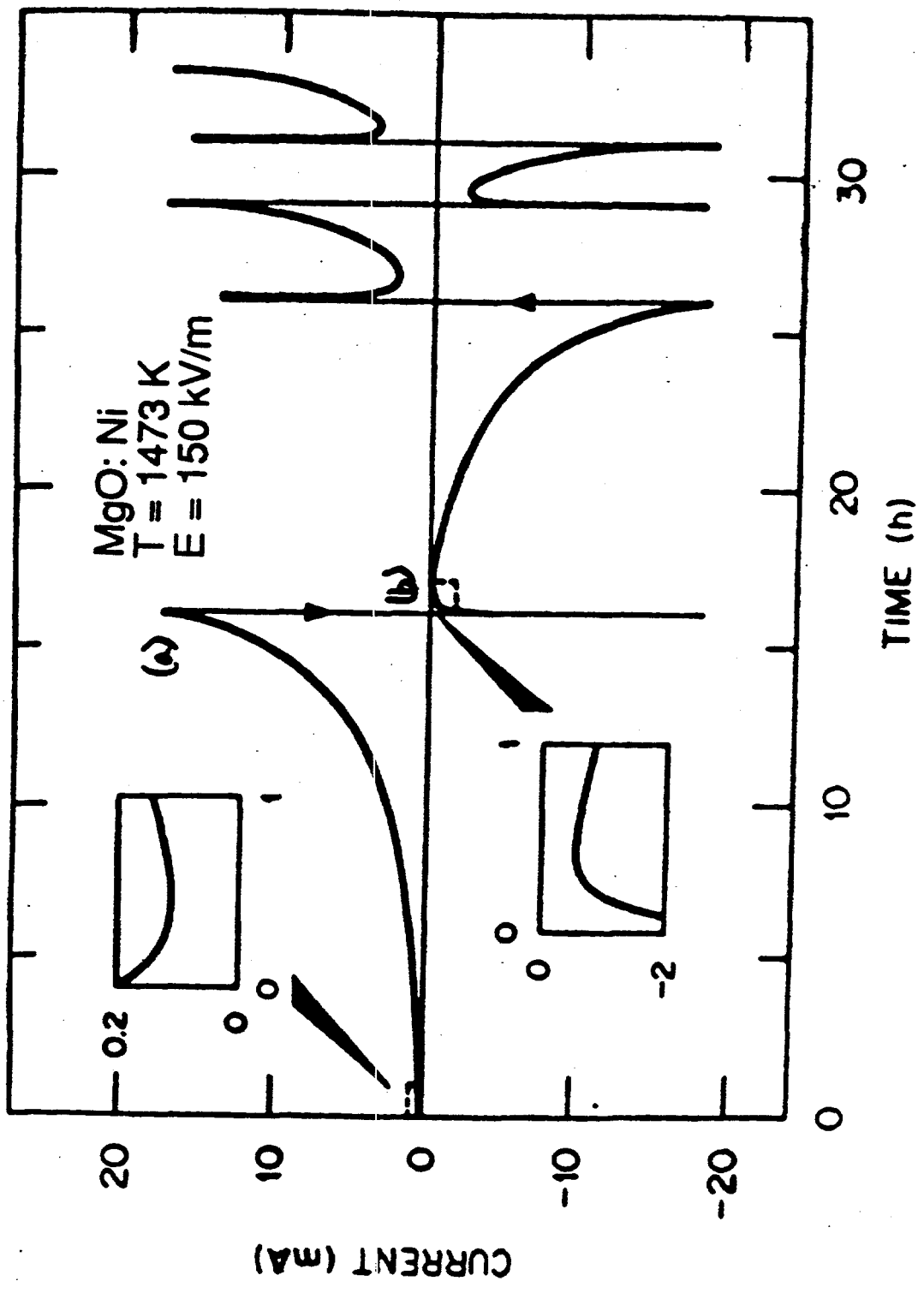
(a) MgO crystals
Mechanism: carrier injection
defect --> ? ? ?
(1982 - 84)

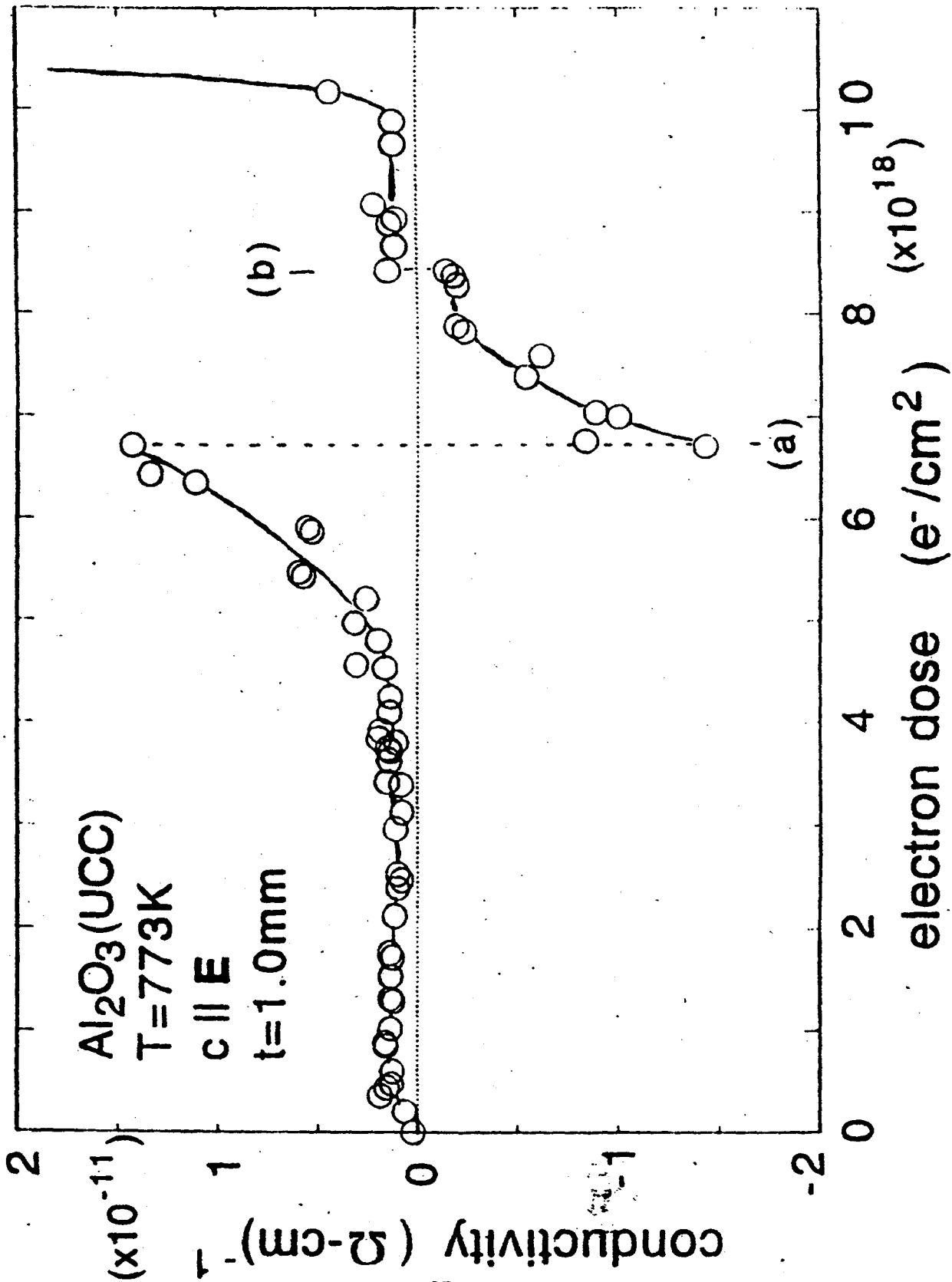
(b) Al_2O_3 crystals
no breakdown observed
(1982 - 84)

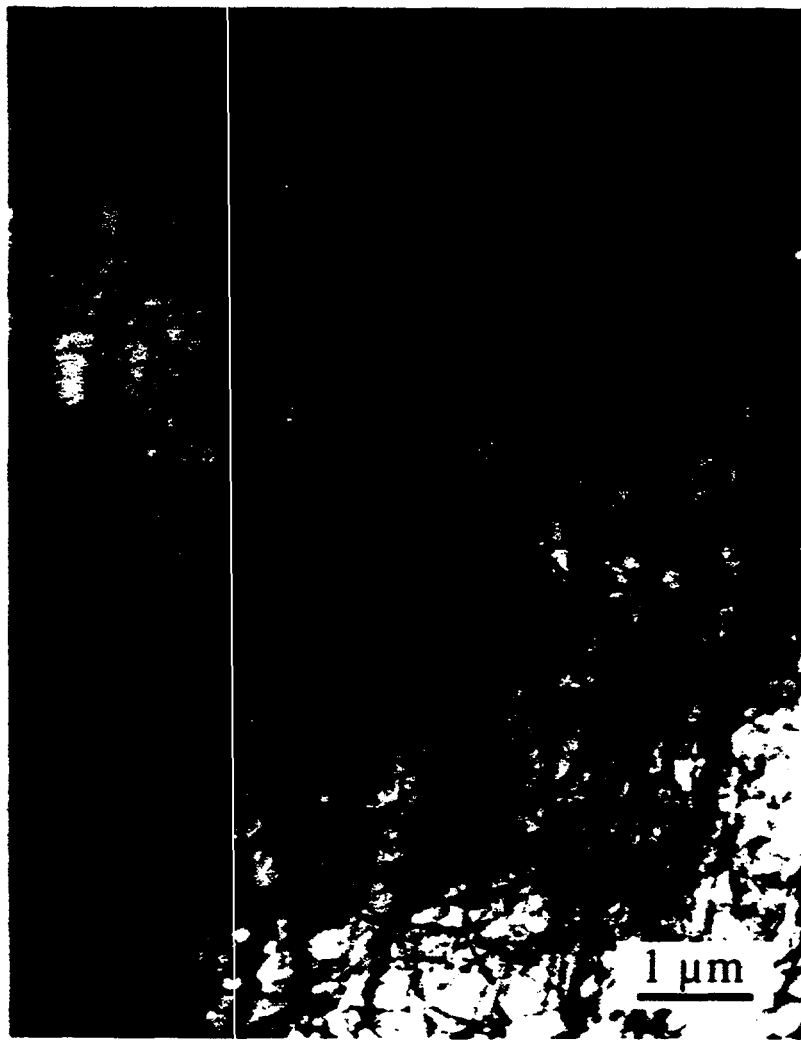
Al_2O_3 crystals
Mechanism: carrier injection
defect --> dislocs 10^8 cm^{-2}
(1994 - 96)

MgO crystals
Mechanism: carrier injection
defect --> dislocations 10^{10} cm^{-2}
(1997, unpublished)

MgO crystals
no RIED observed
(1997, in progress)







Content

- (1) RIED observed in $\alpha\text{-Al}_2\text{O}_3$ at 773K
- (2) Impurities or radiation-induced vacancies
- (3) "Radiation Damage" issue? or carrier injection from electrodes?
- (4) Defects responsible for RIED?
- (5) A model for RIED
- (6) Implications: bulk vs. surface effects

Point Defects

- 1.8 MeV electrons

primarily mono-vacancies → F centers
low production cross section
concentration saturates at $<10^{17} \text{ cm}^{-3}$ at RT

- Defects anneal at 500K

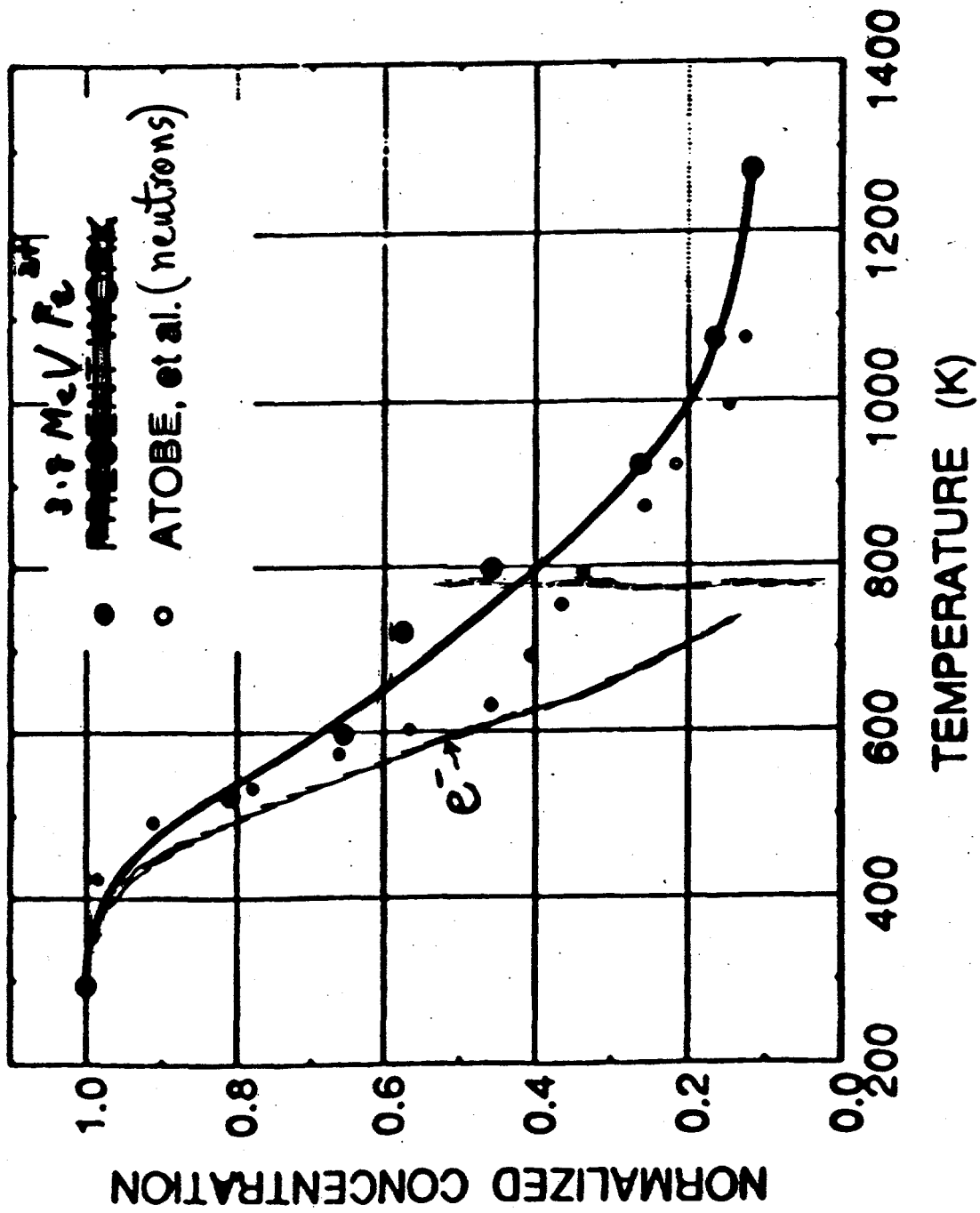
at 773K, few survive, $<10^{15} \text{ defects/cm}^3$
no detectable F centers from RIED

- Thermochemically reduced crystals:

stoichiometric imbalance; no interstitials
 $> 10^{18} \text{ cm}^{-3}$ F centers; no enhanced conductivity

Conclude:

It is unlikely that RIED is caused by anion vacancies produced during Rad-E-T



Impurities

- vacancies $< 10^{15} \text{ cm}^{-3}$
- impurities $\sim 10^{19} \text{ cm}^{-3}$
- $n(\text{impurities}) \gg n(\text{defects})$

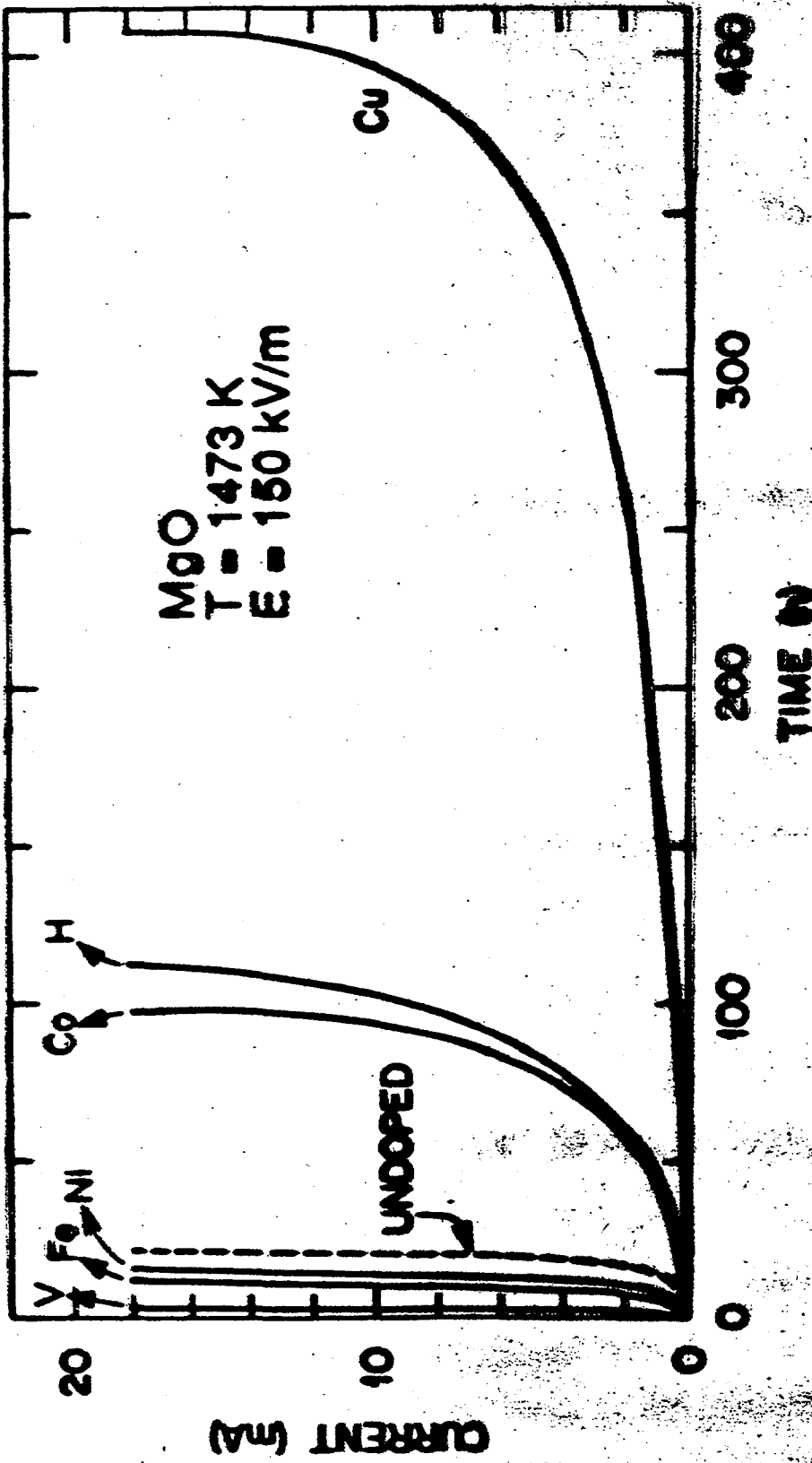
Conclude:

Impurities are expected to play a critical role in RIED

Evidence:

Factor of 4 in critical dose for samples of different sources

Factor of ~ 100 impurity dependence in dielectric breakdown in MgO



Extended Defects

Dislocations

Rad-E-T: 10^8 dislocations/cm²

Virgin: 10^4 dislocations/cm²

Precipitates

None observed

Conclude

10^8 dislocations/cm² - comparable to mechanically deformed crystal. Requires efficient mechanism.

Model

- Carriers injected from electrodes
- Carriers trapped by impurities
- Accumulation of carriers → dislocations
- Dislocations traps e-h created by irradiation
- Charged dislocations affected by **E**
- Diffuse network → conductivity increases
- Reverse **E** → compact network
→ conductivity decreases

Radiation

Radiation is necessary but not sufficient condition for RIED in $\alpha\text{-Al}_2\text{O}_3$

Role:

Provides electrons and holes

Field reversal (a.c.)

1. Kestemick: a.c. σ independent of E surface

2. Zong: E reversal σ dependent of E bulk

3. Hodgson: a.c. σ independent of E surface



On the Electrical Conductivity of Al_2O_3 Under Irradiation

W. Kesternich

Abstract

The validity of the electrical guard technique in the measurements of the electrical conductivity in highly insulating materials has been tested in alpha particle irradiations of Al_2O_3 . Depending on the irradiated specimen area, increases as well as decreases of the apparent bulk conductivity have been observed as a result of "extrinsic" surface leakage currents. They are explained by radiation-modified surface contamination.

Large increases of the apparent bulk conductivity were observed also as an effect of radiation-enhanced "intrinsic" surface conductance through microcracks. Sealing of the cracks resulting in a reversal of this conductivity increase was obtainable by changing the irradiation conditions. Thus, microcracks can be a second reason of systematic error in bulk conductivity measurement. Inspection for microcracks by SEM on pre-polished specimens is recommended. It is shown that $0.3 \mu\text{m}$ wide cracks can be identified by this method.

In search of RIED, experiments by several research groups on several types of Al_2O_3 (including Vitox) have recently been performed with standardized experimental conditions (control of Rpg, Rg, and Rcg). None of these experiments did confirm the existence of permanent bulk conductivity increases. It is concluded that previous RIED-like effects in electron, proton, and neutron irradiations have possibly been caused by either surface or microcrack leakage conductances. Unless these earlier RIED results can be reconfirmed in repeating those experiments under the now standardized conditions, including post-irradiation tests for microcracking, it has to be assumed that RIED as a bulk effect is not existing.

Electrical leakage conductances both, along the outer specimen surface as well as through microcracks in the specimen interior, can be radiation-enhanced by many orders of magnitude. Thus, RIED as an effect of radiation enhanced surface conductivity needs to be further investigated, and the impact of "surface RIED" on electrically insulating fusion reactor components needs to be studied. In these studies outer surfaces as well as cracks within the components need to be taken into consideration.

IEA workshop on Ceramic Insulators for Fusion Energy Applications,
Cincinnati, May 8-9, 1997

On the Electrical Conductivity of Al_2O_3
under irradiation

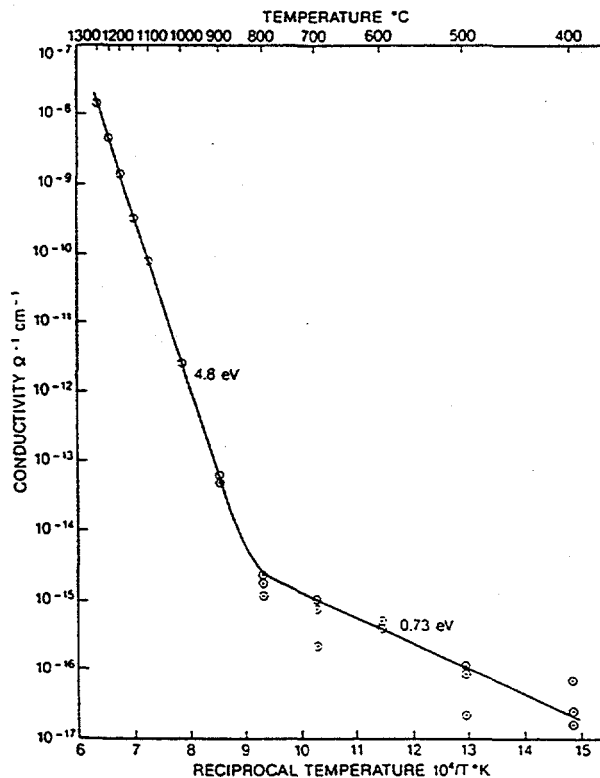
(RIED an Effect of Surface Conductance
and Micro-cracking)

Wilto Kesternich

Electrical Conductivity of Alumina

Temperature dependence > Indication on the conduction mechanism. Intrinsic electronic conduction, extrinsic electron-hole conduction, or ionic conduction ?

Discrepancies: At 600°C the data vary between 10^{-8} and 10^{-14} S/m, i.e. 6 orders of magnitude



Will and Janora

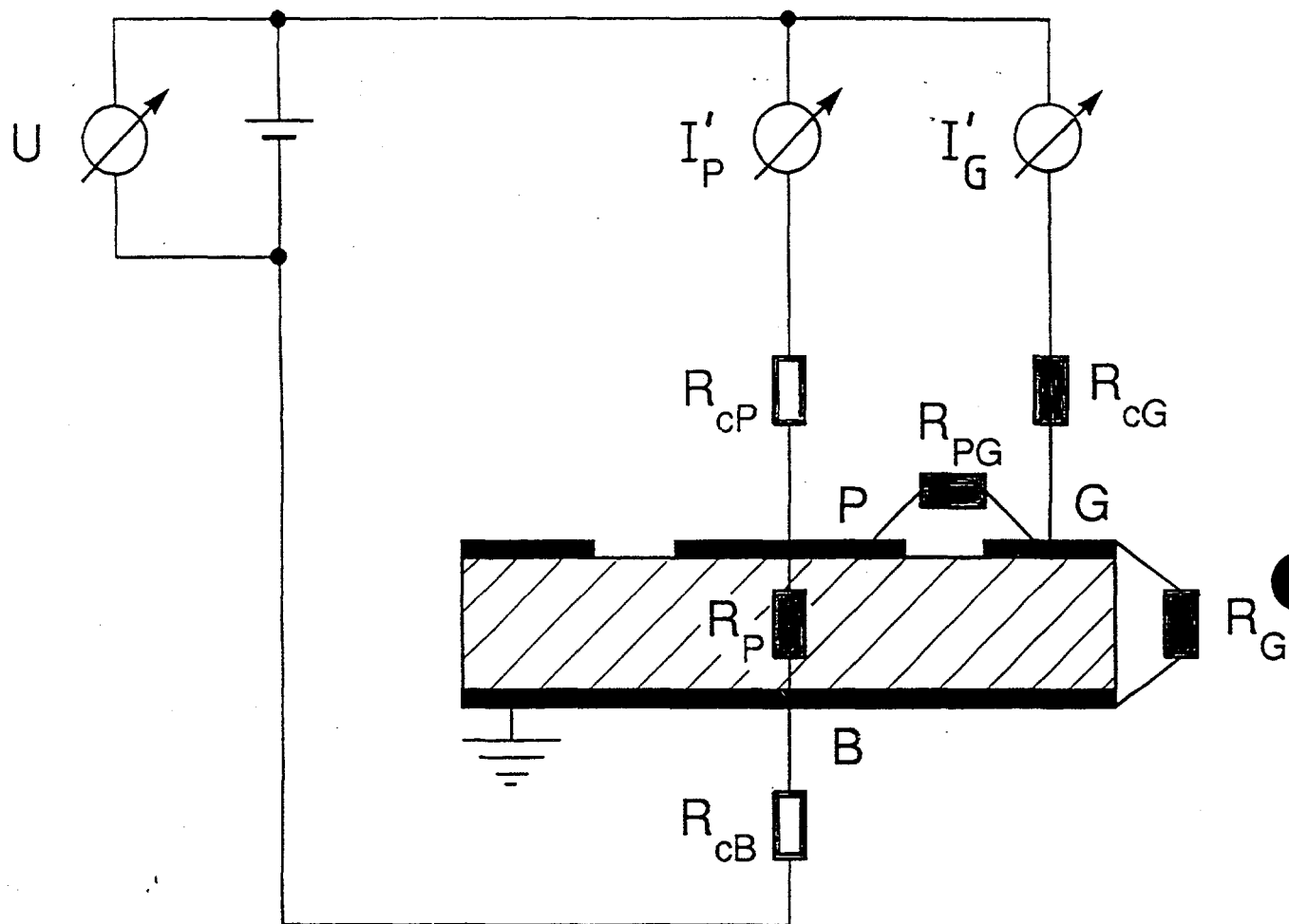
Three-terminal guard technique (TTEG) against surface conduction

Shields against gas conduction at high temperatures

Will and Janora discuss in detail the possible errors in conduction measurement of highly insulating materials

Limits of the TTEG have never been considered

Three-Terminal Electric Guard System (TTEG)



Limit of the three-terminal electric guard (TTEG) technique

$$\sigma = \frac{1}{f} \frac{1}{R_p}$$

$$\sigma_{meas} = \frac{1}{f} \frac{I_p}{U} = \sigma + \Delta\sigma$$

Assumptions:

$$R_{cB}, R_{cP}, R_{cG} \ll R_{PG}, R_G, R_p$$

$$\frac{R_p}{R_{cP}} \gg \frac{R_G}{R_{cG}}$$

Error of the TTEG method

$$\Delta\sigma = \frac{1}{f} \frac{R_{cG}}{R_{PG} \cdot R_G}$$

R_{cP} no influence

For $R_G \gg R_p: \Delta\sigma = 0$

Critical relation

$$R_p \cdot R_{cG} \ll R_{PG} \cdot R_G$$

volume
contact
surface

example:

$$10^{12} \Omega \quad 10 \Omega \quad > 10^7 \Omega$$

Effect of irradiation on the electrical conductivity

(1) RIC Radiation Induced Conductivity

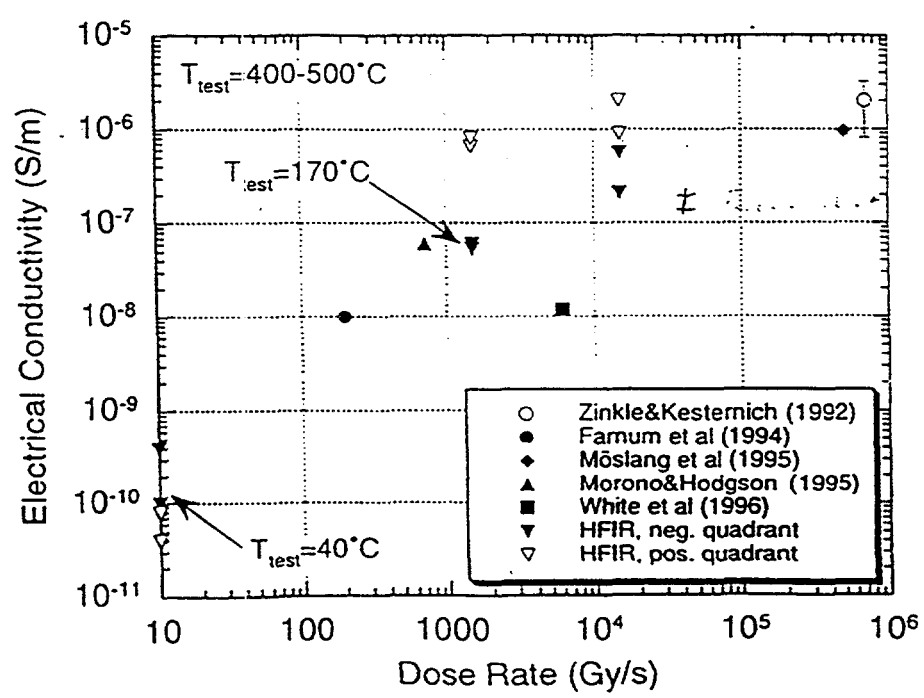
$$\sigma_{RIC} = \sigma_0 + K \cdot R^\delta$$

Ionizing radiation dose rate R

Dose rate exponent $\delta \approx 1$ ($0.5 < \delta < 1.6$)

constant $K_{RT} \approx 10^{-12}$ to $10^{-9} \frac{s}{Gy \Omega m}$

recombination + trapping



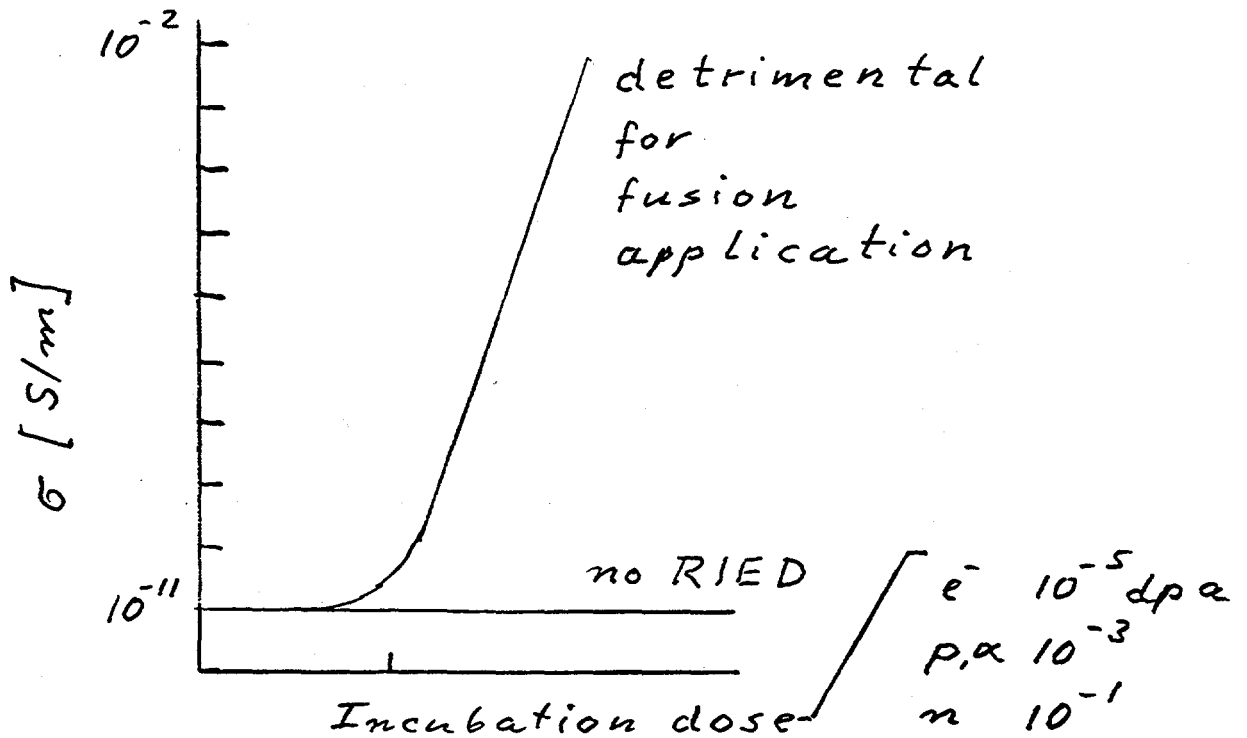
Effect of irradiation on the electrical conductivity

(2) RIED Radiation-Induced Electrical Degradation

{	Irradiation	Oxide Ceramics
	e ⁻ , ion, n	
	Temperature	
	200 to 600°C	
	Electric Field	
	150 to 500 V/mm	

Contradictions

○ electrical conductivity



○ microstructure

precipitates = colloids
 precipitates = gamma-alumina
 dislocations
 grain boundaries

no microstructural changes

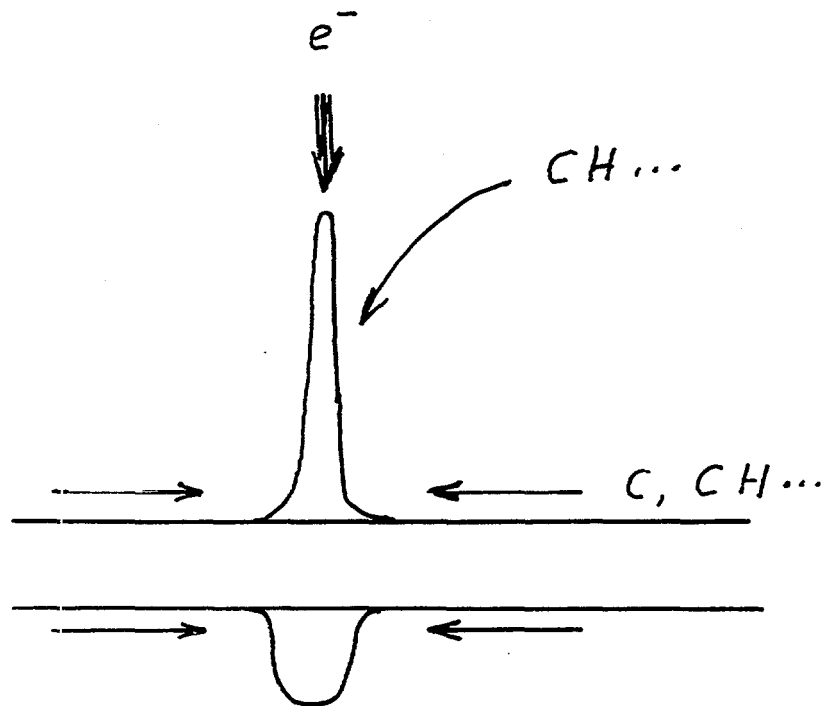
7

Experimental Difficulties in RIED experiments

(A) Surface leakage currents

= Enhancement of surface conductivity by irradiation

The problem may be explained by the experimental conditions observed in transmission electron microscopy.



Solution: Measurement of R_{PG} , R_G and R_{cG}



(B) Leakage currents through the specimen

= Microcracks due to differential thermal expansion of specimen and specimen holder

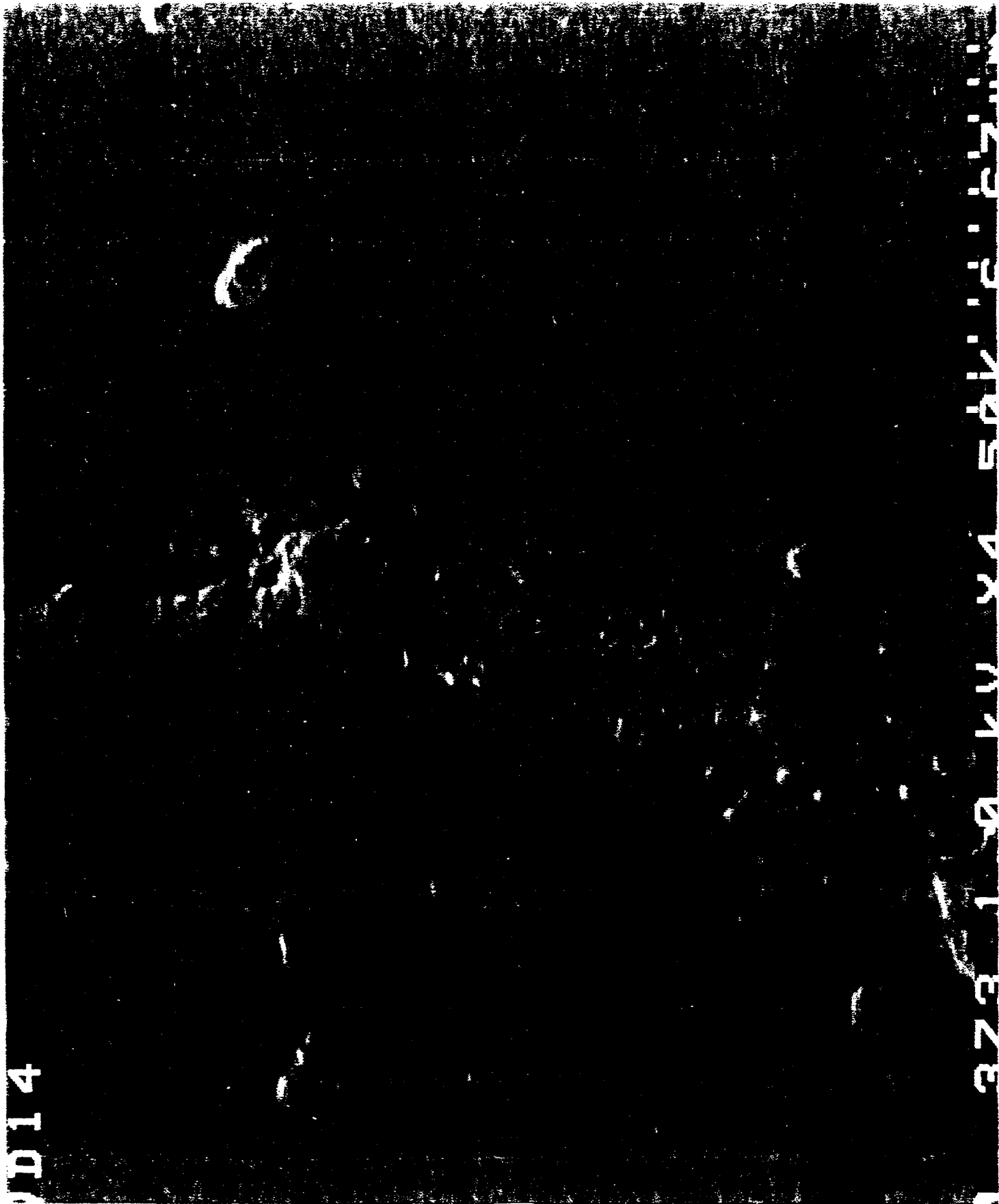
(= Diffusion from metal contact into the grain boundaries)

Brazing of specimen to the holder is mandatory in most accelerator experiments for allowing sufficient heat transfer.

There might be other reasons for crack formation, e.g. specimen grinding during specimen preparation.

Solution: Polishing of specimen surface and inspection by SEM

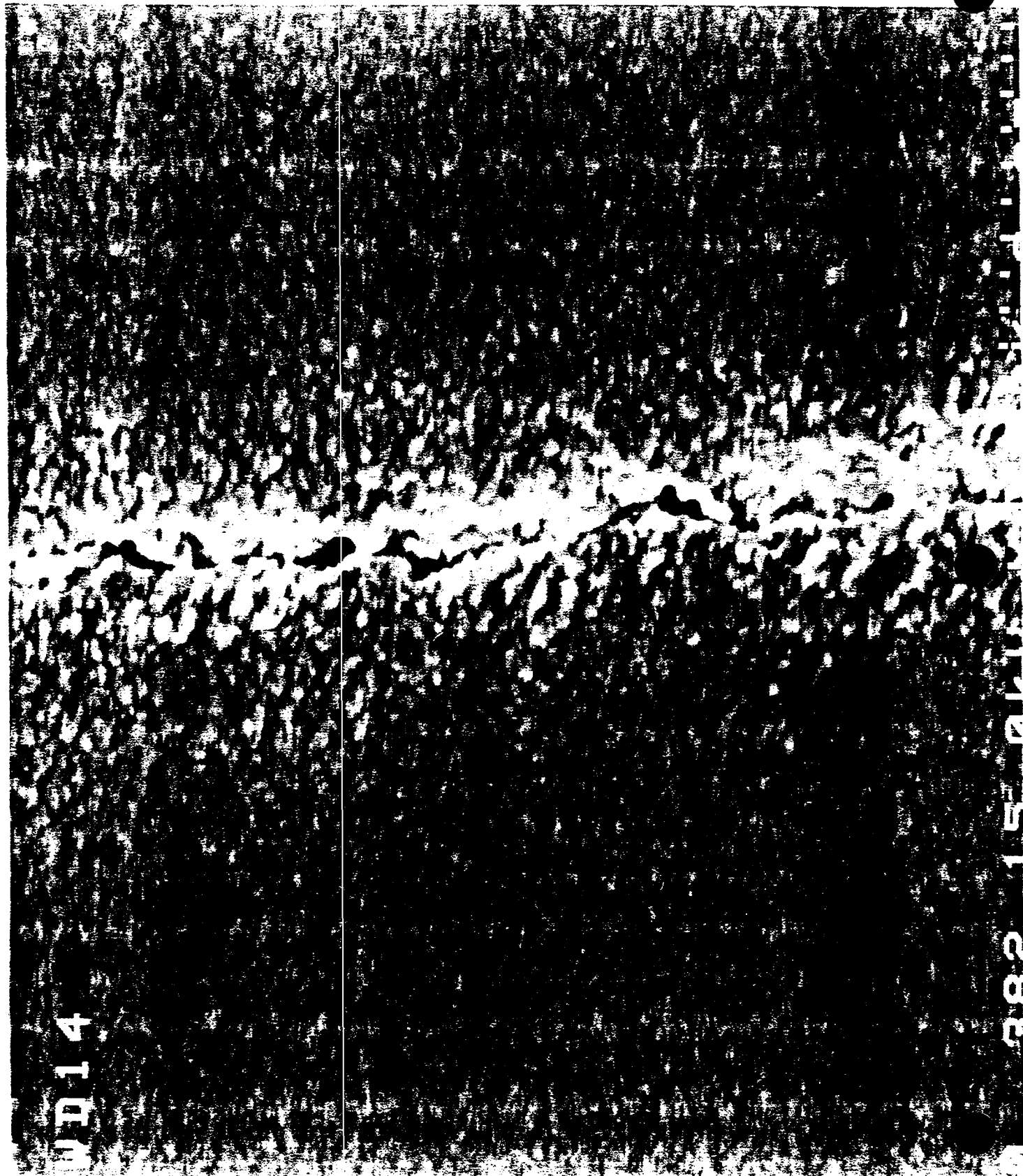
Microcrack in sapphire covered with 2 μ m Au



JD14

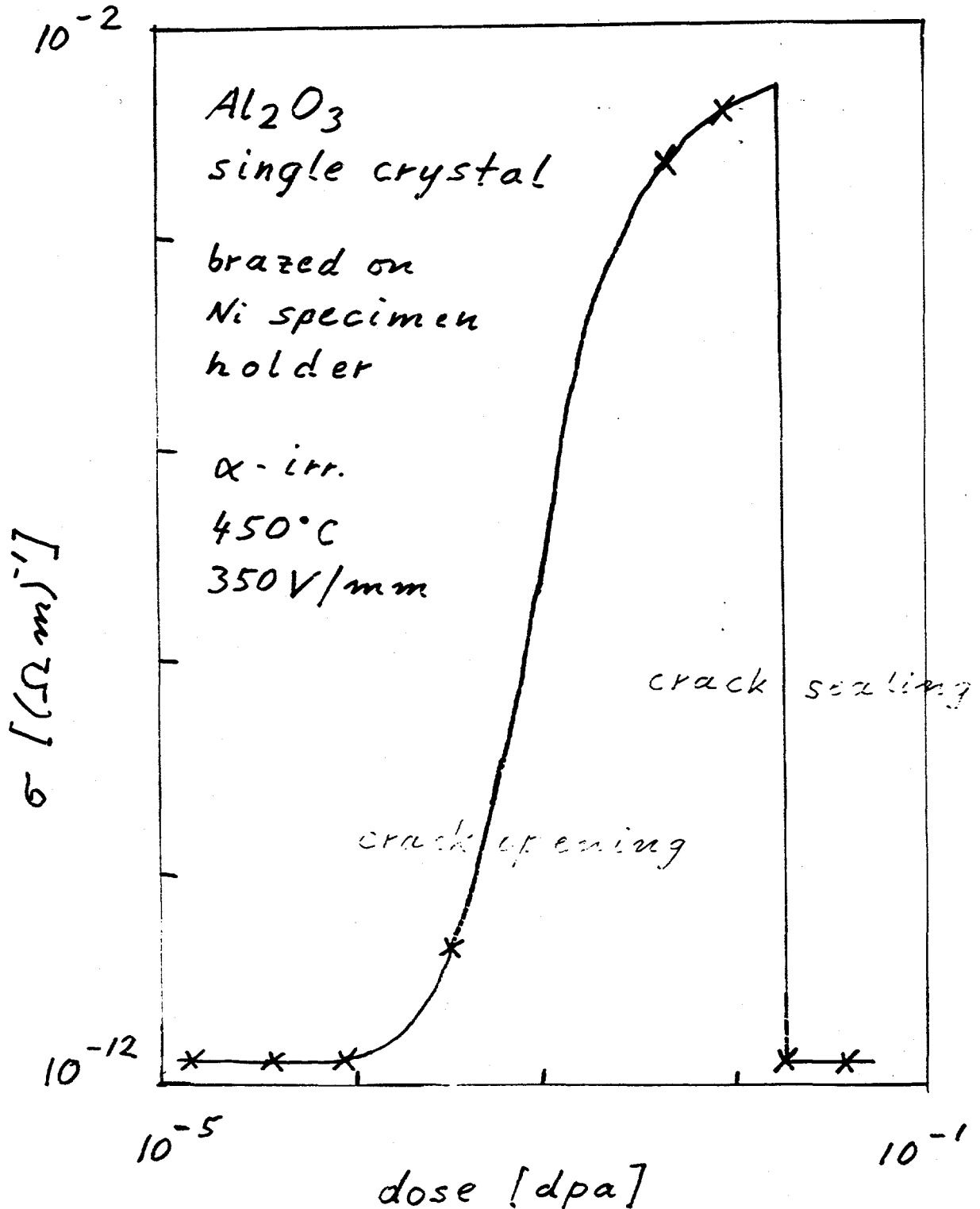
373 1 0 KW YA 54K 12 65 11

post-irradiation



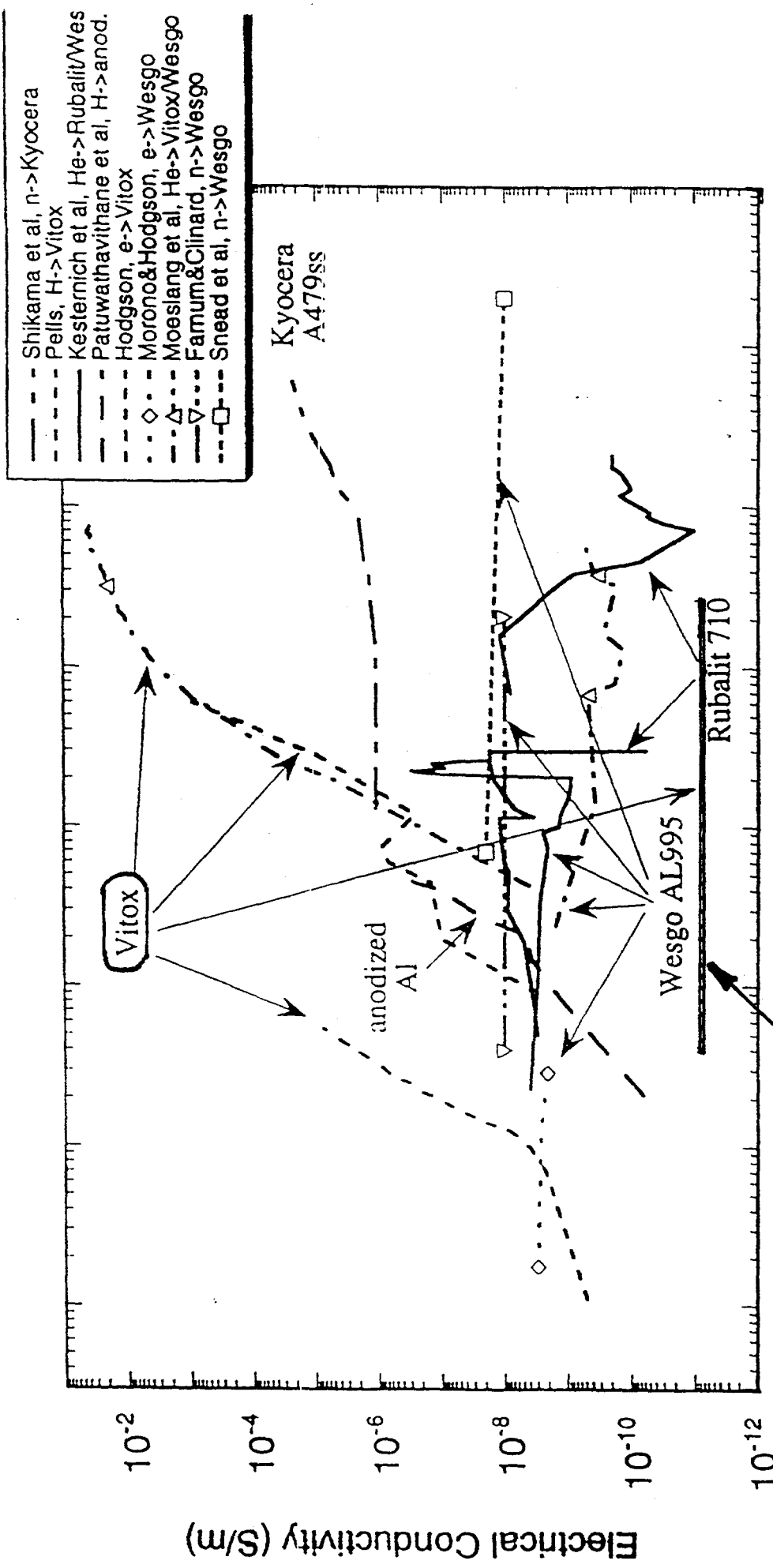
Microcracks - σ increase by 10^3

Microcracks do not necessarily lead to conductivity increase



post-irradiation conductivity $< 10^{15} \Omega^{-1} m^{-1}$

SEM - Restructuring of the surface by α -beam



present result

Dose (dpa) compilation from Einkle & Kinoshita

Conclusions

Electrical conductivity measurements in highly insulating materials: Limitations of the guard technique have previously been neglected. They need to be taken into consideration (also in non-irradiation experiments). In particular surface and contact resistances need to be measured. A formula is given for calculating the error.

Microcracks can be a second reason of error in bulk conductivity measurements. Inspection for microcracks by SEM on pre-polished specimens is recommended (sensitivity ~0.03 μm crack width).

RIC: Data of different experimentors show large scatter. Experimental conditions need to be standardized.

RIED: In search for RIED, experiments by several research groups have been performed with standardized experimental conditions as defined at the IEA workshop in Stresa (control of R_G , R_{PG} , and R_{CG}). None of these experiments did confirm the existence of permanent conductivity increases.

Unless the earlier RIED results can be reconfirmed in repeating those experiments under the now standardized conditions, it has to be assumed that RIED as a bulk effect is not existing.

Surface RIED: Electrical leakage currents along the outer specimen surface as well as through microcracks in the specimen interior can be radiation-enhanced by many orders of magnitude. Thus RIED as an effect of radiation-enhanced surface conductivity needs to be further investigated, and the impact of "surface RIED" on ceramic fusion reactor components needs to be studied. In these studies outer surfaces as well as cracks within the components have to be taken into consideration.



Electrical conductivity measurements on VITOX, DERANOX and WESGO alumina during and after alpha-particle irradiation

A. Möslang
Institut für Materialforschung I

Alumina samples with typical dimensions of $8 \times 10 \times 0.4 \text{ mm}^3$ have been cut from plates made of polycrystalline VITOX (99.9%), CERANOX (99.9%) and WESGO (99.2%). These specimens were equipped by vacuum evaporation of about $1 \text{ }\mu\text{m}$ Au with central, guard and back electrodes which themselves were solid state bonded to leads at the front side and to a temperature controlled metal substrate (hollow fatigue specimen) at the back side. All irradiations were performed in high vacuum using a high energy α -particle beam with an applied DC electric field. The test conditions and the experimental set up are given in table 1 and figs. 1-2, respectively. It should be emphasized that due to the high range (1.35 mm in Fe) and the small range straggling, the 104 MeV α -particles are stopped in the faraday cup behind the substrate. That is, they completely penetrate the alumina layer. While the in-beam electrical conductivity σ was recorded continuously during irradiation, the out-of-beam electrical conductivity σ_0 was measured always 3 minutes after turning off the α -particle beam. During these beam off times the resistance between central and guard electrode as well as between guard electrode and substrate was also recorded. Table 2 summarizes key results of the electrical conductivity measurements.

1. Vitox :

- In the high purity Vitox alumina σ and σ_0 show at both irradiation temperatures a huge increase (fig.3) of several orders of magnitude. This degradation has an ohmic behavior, only a small temperature dependency (fig. 6) and is stable against thermal annealing treatments.
- Optical microscopy and SEM investigations have clearly shown, that both ceramic samples cracked completely during the experiments. That is, a few cracks propagated directly across the ceramic from the back side to the center electrode. In both cases, the huge electrical conductivity increase can be explained easily by the formation of a surface layer along the cracks leading to low resistance pathways between the electrodes. The cracks could be initiated before irradiation by thermal cycling during the $1/T$ -measurements of σ_0 . Integral failure by subcritical crack growth caused by a misfit of the thermal elongation between the ceramic and a metal substrate is well known in thermal cycling experiments.
- After electron irradiation, a significant increase of the dislocation density has been reported in crystalline Al_2O_3 . From the polycrystalline VITOX specimen irradiated at $350 \text{ }^\circ\text{C}$ we have prepared two TEM samples (figs. 9 and 10). Both samples show a very low dislocation density very similar to the unirradiated ones. Although other elements were not detected in EDAX analyses (fig. 11), a re-deposition of sputtered Al on the TEM specimen surface could also explain the very fine,

irregular background on the TEM micrographs of irradiated VITOX. Small γ -alumina phases were not found in the diffraction analyses. That is, up to now we were not able to detect clearly irradiation induced point defects. May be, they are too small (sub nm) after 0.08 dpa light ion irradiation.

2. Deranox999:

- As the dpa dependency in fig. 5 shows, the out-of beam conductivity σ_0 increased at 400 °C after some fluctuations during the early stage of irradiation by about one order of magnitude. During the 250 °C irradiation, however, σ_0 could not be measured because it remained below the resolution limit of about $2 \times 10^{-12} (\Omega m)^{-1}$.
- The temperature dependency of σ_0 is given in fig.7 before and after irradiation for the specimen irradiated at 400 °C. The moderate irradiation induced increase of the electrical conductivity is confirmed (open symbols). As expected, the electrical conductivity at a given ionizing rate (closed symbols) is practically independent of the temperature at low temperatures and follows closely the thermal induced conductivity at high temperatures. However, it should be emphasized, that the indicated ionizing dose rates has been calculated directly from the energy loss of the α -particles inside the ceramic (heat production). The related heat deposition and consequently the actual Gy-rate is considered to be much smaller because the majority of the x- and γ -rays can escape from the ceramic during the light ion irradiations.
- The in-beam conductivity σ decreases as expected by at least one order of magnitude during the early stage of irradiation at all temperatures investigated (fig. 5). After the saturation level has been reached, σ -variations can be directly attributed to beam current fluctuations.
- Both, Vitox and DERANOX999 are fabricated by „Morgan Matroc“ and have the same small grain size (fig.8) and low dislocation density. The 10 times higher silicon content of Ceranox999 is the only obvious difference (table 3).

3. Wesgo:

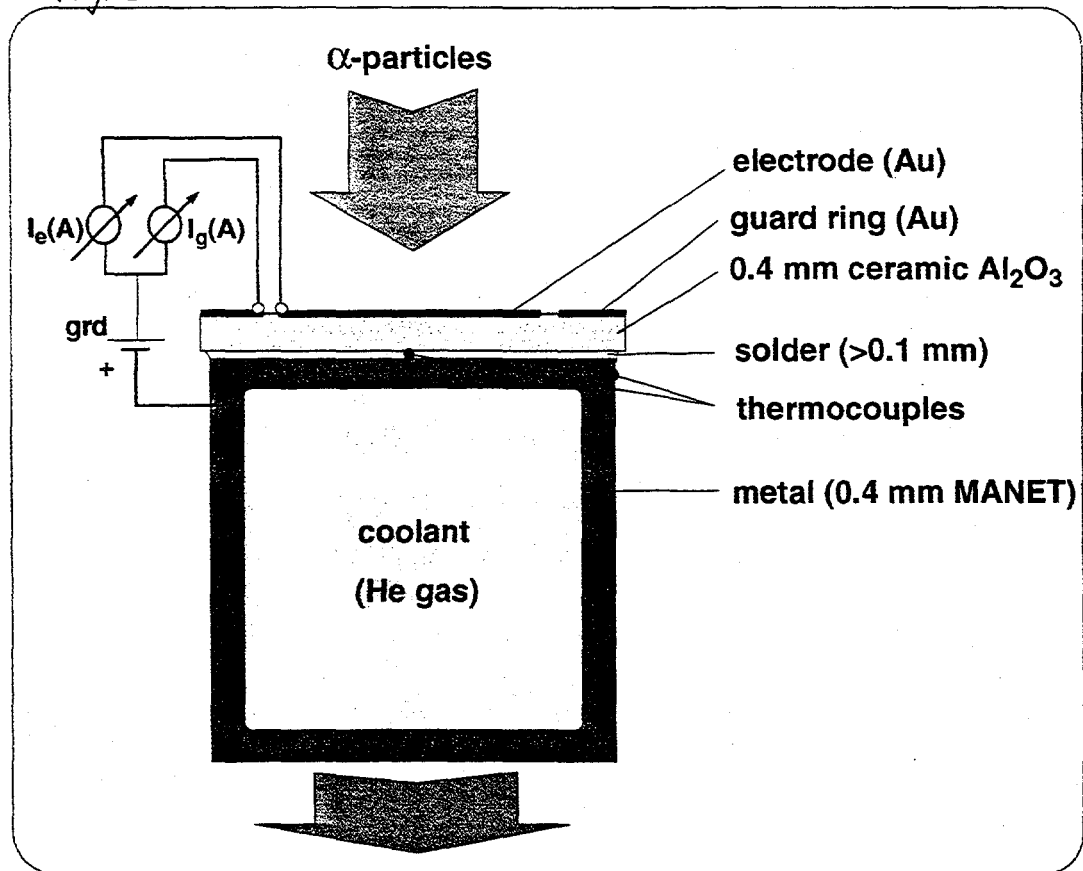
- Immediately after the irradiation has been started, the initial σ and σ_0 values decrease. Although a moderate re-increase was observed during further irradiation, σ_0 remained below the initial value of the unirradiated specimen.
- In contrast to Vitox and Deranox999, Wesgo has a much larger grain size (fig. 8), it shows a moderate porosity and a much higher amount of impurities like Ca, Fe, Mg, Si and Ti (table 3).

table 1

Test Conditions

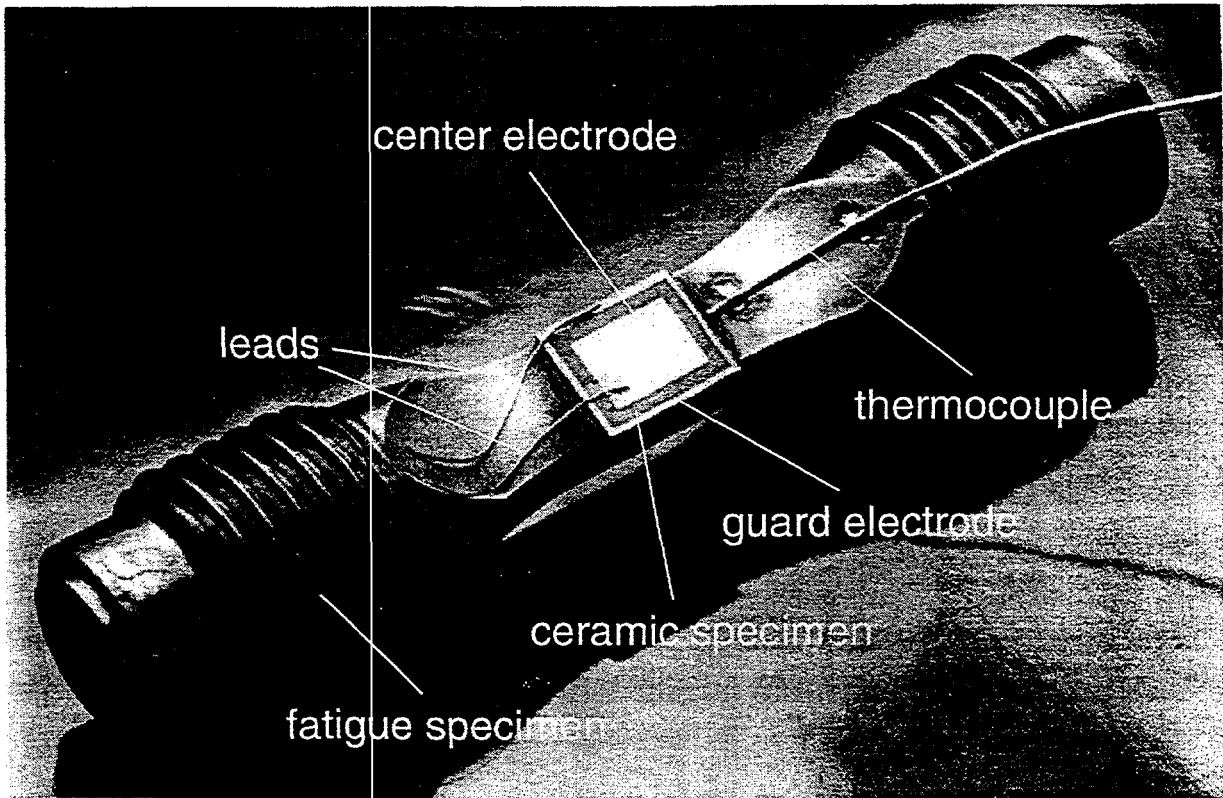
Ceramics	Al ₂ O ₃ 0.40 mm
E-field (DC)	100V/mm
α-particle energy	94-104 MeV
Displacement rate (total)	(3.7-4.9)x10 ⁻⁷ dpa/s
Ionization rate	(2.8-3.7)x10 ⁶ Gy/s
Irradiation temperature	250-550 °C
Beam spot	Ø = 4 mm; A = 12.6 mm ²
α-particle beam density	(1.3-1.7) μA/12.6 mm ²
Vacuum (total pressure)	(5±4)x10 ⁻⁶ mbar

fig. 1



Electrical conductivity measurements on Ceramics
at the Karlsruhe Cyclotron Facility

fig. 2

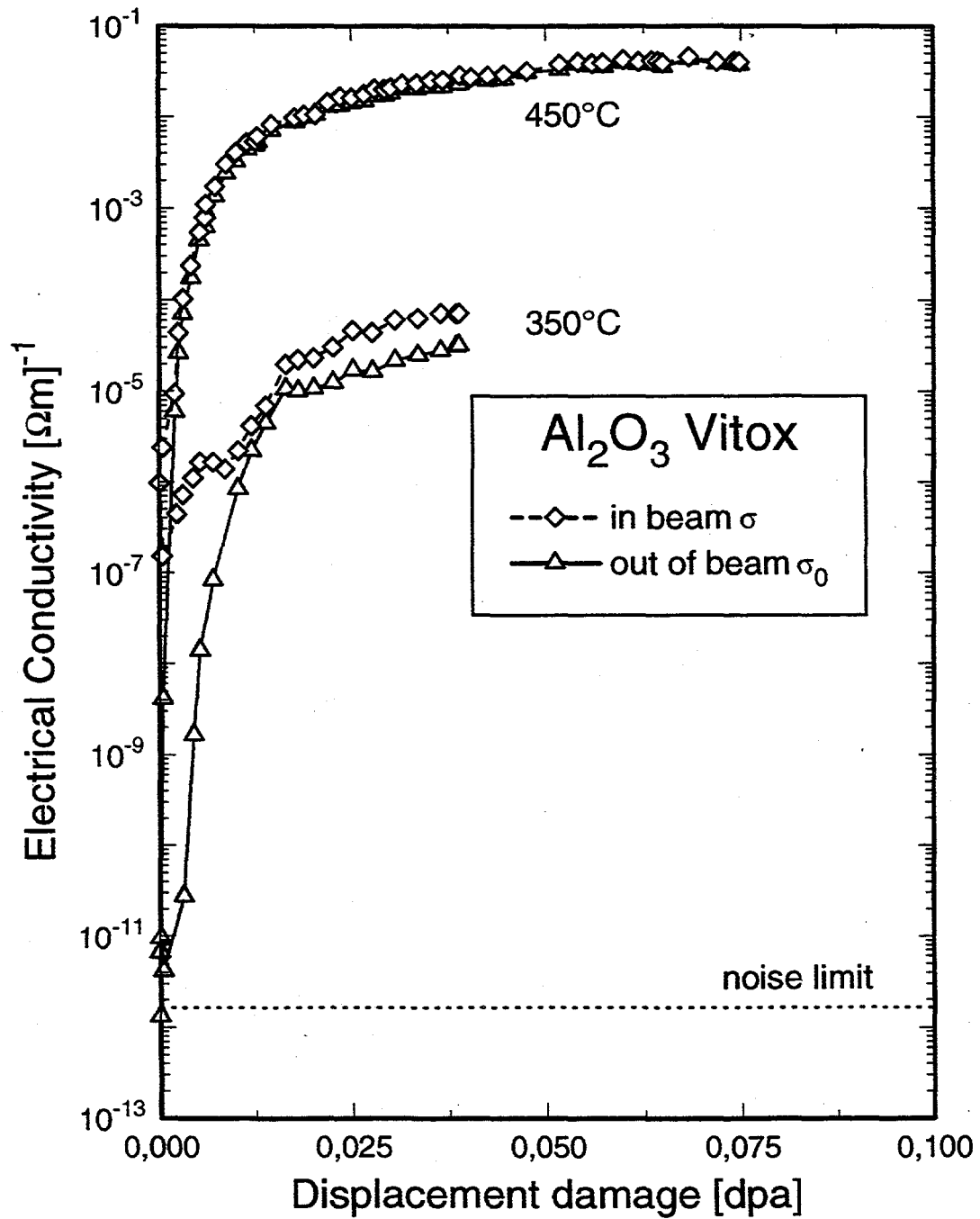


Test matrix and main results

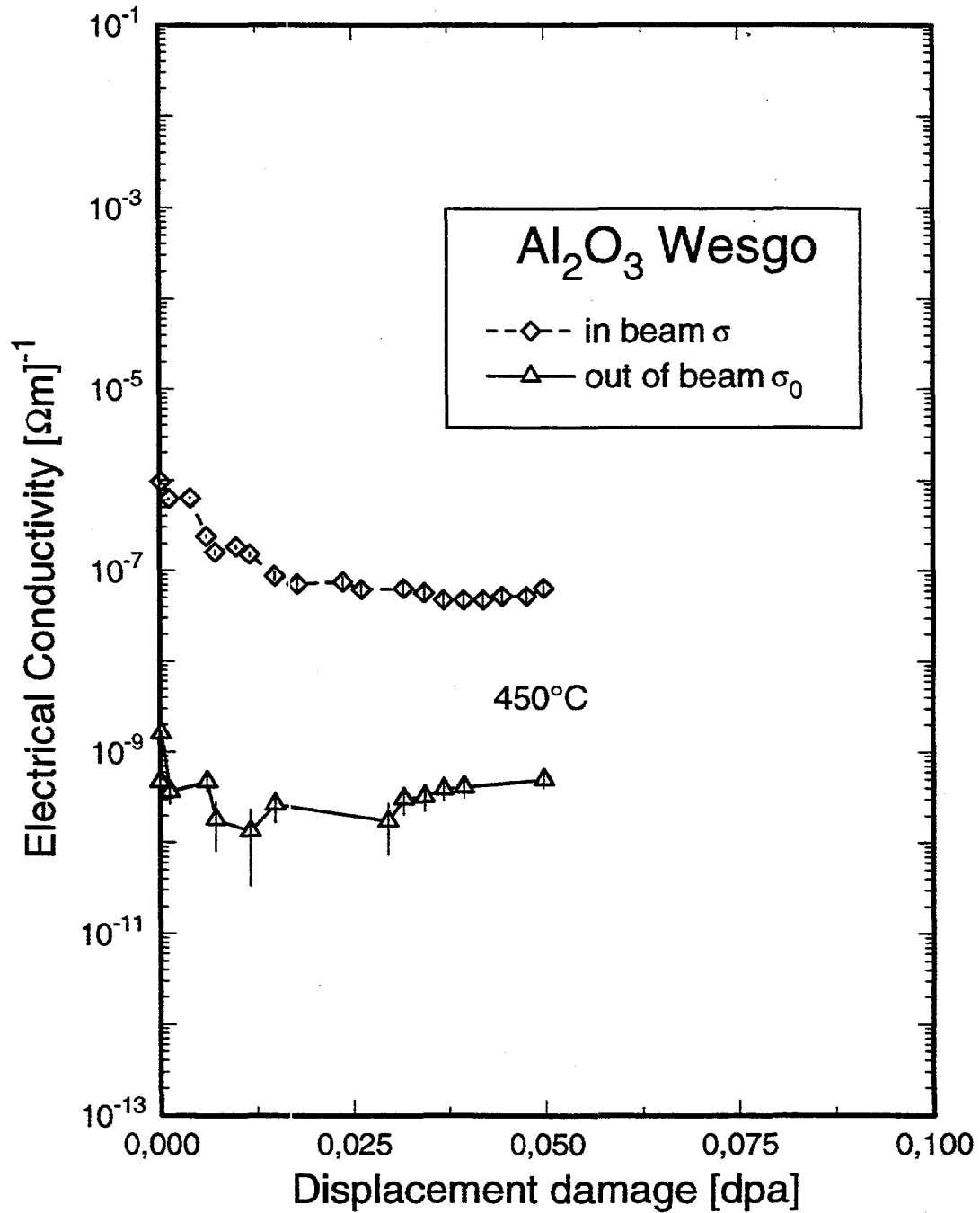
table 2

Ceramic	T_{irr} (°C)	DPA dose	electrical degradation	Structural integrity
Vitox	350	0.04	significant	both specimens cracked during irradiation experiment
	450	0.08	significant	
Deranox999	250	0.05	minor at all temperatures irradiated	no visible cracks during all irradiation experiments
	400	0.035		
	550	<0.03		
Wesgo	450	0.05	no	no visible cracks during irradiation experiment

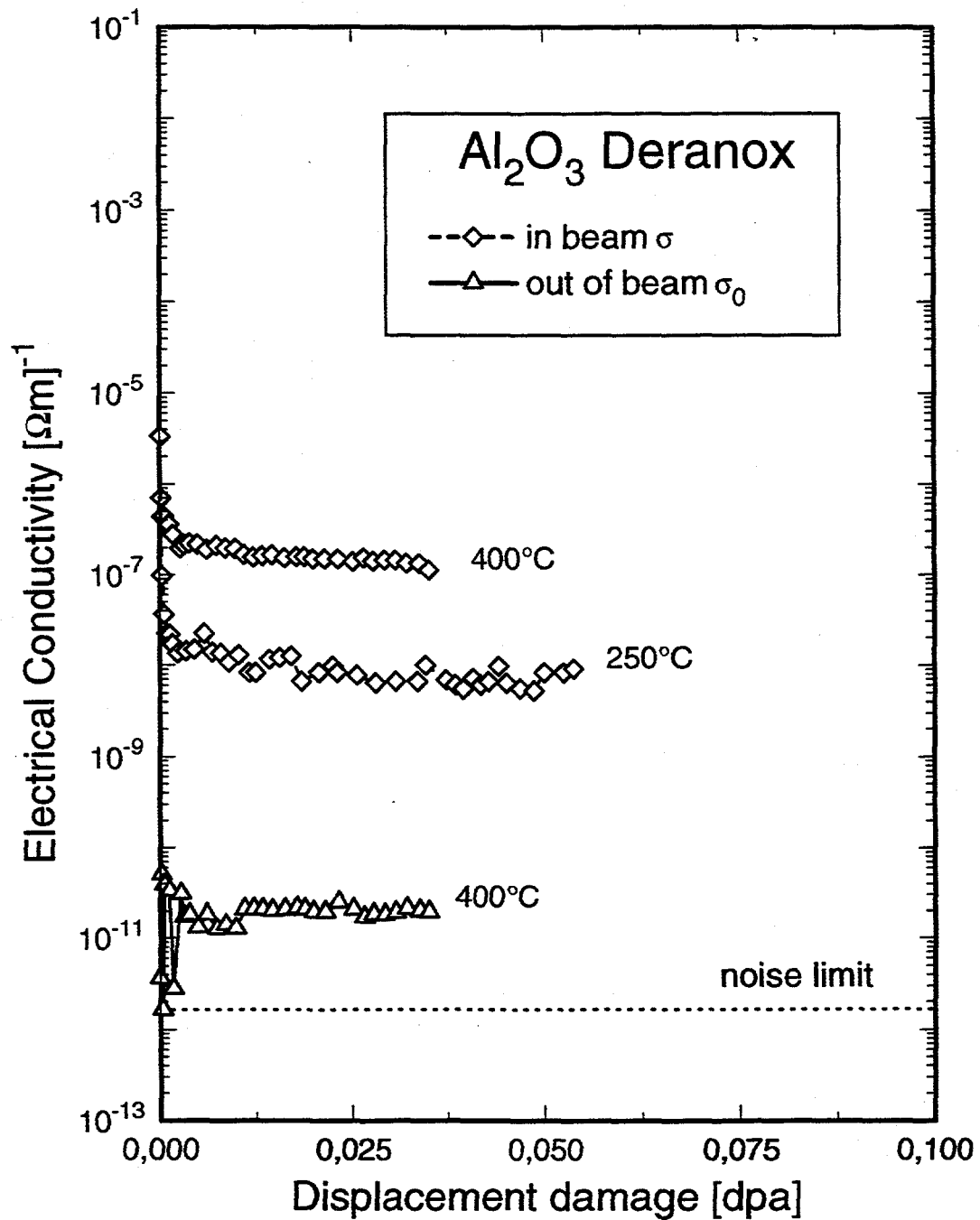
Displacement Damage Dependency



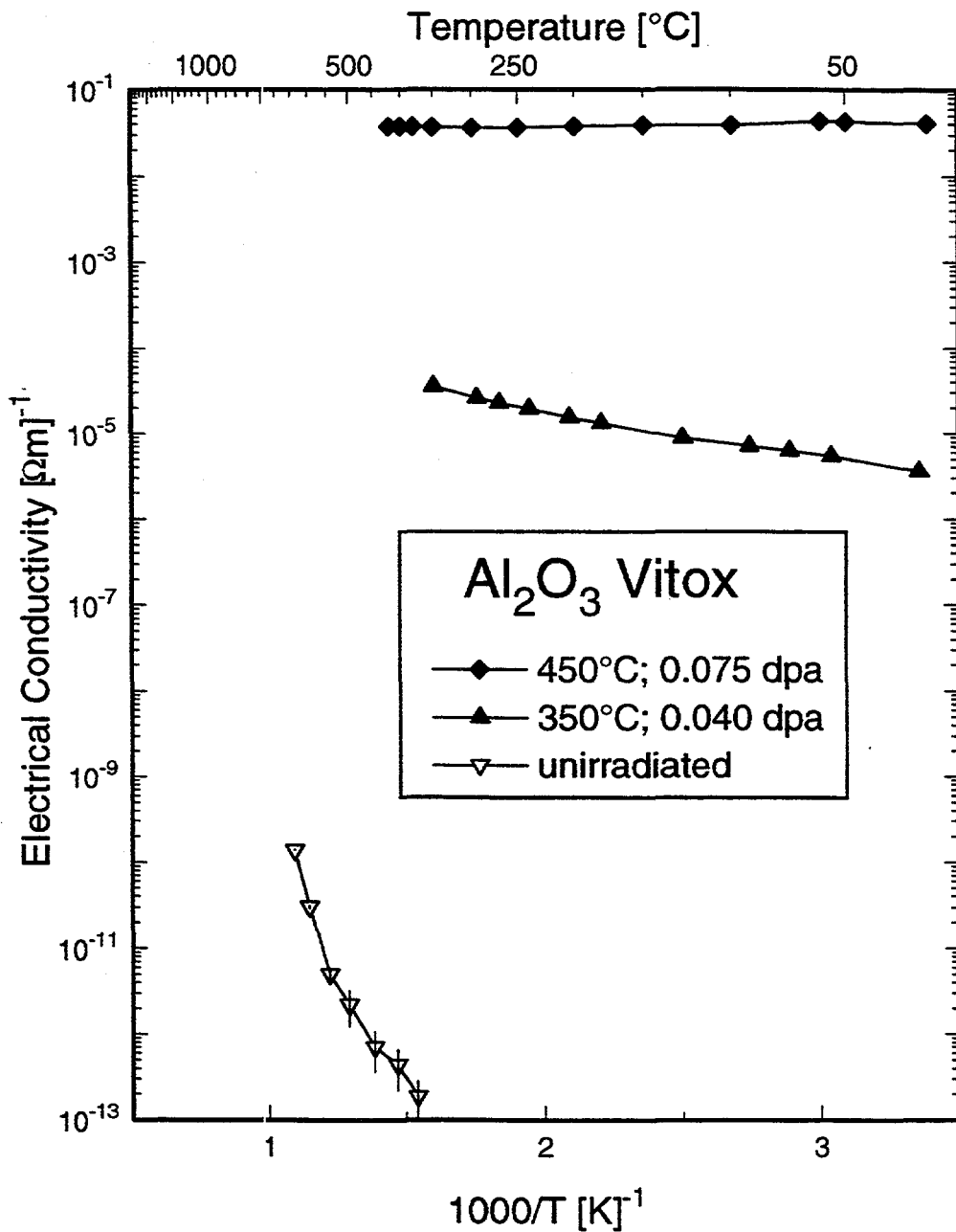
Displacement Damage Dependency



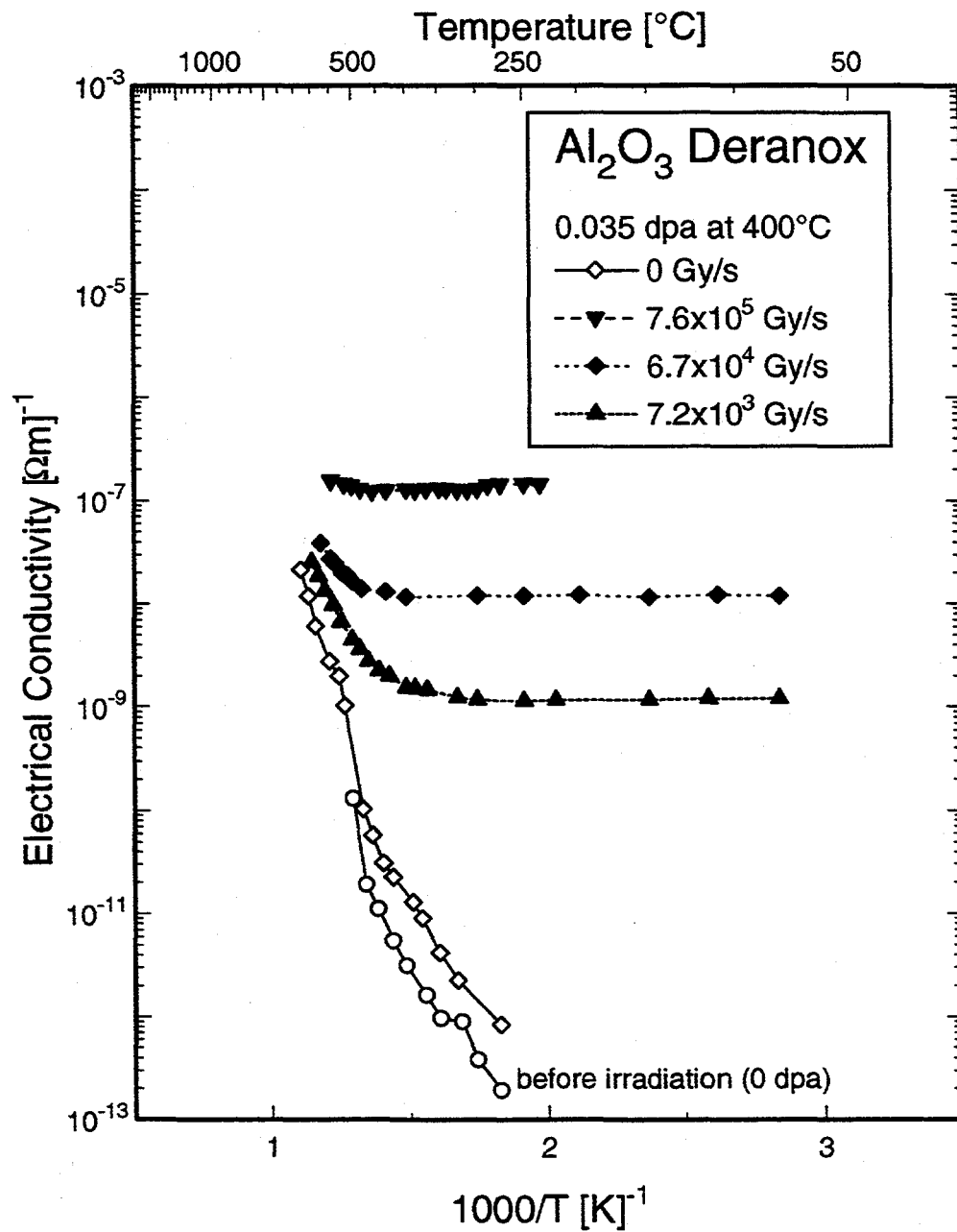
Displacement Damage Dependency



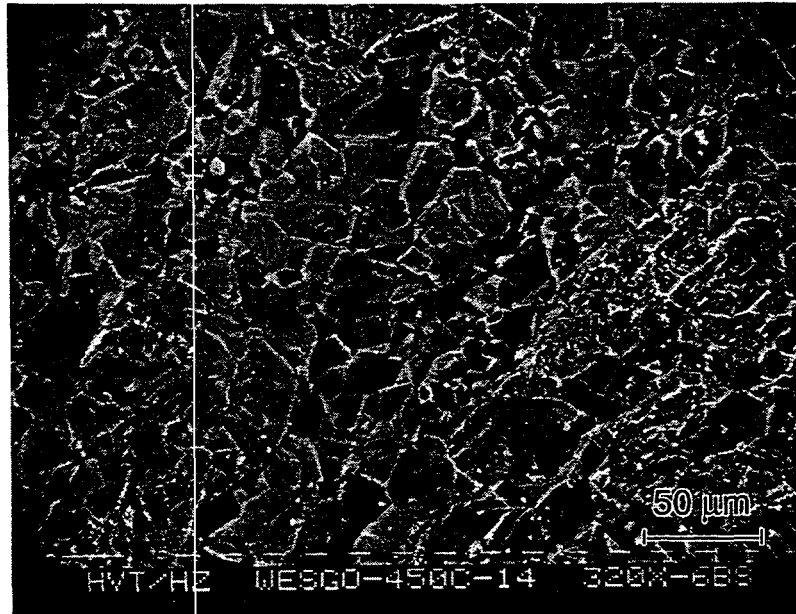
Temperature Dependency



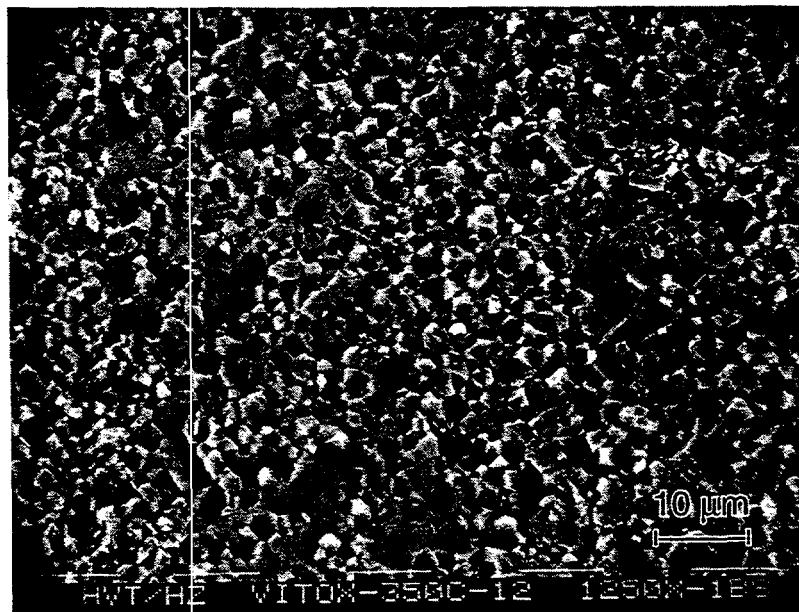
Temperature Dependency



Al_2O_3 irradiated with 104 MeV α -particles
- grain structure -

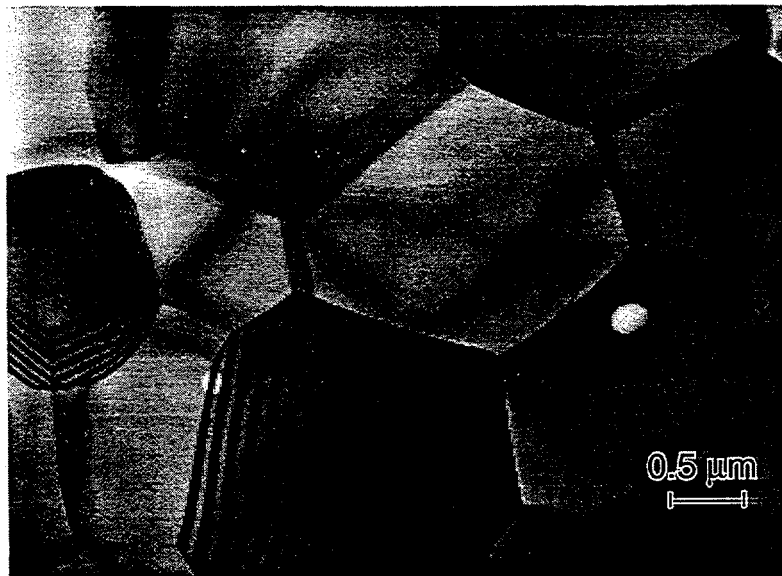


Wesgo
450 °C
0.014 dpa



VITOX
350 °C
0.011 dpa

TEM-micrographs of unirradiated Al_2O_3
and irradiated with 104 MeV α -particles

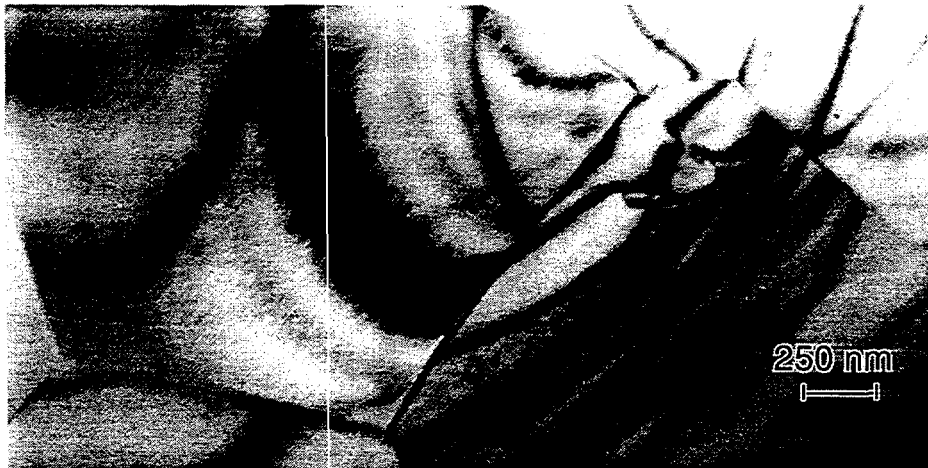


VITOX
unirradiated



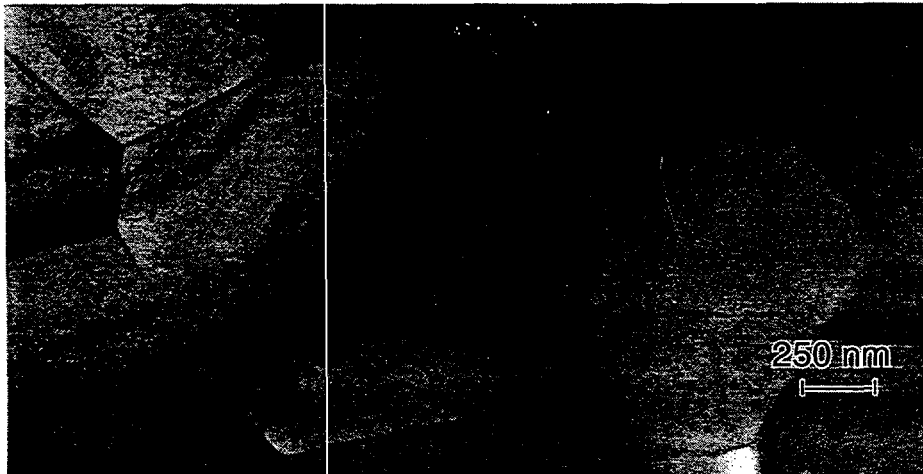
VITOX
350 °C
0.011 dpa

TEM-micrographs of unirradiated Al_2O_3
and irradiated with 104 MeV α -particles



VITOX
unirradiated

specimen 12-3
40 000 x



VITOX
350 °C
0.011 dpa

specimen 12-1
40 000 x



VITOX
350 °C
0.011 dpa

specimen 12-5
40 000 x

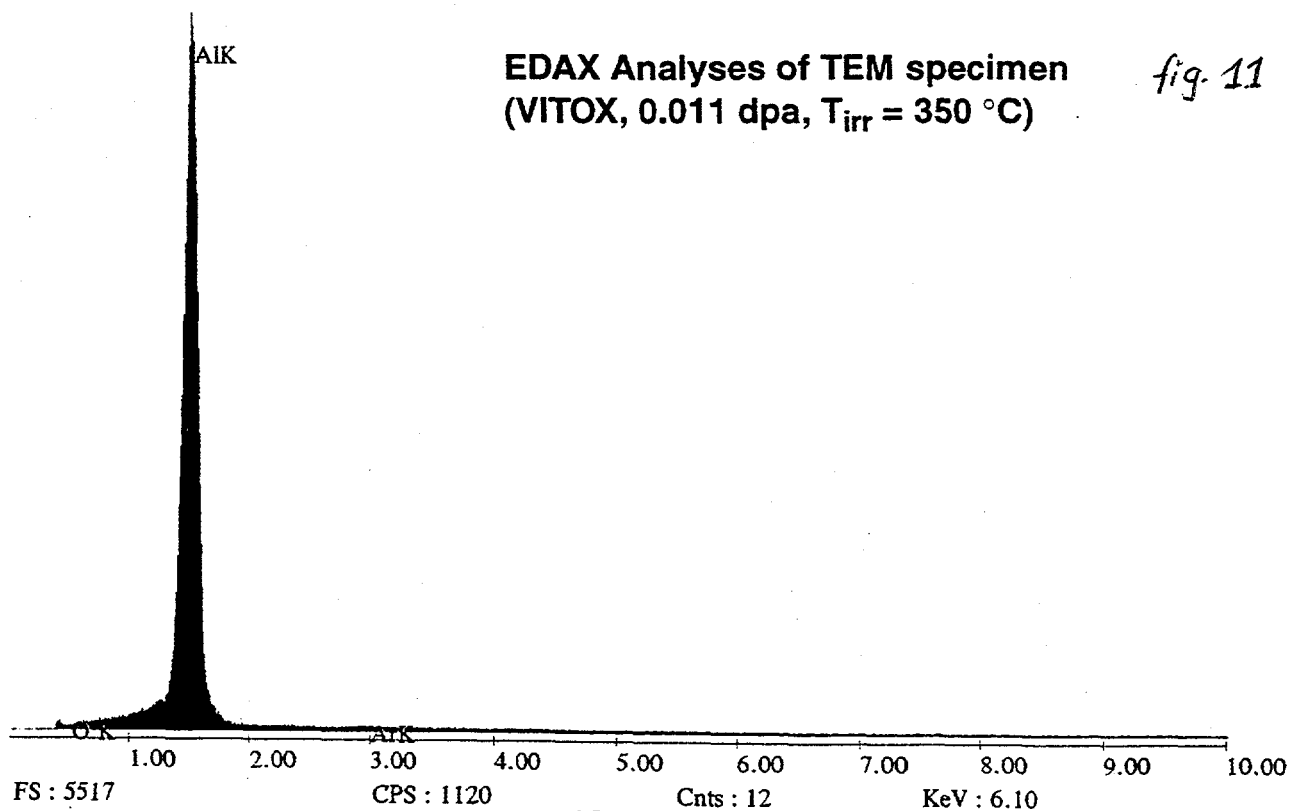
fig. 10

Al₂O₃ - Chemical Analyses

table 3

Element	Deranox (wt-%)	Vitox (wt-%)	Wesgo (wt-%)	Konz. Wesgo Konz. Vitox
B	<0.0005 0.017±0.007			
Ba	<0.0002	<0.0002	<0.0002	
Ca	<0.001	<0.001	0.0424±0.0004	42.2
Co	<0.0005	<0.0005	<0.0005	
Cr	<0.001	<0.001	<0.001	
Fe	<0.006	<0.005	0.034±0.001	6.8
K	<0.002	<0.002	<0.002	
Li	<0.002			
Mg	0.030±0.001	0.030±0.001	0.249±0.005	8.3
Na	<0.005	<0.01	<0.021±0.0005	2.1
Ni	<0.001	<0.002	<0.002	
Si	0.069±0.009	0.006±0.003	0.137±0.006	22.8
Ti	<0.0005	0.0027±0.0003	0.0100±0.0005	3.7
Zr	<0.001	0.0038±0.0004	0.0070±0.0004	1.8

Live Time : 300.0





In-Situ Measurement of the Electrical Conductivity of Aluminum Oxide in HFIR: Summary of the TRIST-ER1 Experiment

S.J. Zinkle¹, T. Shikama², K. Shiiyama³, E.H. Farnum⁴, K. Scarborough⁴, D.P. White^{1,5},
L.L. Snead¹, W.S. Eatherly¹, D.G. Raby¹, A.L. Qualls¹, D.W. Heatherly¹, R.G. Sitterson¹,
R.L. Wallace¹, M. Narui² and T. Sagawa⁶

¹Oak Ridge National Laboratory, Oak Ridge, TN 37831 USA

²Oarai Branch, IMR, Tohoku University, Ibarakiken, Japan

³Kyushu University, Fukuoka, Japan

⁴Los Alamos National Laboratory, Los Alamos, NM USA

⁵Merrimack College, North Andover, MA 01845 USA

⁶Japan Atomic Energy Research Institute, Ibarakiken, Japan

A collaborative DOE/Monbuscho irradiation experiment has been completed which measured the in-situ electrical resistivity of 12 different grades of aluminum oxide during neutron irradiation at 450-500°C. The main objective of the Temperature Regulated In-Situ Test - Electrical Resistivity (TRIST-ER1) experiment was to determine if radiation induced electrical degradation (RIED) occurred in several different grades of aluminum oxide during irradiation in a fusion-relevant irradiation environment (appropriate ionizing/displacive radiation levels) up to relatively high doses.

The experiments were performed in a Removable Beryllium position of the High Flux Isotope Reactor (HFIR) at Oak Ridge National Laboratory. The specimen matrix included 12 different grades of polycrystal and single crystal alumina in order to determine whether the threshold dose for initiation of RIED depended on specimen purity. Two of the single crystal specimens and one of the polycrystal specimens were irradiated without dc bias and served as control specimens for the RIED experiment. The alumina specimens were irradiated as disks with dimensions of 8.5 mm diameter by 0.75 mm thick. The TRIST-ER1 experiment was performed following the guidelines outlined in ASTM Standard Test Method for DC Resistance or Conductance of Insulating Materials (ASTM D257-91), and in accordance with the stringent experimental technique conditions adopted by the participants to an IEA ceramic insulator workshop held in Stresa, Italy in September 1993. In particular, the electrical contacts were brazed onto the specimen surface so that contact resistances were negligible, and the leakage resistances between the back (high voltage) and low-voltage guard and center electrodes was measured periodically throughout the irradiation. The specimen temperatures were monitored continuously by two thermocouples located in each subcapsule. All of the subcapsules were sealed to minimize the amount of surface contamination buildup during irradiation.

A dc potential of 150 V was continuously supplied to the brazed base surface of 12 of the specimens (except for brief periods when electrical measurements were taken) by two HP 6035A power supplies, producing an electric field of 200 V/mm in the specimens. As described elsewhere [1,2], several different types of electrical measurements were performed on the specimens in order to differentiate between bulk conductivities and surface conductances. These tests included frequent measurement of the specimen and guard ring currents at 100 V and periodic measurement of the ohmic nature of the electrical currents in the alumina samples and coaxial MI cables over a typical potential range of +100 V to -100V. Diagnostic measurements were also performed periodically which allowed the surface resistance and cable insulation conductivities to be measured. For each electrical measurement, an electrification time of 10 to 30 seconds was typically used from the time the specimen was switched to the power supply until an electrical current was measured in order to eliminate signal noise associated with the cable and specimen capacitance. Data obtained during full-power reactor irradiation were comparable for electrification times ranging from 5 to 180 s.

The irradiation was accomplished over a time period of about 3 1/2 months, and involved three irradiation cycles (each ~26 days long) of the HFIR reactor operating at 85 MW. The electrical conductivity of the specimens was measured before, during and following each of the three HFIR irradiation cycles. The specimen temperatures ranged from 30 to 50°C when the reactor was off, and between 50 and 170°C (depending on the control gas mixture) when the reactor was at 10% power. The irradiation temperature was maintained at 440 to 500°C for all 15 specimens during full-power irradiation. The full-power reactor ionizing dose rate was 10 to 16 kGy/s and the average displacement damage rate was ~ 2.4 to 4.3×10^{-7} dpa/s, depending on specimen position.

The current vs. applied voltage data generated from the HFIR TRIST-ER1 experiment were analyzed to determine the electrical conductivity of the 15 alumina specimens and the MgO-insulated electrical cables as a function of irradiation dose. With the exception of the 0.05%Cr-doped sapphire (ruby) specimen, the electrical conductivity of the alumina specimens remained at the expected radiation induced conductivity (RIC) level of $\leq 10^{-6}$ S/m during full-power reactor irradiation (10-16 kGy/s) at 450-500°C up to a maximum dose of ~ 3 dpa. It is particularly noteworthy that RIED was not observed in the sapphire specimens, which were found to have an incubation dose of < 0.0001 dpa for significant RIED ($\sigma_e \geq 10^{-5}$ S/m) in electron irradiation studies. The ruby specimen showed a rapid initial increase in conductivity to $\sim 2 \times 10^{-4}$ S/m after ~ 0.1 dpa, followed by a gradual decrease to $< 1 \times 10^{-6}$ S/m after 2 dpa. Nonohmic electrical behavior was observed in all of the specimens, and was attributed to preferential attraction of ionized electrons in the capsule gas to the unshielded low-side bare electrical leads emanating from the subcapsules. The electrical conductivity was determined from the slope of the specimen current vs. voltage curve at negative voltages, where the gas ionization effect was minimized. Dielectric breakdown tests performed on unirradiated mineral-insulated coaxial cables identical to those used in the HFIR TRIST-ER1 experiment indicate that the electrical shorting which occurred in many of the high voltage coaxial cables during the 3-month irradiation is attributable to thermal dielectric breakdown in the glass seals at the end of the cables, as opposed to an RIED effect.

Previous electron irradiation studies of the RIED phenomenon indicated that RIED would be most pronounced in high-purity single crystal specimens, and would be the least pronounced in low-purity polycrystal specimens. In the TRIST-ER1 experiment, two single crystal specimens of alumina were successfully irradiated to the highest doses ever studied in an RIED experiment (> 2 dpa) without any evidence of degradation above the normal RIC level. There are several possible explanations for the discrepancy between the electron RIED studies and the present work. One possibility is that the large amount of implanted charge associated with electron irradiation may somehow trigger the initiation of RIED. Further work is needed to understand the physical mechanism(s) responsible for producing RIED in electron-irradiated samples.

A moderate amount of RIED that apparently is not due to surface leakage currents was observed in the Cr-doped sapphire specimen; the full-power conductivity increased by nearly 3 orders of magnitude after the first few days of irradiation and then gradually decreased over the ensuing 3 months. Further work is needed to determine the cause of the high apparent bulk conductivity of the ruby specimen which occurred at a dose of ~ 0.1 dpa.

Disassembly of the HFIR TRIST-ER1 capsule is currently in progress. Several different post-irradiation measurements are planned, including electrical resistivity vs. temperature for all 15 alumina specimens and examination of the shorted coaxial cables. Microstructural examination of selected alumina specimens may also be performed.

- [1] S.J. Zinkle et al., in Fusion Materials Semiannual Progress Report for Period ending June 30, 1996, DOE/ER-0313/20 (Oak Ridge National Lab, 1996) p. 257.
- [2] S.J. Zinkle et al., in Fusion Materials Semiannual Progress Report for Period ending June 30, 1997, DOE/ER-0313/22 (Oak Ridge National Lab, 1997) p. 188.

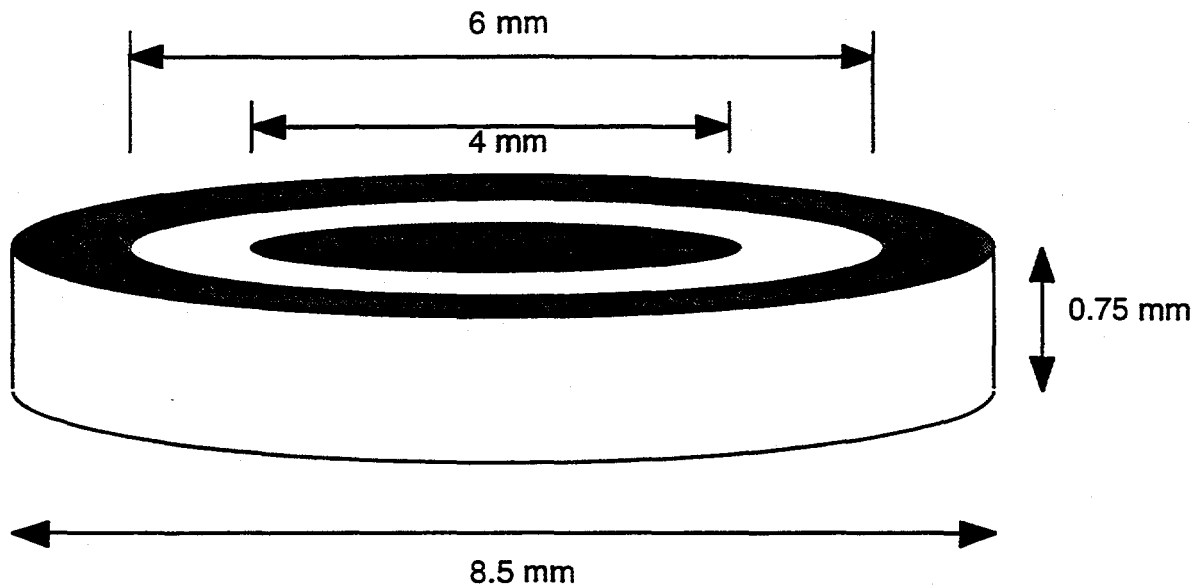
Experimental Technique

- 15 specimens irradiated in separate, sealed subcapsules; the radiation flux was about 40% lower at the ends of the capsule compared to the center
- damage rate varied from $\sim 2.4 \times 10^{-7}$ dpa/s (samples 1,15) to $\sim 4.3 \times 10^{-7}$ dpa/s (sample 8)
- ionizing dose rate varied from ~ 10 kGy/s (samples 1,15) to ~ 16 kGy/s (sample 8)
- Electrical resistivity measured in-situ before, during and after HFIR reactor irradiation at $T_{irr} \sim 450^\circ\text{C}$. 150 V DC (200 V/mm) continuously applied to 12 of the samples during irradiation to $\sim 3 \times 10^{25}$ n/m², $E > 0.1$ MeV (~ 3 dpa)
 - HFIR irradiation started 3/8/96
 - Final (3rd) cycle completed 6/20/96
- 5 sets of in-situ diagnostics tests (e.g., surface leakage resistances) periodically performed to verify quantitative accuracy of electrical conductivity data
- The specimen temperatures were continuously monitored by two thermocouples in each subcapsule
- Scheduled postirradiation examinations (to begin summer 1997?): electrical resistivity; also possibly TEM, thermal conductivity, optical spectroscopy

KEY FEATURES OF TRIST-ER1 DESIGN

- Electrical measurements are made in accordance with ASTM Standard Test Method for DC Resistance or Conductance of Insulating Materials (ASTM D257-91)
- Well-defined path for heat flow (no unknown heat transfer gaps)
 - ceramic specimens and insulating pedestal brazed to metal heat sink, 2 thermocouples used per subcapsule
- Well-defined, low resistance electrical contacts and lead wires
 - electrical wires laser-welded to braze pads in the center and guard ring regions of the specimen
- Electrical resistance between center and guard ring electrodes, and between guard ring and back electrodes is sufficiently high (must be $>10 \text{ k}\Omega$, preferably $>>1 \text{ M}\Omega$)
 - surface leakage resistances measured during irradiation

GUARDED ELECTRODE GEOMETRY FOR HFIR ELECTRICAL RESISTIVITY EXPERIMENTS ON CERAMIC INSULATORS



- Guard ring geometry conforms to ASTM Standard Test Methods for DC Resistance of Conductance of Insulating Materials, D257-91
- Center and guard electrodes are $\sim 1 \mu\text{m}$ sputter-deposited Pt (with $\sim 0.1 \mu\text{m}$ Ti underlayer)
 - back electrode is TiCuSil braze metal
- Wire leads for guard and center electrode are brazed onto the specimen before depositing the Pt electrodes
- Voltage is applied to the back electrode; specimen current is measured on the low (guarded) side
- Specimens are enclosed inside of sealed subcapsules to minimize surface contamination effects (high purity He environment)

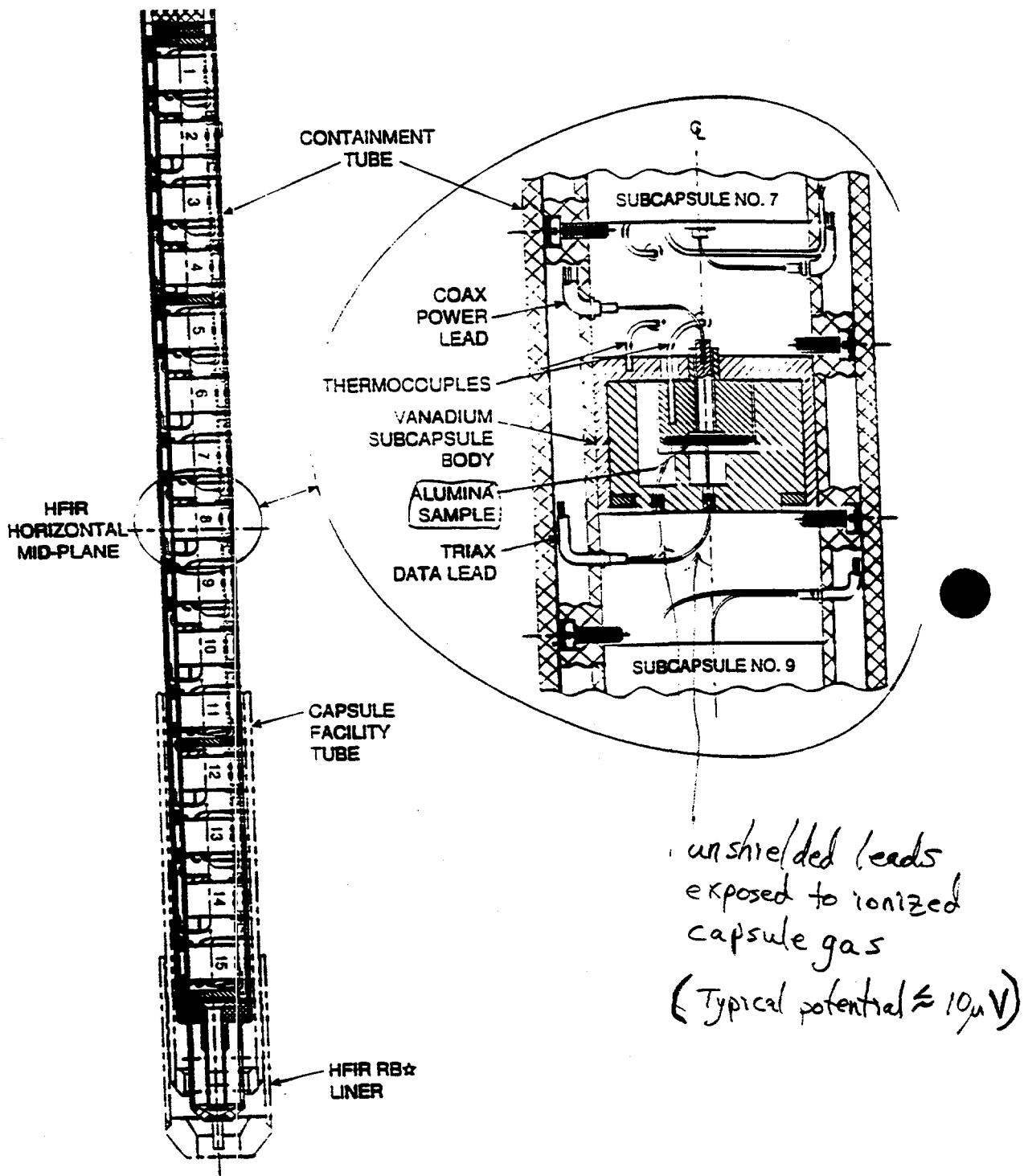


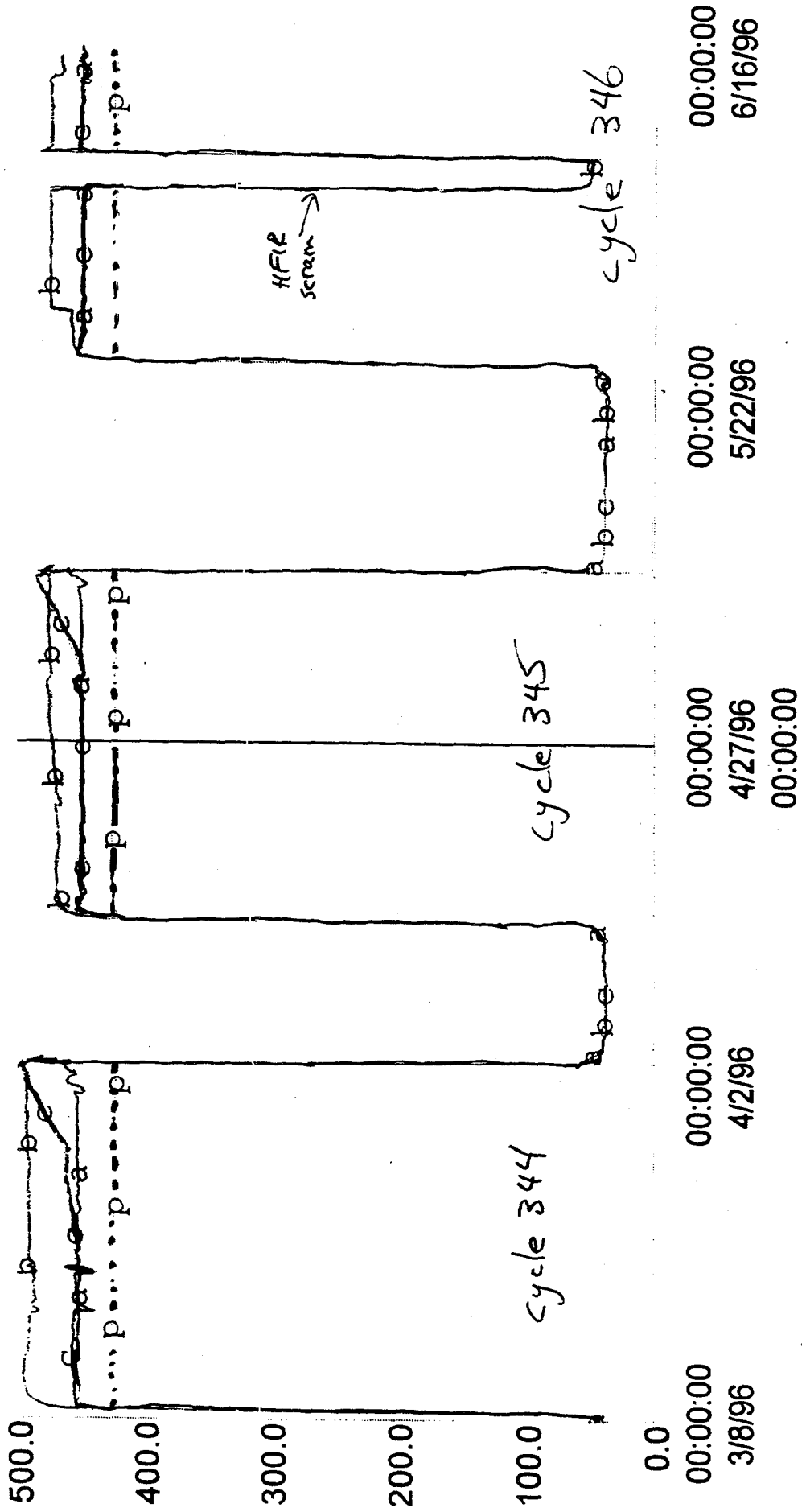
Fig. 2. Axial cross-section of the irradiation capsule.

SPECIMEN MATRIX FOR THE IR TRIST-ERI EXPERIMENT
450°C, 3 Cycles in RB* Position (~3x10²⁵ n/m², E>0.1 MeV; ~3 DPA in Al₂O₃)

HFIR

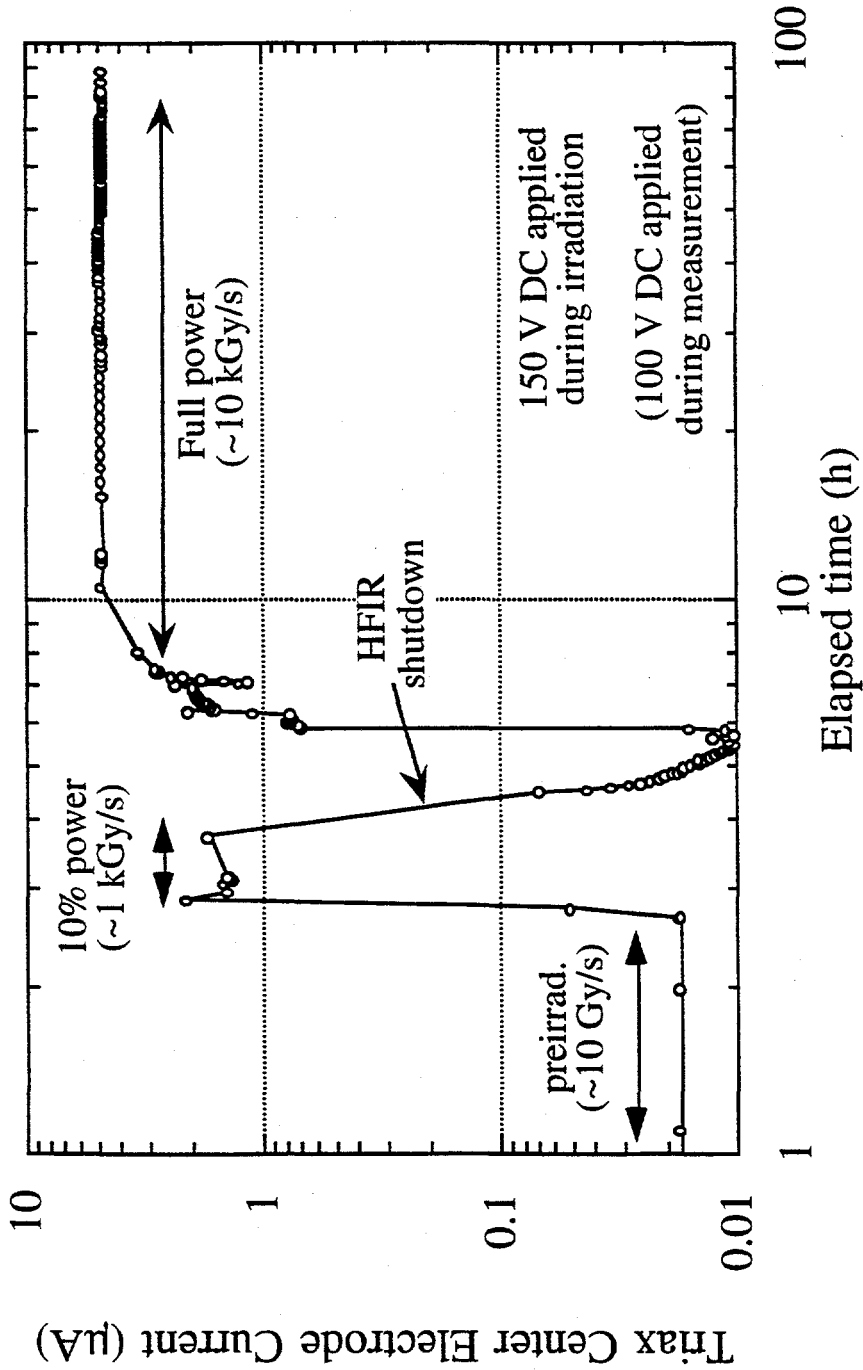
<u>Position</u>	<u>Material</u>	<u>Appl. Voltage</u>	<u>Vendor and grade</u>
1.	Al ₂ O ₃ , single crystal	150 V	Crystal Systems (Hemex UV grade) a-axis
2.	Al ₂ O ₃ , single crystal	150 V	Crystal Systems (Hemex UV grade) c-axis
3.	Al ₂ O ₃ , single crystal	150 V	Crystal Systems (Hemex regular), c axis
4.	Al ₂ O ₃ , single crystal	150 V	Crystal Systems (Hemex regular), a axis
5.	Al ₂ O ₃ , polycrystalline	150 V	Vitox (99.9% purity, Morgan Matroc, Anderman Div.)
6.	Al ₂ O ₃ , polycrystalline	150 V	Kyocera A-480 (99.9% purity)
7.	Al ₂ O ₃ , polycrystalline	150 V	Wesgo AL300 (97.0% purity)
8.	Al ₂ O ₃ , polycrystalline	150 V	Kyocera A-479 (99.0% purity)
9.	Al ₂ O ₃ , polycrystalline	150 V	Coors AD998 (99.8% purity)
10.	Al ₂ O ₃ , polycrystalline	150 V	Wesgo AL995 (99.5% purity)
11.	Al ₂ O ₃ , polycrystalline	0 V	Wesgo AL995 (99.5% purity)
12.	Al ₂ O ₃ , single crystal	0 V	Crystal Systems (Hemex regular), c axis
13.	Al ₂ O ₃ +Cr, single crystal	150 V	Union Carbide (UV grade), 60° from c axis
14.	Al ₂ O ₃ , single crystal	150 V	Kyocera SA100 (1̄102 orientation)
15.	Al ₂ O ₃ , single crystal	0 V	Kyocera SA100 (1̄102 orientation)

Temperature History of TRIST-ERI Capsule



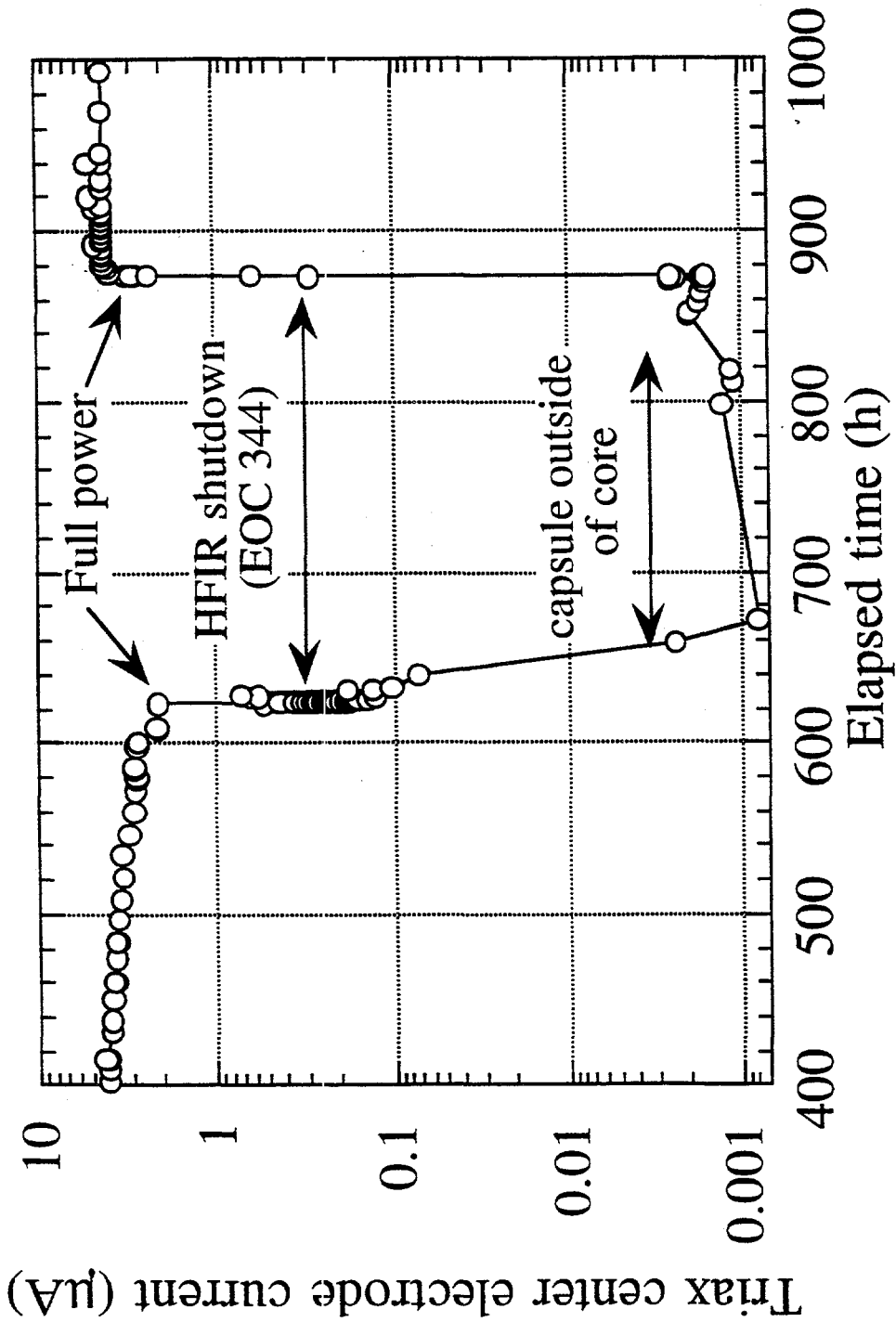
a samples 1-4
 b samples 5-11
 c samples 12-15
 p reactor power

Conductance of Sapphire Measured during HFIR Irradiation (Crystal Systems "Hemex" UV grade, a-axis)

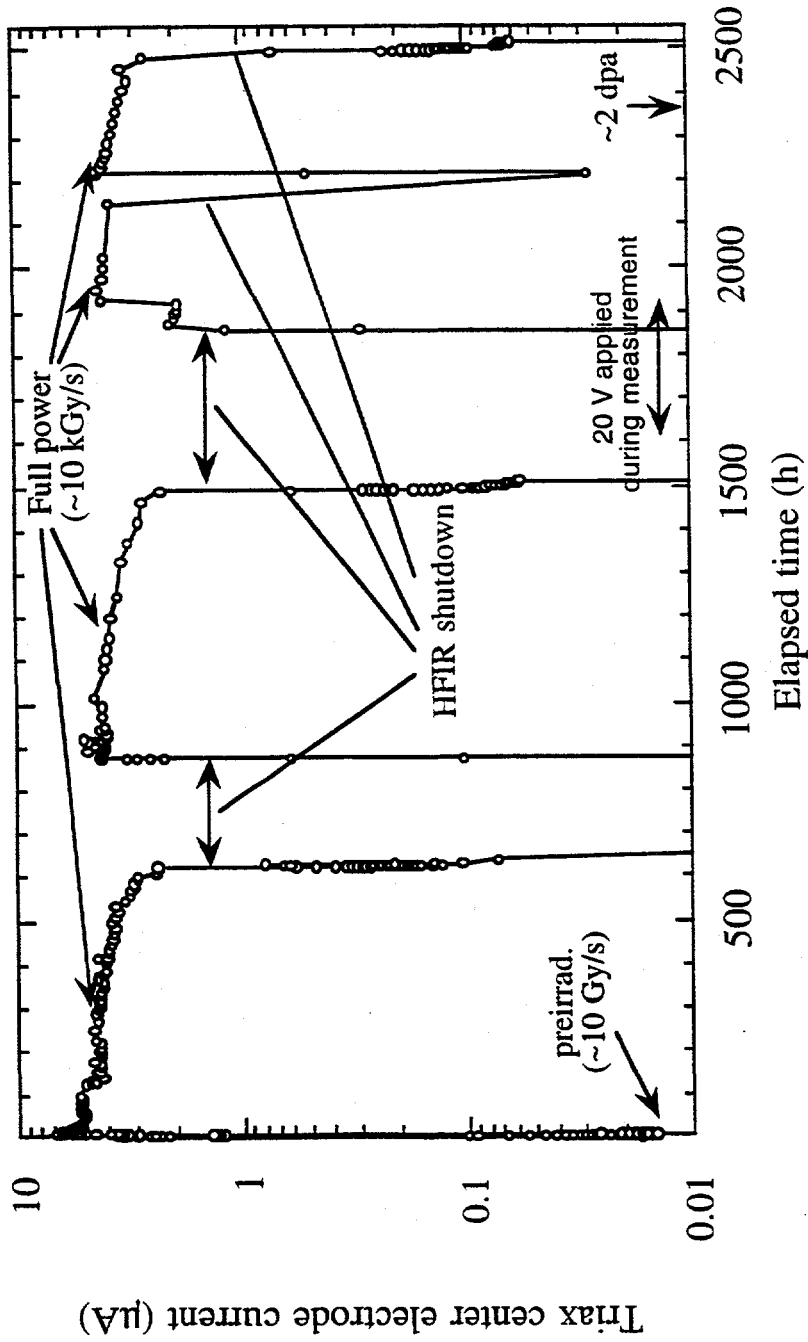


- Startup procedure for 1st cycle (#344): rapid increase to 10% power, hold for ~1.5 h, reactor scram, then "conventional" ascension to full power operation

Measured current from Crystal Systems regular grade, c-axis sapphire between HFIR cycles 344 and 345

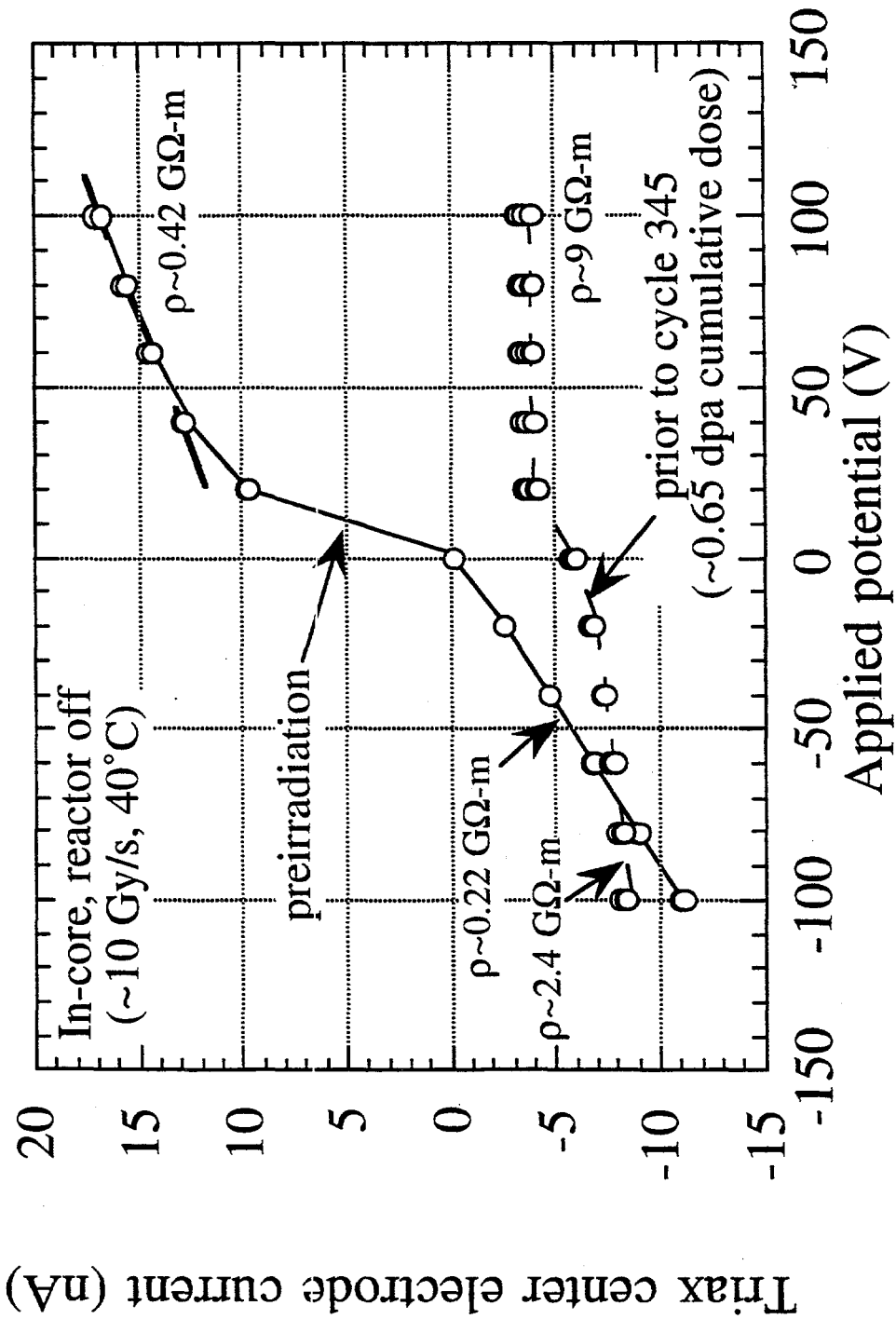


Conductance of Sapphire Measured During HFIR Irradiation
 (Crystal Systems "Hemex" UV grade, c-axis)



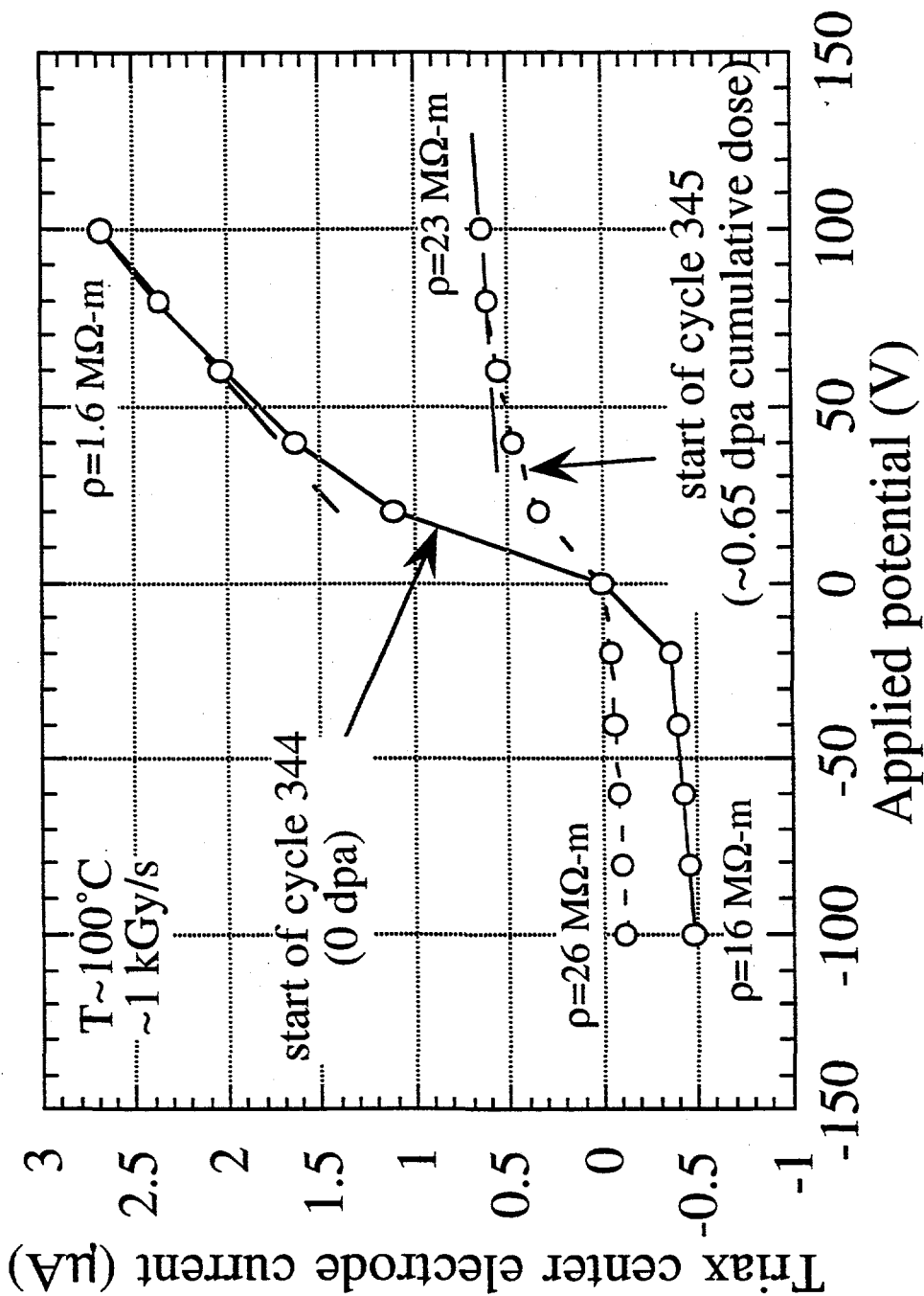
- Inadvertant reactor scram during the 3rd HFIR irradiation cycle (~ 2100 h) due to power outage

**In-core ohmic check on Crystal Systems
"Hemex" UV-grade sapphire, c-axis (reactor off)**



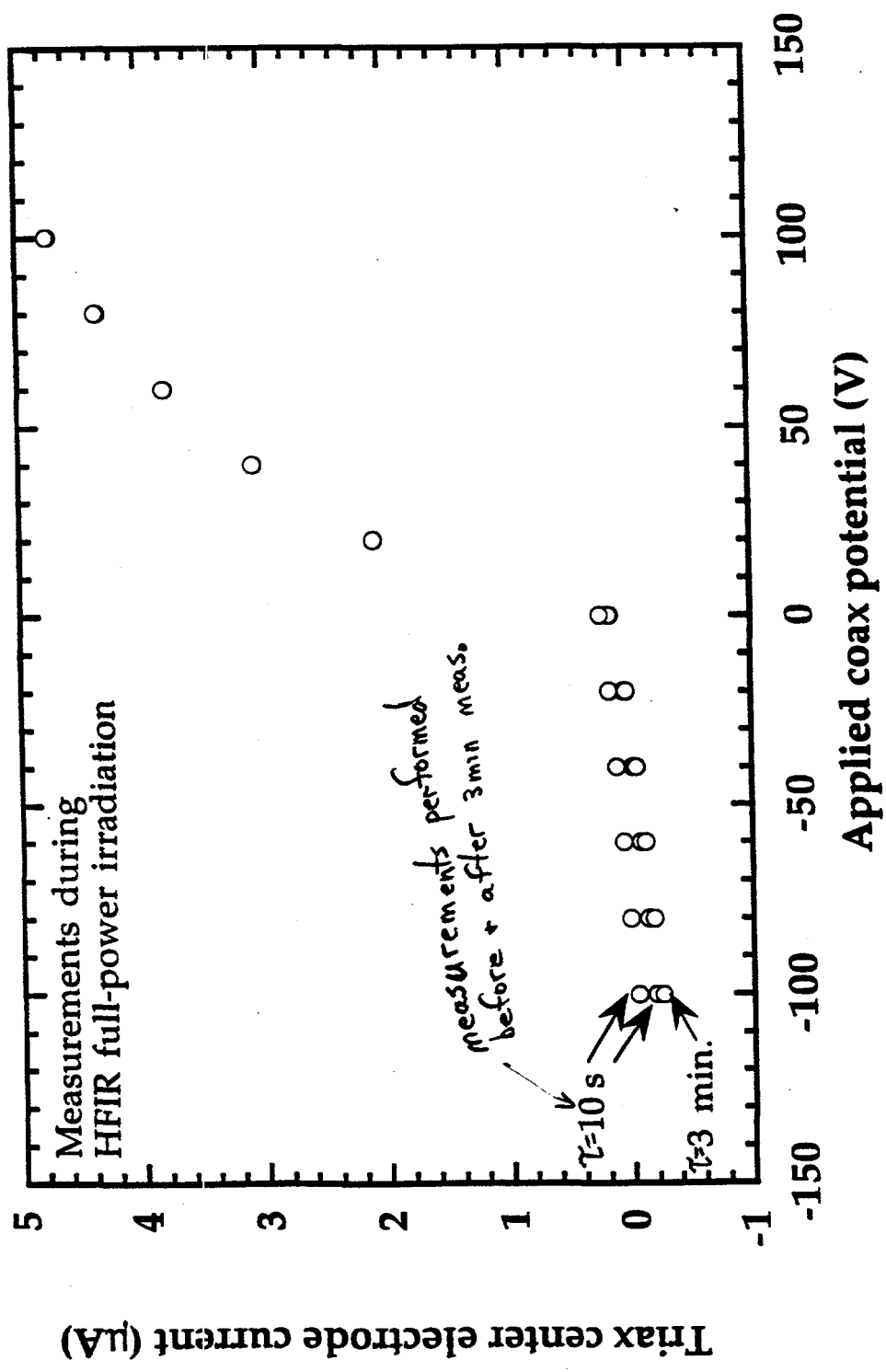
- Non-ohmic response to applied voltage

Ohmic check during HFIR irradiation at 10% power
 (Crystal Systems Hemex UV grade sapphire, c-axis)

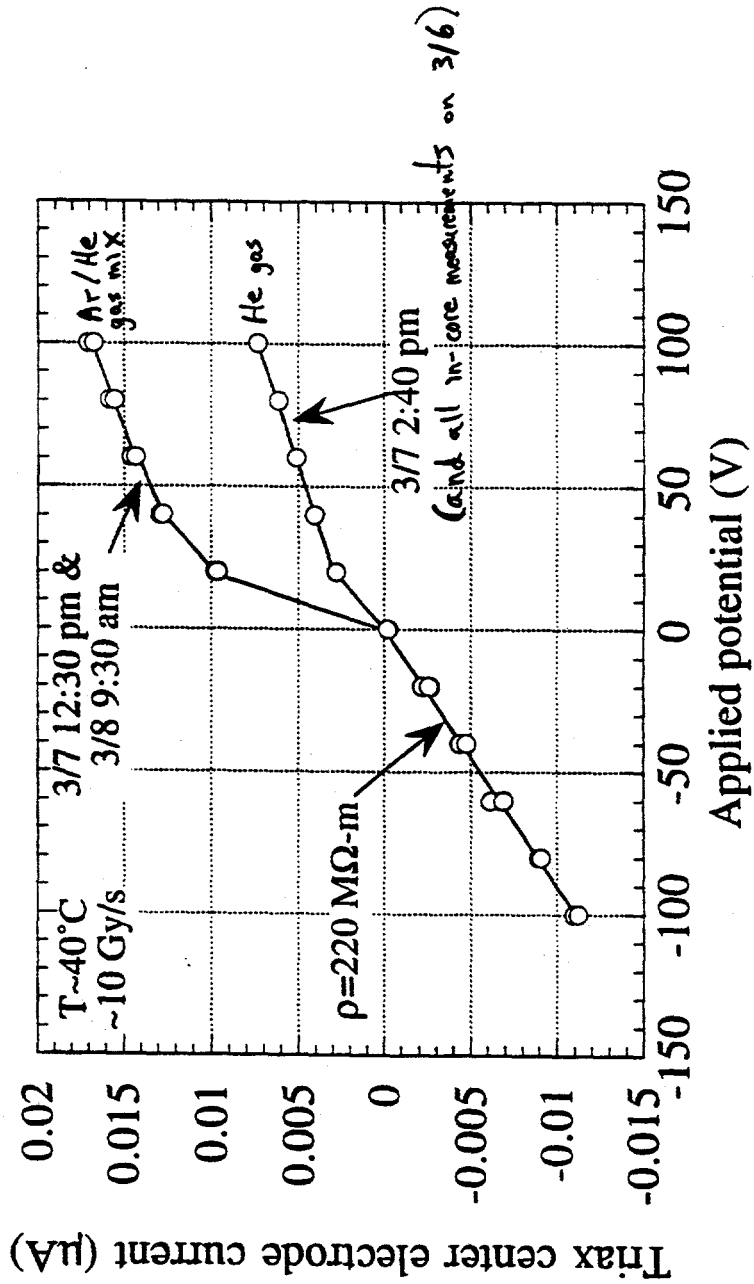


calculated RC time constant = $\begin{cases} < 0.1 \text{ ms specimen} \\ (C = 7 \text{ pF}) \\ \sim 10 \text{ ms coax cable} \\ (C = 7 \text{ nF}) \end{cases}$

Check of effect of RC wait time on the electrical response of CSI sapphire (UV grade, a-axis, exp21)



**Preirradiation ohmic check on sapphire
(Crystal Systems "Hemex", UV grade, c-axis)**



Effect of Ionized Gas on RIC Measurements

Theory based on ionization chambers (radiation detectors)

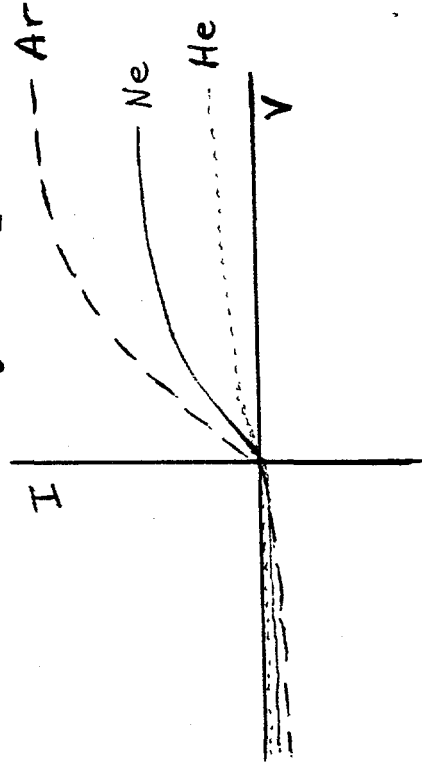
c.f. W.J. Price, Nuclear Radiation Detection (1964), etc.

$$\sigma_e = ne\mu \quad (I = ne\mu EA)$$

$$\sigma_e = KDe\mu_e / \alpha = 3.7 \times 10^{-6} \text{ S/m in air at } 16 \text{ kGy/s}$$

(Chervenak and vanLint, 1982)

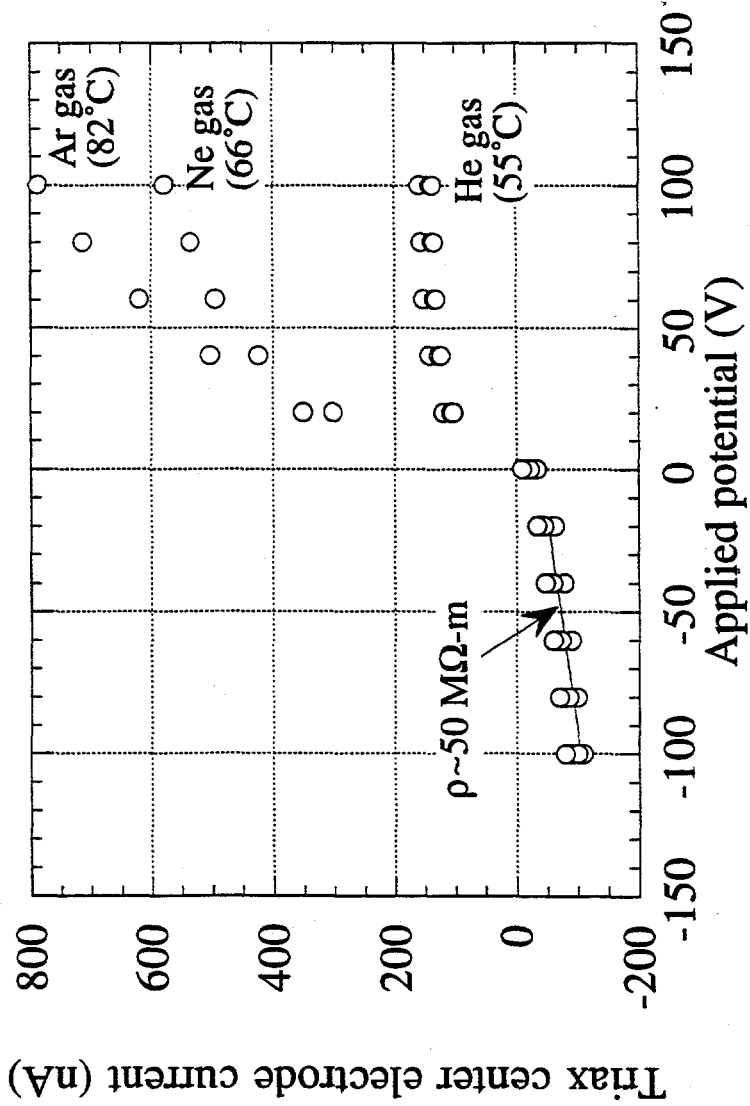
$\mu_{\text{ion}} \sim 10^{-3} \mu_e \Rightarrow$ gas effect occurs mainly for positive applied voltage



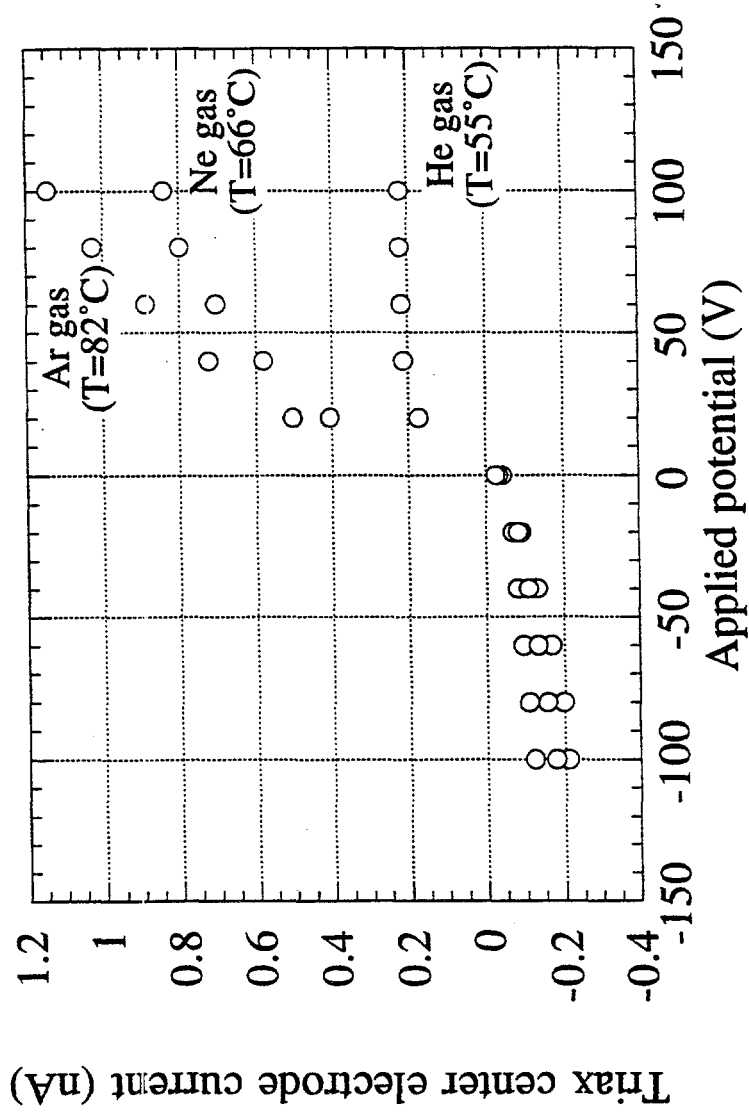
Gas	K (ion pairs/cm ³ -Gy)
He	2.3x10 ¹⁰
Ne	7.0x10 ¹⁰
Ar	17.7x10 ¹⁰

\Rightarrow gas conduction effect should be largest for Ar gas

**Ohmic check following HFIR cycle 344 shutdown
in Crystal Systems UV-grade sapphire (exp22cum.)**

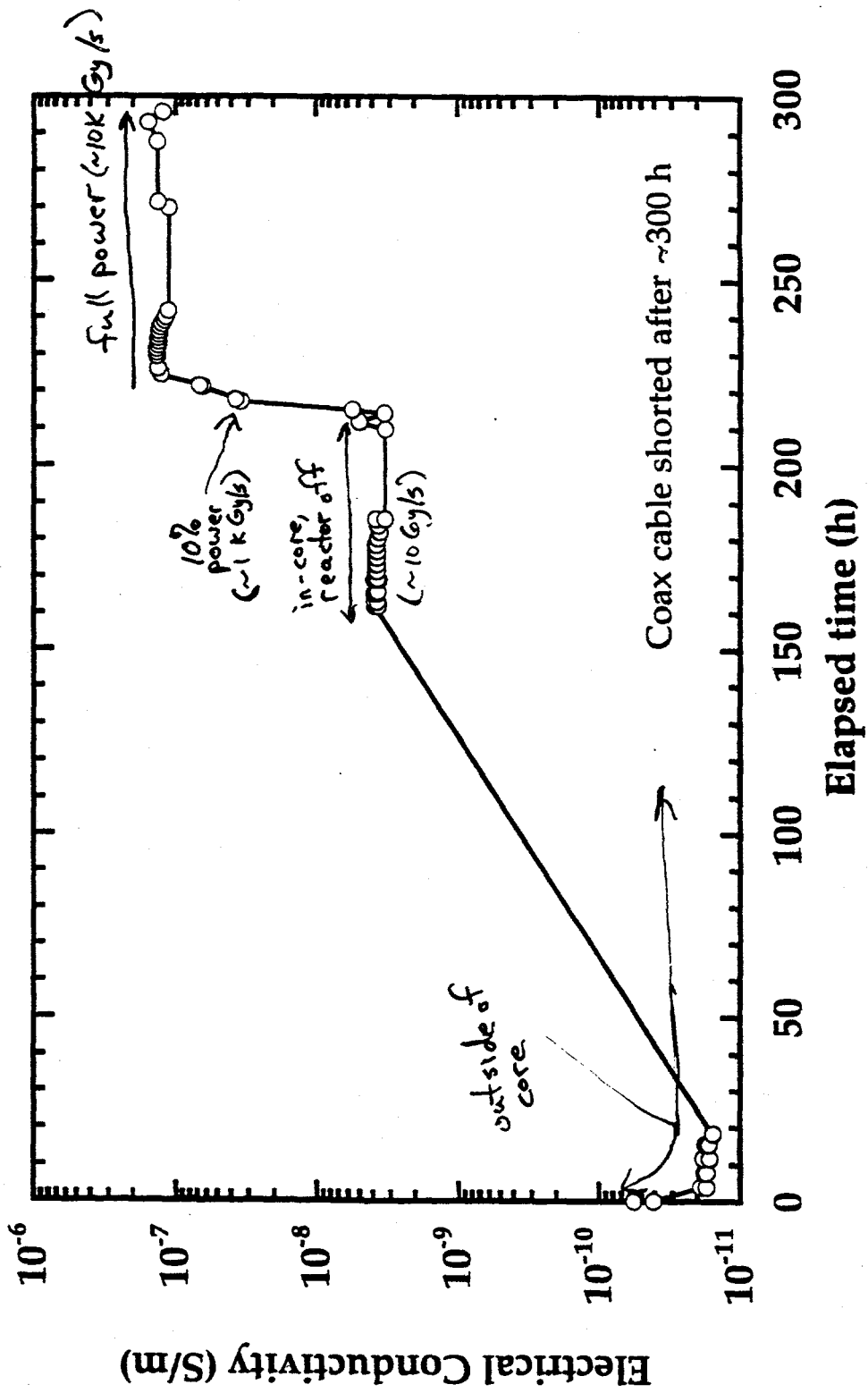


**Ohmic check after HFIR cycle 344 shutdown in
Kyocera A479 polycrystalline alumina (exp28cum.)**

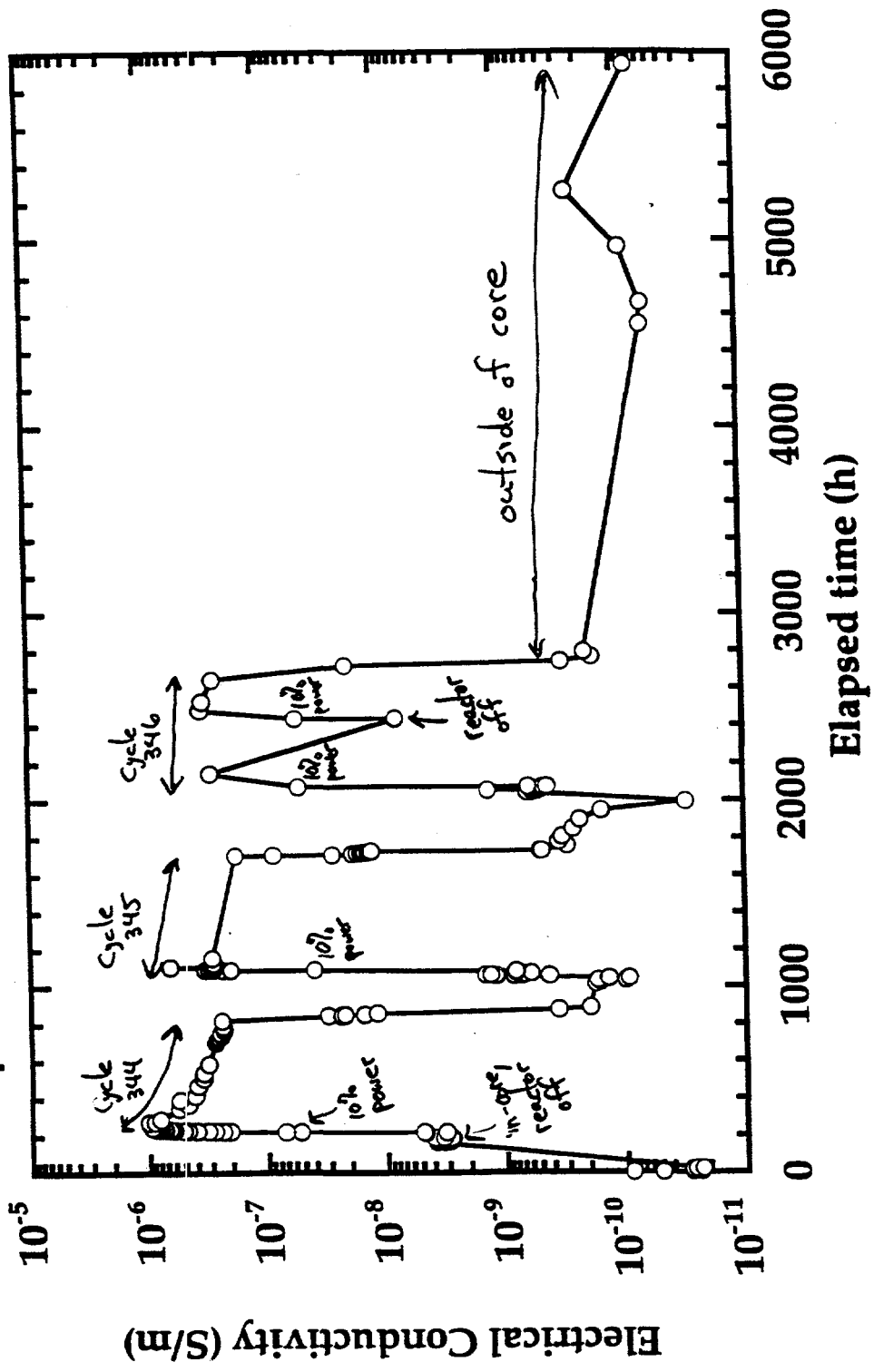


Conductivity calculated from slope
of I vs. V plots at $V < 20V$

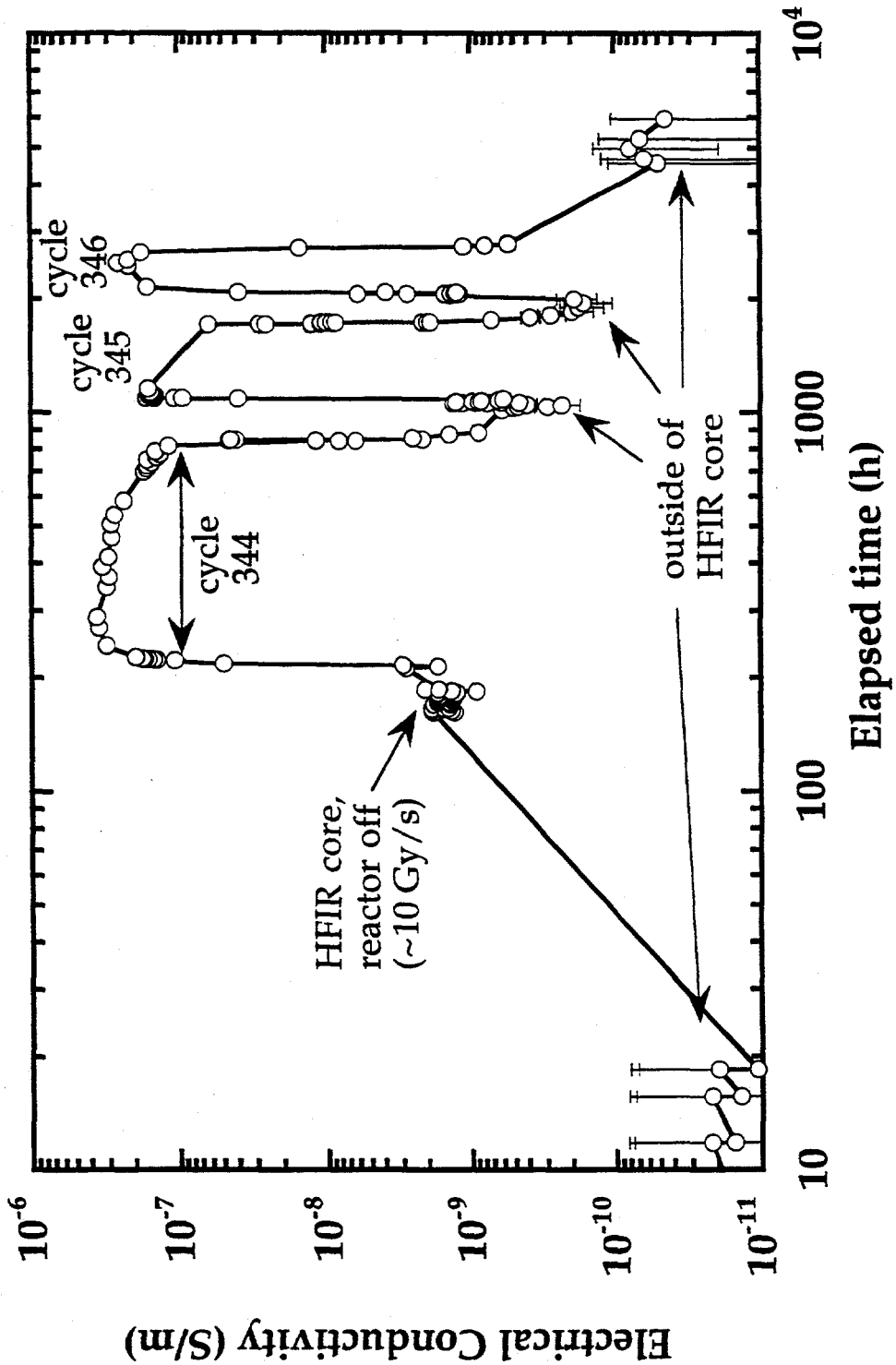
exp21/all (CSI Sapphire, UV grade, a-axis)



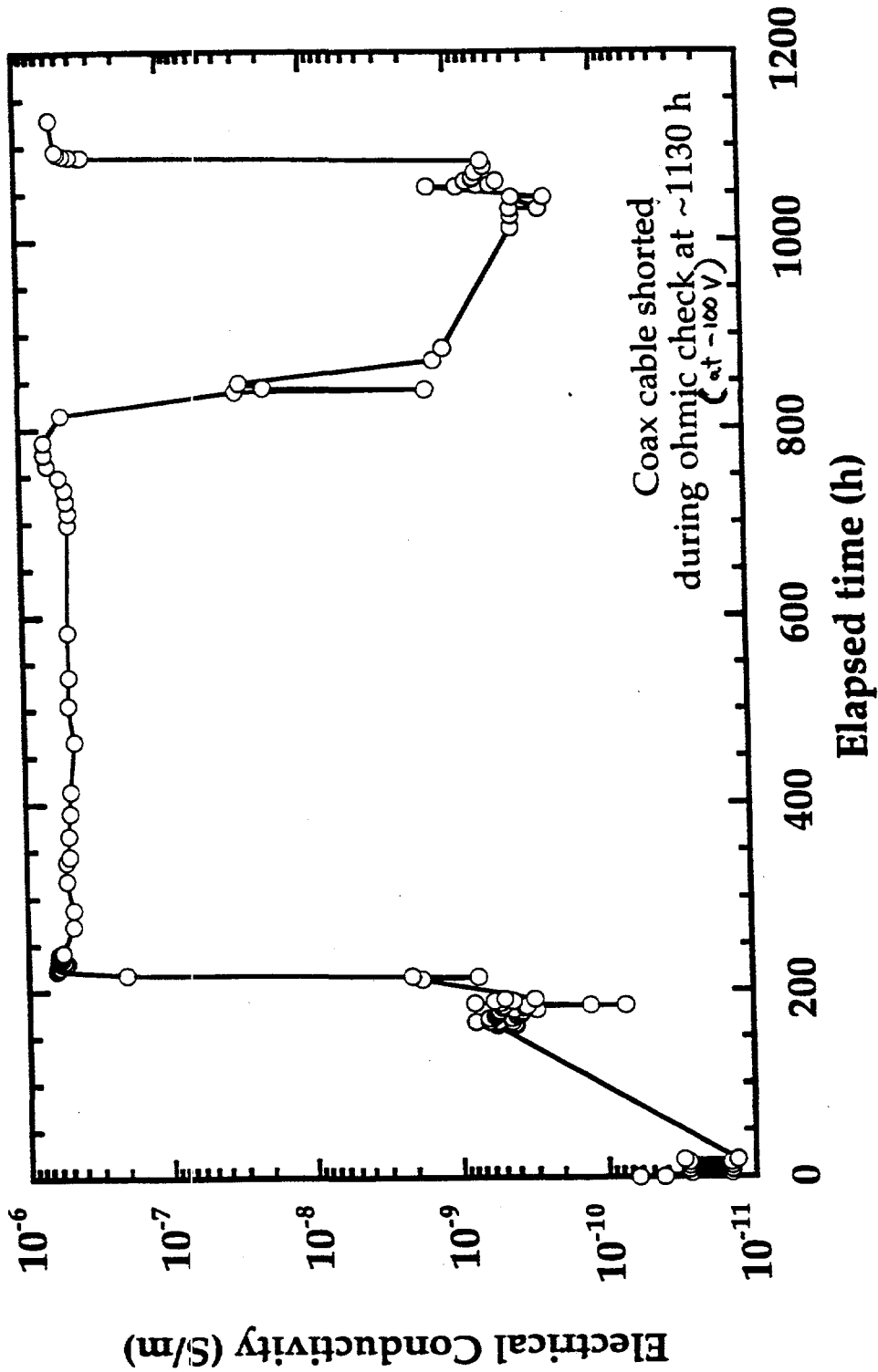
exp22/all (CSI Sapphire, UV grade, c-axis)



Measured Electrical Conductivity of Crystal Systems Sapphire During HFIR Irradiation (regular grade, c-axis, sample #3)

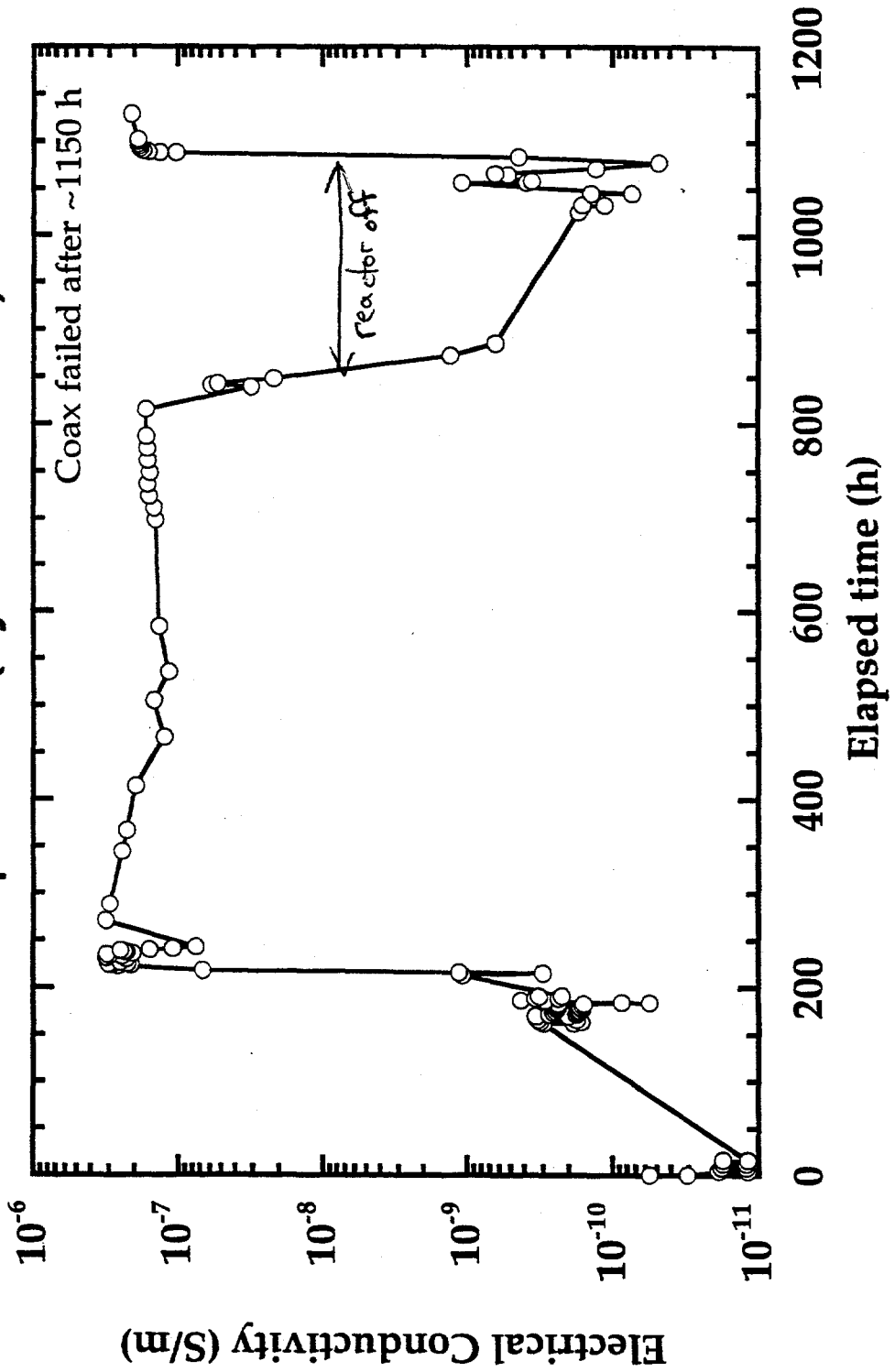


exp27/all (Wesgo AL300 polycrystal alumina)

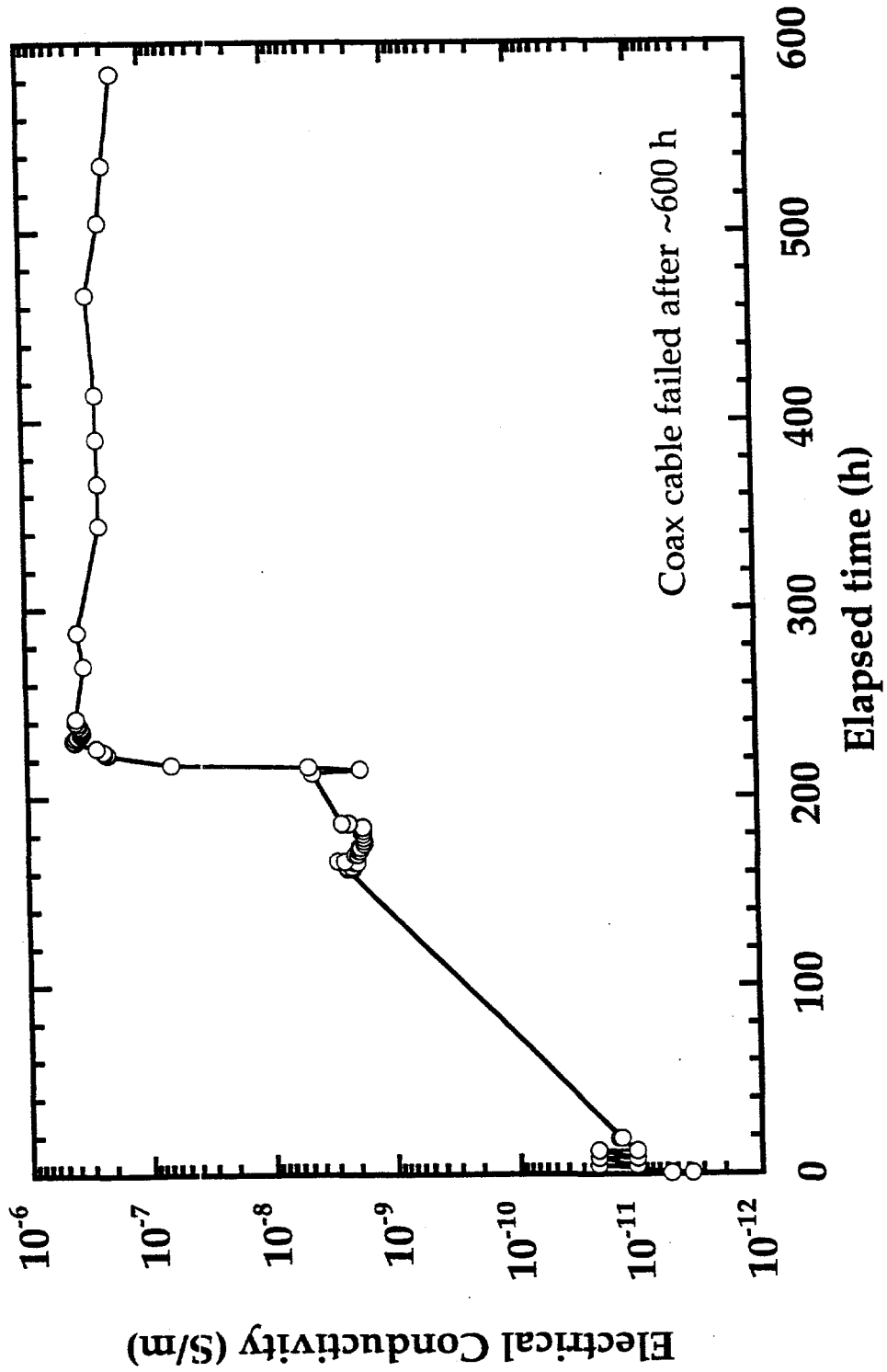


- About half of the coax cables shorted during the 3 month irradiation (most likely due to dielectric breakdown in the glass seals - see discussion)

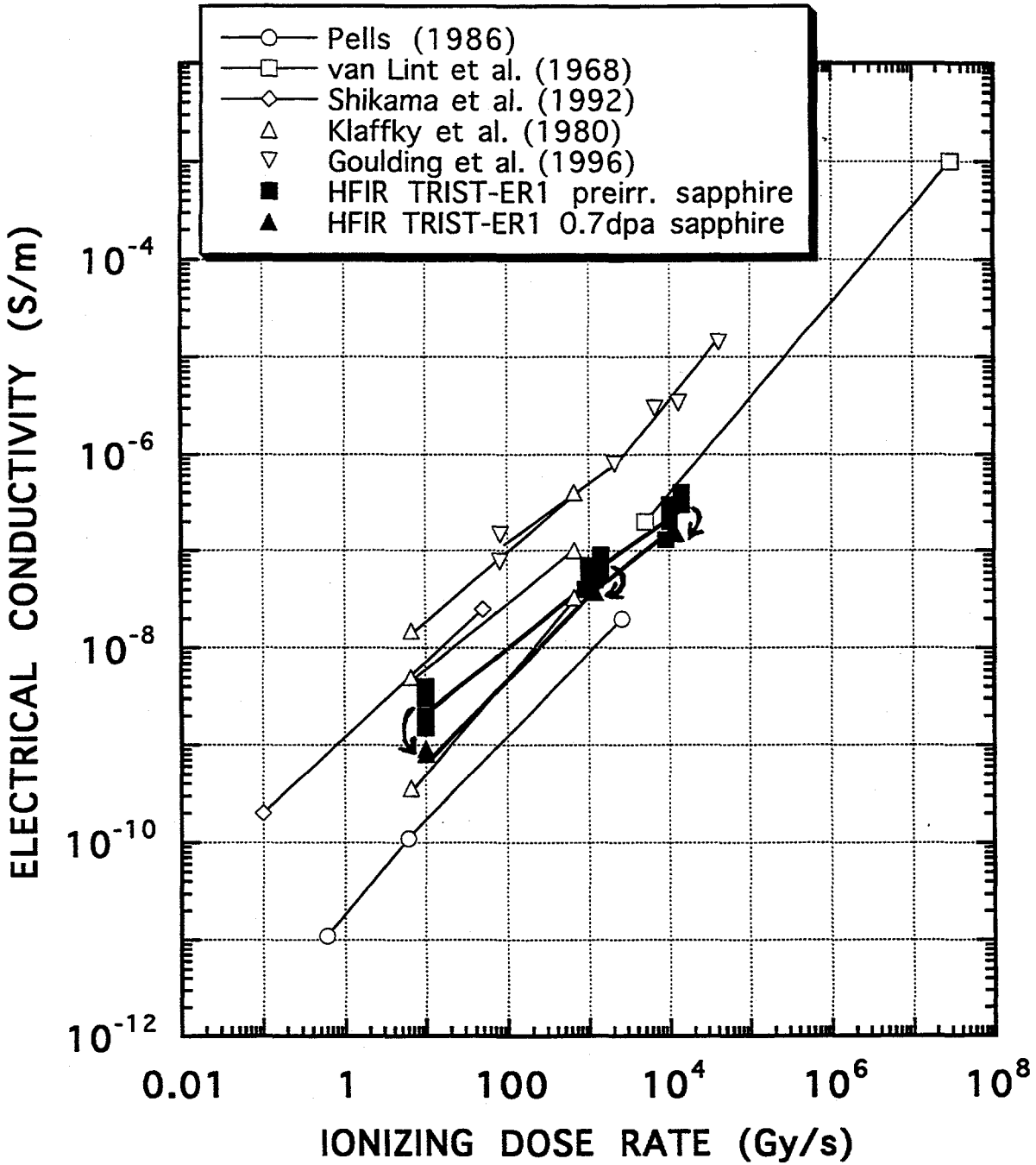
exp28/all (Kyocera A-479)



exp212/all (CSI regular sapphire, c-axis, 0 bias)

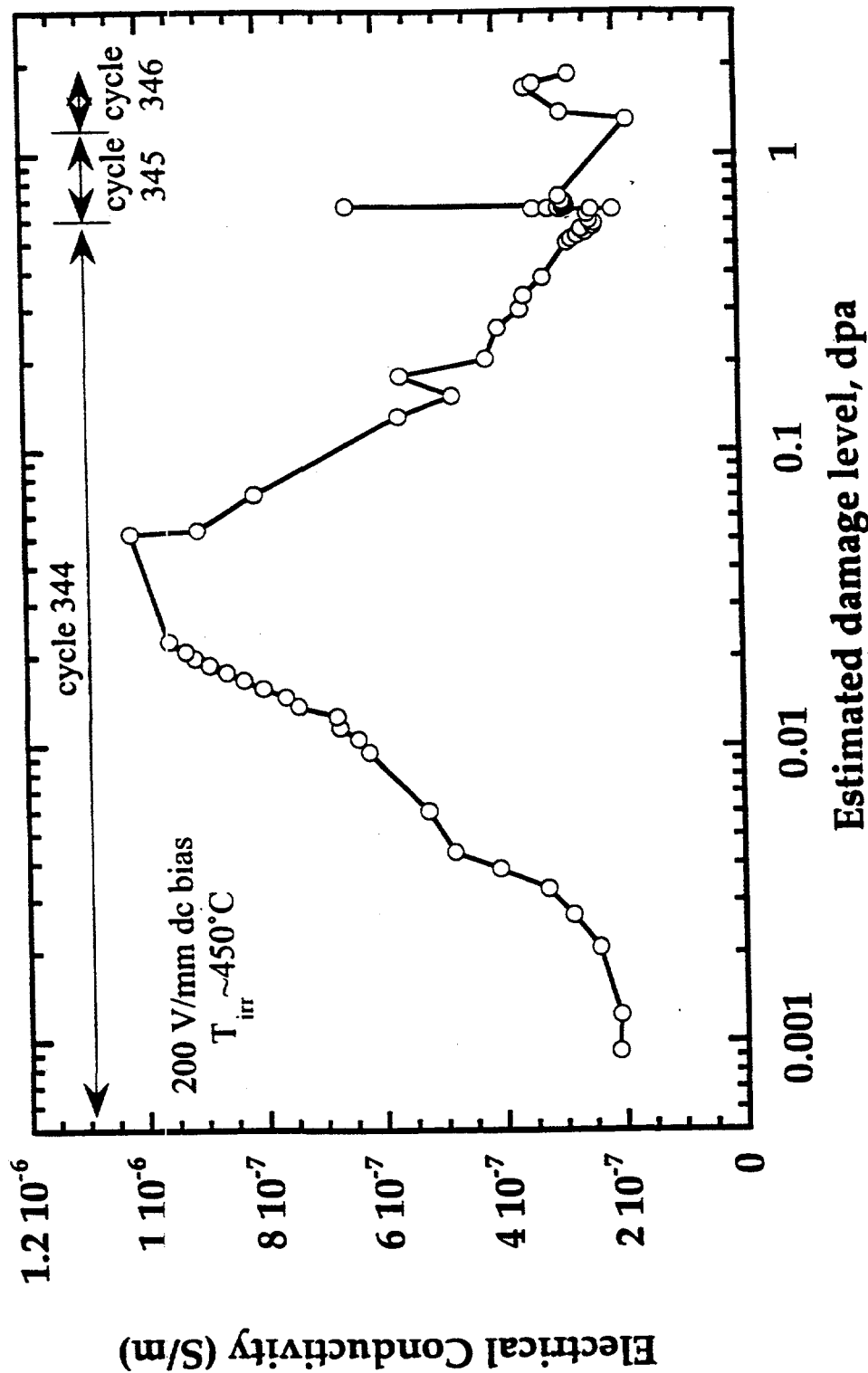


RADIATION INDUCED CONDUCTIVITY IN ALUMINA

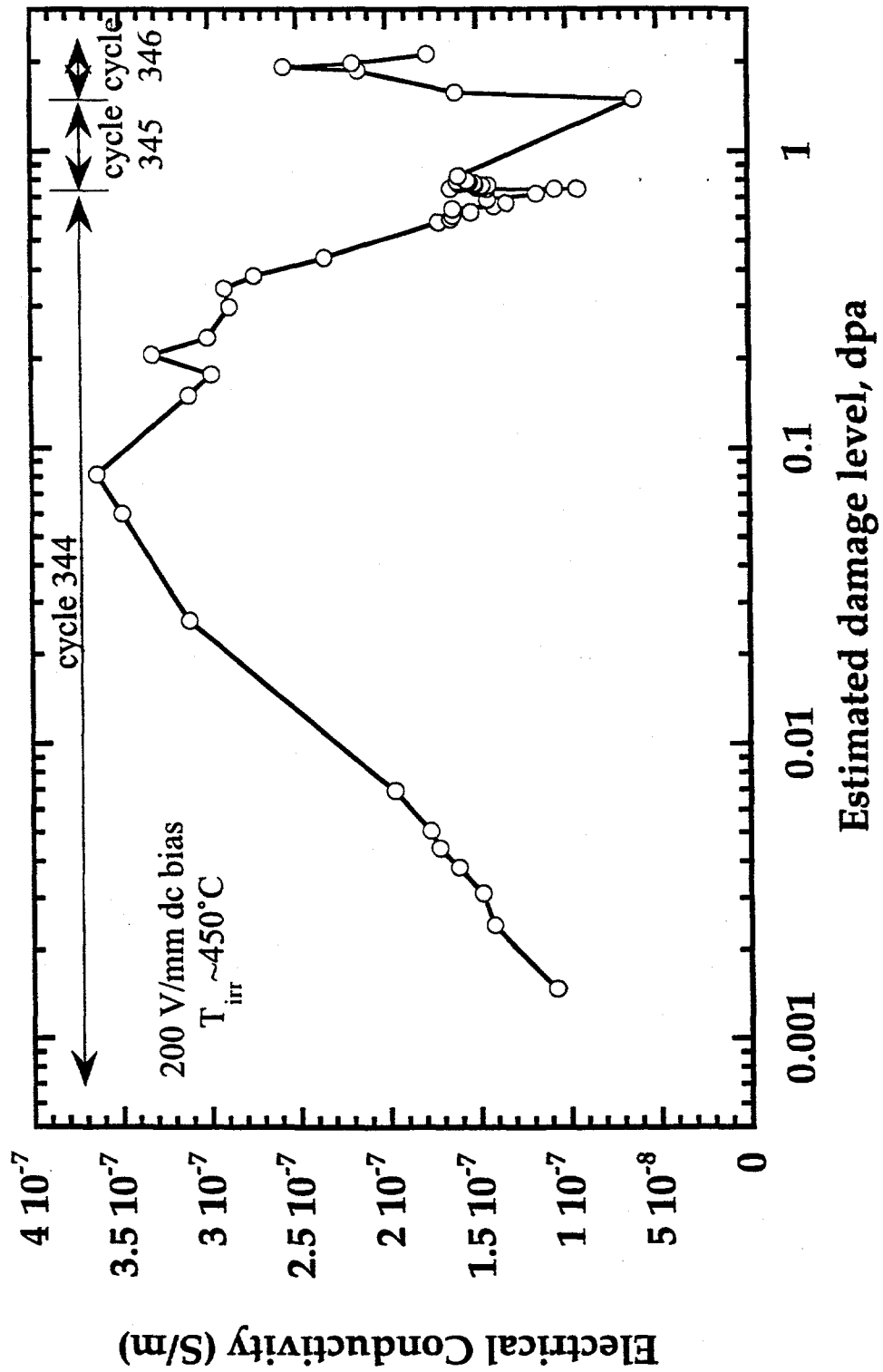


only full-power data plotted

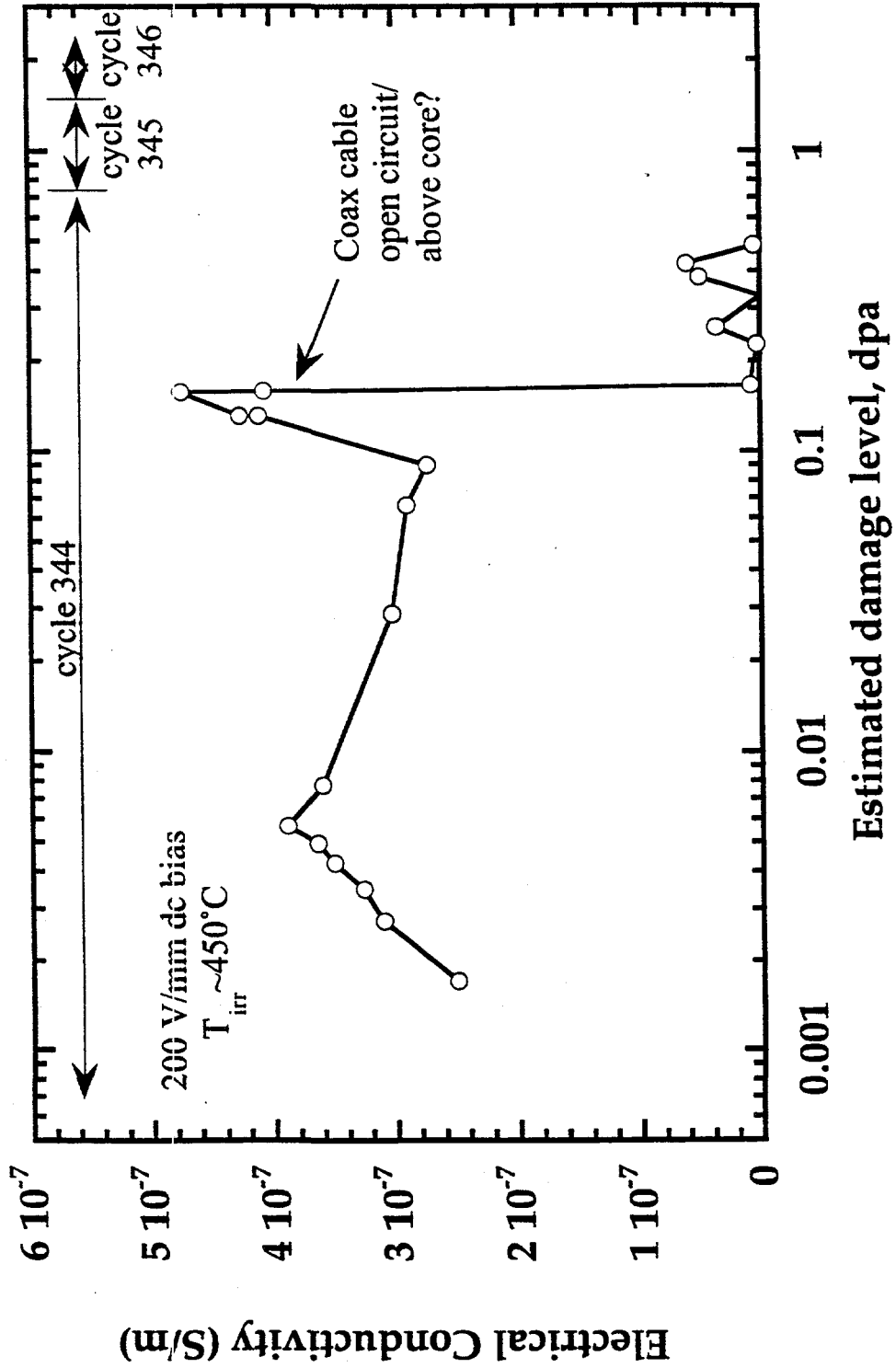
Conductivity of Crystal Systems Sapphire (UV, c-axis) Measured during full-power HFIR Irradiation (exp22)



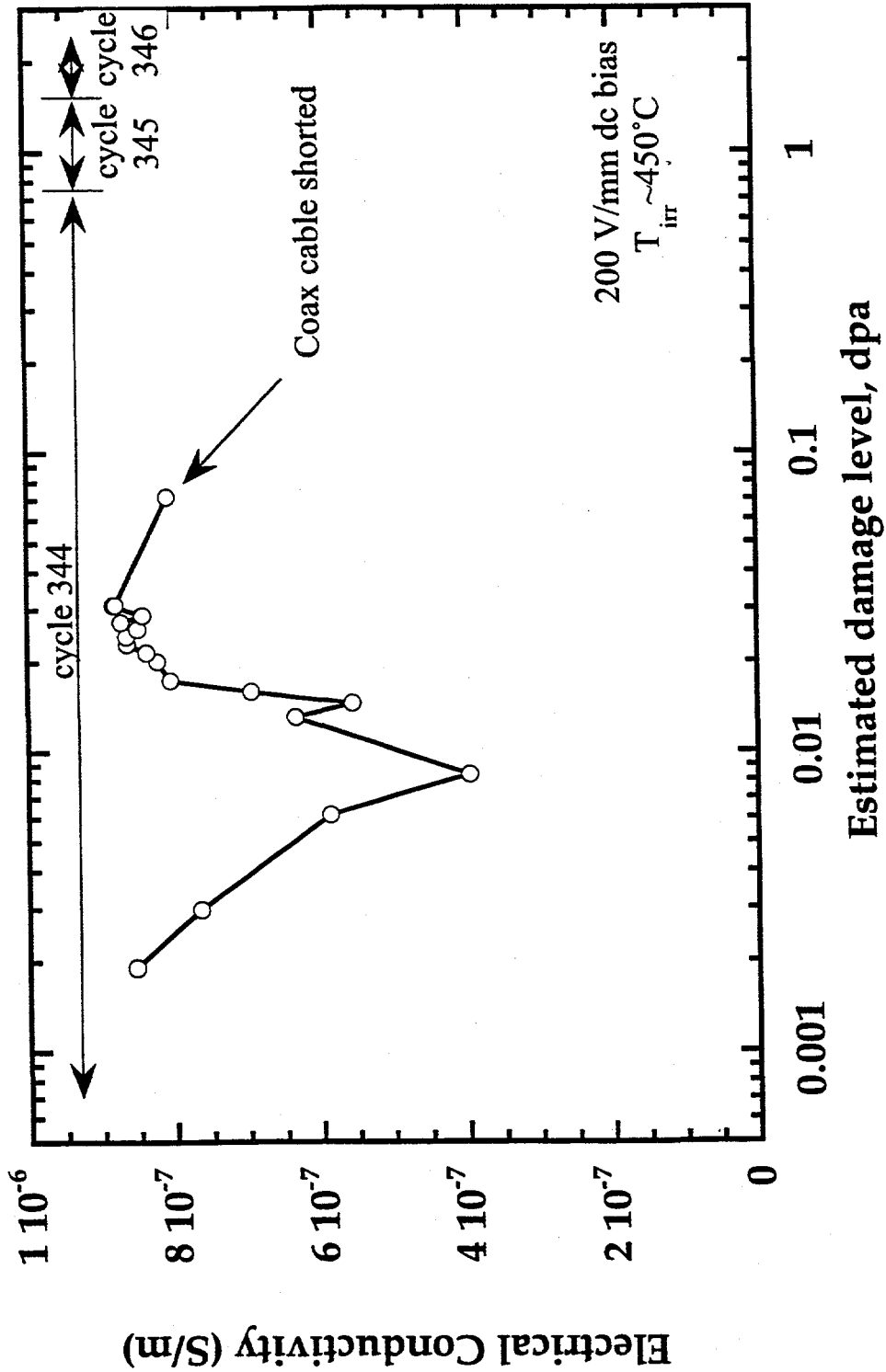
**Conductivity of Crystal Systems Sapphire (regular, c-axis)
 Measured during full-power HFIR Irradiation (exp23)**



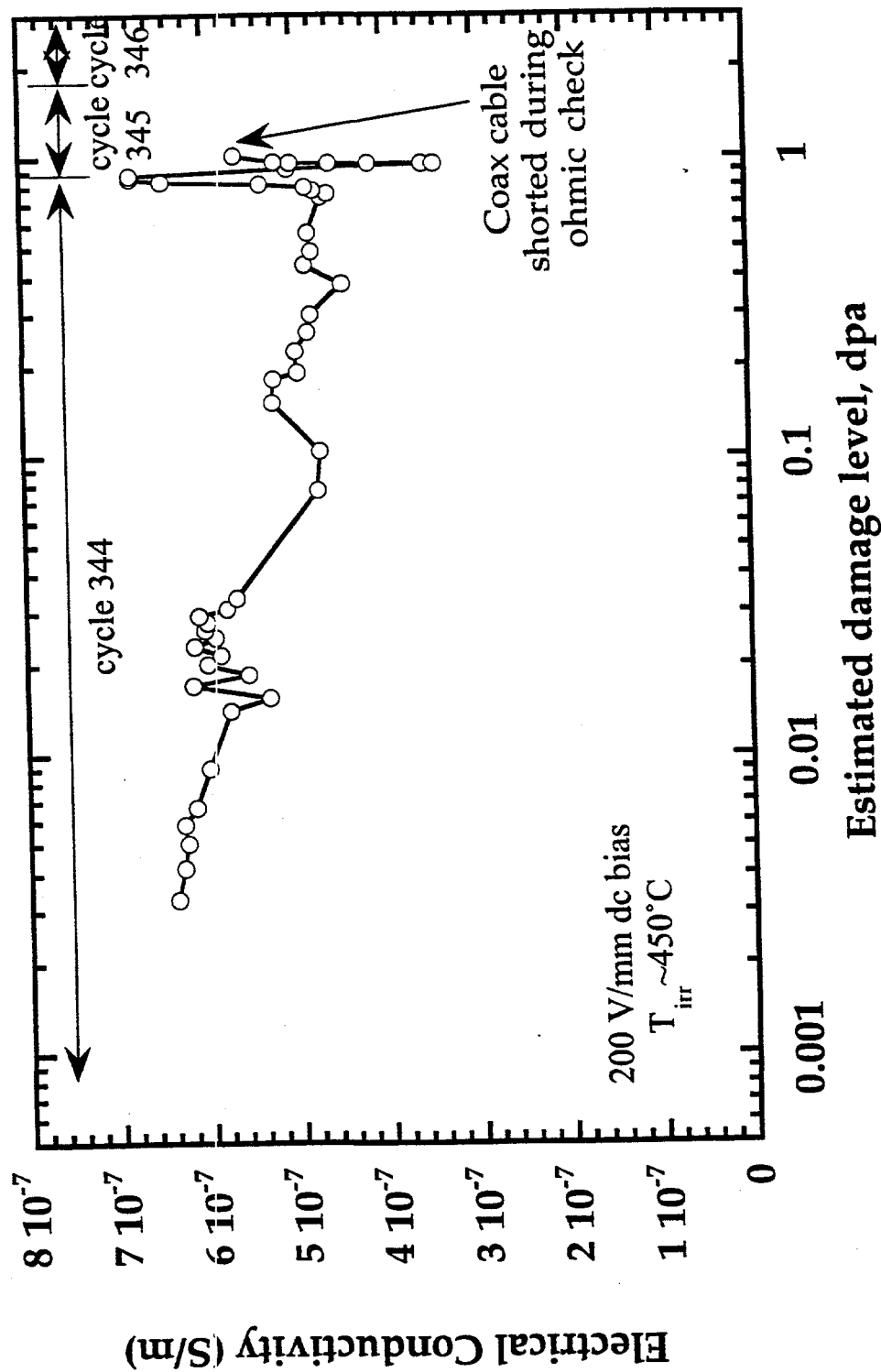
**Conductivity of Crystal Systems Sapphire (regular, a-axis)
Measured during full-power HFIR Irradiation (exp24)**



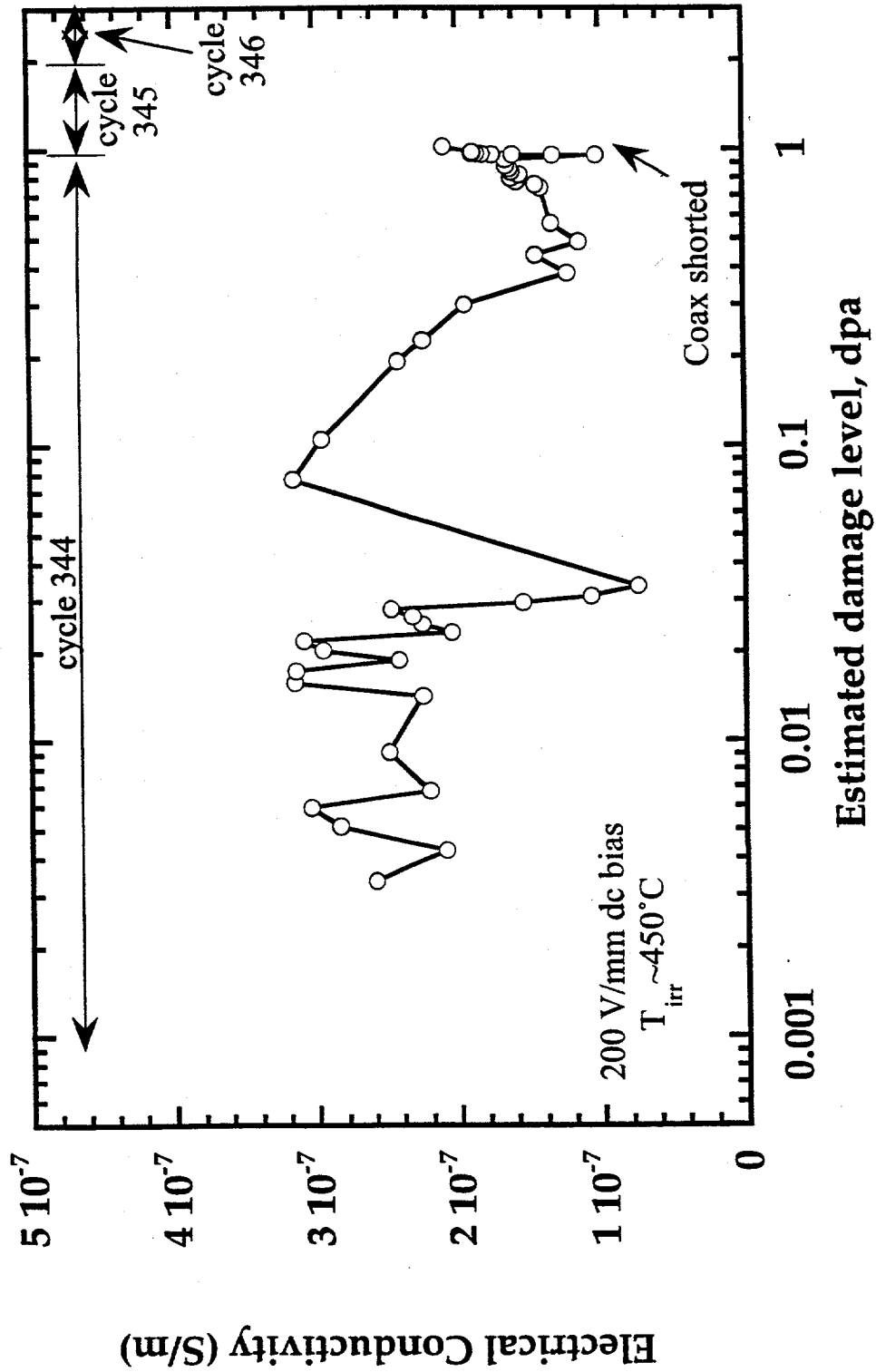
Conductivity of Vitox polycrystalline alumina
 Measured during full-power HFIR Irradiation (exp25)



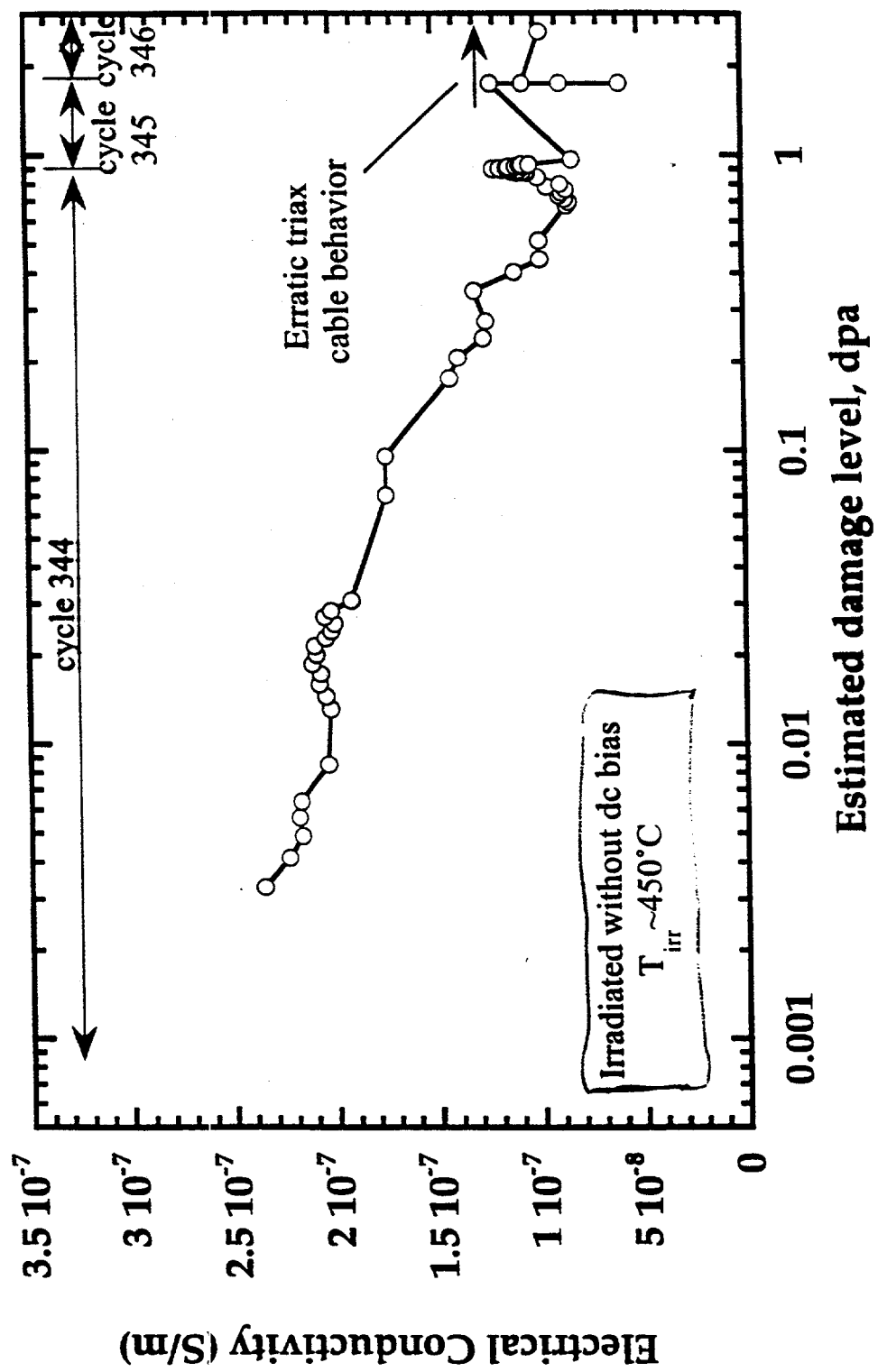
**Conductivity of Wesgo AL300 polycrystal alumina
Measured during full-power HFIR Irradiation (exp27)**



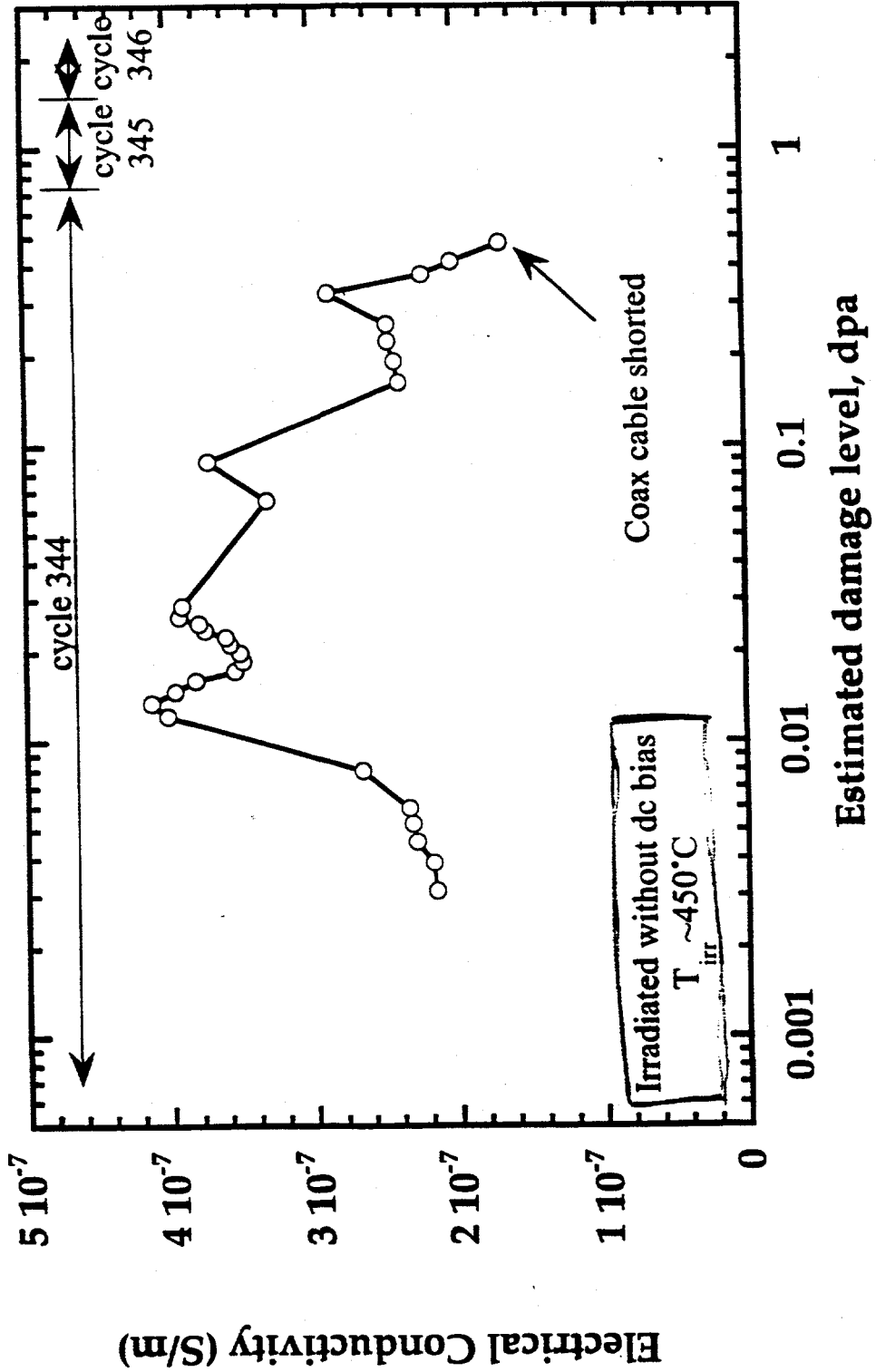
Conductivity of Kyocera A479 polycrystal alumina
 Measured during full-power HFIR Irradiation (exp28)



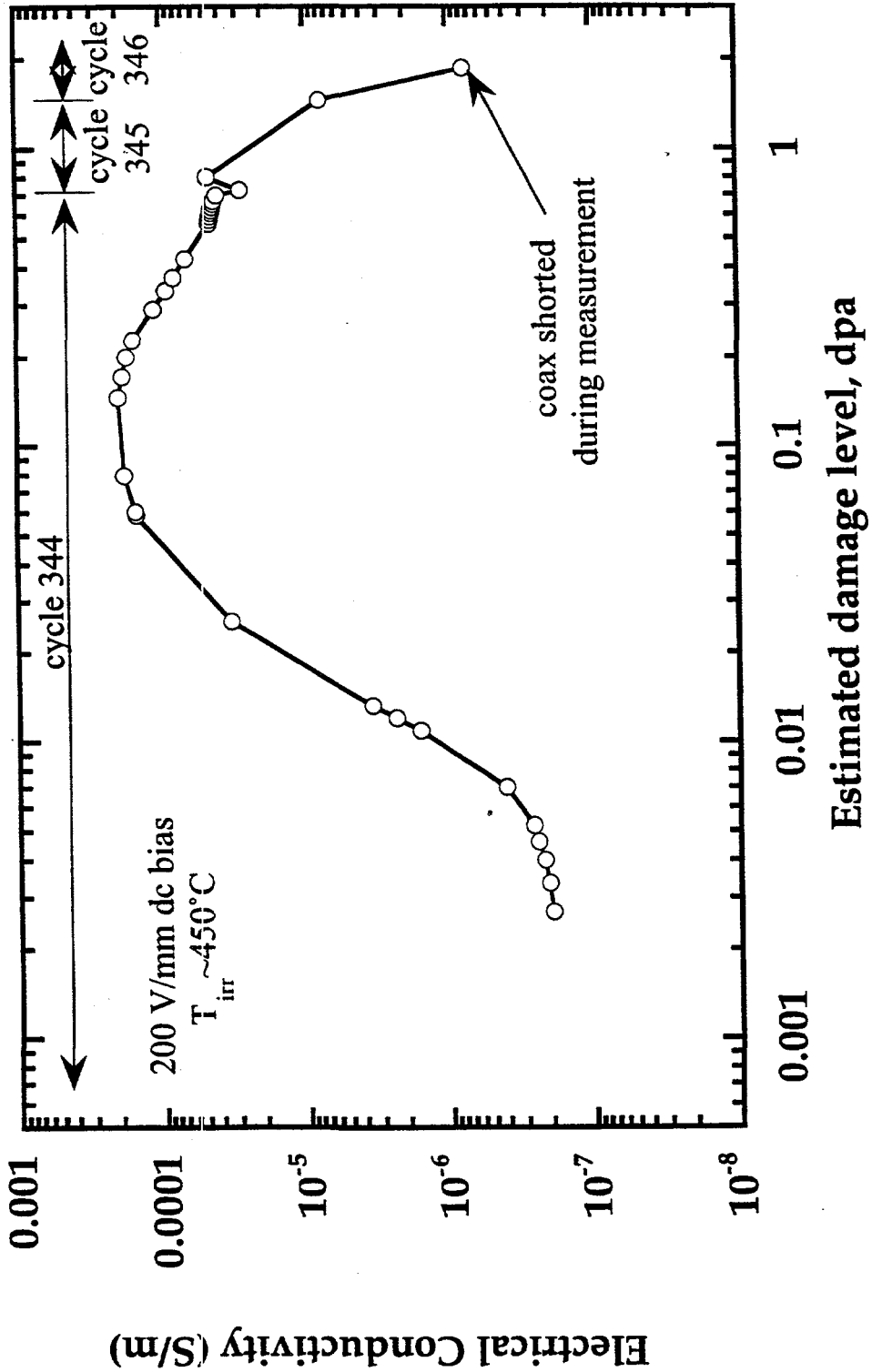
**Conductivity of Wesgo AL995 polycrystal alumina
Measured during full-power HFIR Irradiation (exp211)**



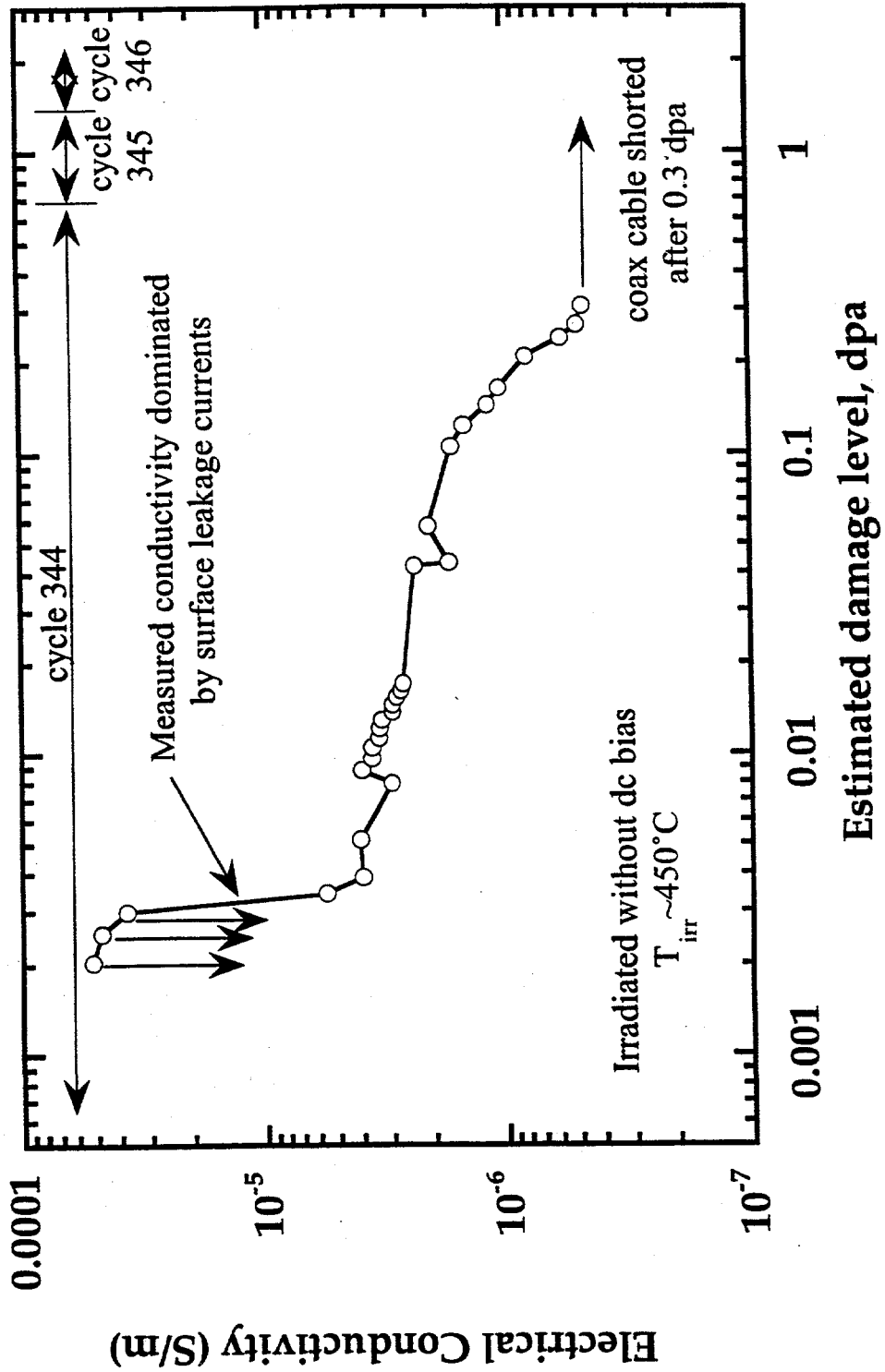
**Conductivity of Crystal Systems Sapphire
Measured during full-power HFIR Irradiation (exp212)**



Conductivity of Cr-doped Sapphire Measured during full-power HFIR Irradiation (exp213)



Conductivity of Kyocera SA100 Sapphire Measured during full-power HFIR Irradiation (exp215)



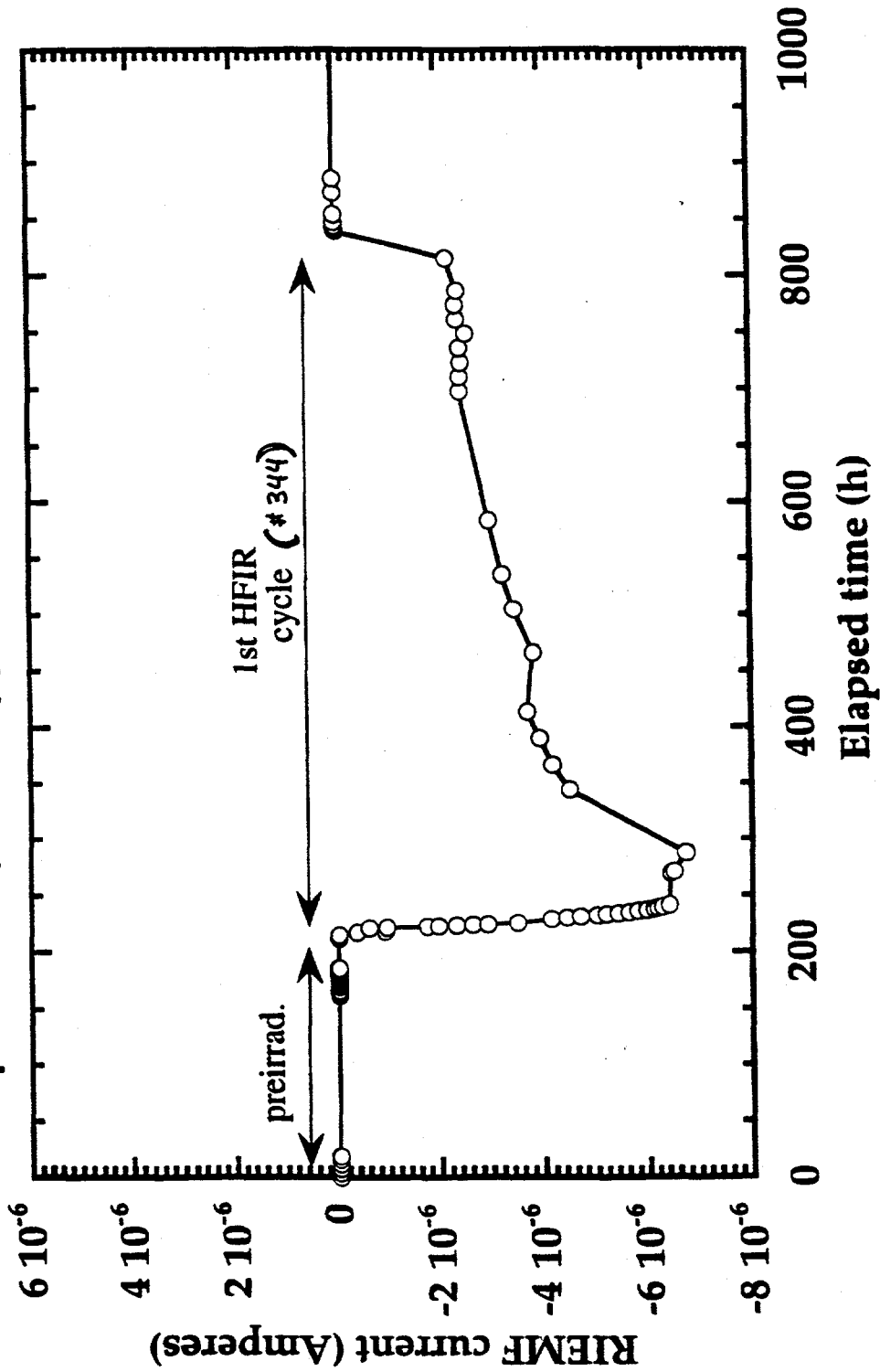
Summary of HFIR Electrical Conductivity Measurements at Startup

Position # and material	Electrical Conductivity (S/m)		
	In-core, reactor off (10 Gy/s, 60°C)	10% power (1-1.6 kGy/s, 170°C)	100% power (10-16 kGy/s, 450°C)
1. CSI sapphire, UV, a-axis	4x10 ⁻⁹	4x10 ⁻⁸	1.2x10 ⁻⁷
2. CSI sapphire, UV, c-axis	3x10 ⁻⁹	6x10 ⁻⁸	3x10 ⁻⁷
3. CSI sapphire, regular, c-axis	2x10 ⁻⁹	5x10 ⁻⁸	3x10 ⁻⁷
4. CSI sapphire, regular, a-axis	1.5x10 ⁻⁹	9x10 ⁻⁸	4x10 ⁻⁷
5. Vitox (99.9%)	(<7x10 ⁻⁸)*	(<4x10 ⁻⁷)*	1x10 ⁻⁶
6. Kyocera A480 (99.9%)	3x10 ⁻¹⁰	1x10 ⁻⁷	1x10 ⁻⁶
7. Wesgo AL300 (97%)	5x10 ⁻¹⁰	2x10 ⁻⁷	5x10 ⁻⁷
8. Kyocera A479 (99.0%)	3x10 ⁻¹⁰	6x10 ⁻⁸	3x10 ⁻⁷
9. Coors AD998 (99.8%)	3x10 ⁻¹⁰	1x10 ⁻⁷	---
10. Wesgo AL995 (99.5%)	3x10 ⁻¹⁰	6x10 ⁻⁸	8x10 ⁻⁷
11. Wesgo AL995 (99.5%)	4x10 ⁻¹⁰	4.5x10 ⁻⁸	2x10 ⁻⁷
12. CSI sapphire, regular, c-axis	2x10 ⁻⁹	6x10 ⁻⁸	3x10 ⁻⁷
13. Un. Carbide Cr-doped sapphire	1x10 ⁻⁹	7x10 ⁻⁸	2x10 ⁻⁷
14. Kyocera SA100, [1102]	3x10 ⁻⁹	7x10 ⁻⁸	2x10 ⁻⁷
15. Kyocera SA100, [1102]	(<1x10 ⁻⁷)*	(<1x10 ⁻⁶)*	(<3x10 ⁻⁶)*

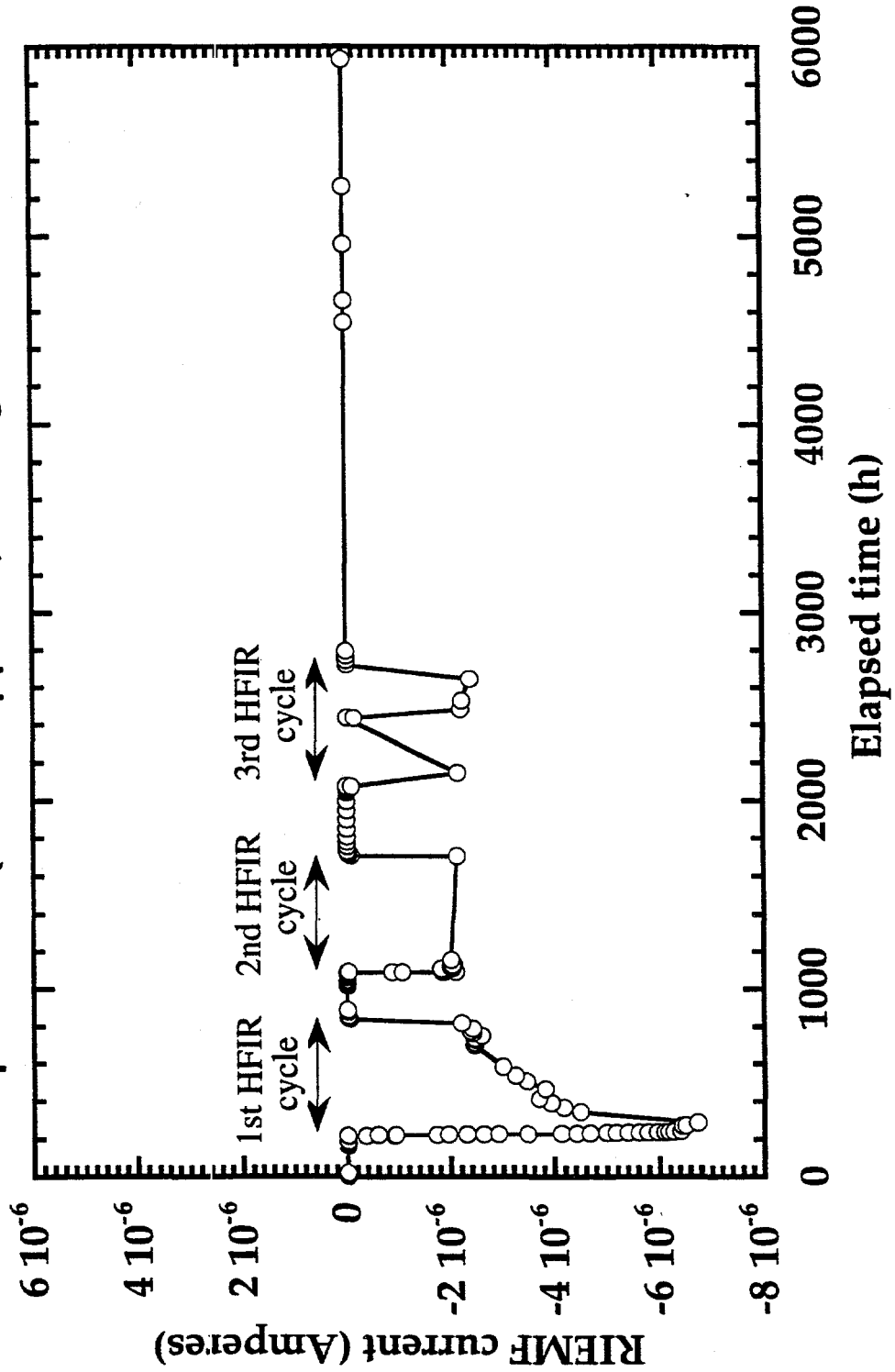
*values in parenthesis denote upper limits to bulk conductivity due to high surface leakage currents

- Conductivity of polycrystalline specimens was ~10x lower than single crystal specimens at 10 Gy/s
- RIC values for polycrystal and single crystal specimens became comparable at high dose rates (1-16 kGy/s)

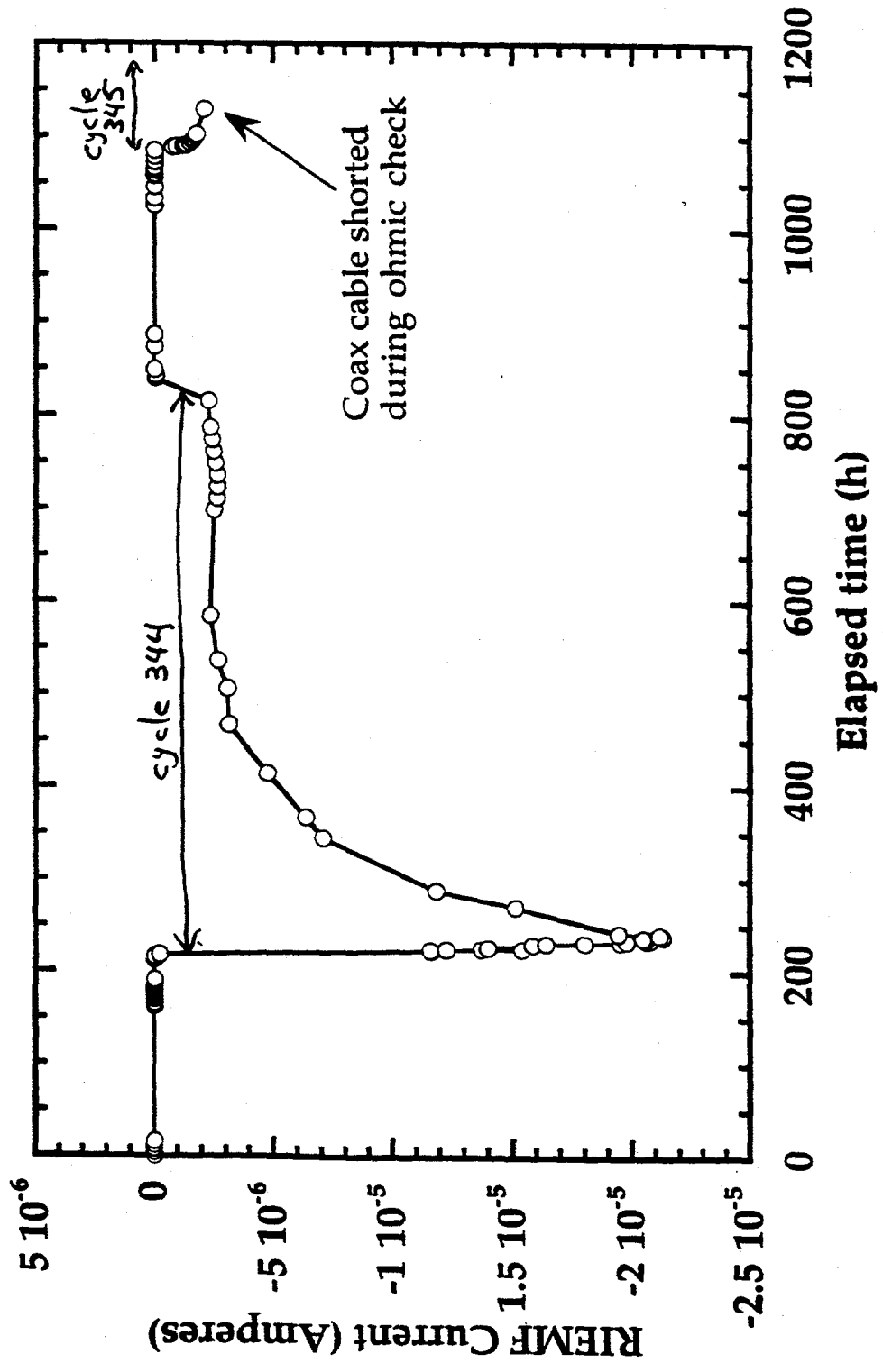
exp22/all (CSI Sapphire, UV grade, c-axis)



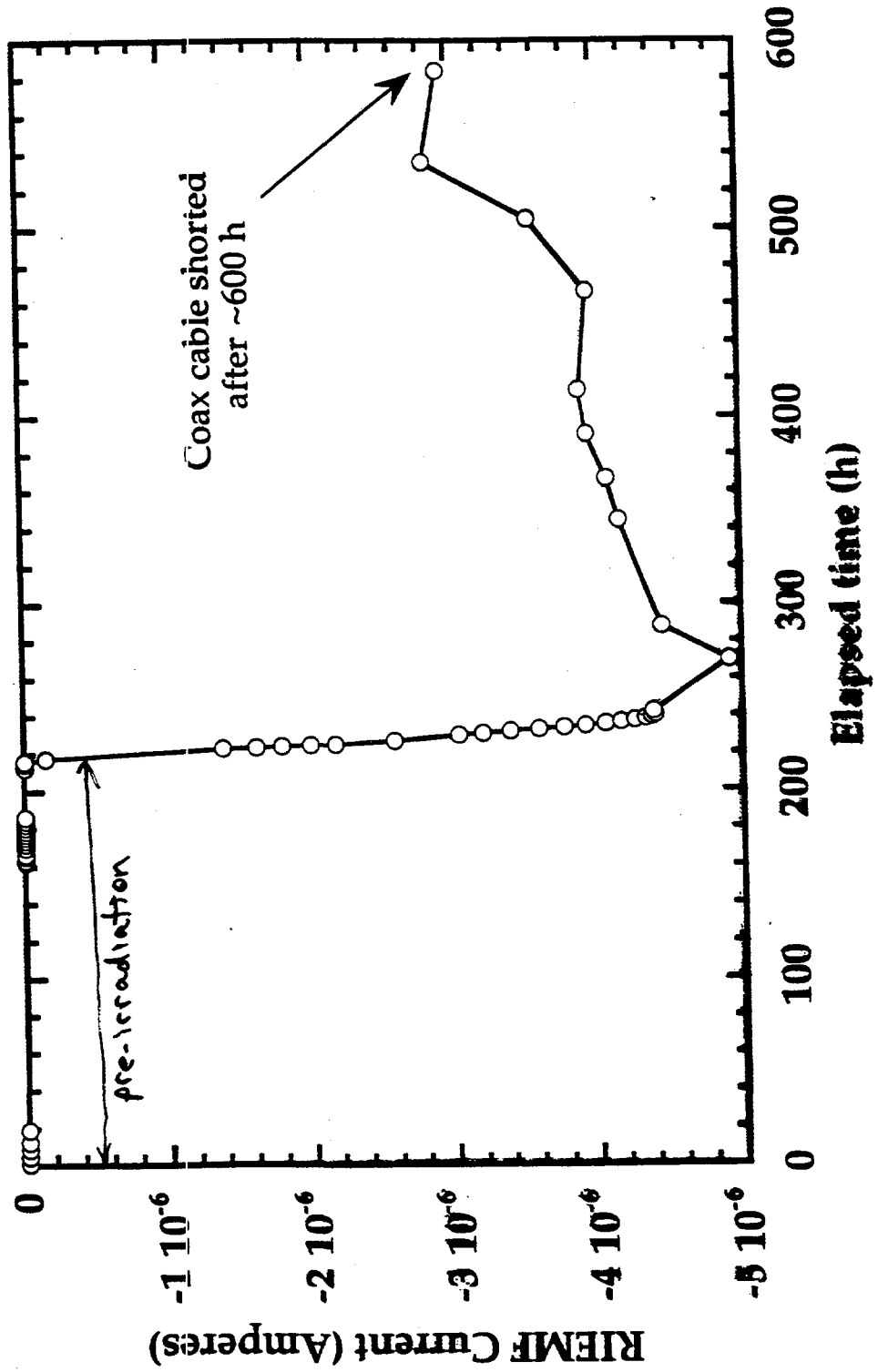
exp22/all (CSI Sapphire, UV grade, c-axis)



exp28/all (Kyocera A479 polycrystal alumina)

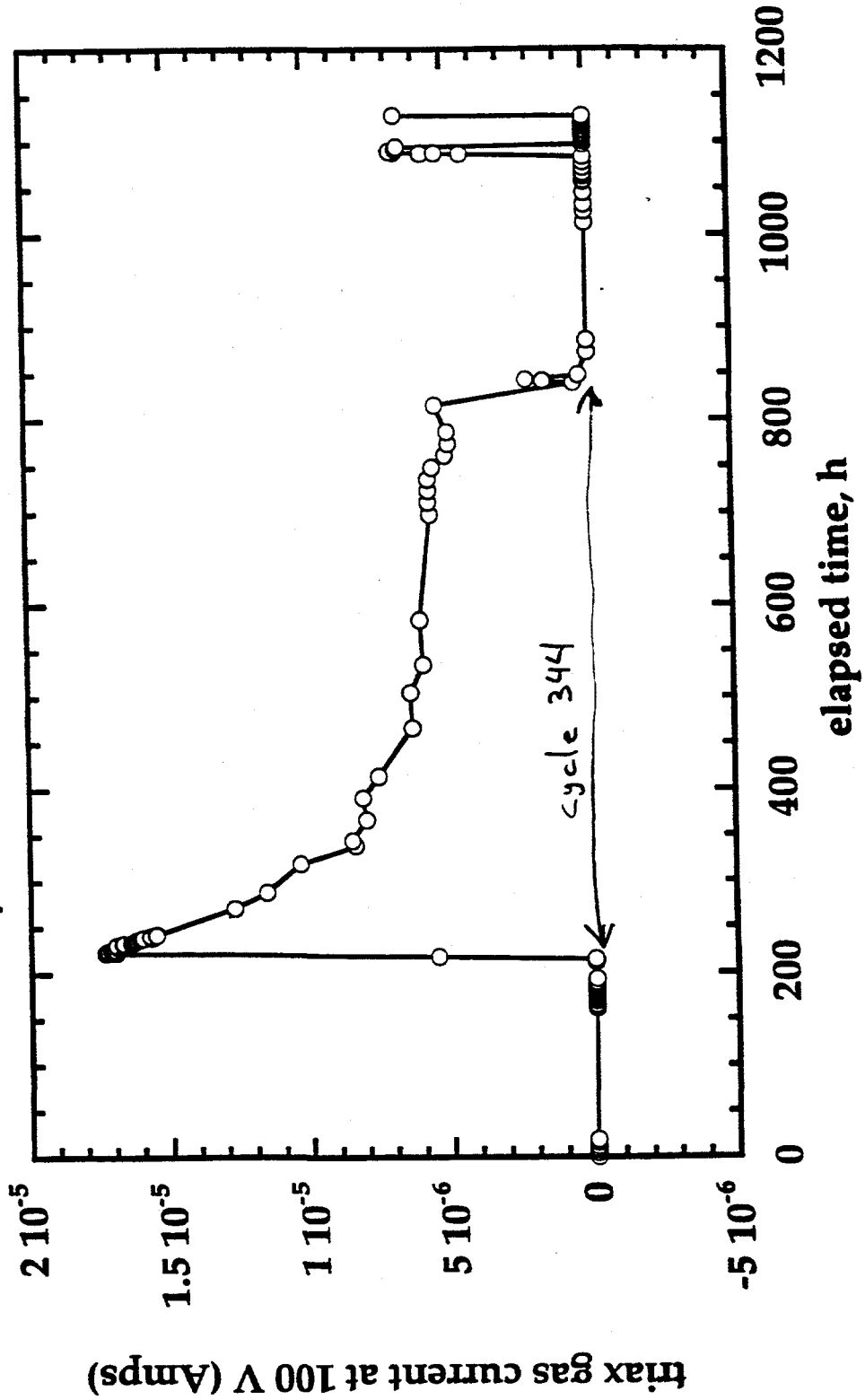


exp212/all (CSI sapphire, regular grade, c-axis/no bias)



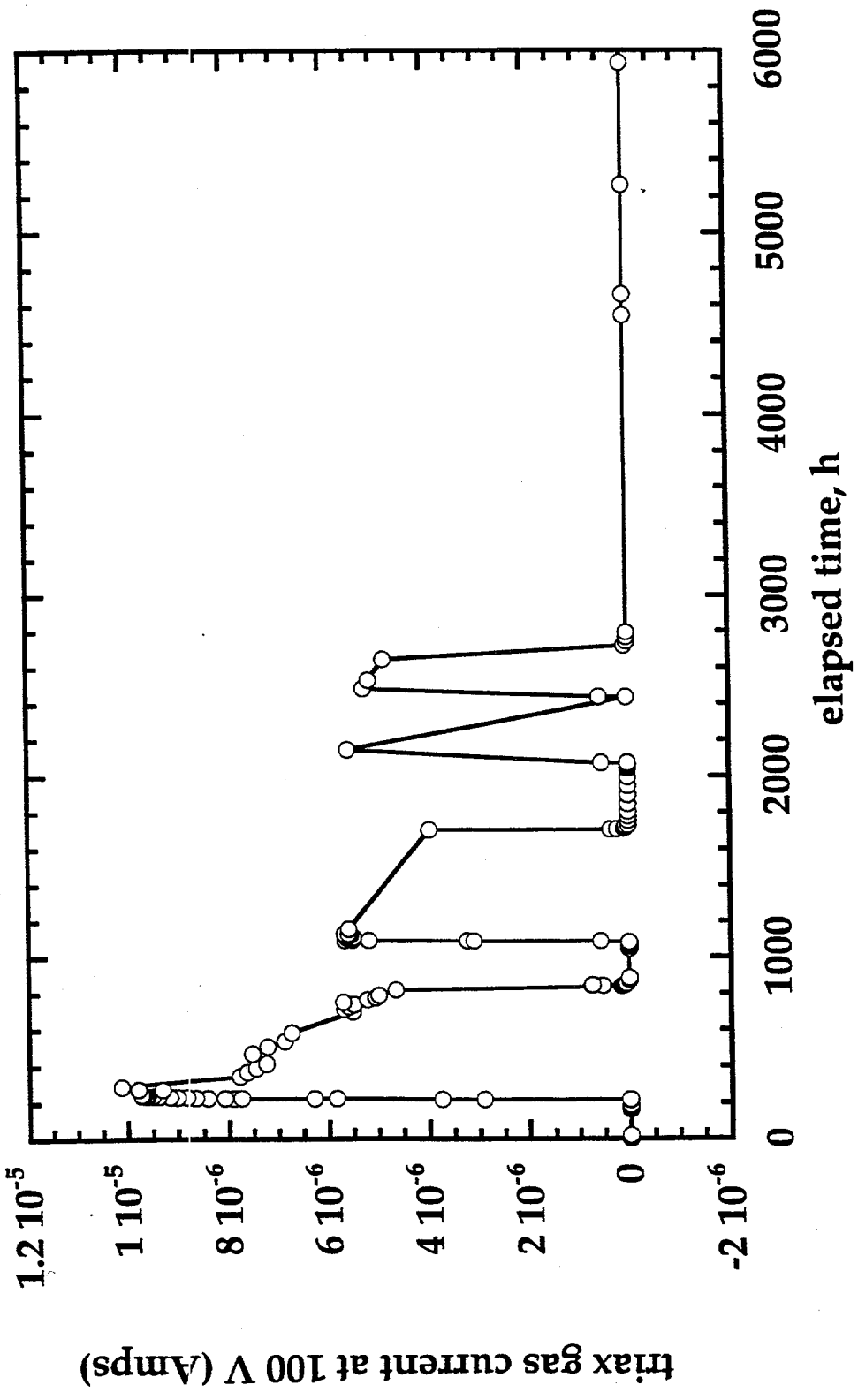
—○— triax gas current at 100 V

exp27cum. 2:46:12 PM 4/18/97



—○— triax gas current at 100 V

exp22cum. 2:40:31 PM 4/18/97



—○— triax gas current at 100 V

exp23cum. 2:42:09 PM 4/18/97

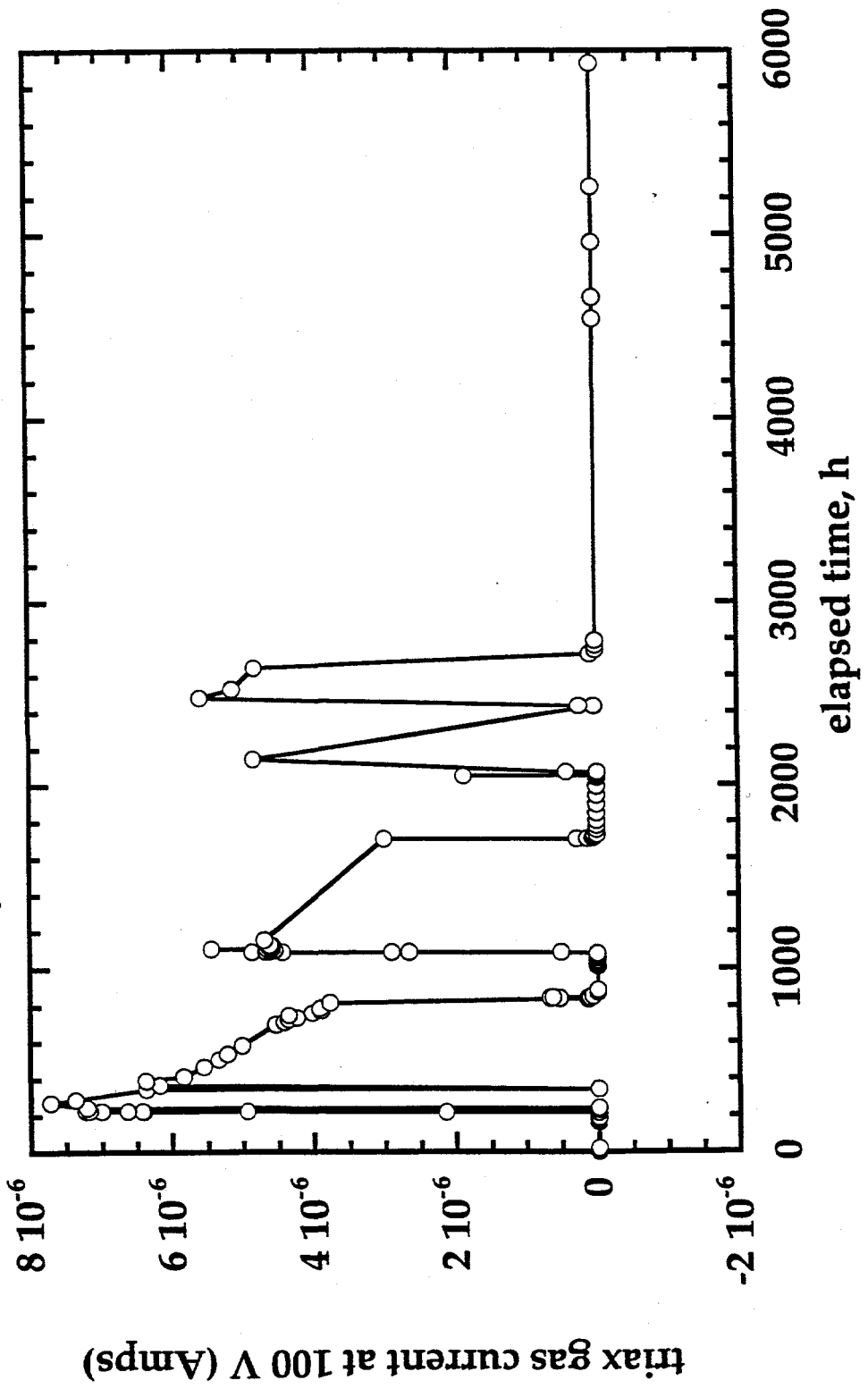


Table 1. Summary of measured in-core conductivities (S/m) for the coax cables at the start of the HFIR irradiation (from the negative quadrant of the ohmic check plots). The data marked with an asterisk denote values that are an upper limit to the bulk conductivity due to low (<1 M Ω) surface leakage resistances.

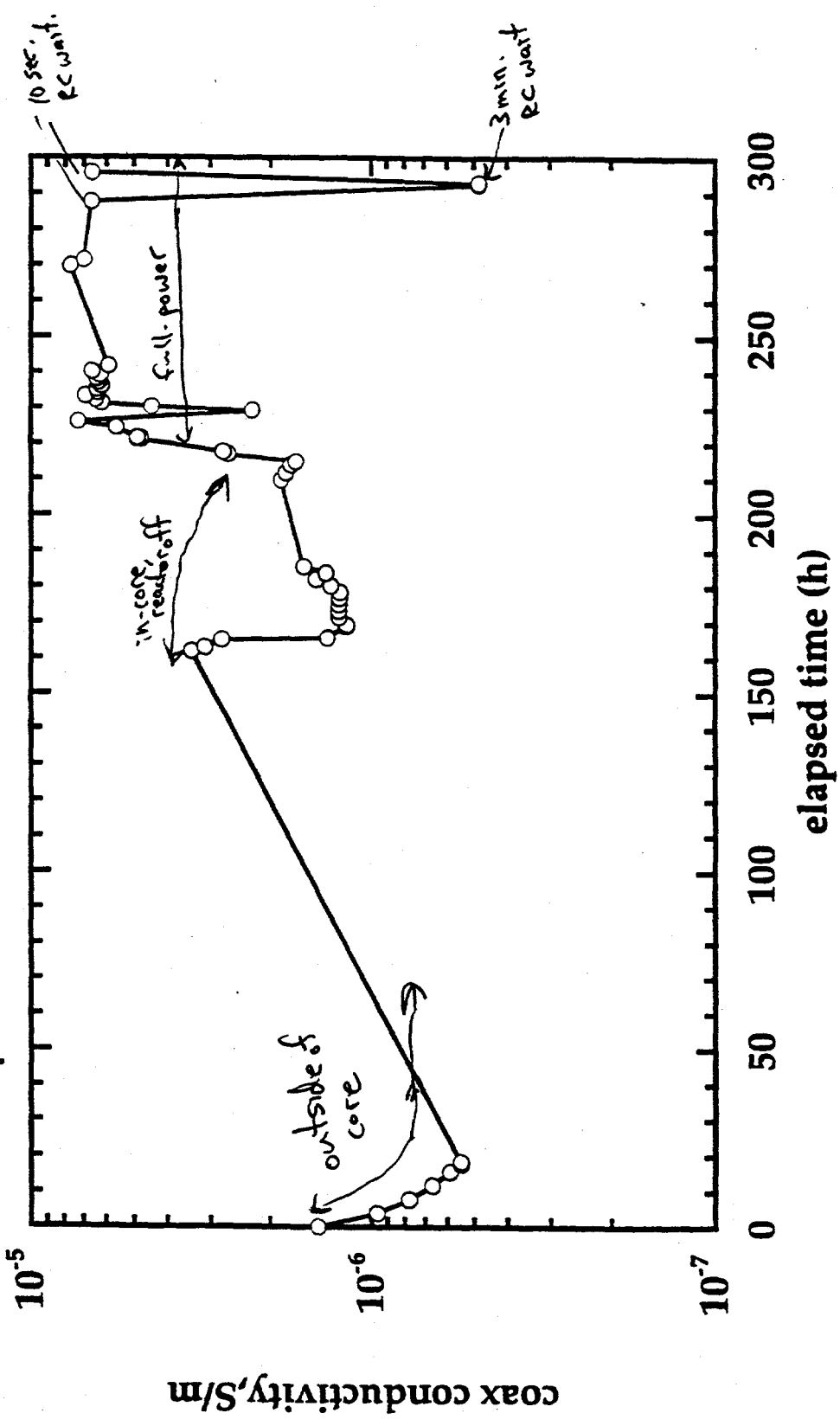
HFIR position	Material	Preirradiation (10 Gy/s, 50°C)	10% power, 0 dpa (1-1.6 kGy/s, 170°C)	full power, 0 dpa (10-16 kGy/s, 440-500°C)	full power, 1st cycle avg. (10-16 kGy/s, 440-500°C)
1	UV sapphire, a-axis	(<1.5x10 ⁻⁶)*	~6x10 ⁻⁶	~6x10 ⁻⁶	~6x10 ⁻⁶
2	UV sapphire, c-axis	(<2x10 ⁻⁷)*	~1x10 ⁻⁶	~4x10 ⁻⁶	~2x10 ⁻⁵
3	regular sapphire, c-axis	~2x10 ⁻⁹	~2x10 ⁻⁷	~5x10 ⁻⁷	~1x10 ⁻⁶
4	regular sapphire, a-axis	(<5x10 ⁻⁸)*	~4x10 ⁻⁷	~3x10 ⁻⁶	---
5	Vitox	(<4x10 ⁻⁵)*	(<2x10 ⁻⁵)*	(<5x10 ⁻⁵)*	(<5x10 ⁻⁵)*
6	Kyocera A-480	(<1.5x10 ⁻⁸)*	~2.5x10 ⁻⁷	~2x10 ⁻⁶	---
7	Wesgo AL300	~2x10 ⁻¹⁰	~8x10 ⁻⁸	~5x10 ⁻⁷	~5x10 ⁻⁷
8	Kyocera A-479	(<1x10 ⁻⁷)*	~4x10 ⁻⁷	~8x10 ⁻⁷	~4x10 ⁻⁷
9	Coors AD998	(<3x10 ⁻⁷)*	~2x10 ⁻⁷	~5x10 ⁻⁷	~4x10 ⁻⁷
10	Wesgo AL995	(<1x10 ⁻⁷)*	~1x10 ⁻⁷	~1x10 ⁻⁵	---
11	Wesgo AL995	~1.5x10 ⁻⁹	~5x10 ⁻⁸	~5x10 ⁻⁷	~2x10 ⁻⁷
12	regular sapphire, c-axis	~1x10 ⁻⁹	~7x10 ⁻⁸	~1x10 ⁻⁶	~2x10 ⁻⁶
13	Cr-doped sapphire	(<2x10 ⁻⁸)*	~2x10 ⁻⁷	~5x10 ⁻⁷	~2x10 ⁻⁶
14	SA100 sapphire (1102)	~5x10 ⁻¹⁰	~5x10 ⁻⁸	~3x10 ⁻⁷	---
15	SA100 sapphire (1102)	(<5x10 ⁻⁵)*	(<7x10 ⁻⁵)*	(<1x10 ⁻⁴)*	(<3x10 ⁻⁵)*

↑ 0.5-2 x10⁻⁷ S/m 0.3-5 x10⁻⁶ S/m

dominated by specimen + scanner card leakage resistances

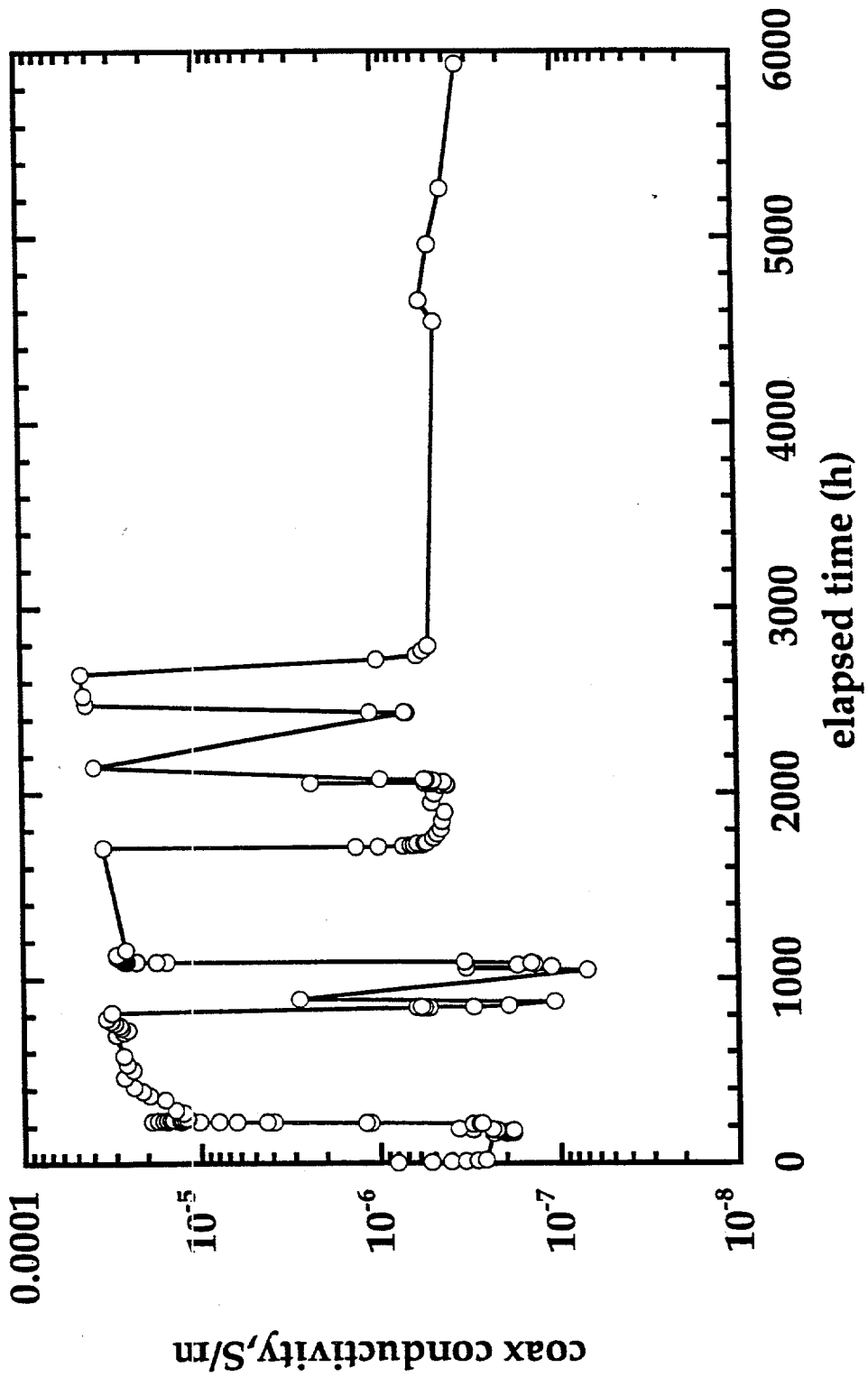
—○— coax conductivity, S/m

exp21/master/all 12:20:45 PM 3/4/97



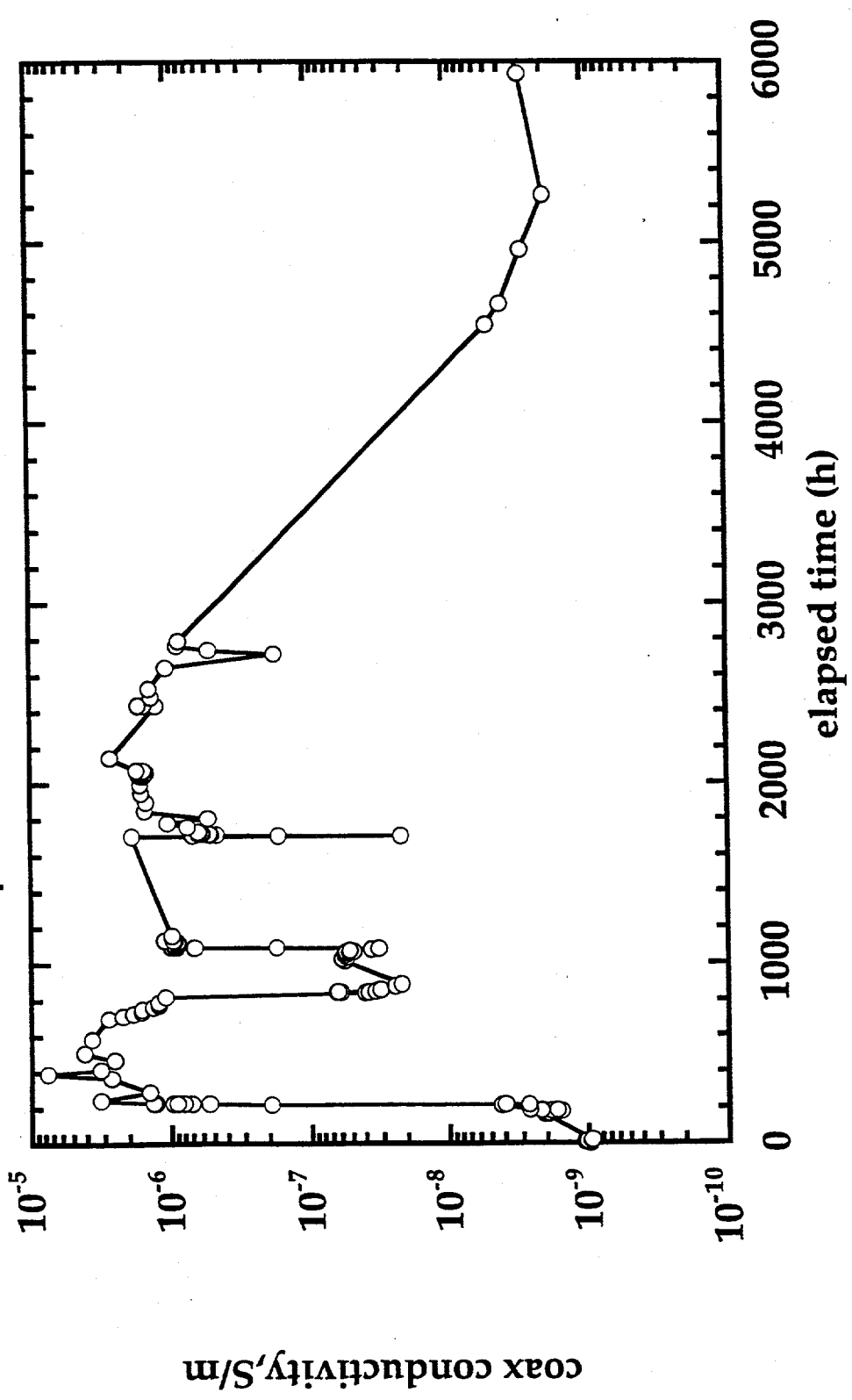
—○— coax conductivity, S/m

exp22cum. 5:30:21 PM 4/11/97



—○— coax conductivity, S/m

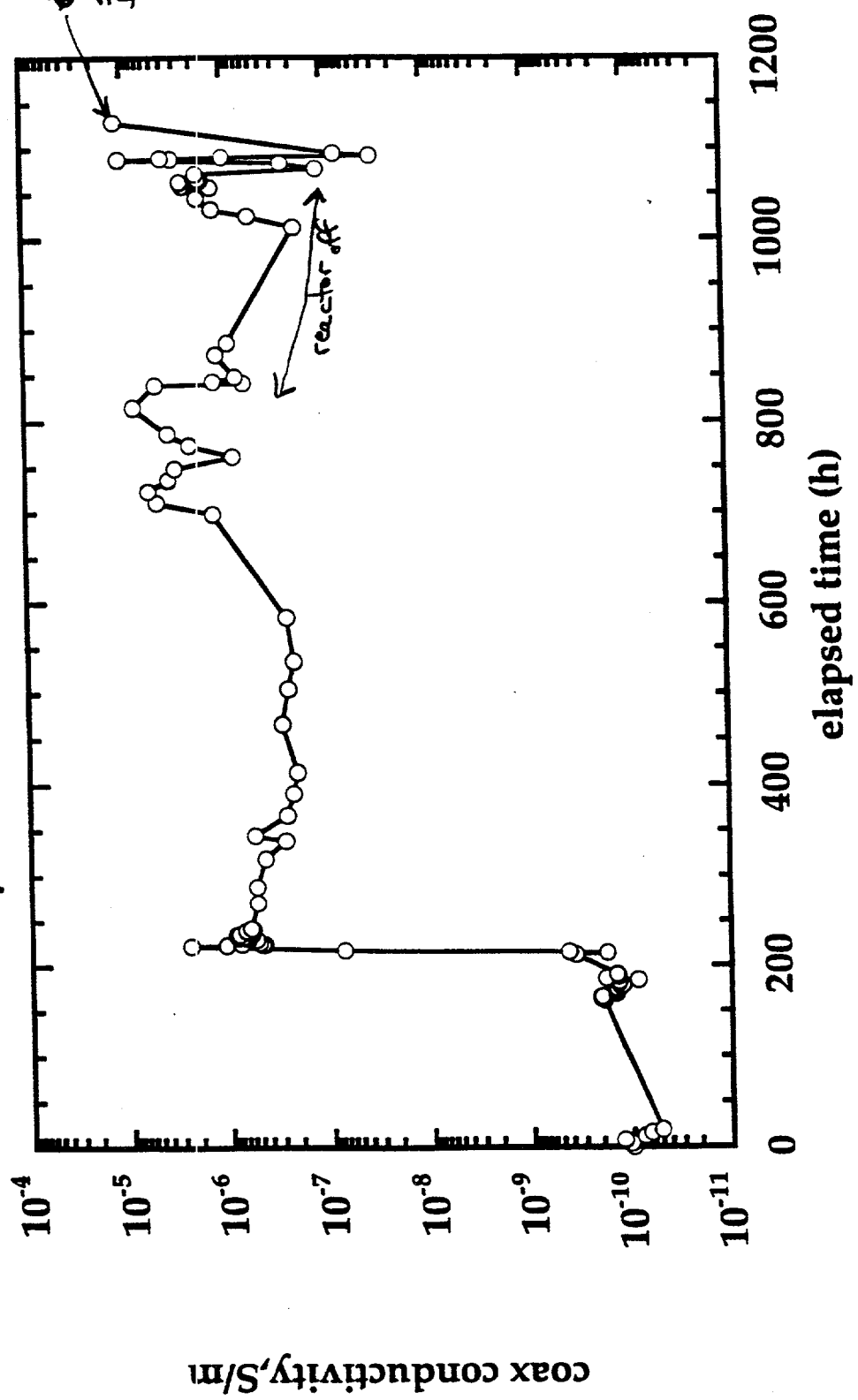
exp23cum. 3:03:16 PM 3/4/97



Wesgo AL300 coax cable

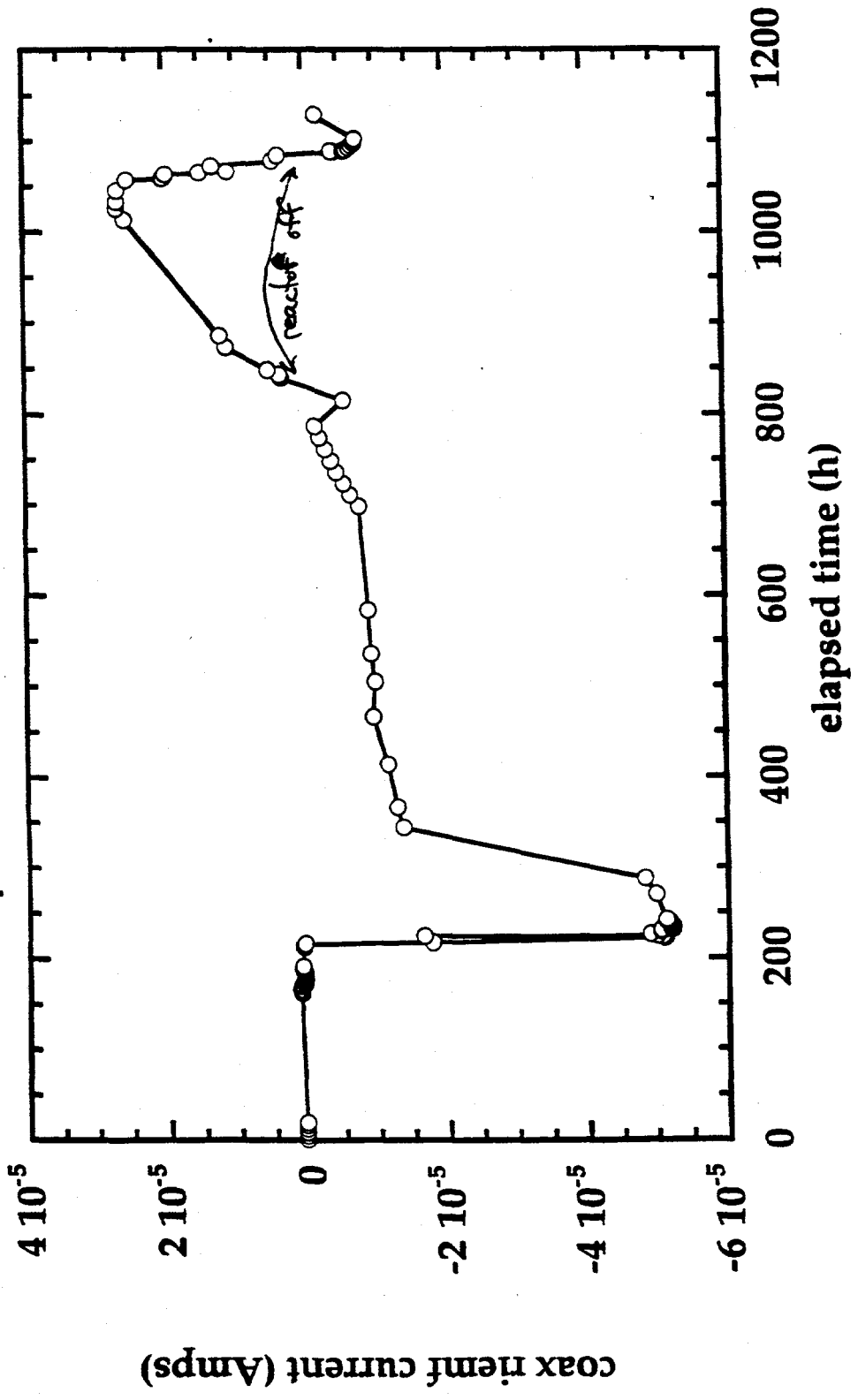
exp27 cum. 2:33:21 PM 3/5/97

—○— coax conductivity, S/m



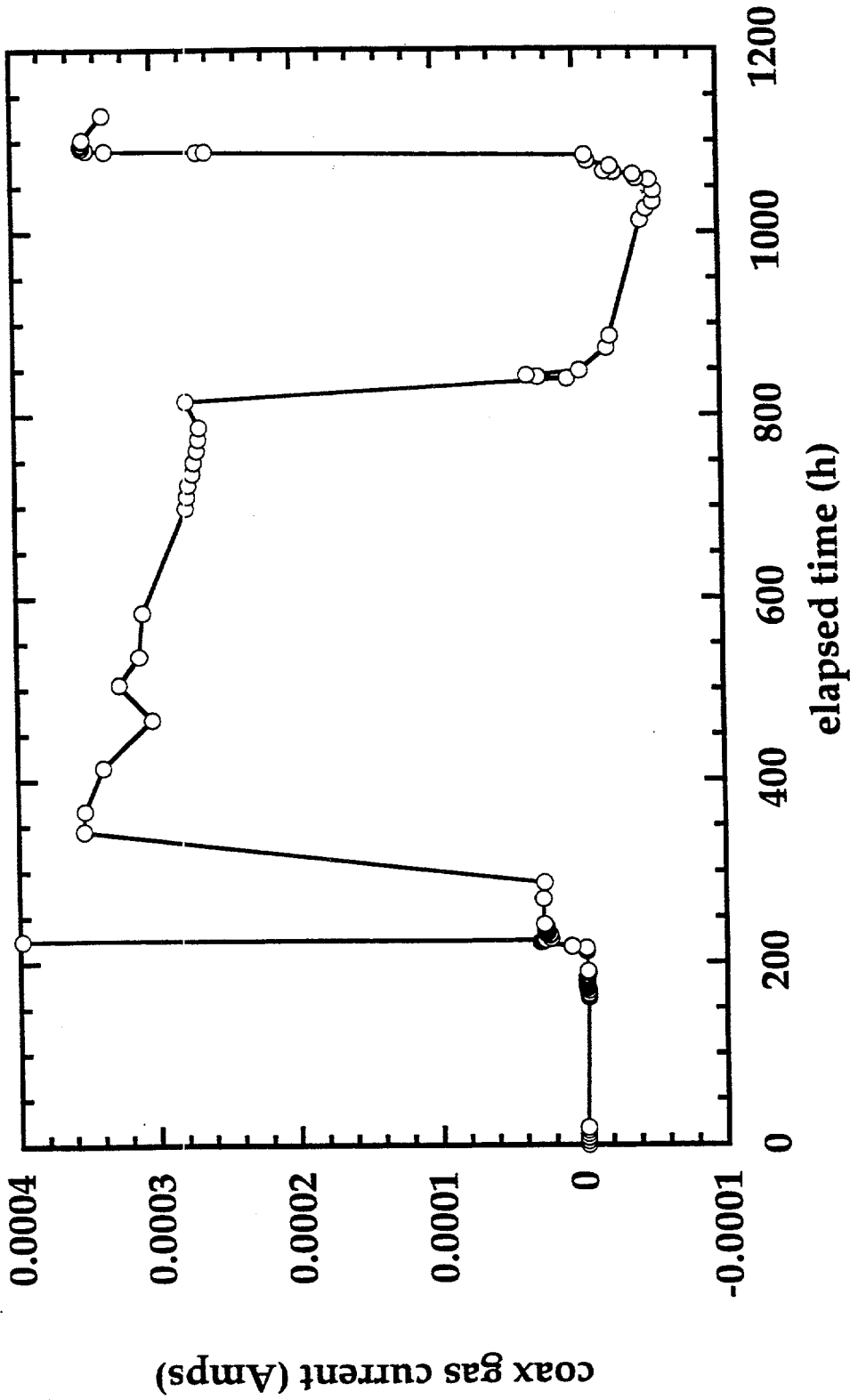
—○— coax riemf

exp28cum. 3:52:04 PM 4/14/97



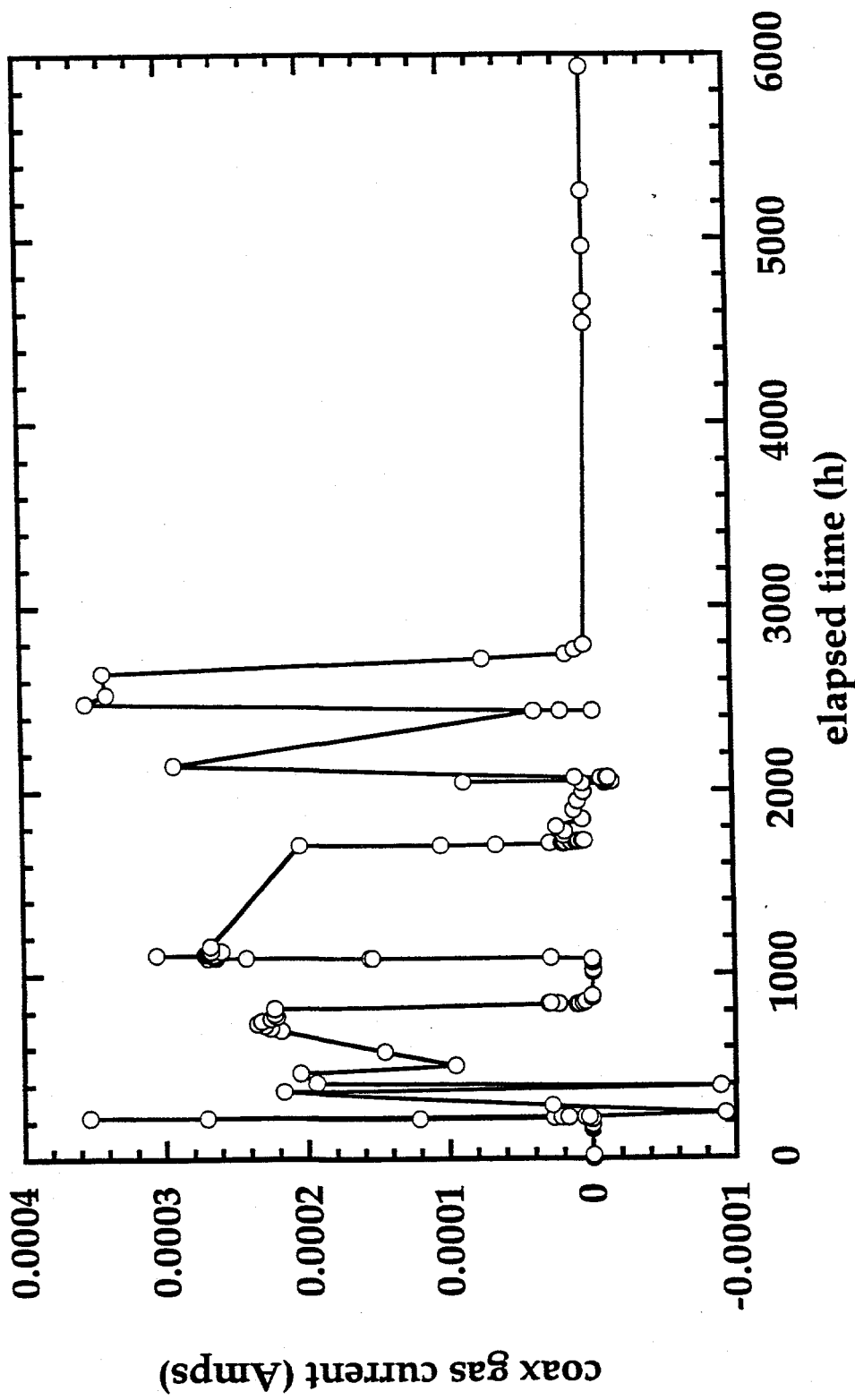
—○— coax gas current

exp28cum. 3:52:04 PM 4/14/97



—○— coax gas current

exp23cum. 11:07:22 AM 4/15/97



Summary of Key Results

- The measured RIC values for alumina are in good agreement with previous studies. The quantitative level of RIC decreased slightly following irradiation, in agreement with previous irradiation studies performed without an applied electric field during irradiation
- decrease in conductivity may be attributable to increased electron-hole trapping at radiation-produced defects
- Shorting of several of the coax cables is attributed to dielectric breakdown of the glass used to seal the ends of the cables, based on tests performed on several non-irradiated control coax cables at 20-200°C (i.e., up to the maximum expected operating temperature of the glass seals in HFIR)
- the dielectric breakdown strength (DBS) decreased with increasing temperature, and the breakdown was confirmed to occur in the glass ^{temperature DBS for} _{glass @ 20°C is 10-100 MV/m}
* DBS > 1100V for short-term tests at 20°C (max glass seal E field ~ 8 MV/m)
- the DBS was ~600 V for short-term tests at 200°C (positive voltage only)
- the DBS was ~500 V for short-term tests at 200°C, alternating positive and negative voltage

- approximately half of the cables failed within 2 days at 200°C for a continuously applied voltage of 300 V ^{corresponding} _{Max E field in glass seal ≈ 2 MV/m}

* from in-situ diagnostic tests, cable failure is not associated with catastrophic RIED in the ceramic samples

- Simple calculations suggest that the observed non-ohmic electrical behavior during HFIR irradiation is due to preferential attraction of ionized electrons
- the capsule gas to the unshielded low-side electrical leads

Conclusions and Future Work

- Catastrophic radiation-induced electrical degradation ($\sigma_e > 10^{-4}$ S/m) was not been observed in any of the HFIR-irradiated high-purity alumina specimens (~3 dpa maximum dose); a slight increase in the resistivity was observed in several specimens
- A moderate amount of RIED that apparently is not due to surface leakage currents was observed in the Cr-doped sapphire specimen; the full-power conductivity increased by nearly 3 orders of magnitude after the first few days of irradiation and then gradually decreased over the ensuing 3 months
- Previous reports of RIED in alumina may be due to
 - 1) charge storage effects (nonpenetrating electron irradiation studies)
 - 2) experimental artifacts (surface leakage currents, cracked specimens, etc.)
- Non-ohmic electrical behavior was observed in the irradiated specimens - analysis suggests it is due to ionized gas effects (and RIEMF)
- Capsule disassembly and post-irradiation examination is currently in progress
 - electrical resistivity vs. temperature; possibly TEM
 - examination of shorted coax cables



In-situ Measurements Electrical Conductivity of Al_2O_3 and MgO in JRR-3

K. Noda, T. Tanifuji, Y. Katano and T. Nakazawa

Japan Atomic Energy Research Institute
Tokai-mura, Naka-gun, Ibaraki-ken, 319-11 Japan

IEA Workshop on Radiation Effects in Ceramic Insulators

Omni Netherland Plaza Hotel, Cincinnati, OH, USA
May 7-8, 1997

Many ceramic materials will be used as electrical insulator materials for various diagnostics components, the first wall current break, reduction of electromagnetic force to various in-vessel components, the RF windows, etc. in D-T fusion reactors. These ceramic materials will be subjected to severe neutron and gamma-ray irradiation during operation of the fusion reactors. Severe permanent increase in electrical conductivity of ceramic insulators, i.e., RIED has been reported to occur for irradiation under applied electric field in addition to RIC. Mechanism of RIED still remain uncertain.

In-situ electrical conductivity measurements under reactor irradiation were carried out for Al_2O_3 and MgO specimens using JRR-3 at JAERI. The DC three terminal method with guard ring was used to evaluate the conductivity of the specimens. The specimens were irradiated in the temperature range 573 to 723 K for two cycles (about 0.2 dpa) with an applied DC electric field of 100V/mm in flowing He and N_2 mixture gas in JRR-3. The measured currents, i.e., center, guard and HV source currents, increased with reactor power. The HV source current was much larger than the center current. This large HV source current was considered to be attributed to leak current due to photoelectrons through ionized gas atmosphere in the irradiation capsule. On the other hand, the influence of the leak current on the center current, which prevented proper evaluation of the specimen conductivity from the center current data, was considered to be not so large.

The center current at the reactor shutdown decreased substantially, to be much smaller than that during the reactor operation. Thus, it was considered that RIED did not occur or was negligibly small level up to 0.2 dpa for the Al_2O_3 and MgO specimens.

The conductivity of the Al_2O_3 specimen evaluated from the center current data at various reactor powers in JRR-3 was in good agreement with the other RIC data of high-purity Al_2O_3 .

In-situ Measurements Electrical Conductivity of Al₂O₃ and MgO in JRR-3

K. Noda, T. Tanifuji, Y. Katano and T. Nakazawa

**Japan Atomic Energy Research Institute
Tokai-mura, Naka-gun, Ibaraki-ken, 319-11 Japan**

IEA Workshop on Radiation Effects in Ceramic Insulators

**Omni Netherland Plaza Hotel, Cincinnati, OH, USA
May 7-8, 1997**

Experimental Procedure

Materials

Materials	Form	Dimension(mm)	Annealing	Vendor
1. Al ₂ O ₃	Single crystal	8.5 φ x 0.2t	1273K x 4h in air	Kyosera SA 100, c-axis
2. MgO	Single crystal	8.5 φ x 0.2t	1273K x 6h in oxgen atmosphere	Tateho T98, {100}

Irradiation condition

● Neutron:

JAERI Tokai; JRR-3

Thermal flux; $2 \times 10^{18} \text{n/m}^2 \cdot \text{s}$

Fast flux; $0.5 \times 10^{18} \text{n/m}^2 \cdot \text{s}$, γ -ray level; 3.4 kGy/s

Dose; 0.1dpa/cycles, Total dose; about 0.2 dpa

Temperature range; 573K - 723K in He+ N₂ gas mixtures(Average gas flow ; 2 - 2.5ml/s)

● γ -ray:

Energy; ⁶⁰Co source 1.17 and 1.33 MeV

Dose rate; 5Gy/s

Total dose; 1.4×10^5 Gy

Irradiation temperature: 573K

In-situ measurement method

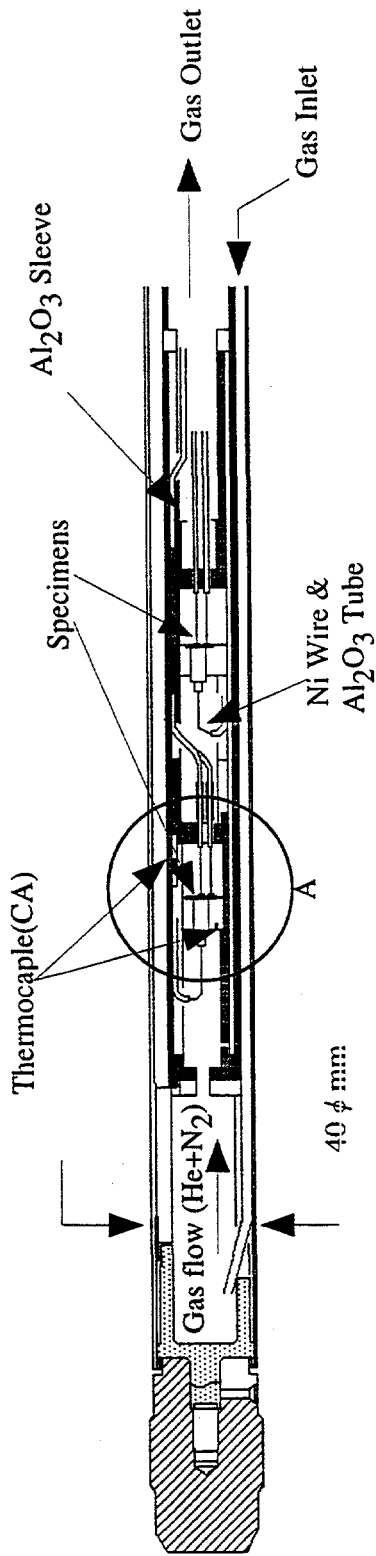
Tree-terminal electric guard system

DC fields ; 100V/mm

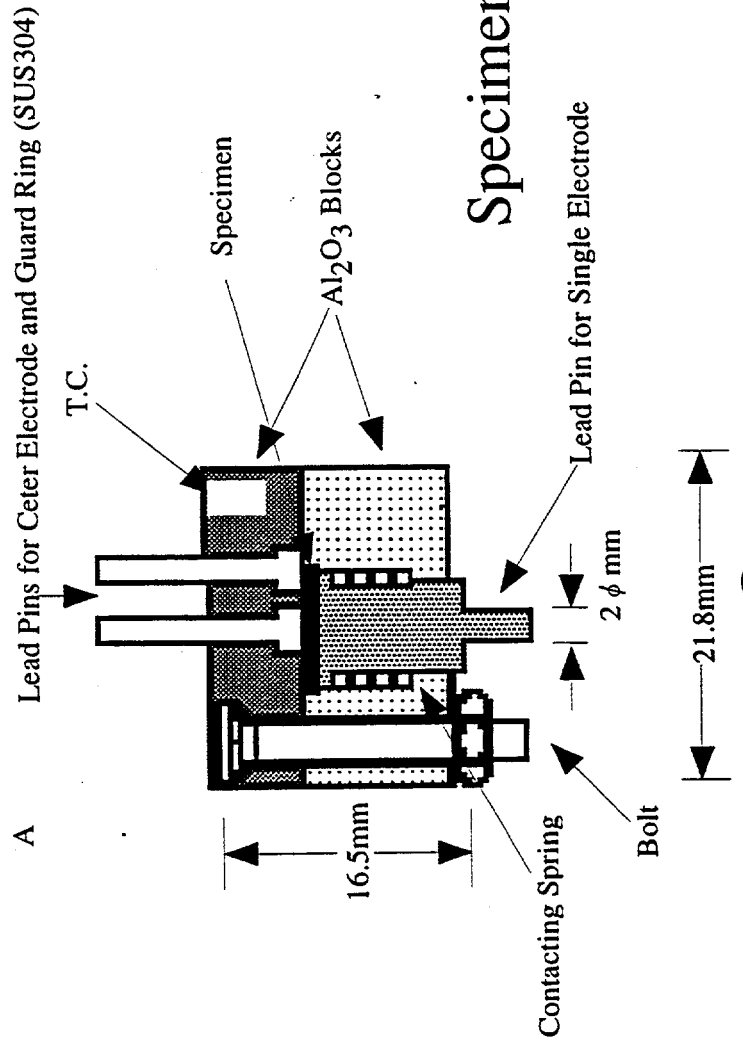
Current measurement; Keithley 6517 high-resistance electrometer (center and guard current)

Keithley 237 source measure unit (HV source current)

JRR-3 Irradiation Capsule and Specimen Holder

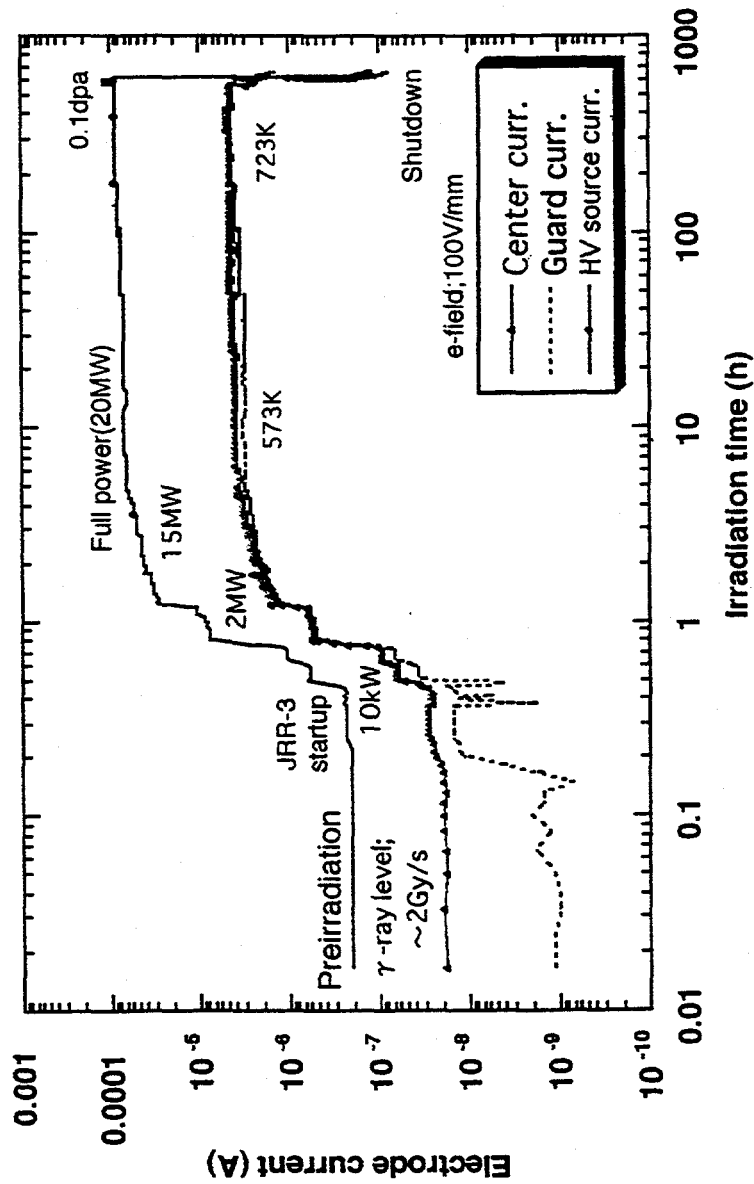


Capsule

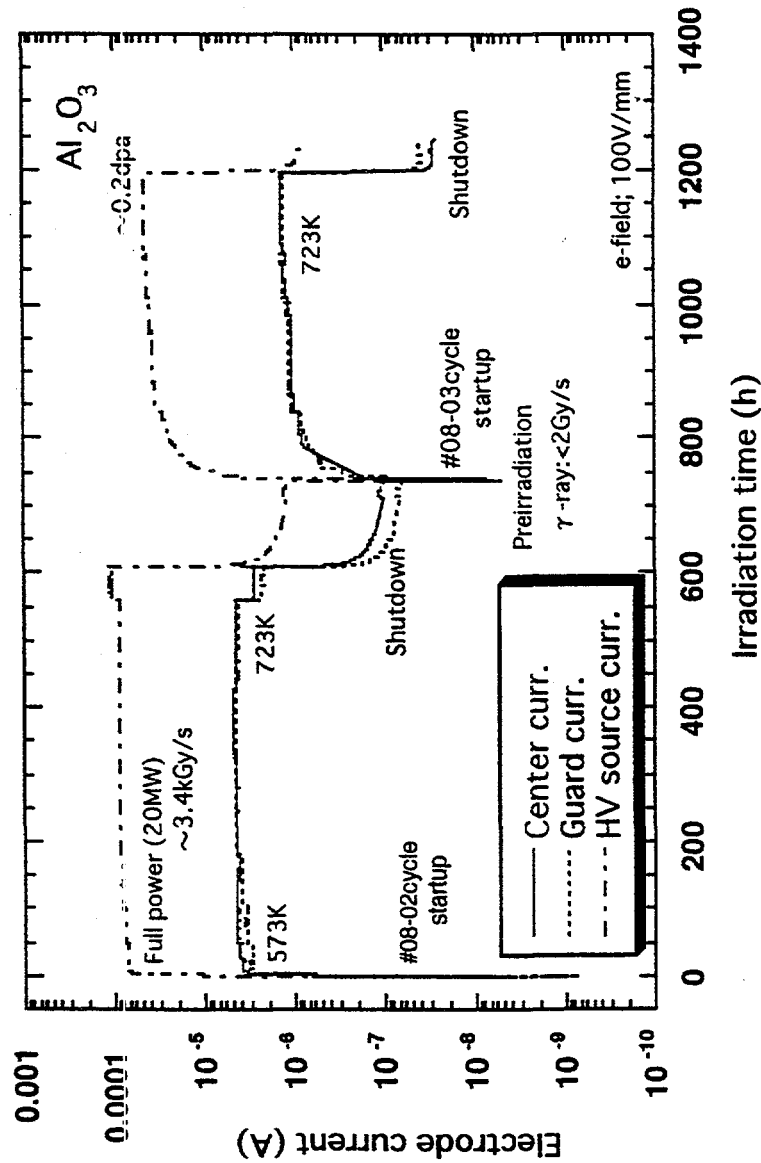


Specimen Holder

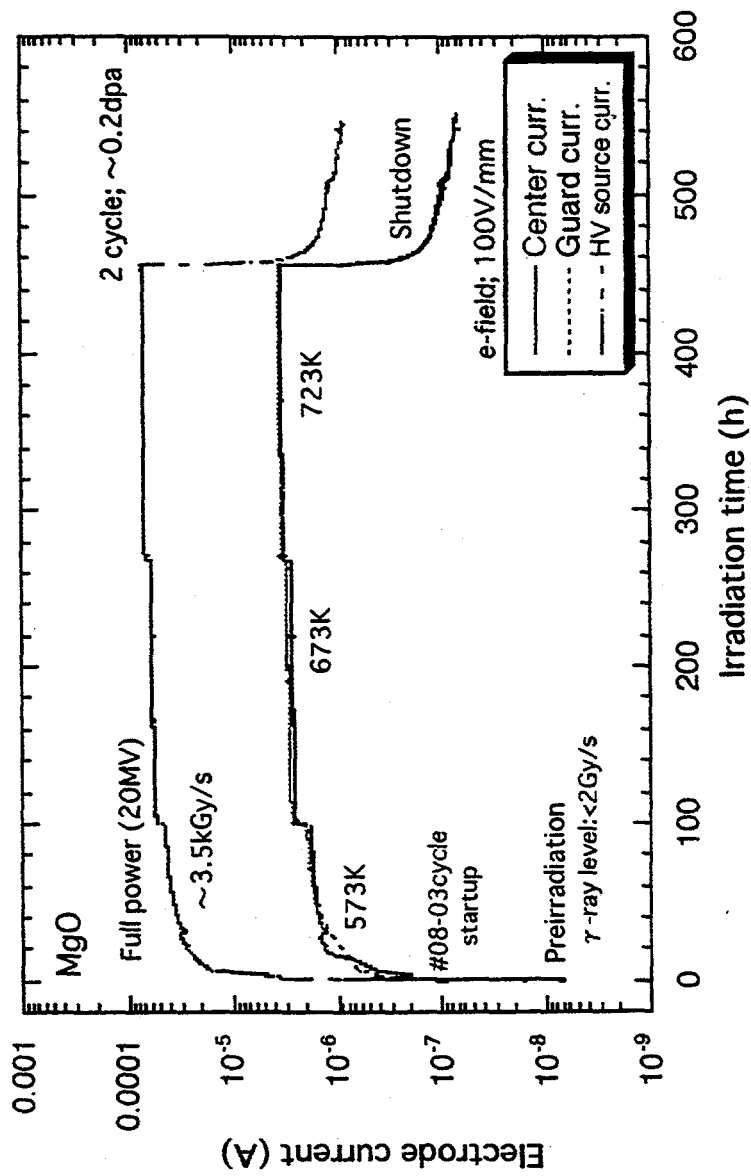
Behavior of center, guard and HV source currents for Al₂O₃ specimen in the first irradiation cycle



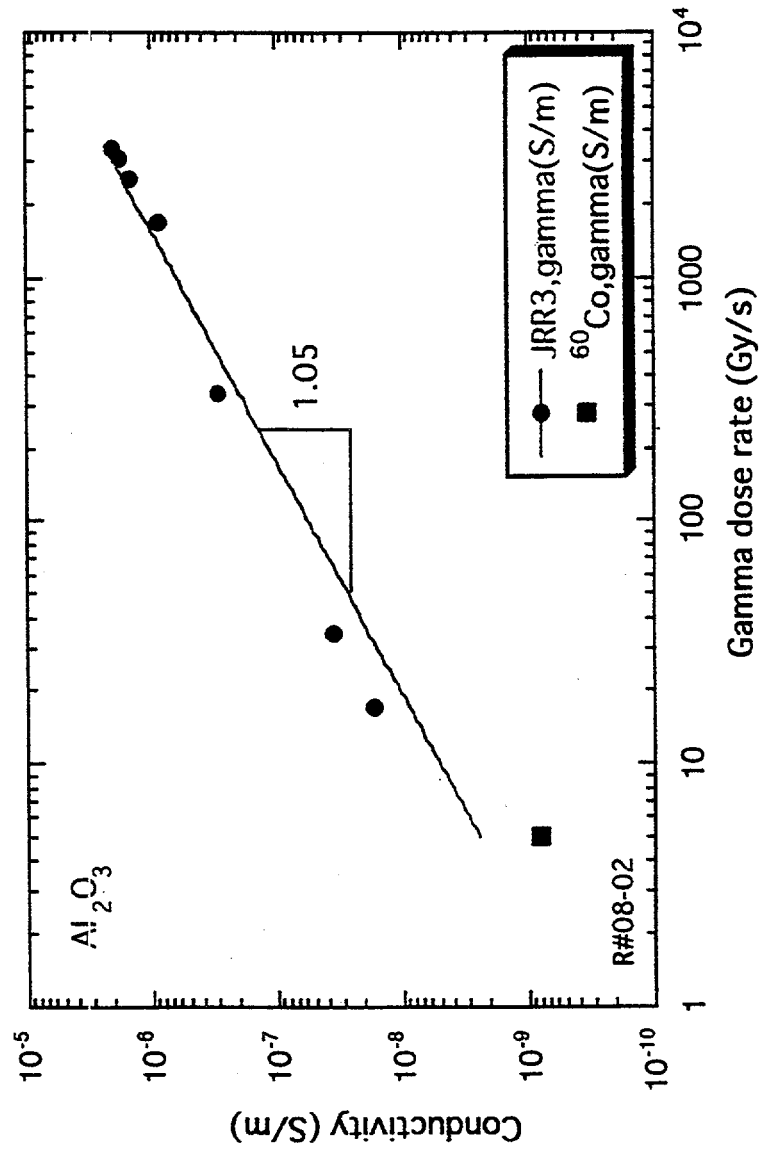
*Center, guard and HV source currents for Al₂O₃ specimen
in the first and the second irradiation cycles
versus the irradiation time*



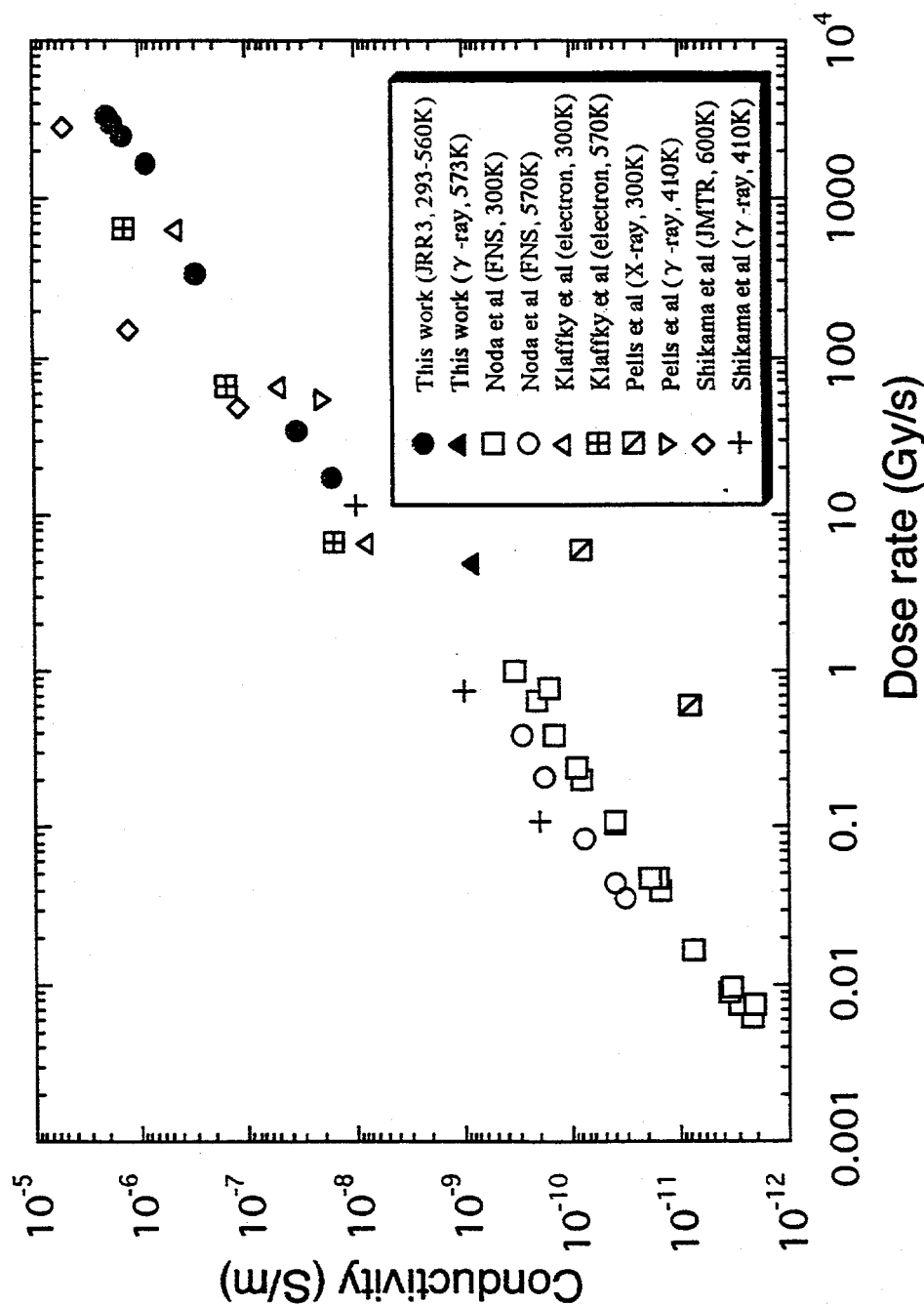
*Center, guard and HV source currents for the MgO specimen
in the second irradiation cycle versus the irradiation time*



Conductivity calculated for Al₂O₃ specimen as a function of gamma-ray dose rate evaluated from the reactor power



Comparison of dose rate dependence of conductivity calculated from center current in JRR-3 data for Al₂O₃ specimen in the present study with the other RIC data of Al₂O₃



Neutron RIED experiment at Mol

E.R.Hodgson

Euratom/CIEMAT Fusion Association, Madrid, Spain

Irradiation will be performed in the Mol BR1 air cooled reactor at 350, 400 and 450 C

Active heating, nuclear heating minimum

In high vacuum ($< 10^{-5}$ mbar) see fig. 1

Dose rates of approximately 50 Gy/s and 10^{-9} dpa/s will be employed.

5 cylindrical samples (10 mm ID, 14 mm OD, 50 mm long) Union Carbide UV grade sapphire

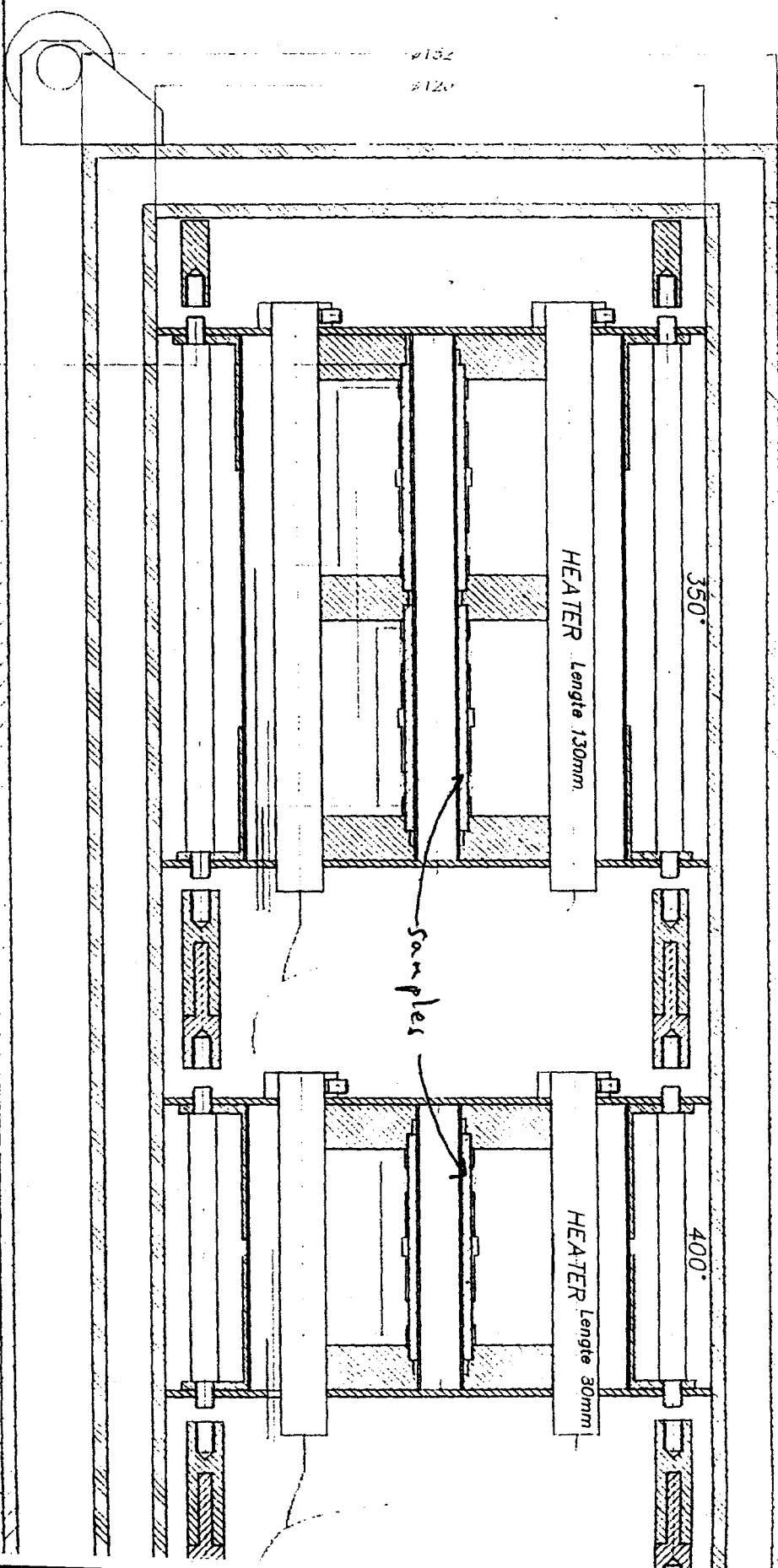
Present status;

Experimental rig is under construction

Samples are ready with platinum contacts

First tests in June this year

Expected sensitivity $\approx 7 \times 10^{-13}$ S/m





Possible explanations for conflicting results
(dose rate - temperature - electric field - material - test environment)

E.R.Hodgson
Euratom/CIEMAT Fusion Association, Madrid, Spain

1. Dose rate

Both displacement damage and ionization are necessary (fig. 1)

Displacement provides the necessary anion vacancies (F centres)

Ionization provides the F⁺ centres (figs. 2 & 3)

Field increases the F⁺ lifetime --> enhanced mobility (fig. 4)

Difficult to assess relative importance as we can have ionization without displacement but not the reverse

Due to the large difference in cross sections displacement damage will limit RIED

As in void swelling in metals and aggregation processes in the alkali halides we expect a process $\propto (\text{dose rate})^{0.5}$ (fig. 5)

==> higher dose rates require higher total doses (this is observed) fig. 6

2. Temperature

Not in the temperature range;

Lower limit; have observed very slow degradation as low as 250 C and from

F and F⁺ studies lower limit is about 200 C fig. 7

Some reports of searches for RIED at RT !!

Upper limit; by 530 C observed only very slight degradation fig. 8

(Pells by 550 C saw none)

Some experiments at T \geq 550 C

BUT beam heating could take T above the expected temperature

So care must be taken with the temperature measurements

3. Electric field

Threshold is a function of the material, the higher the purity the lower the threshold
Very little data on the threshold value, but based on theoretical model we have now been
able to observe clear RIED in Wesgo AL995 alumina for $E > 1$ MV/m (fig. 9)

So the range of fields from high purity single crystal to low purity polycrystalline
materials should range from about 50 kV/m to 1 MV/m

4. Material

Clearly one should expect differences from material to material, however surprisingly
enough this is often forgotten when comparing RIED results fig. 10

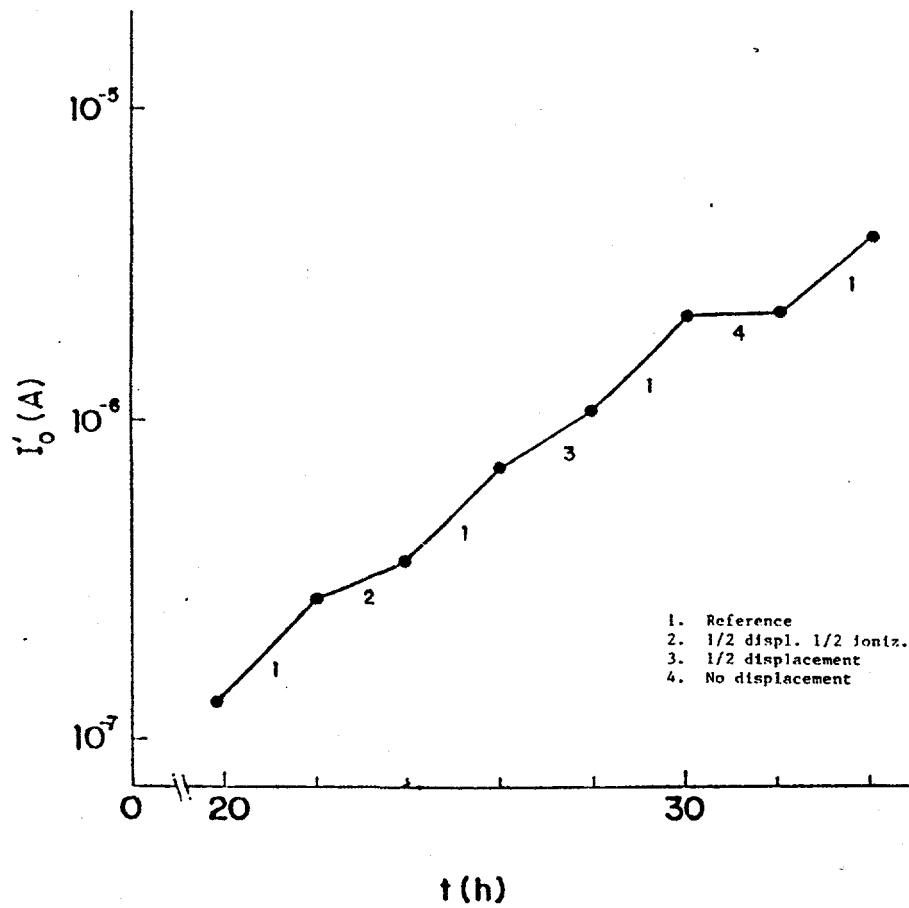
5. Test environment (vacuum, air, He,)

At the present time there is very little data on the role of the irradiation environment.

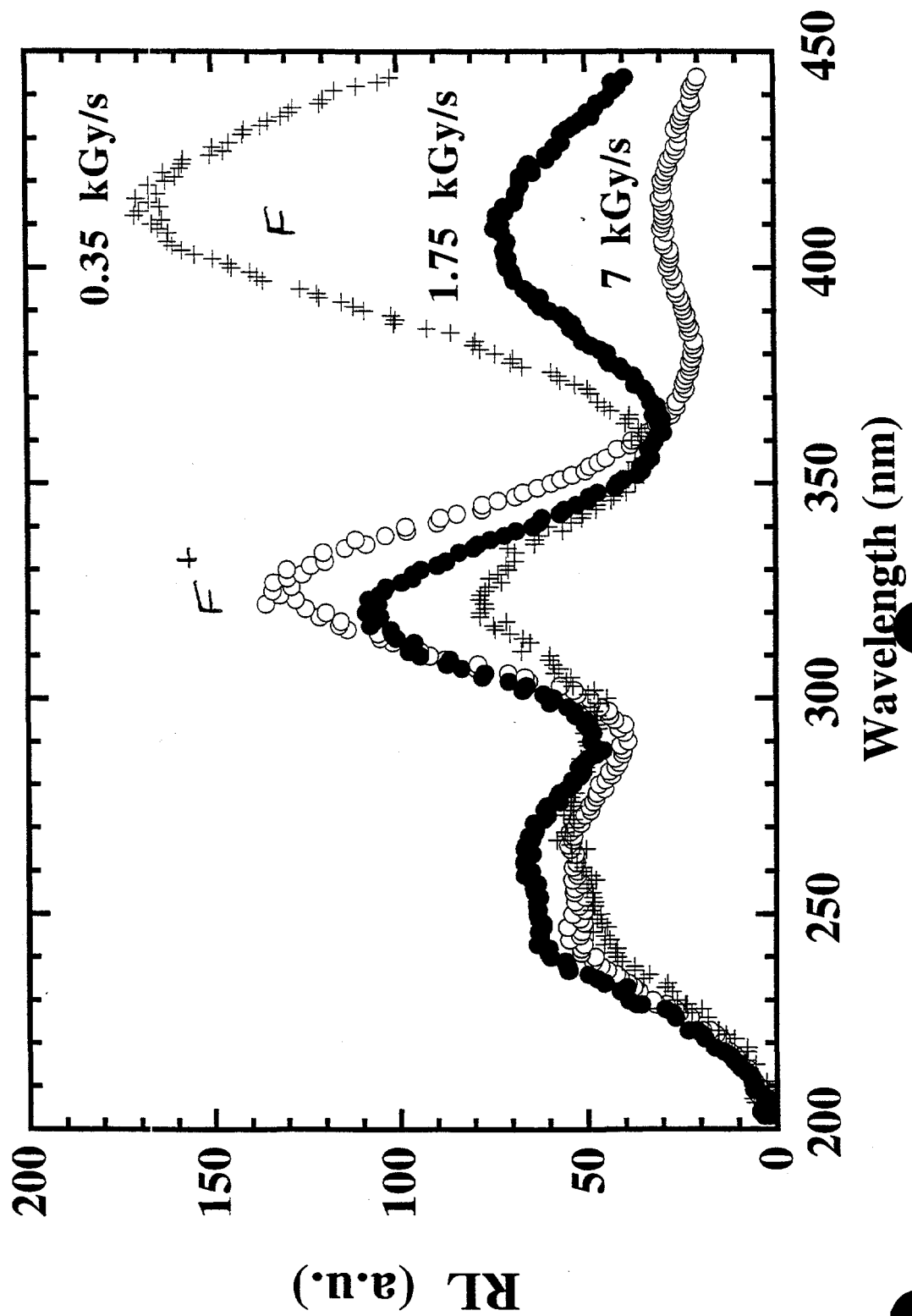
However work on Wesgo AL995 indicates that high surface degradation takes place in
vacuum for this material, but not in air or He. This appears to be related to radiation
enhanced vacuum reduction and electrolysis. This observation agrees with earlier work
by Kesternich and Jung (fig. 11)

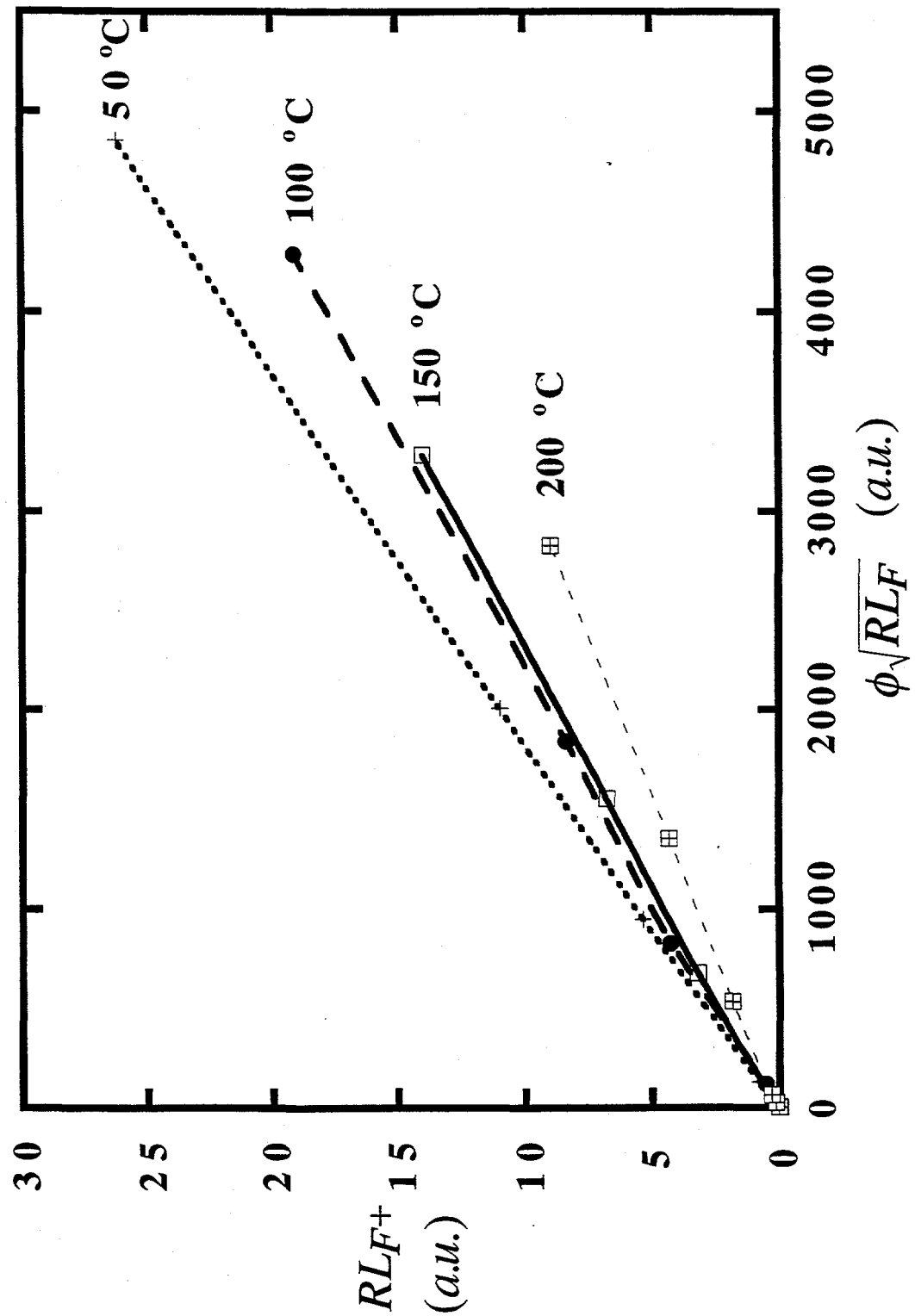
One electron irradiation result in air suggests a saturation in RIED, however such a
saturation has not been observed in RIED observations with e, p, He, or n in vacuum

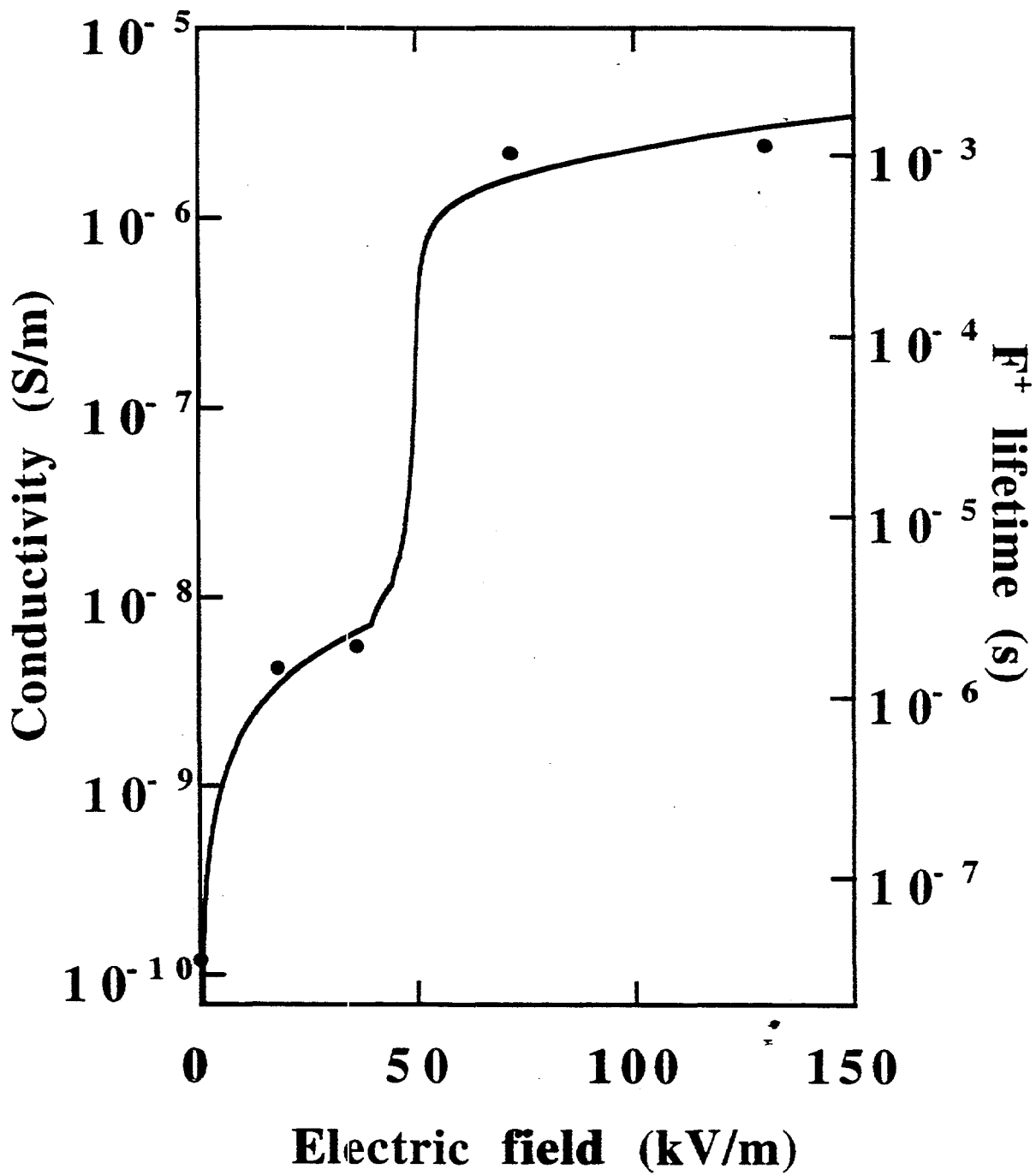
Both ionization and displacement damage are necessary.

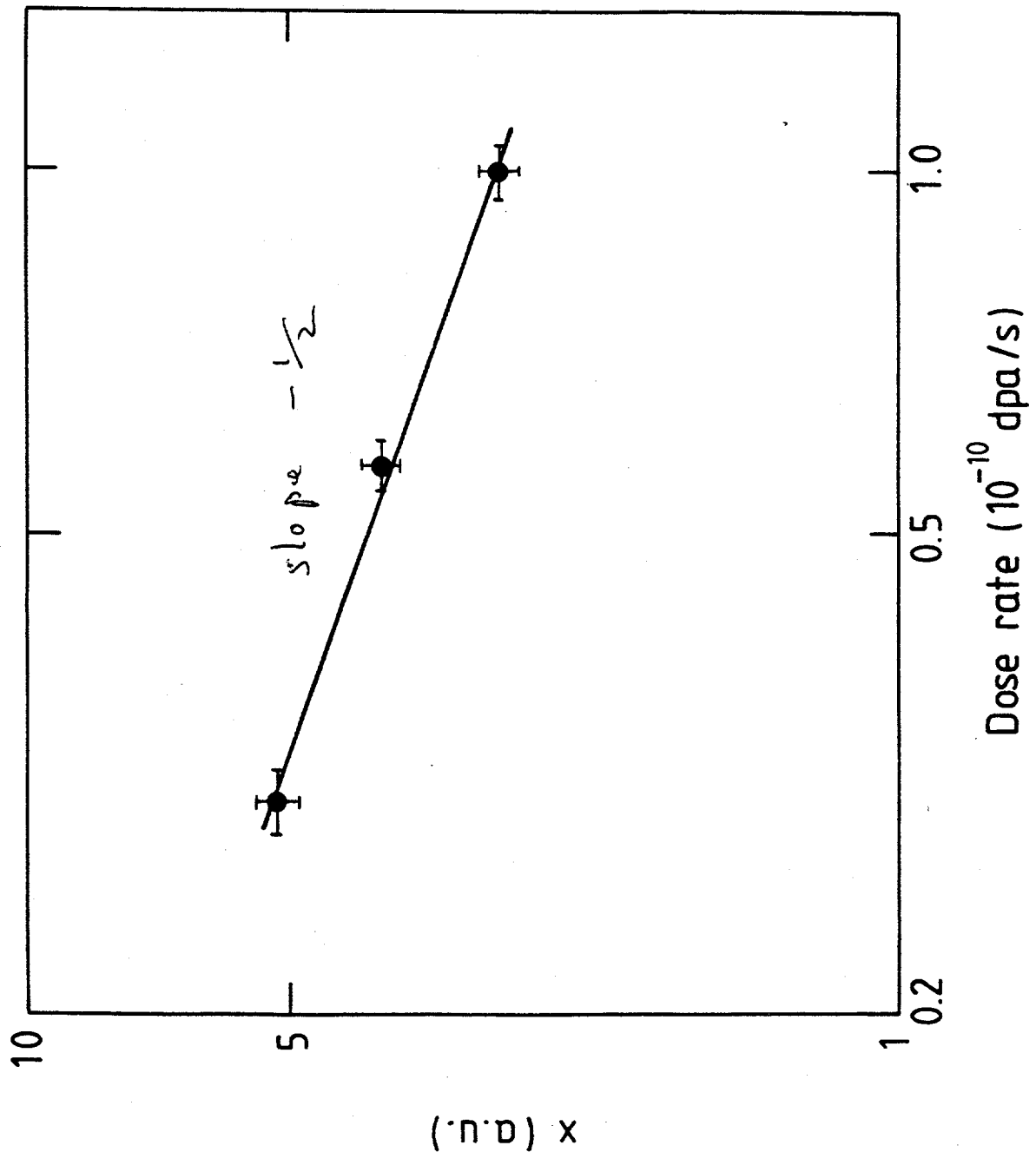


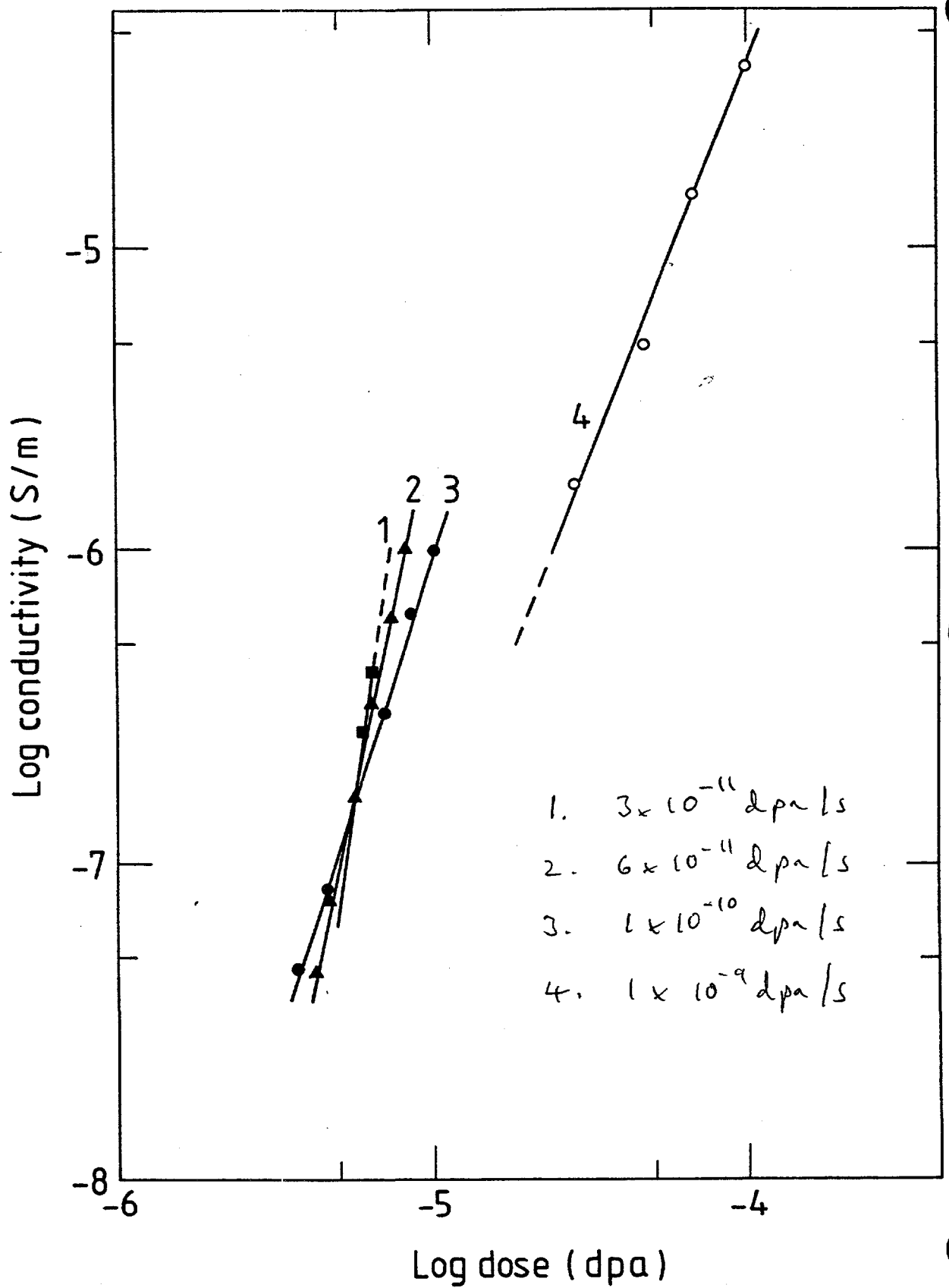
The increasing base conductivity for different irradiation conditions. 1 at 1.8 MeV 10^6 Gy h^{-1} ; 2 at 1.8 MeV 5.7×10^5 Gy h^{-1} ; 3 at 1.0 MeV 10^6 Gy h^{-1} , and 4 at 0.30 MeV 10^6 Gy h^{-1} . All at 500 °C.











Lower T limit ~ 200°C

NUMA 6135 m 5

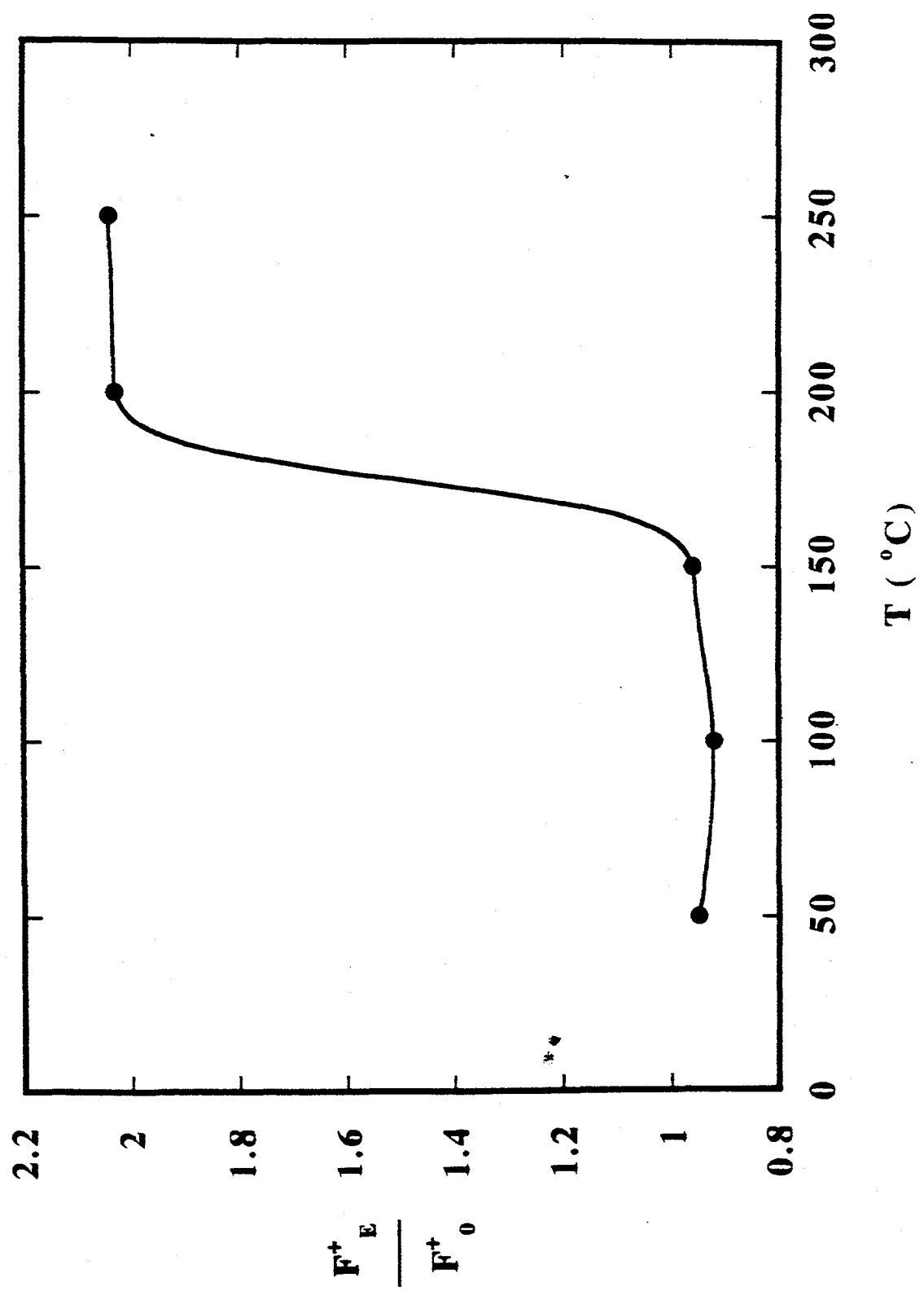


Fig. 7

Upper T limit ~ 550°C

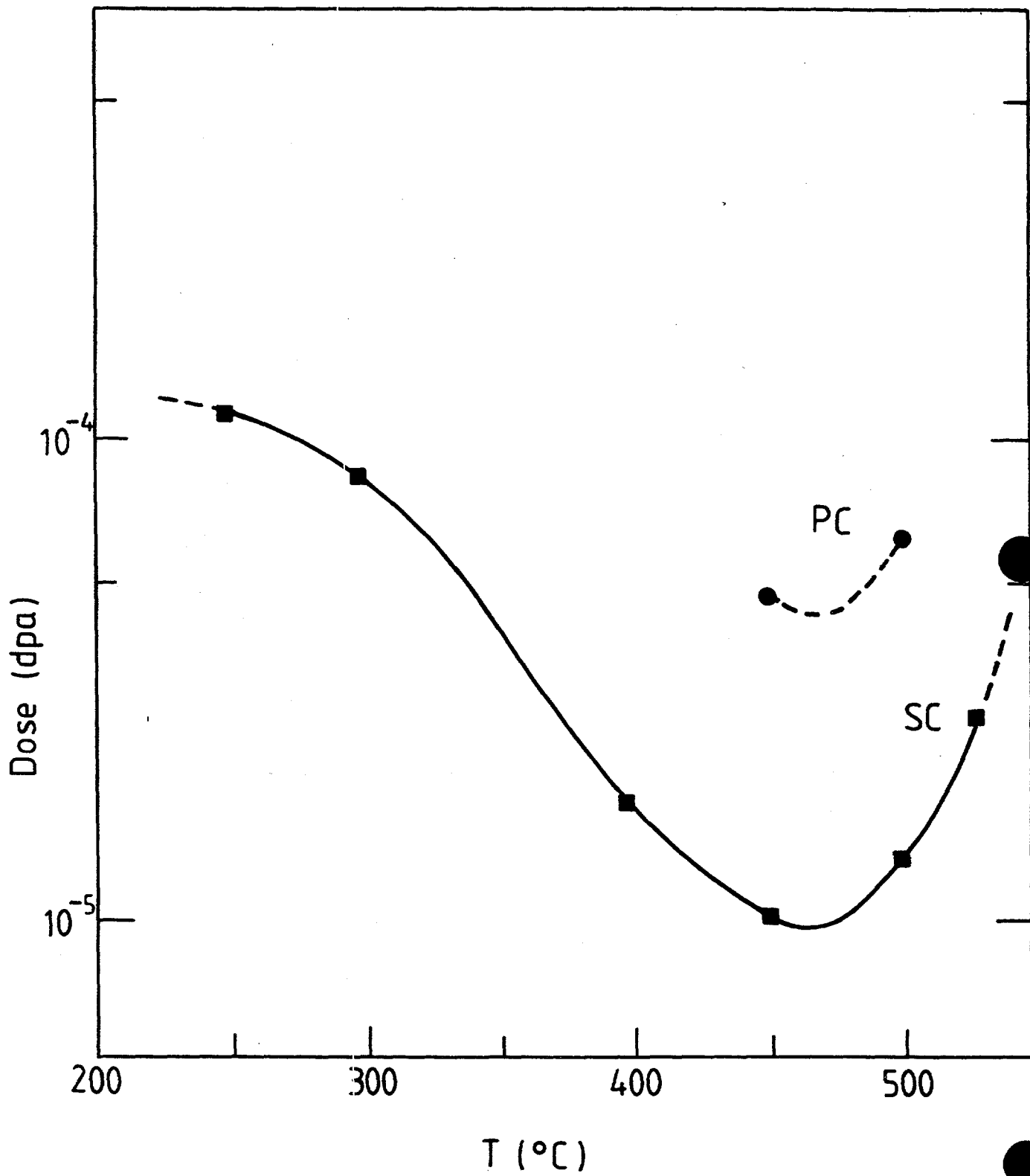
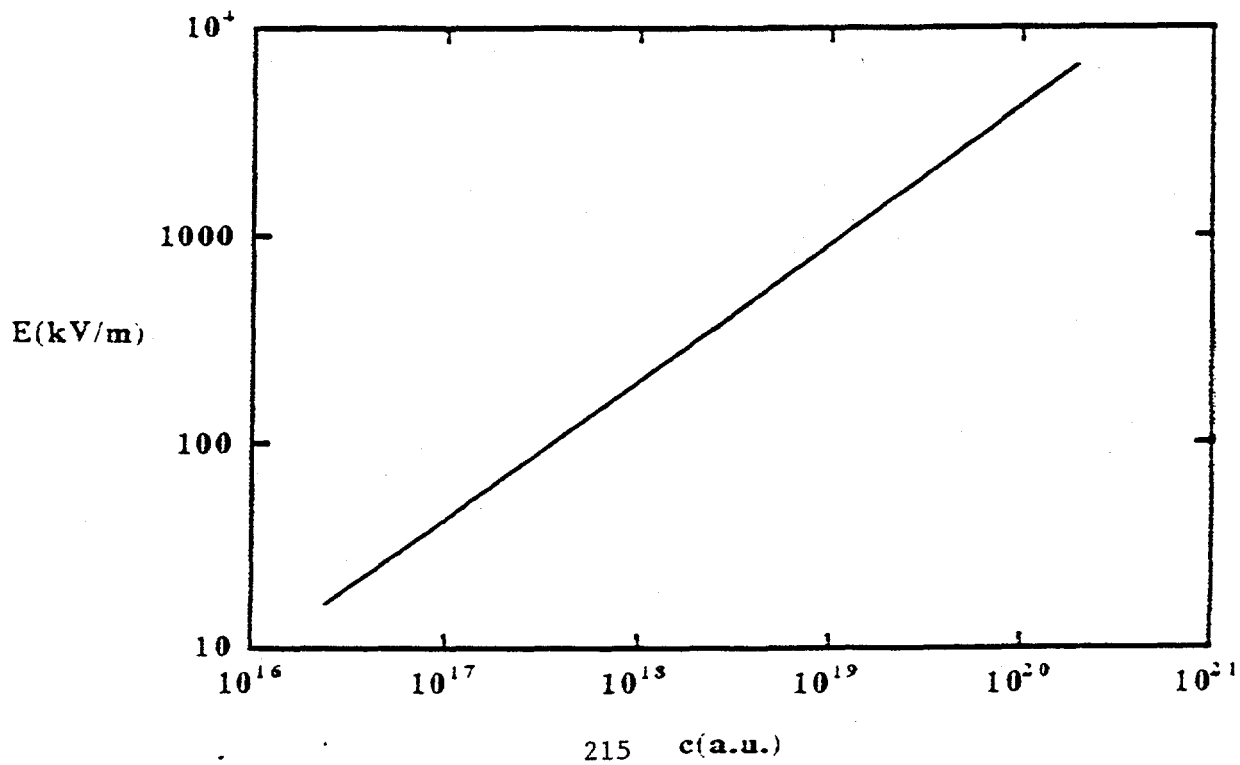
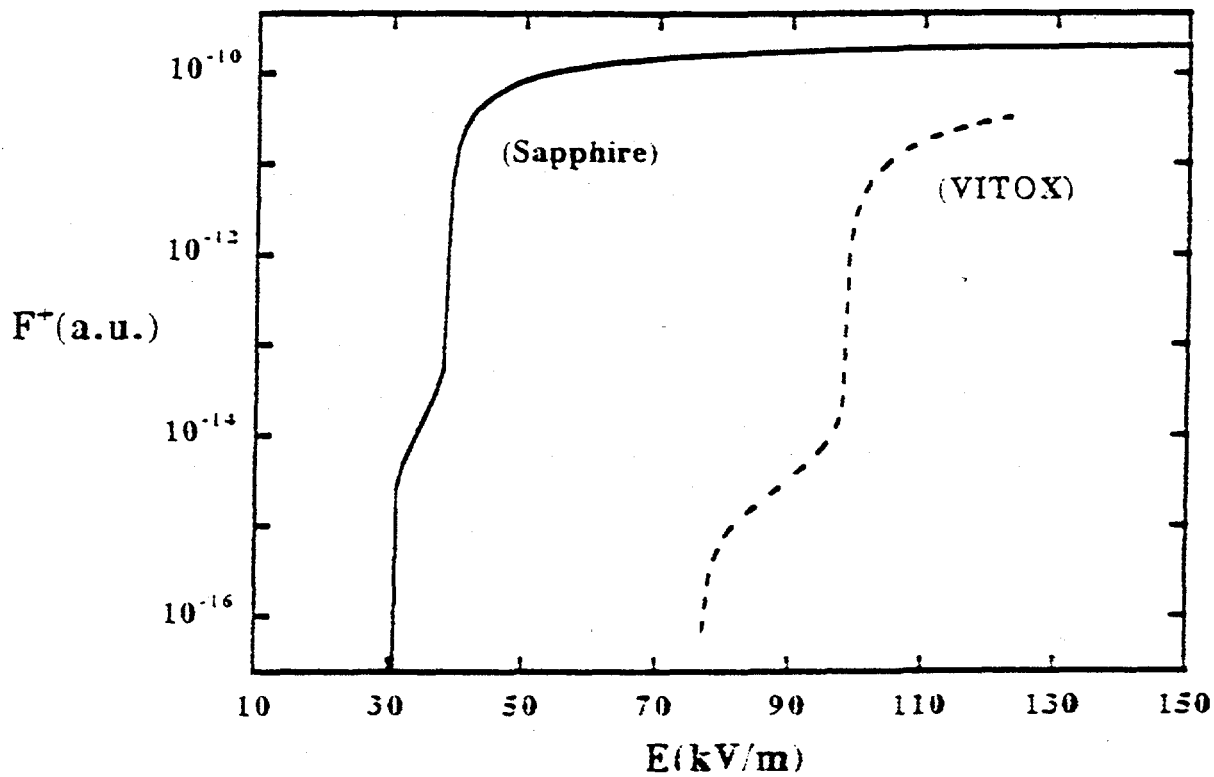
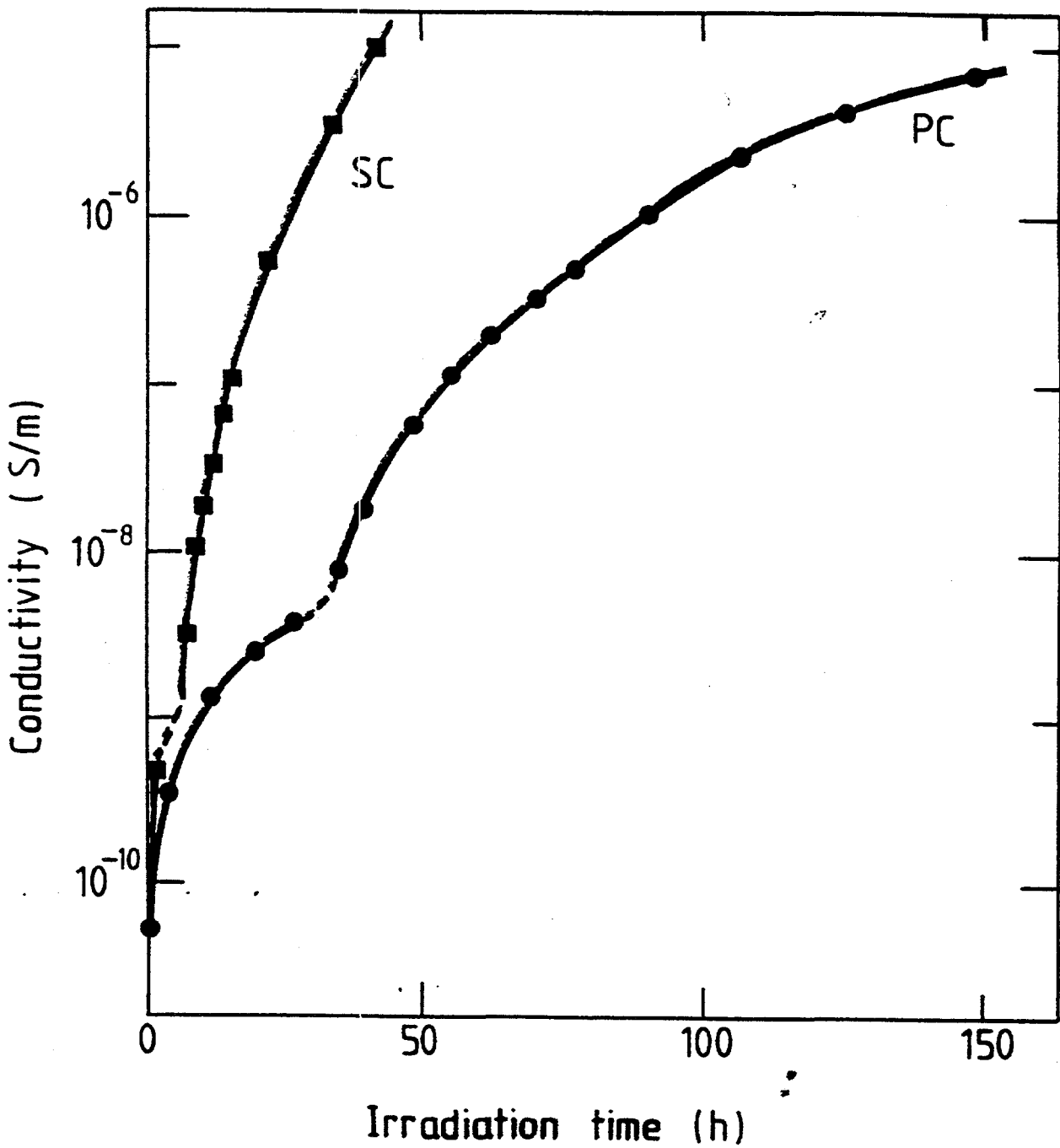


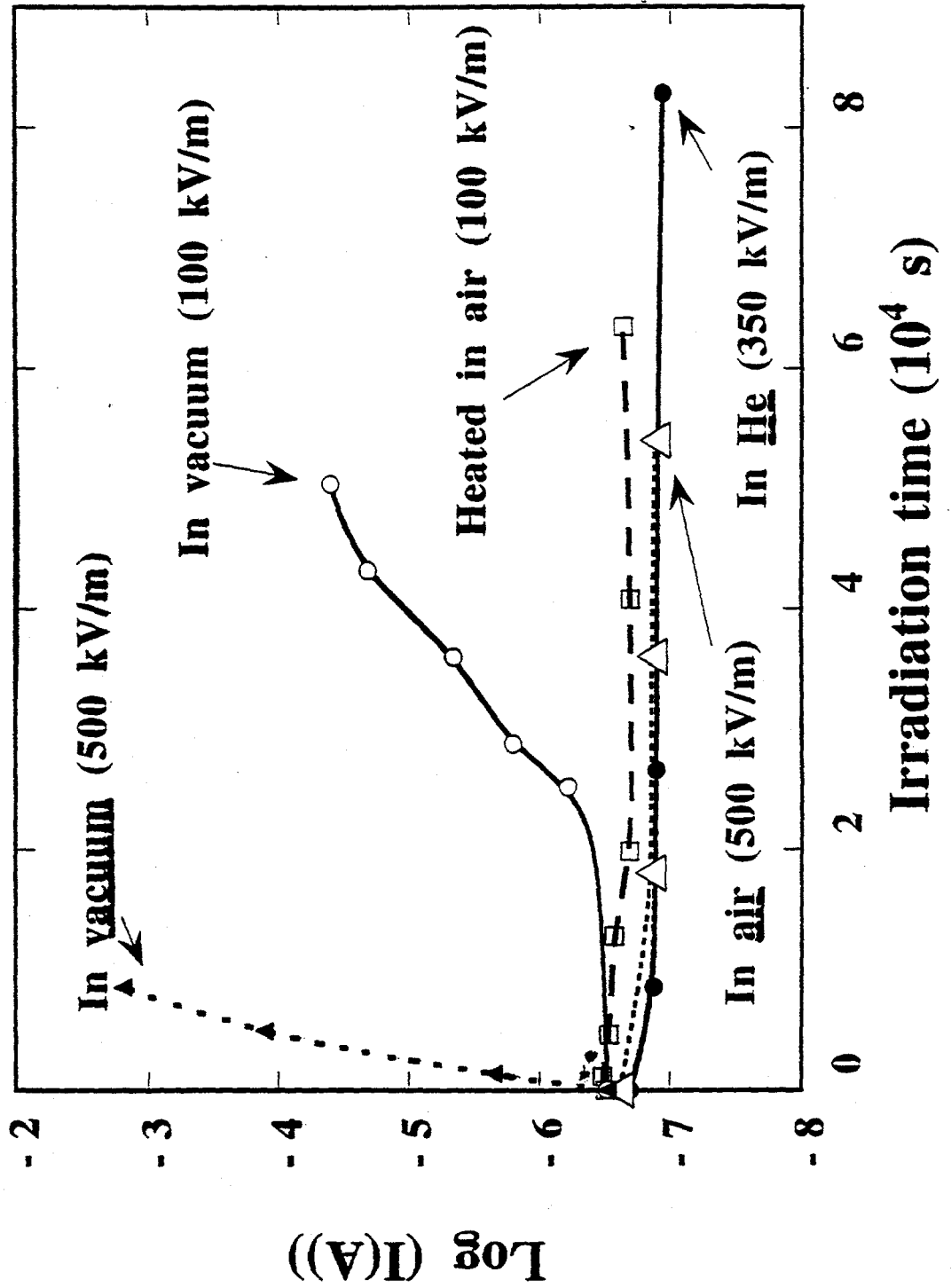
Fig. 8

Impurity/defect effect on RIED threshold





AL995
large grain size
low density alumina





**1.8 MeV Electron Irradiations in Alumina: Transport Calculations
and Implanted Charge Effects**

Y. Lizunov, A. Ryazanov and P. Vladimirov, RRC Kurchatov Institute, Moscow
A. Möslang, Institute of Materials Research I, Research Center Karlsruhe

The calculation method used is based on the solution of the Boltzmann Transport Equations for moving atoms. It is important to note that all calculations of the damage production use the same numerical model. The main results can be summarized as follows:

■ Displacement damage production:

The dashed lines in figure 1 shows the dpa production of the aluminum and oxygen sublattice in an alumina specimen of 1000 μm thickness that is not clamped or solid state bonded to a substrate. Because of the missing backscattered electrons, the dpa rate drops off at the back side. The solid lines represents the dpa rates in an alumina specimen of „infinite“ thickness.

For electron irradiations, the ratios of the sublattice specific damage rates are a function of depth. Within a 1000 μm thick alumina specimen the average value of $\text{dpa}_\text{Al}/\text{dpa}_\text{O}$ is 8 for 1.8 MeV electron irradiations (fig.1), while it is only 3.8 for light ions in the MeV range (fig. 2), and 2.7-2.8 for mixed spectrum and fusion neutrons. If smaller threshold energies E_d would be used for oxygen, this ratios would become also smaller.

■ Implanted charge:

The deposited energy (left axis) and the charge distribution (right axis) are shown in figure 3 again for a 1000 μm „isolated“ alumina specimen (dashed lines) and an infinite thick sample. A specific feature of electrons is the broad distribution of both parameters caused by the high fraction of backscattered electrons. This figure shows also that more than 15% (solid line within the hatched area) of all electrons would come to rest in a 1000 μm thick alumina ceramic pressed on a substrate. If no substrate would be used, still 6% of the electrons would thermalize in the alumina specimen. Even if only a small fraction of these electrons would be trapped in a ceramic, local charge accumulation would occur leading to secondary stresses.

Electron Irradiation of Al_2O_3

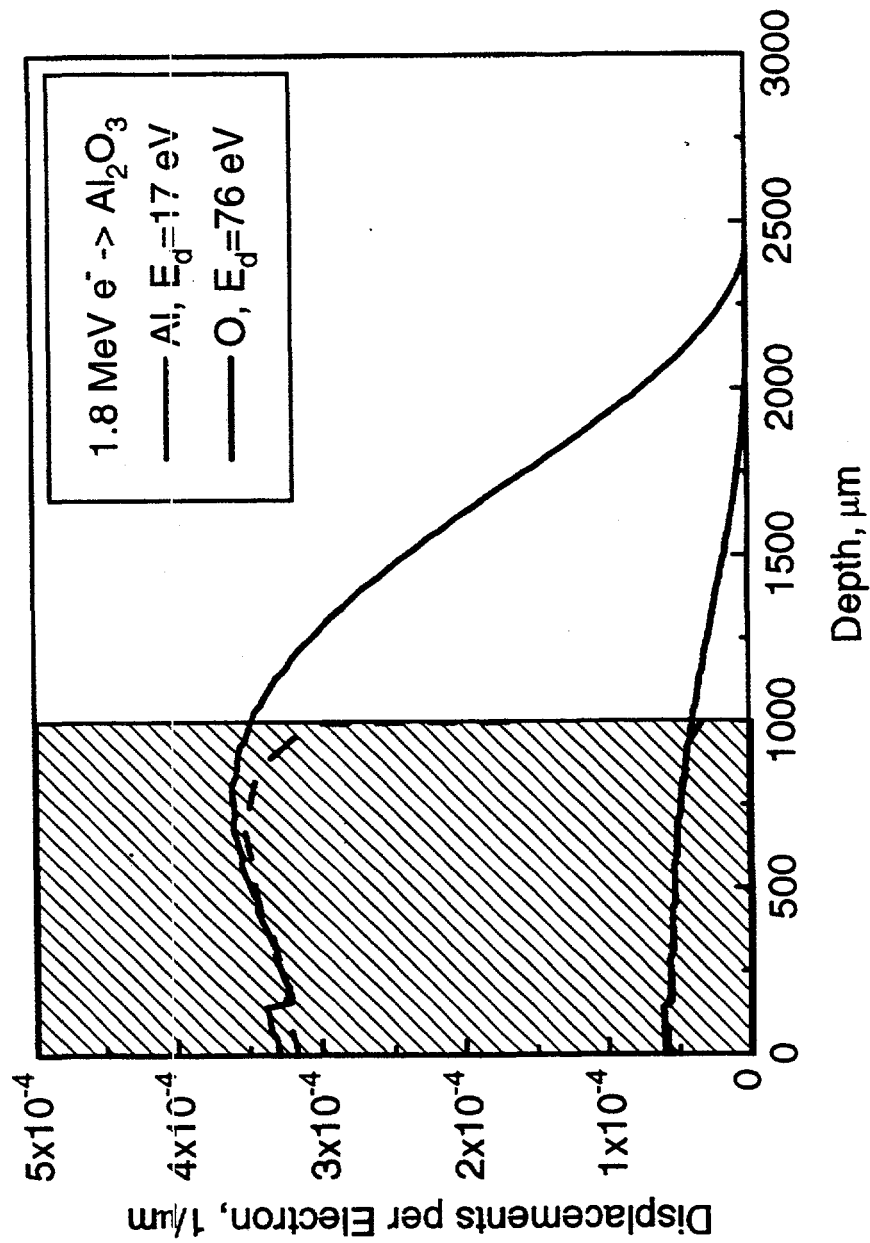


fig. 1

Charged Particle Irradiation of Al_2O_3

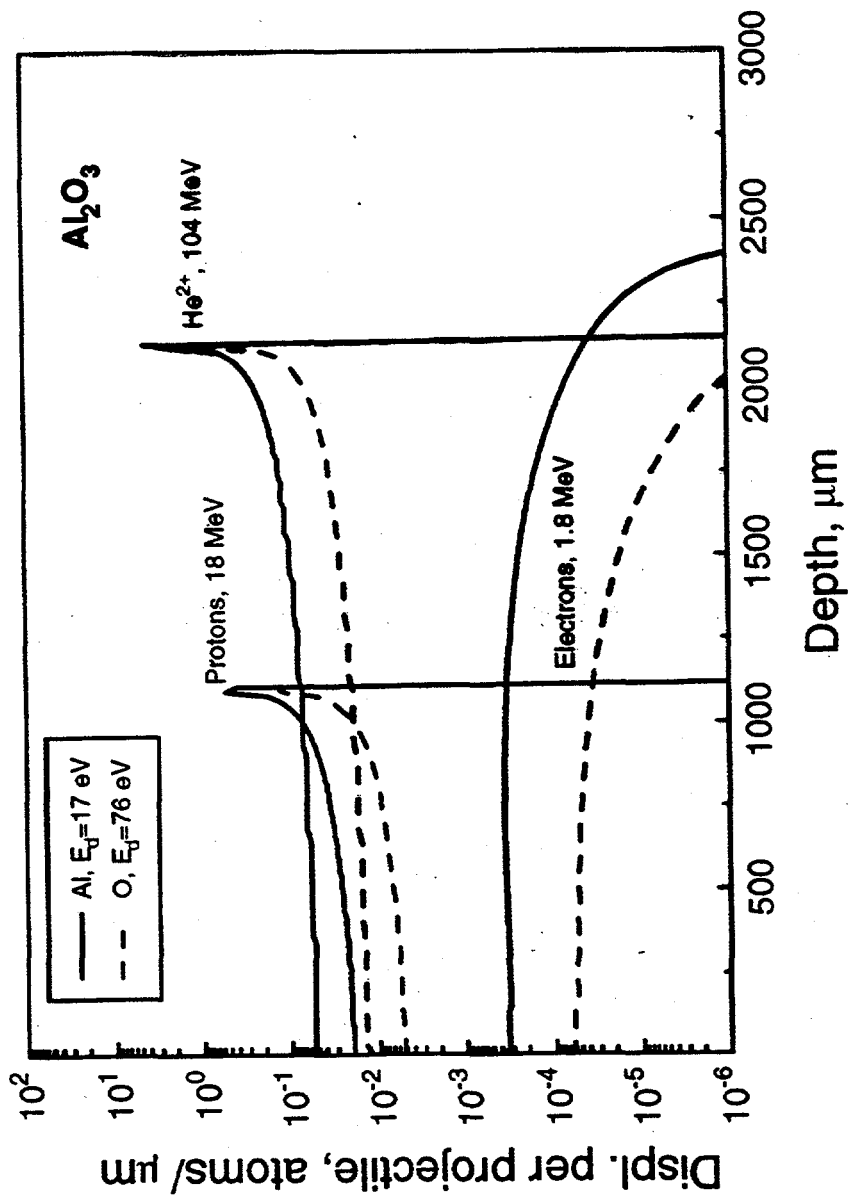


fig. 2

Electron Irradiation of Al₂O₃

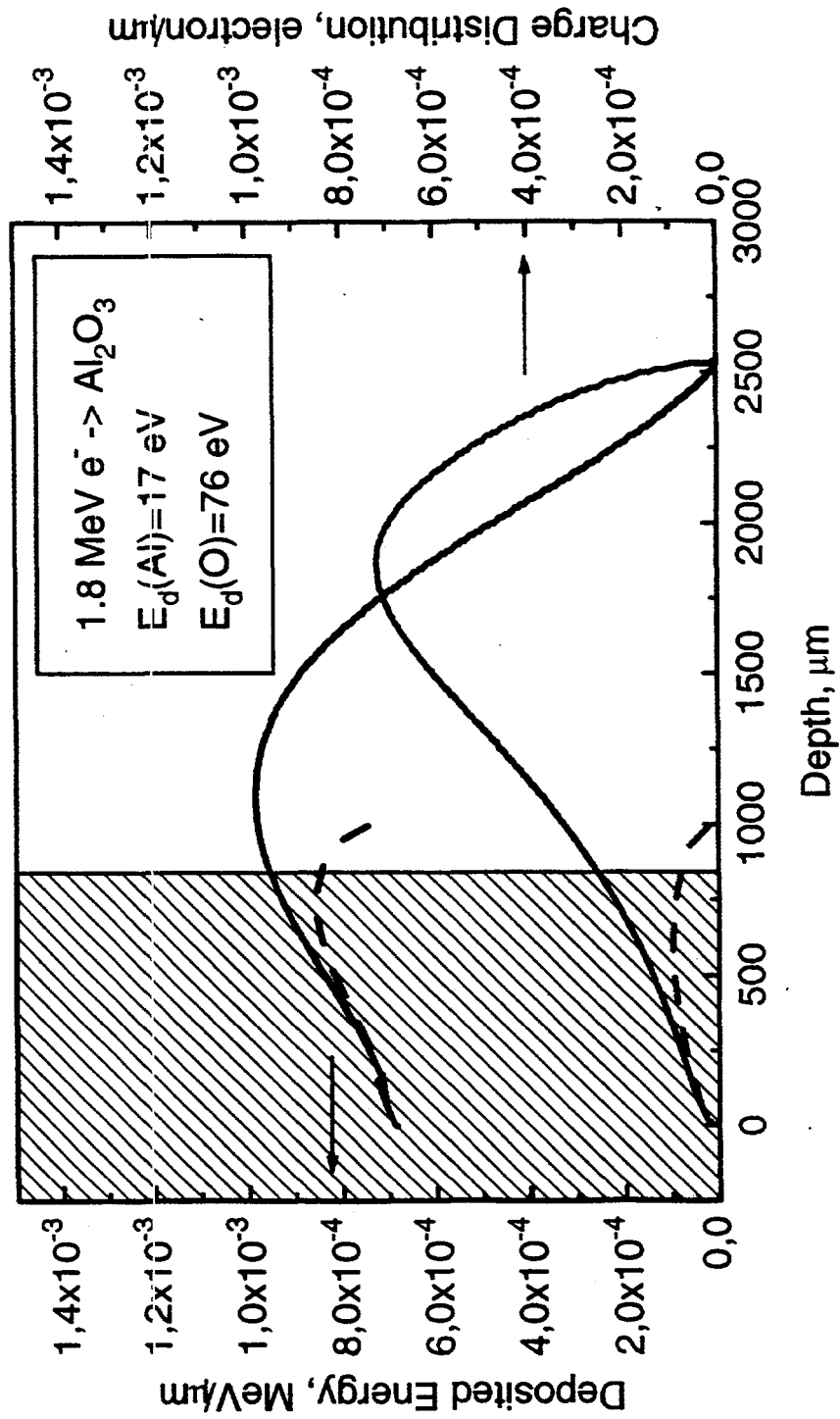


fig. 3

**COMMENTS ON ELECTRON BEAM STRAGGLING AND
CHARGE DEPOSITION IN DIELECTRICS**

S.J. Zinkle

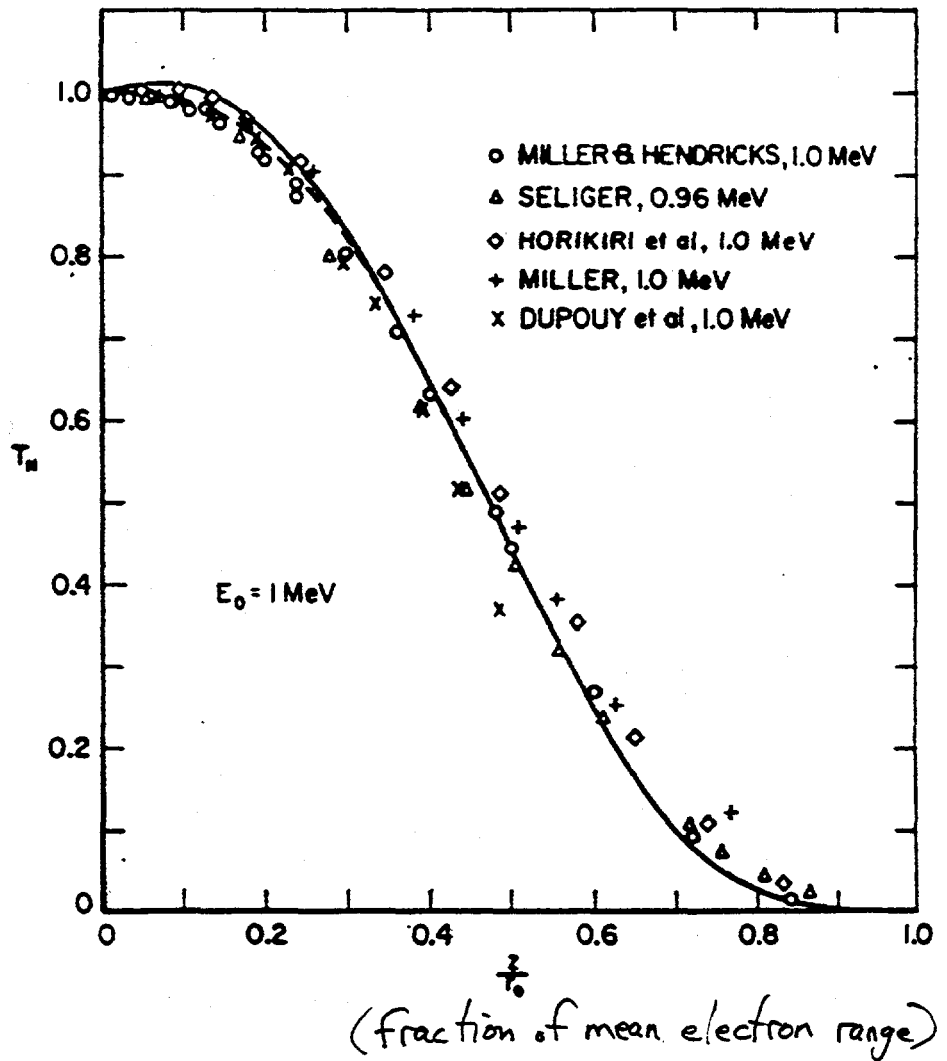
**Metals and Ceramics Division
Oak Ridge National Laboratory, Oak Ridge, TN 37831 USA**

**IEA Workshop on Radiation Effects in Ceramic Insulators
May 7&8, 1997, Cincinnati, OH**

INTRODUCTION

- Due to its low mass, electron irradiation characteristically exhibits very pronounced range straggling
- The maximum in the implanted charge profile (for a thick target) occurs at a depth of ~60% of the projected electron range (cf. B. Gross, in Electrets, 2nd ed. 1987, etc.)
- The large amount of implanted charge associated with electron irradiation needs further consideration
 - e.g., the projected range of 1.8 MeV electrons in Al_2O_3 is ~2.1 mm, but about 50% of the incident electrons are stopped in a 1 mm thick foil (cf. Seltzer & Berger, Nucl. Instr. Meth. 119 (1974) 157, etc.)
 - the injected electrons produce an electric field that causes a further shortening of the range of electrons (B. Gross, in Electrets, Topics in Applied Physics, vol. 33, 1987 and Fredrickson et al, IEEE Trans. Nucl. Sci. 40 (1993) 1393, etc.)

1 MeV electron transmission coefficient for Aluminum



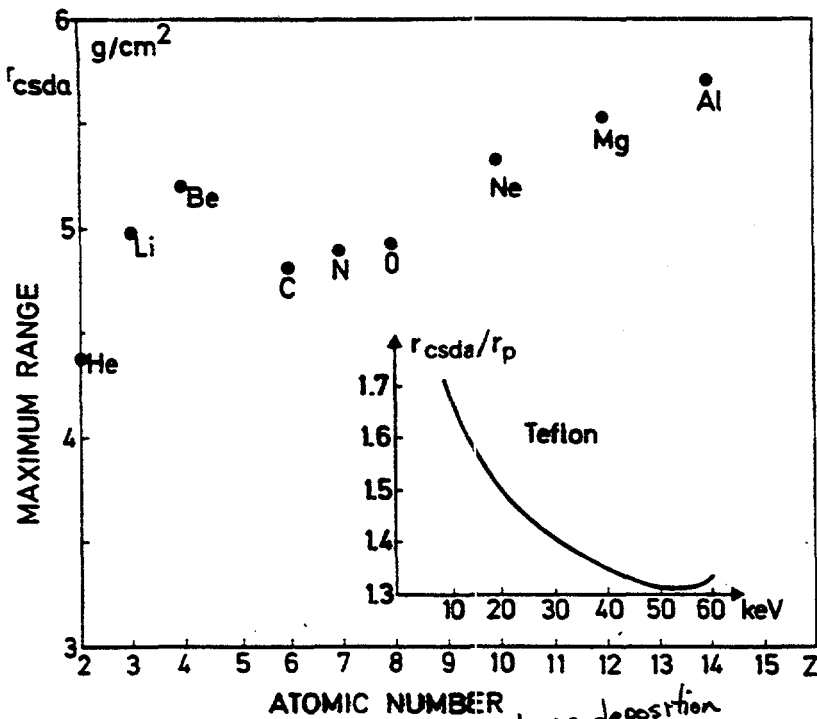


Fig. 4.3. csda range for 50 keV electrons in various elements as a function of atomic number Z [4.70]. Inset: Relation between csda range and extrapolated range for Teflon as a function of energy

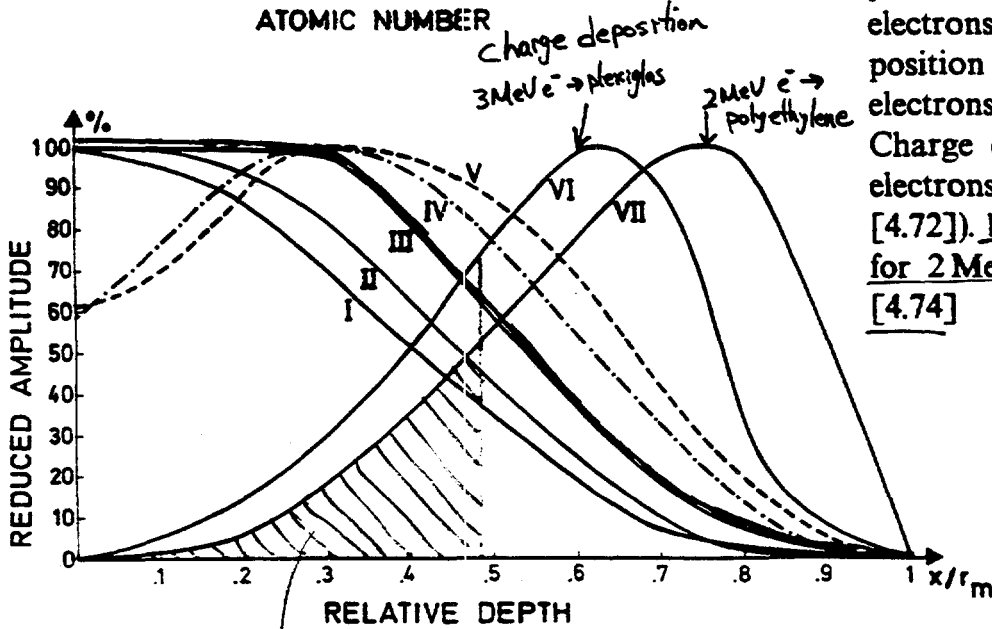


Fig. 4.4. Range relations for electrons - experimental. I: Number transmission curve for 0.159 MeV electrons in Al [4.75]. II: Number transmission curves for 1 MeV electrons in Al [4.71]. III: Charge transmission curve for 2 MeV electrons in plexiglas (Gross-Wright [4.72]). IV: Energy deposition (ionization) curve for 2 MeV electrons in Al [4.73]. V: Energy deposition (dose rate) curve for 2 MeV electrons in polyethylene [4.74]. VI: Charge deposition curve for 3 MeV electrons in plexiglas (Gross-Wright [4.72]). VII: Charge deposition curve for 2 MeV electrons in polyethylene [4.74]

~20% of the charge from 2 MeV incident electrons is deposited in a specimen of thickness $\frac{x}{r_m} \sim 0.5$

(1 mm thick Al_2O_3)

- Numerous studies on electron irradiated dielectrics (which and without applied electric fields) have been performed over the past 40 years
 - the internal electric field generally is not related to the applied electric field in any simple manner (depends on electrode characteristics and other experimental factors)
 - results obtained from Electret research and other fundamental studies on electron-irradiated dielectrics may offer some answers to the RIED puzzle
- Further work is needed to understand the physical mechanism responsible for producing RIED in electron-irradiated samples, including electron irradiation studies on thin film Al_2O_3 specimens

Dielectric Charging by MeV Electron Beams

- According to literature data, the fraction of 1.8 MeV electrons that would be stopped inside an Al_2O_3 foil (projected range ~ 2.1 mm) is:
 - ~ 5 to 10% for 0.5 mm thick foil
 - $\geq 20\%$ for 1.0 mm thick foil
- The electric field associated with these implanted electrons is comparable to the threshold electric field for inducing RIED:

$$\text{In general, } E = - \left[1 - \exp - \frac{\sigma_e t}{\epsilon} \right] \frac{J}{\epsilon} \sigma_e \quad t = \text{time}$$

$$(E = J / \sigma_e \text{ after } \sim 1 \text{ ms for } \sigma_e = 10^{-7} \text{ S/m in } Al_2O_3)$$

where σ_e = electric conductivity, ϵ = dielectric permittivity, and J = electron beam current deposited in specimen

Assuming representative conditions of:

$$\sigma_{RIC} \sim 10^{-7} \text{ S/m and } J \sim 20\% \left[\frac{I_{e \ln}}{A} \right] \sim 0.2 \text{ } \mu\text{A/cm}^2$$

then $E \sim 20 \text{ V/mm} \leftarrow$ (macroscopic E field due to implanted electrons from 1.8 MeV beam for a 1 mm thick specimen)

**POSSIBLE ROLE OF IRRADIATION SPECTRUM
EFFECTS ON THE RIED PHENOMENON**

S.J. Zinkle

**Metals and Ceramics Division
Oak Ridge National Laboratory, Oak Ridge, TN 37831 USA**

**IEA Workshop on Radiation Effects in Ceramic Insulators
May 7&8, 1997, Cincinnati, OH**

Motivation for considering Irradiation Spectrum Effects in RIED

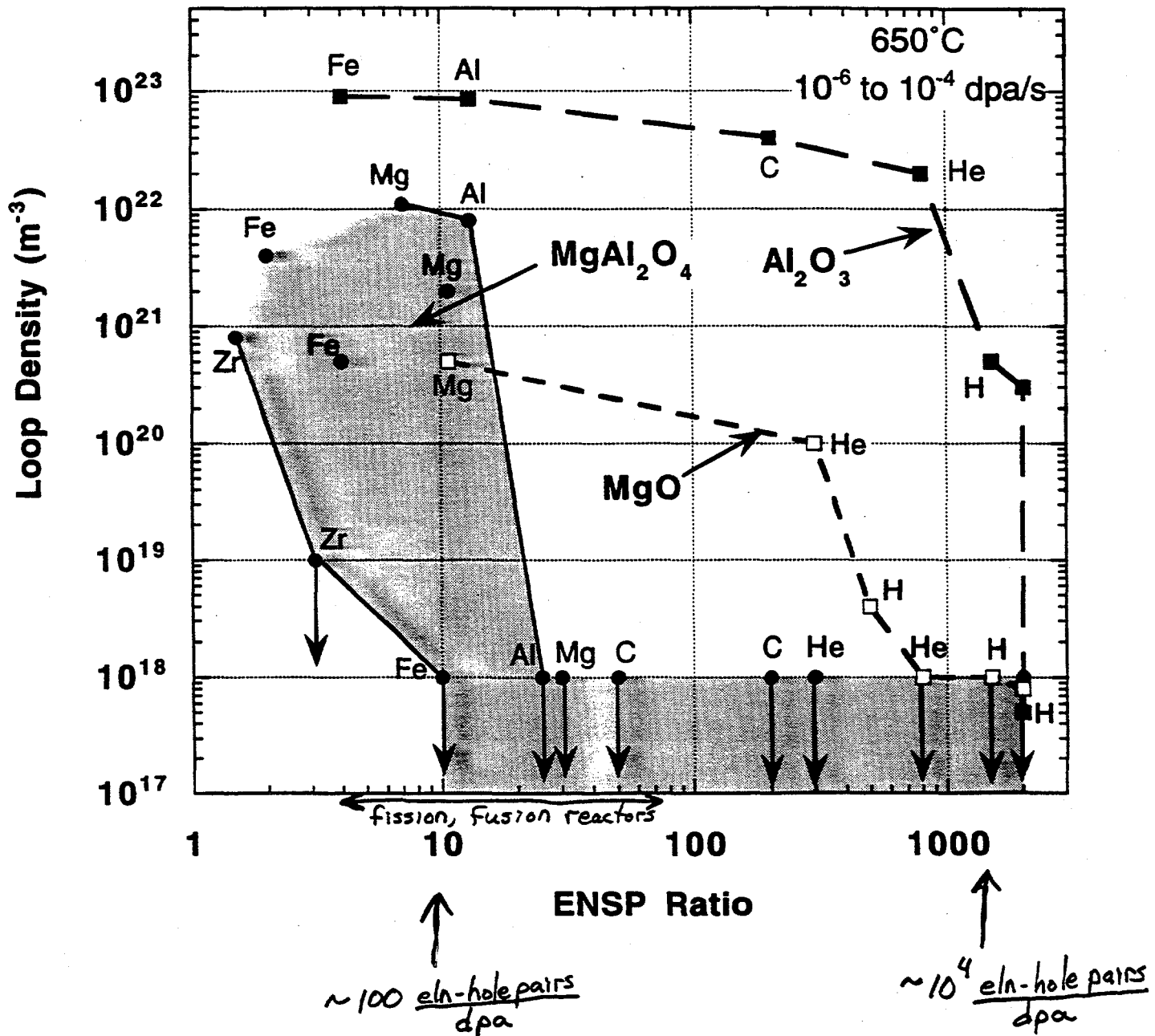
- Bulk RIED observed during electron irradiation of high-purity polycrystalline Al_2O_3 or sapphire by Hodgson and coworkers (numerous studies) and Zong et al (2 studies)
 - however, not seen by Terai and Kinoshita groups
- Definitive levels of bulk RIED have not been observed during energetic ion irradiation or fission neutron irradiation of high-purity Al_2O_3 at 300-530°C
 - Kesternich et al (Deranox, Wesgo Al995, Rubalit 710 grades of Al_2O_3)
 - Möslang et al (Deranox, Wesgo Al995 grades of Al_2O_3)
previous report of RIED in Vitox due to cracked specimen
 - Pells (RIED reported in Vitox and MgAl_2O_4 ; possible influence of cracking is uncertain-- cf. spinel postirradiation annealing results)
 - Patuwathavithane et al (2 MeV proton irradiation of sapphire)
 - Shikama et al (slight RIED observed in one study, "transient RIED" observed in another study, no RIED in 2 other JMTR studies)
 - Tanifuji, Noda et al (no RIED up to 0.2 dpa in JRR-3 reactor)
 - HFIR TRIST-ER1 (no RIED above RIC level of $\sim 5 \times 10^{-7}$ S/m except for ruby-- possible crack effect?)

- Ionizing radiation can anneal pre-existing point defect swelling in oxide ceramics (Walker 1964, Arnold et al 1974, Krefft 1977, Krefft & EerNisse 1978)
- Ionizing radiation converts F centers into F⁺ centers (Krefft 1977, Dalal et al 1988, Brenier et al 1993)
 - F⁺ centers should have higher diffusivities than F centers (ionization-induced diffusion, IID), although direct measurements of IID are limited--Corbett & Bourgoin 1971, Bourgoin & Corbett 1978, Chen et al 1976, Chen et al 1984
 - recent theoretical work indicates that ionization lowers the migration energies for interstitials and vacancies in MgO (Kotomin et al 1996, Brudevoll et al 1996)
- For a given dpa & dpa/s, microstructure depends on bombarding ion mass: defect cluster nucleation is suppressed for light ions (Zinkle 1994, 1995, 1997)
 - MgAl₂O₄ is very sensitive to irradiation spectrum compared to MgO, Al₂O₃
 - lack of defect clusters attributed to ionization enhanced diffusion effects
- If colloid formation is responsible for triggering the onset of RIED in bulk electron irradiations, then the irradiation spectrum (including ionizing radiation) may have an effect; however, colloids have not yet been observed in postirradiation tests on electrically degraded specimens

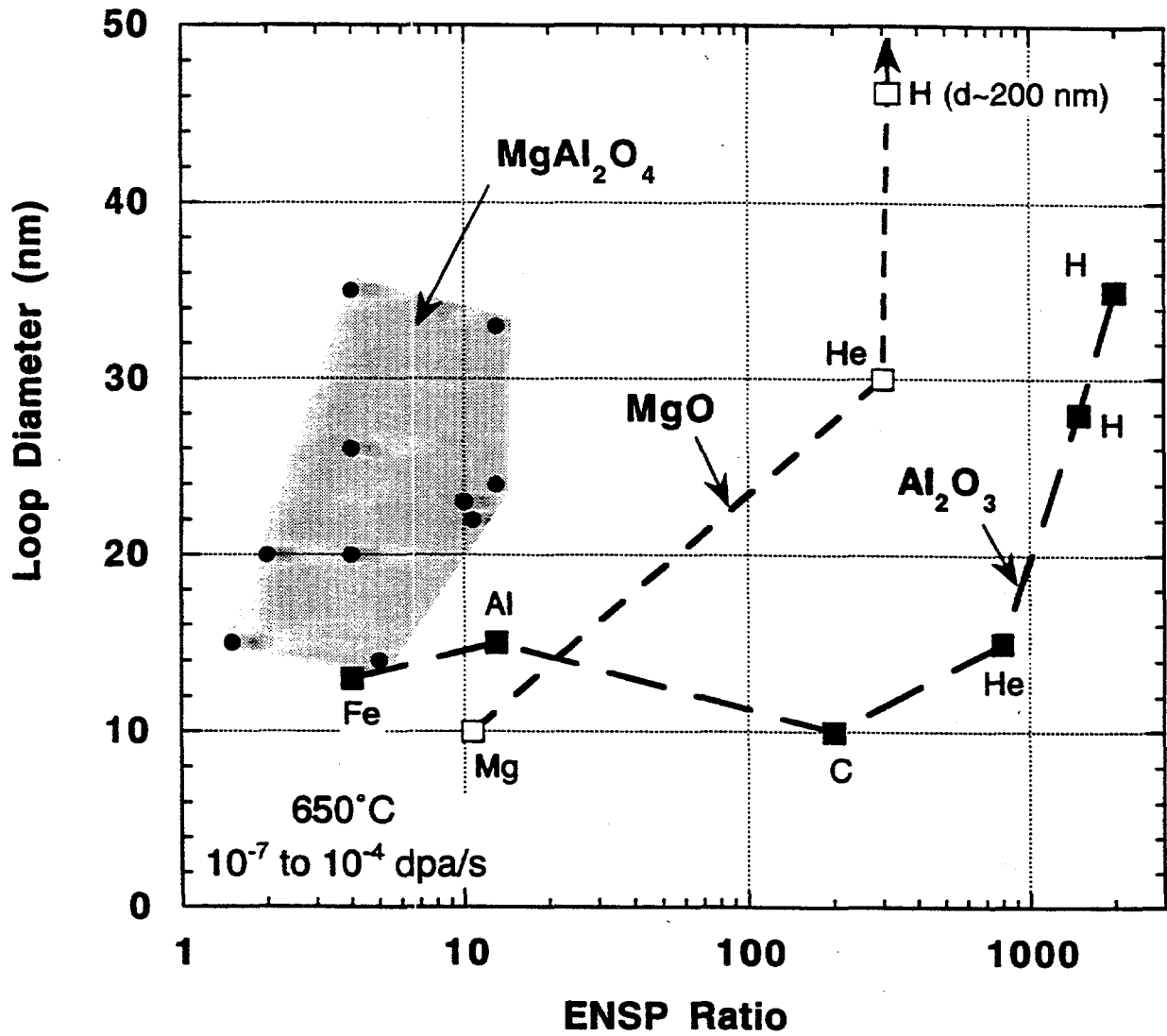
Summary of single ion irradiation results

* measurements made $\geq 0.3 \mu\text{m}$ from surface + implanted ion region.

EFFECT OF ELECTRONIC TO NUCLEAR STOPPING POWER ON THE LOOP DENSITY IN ION IRRADIATED CERAMICS

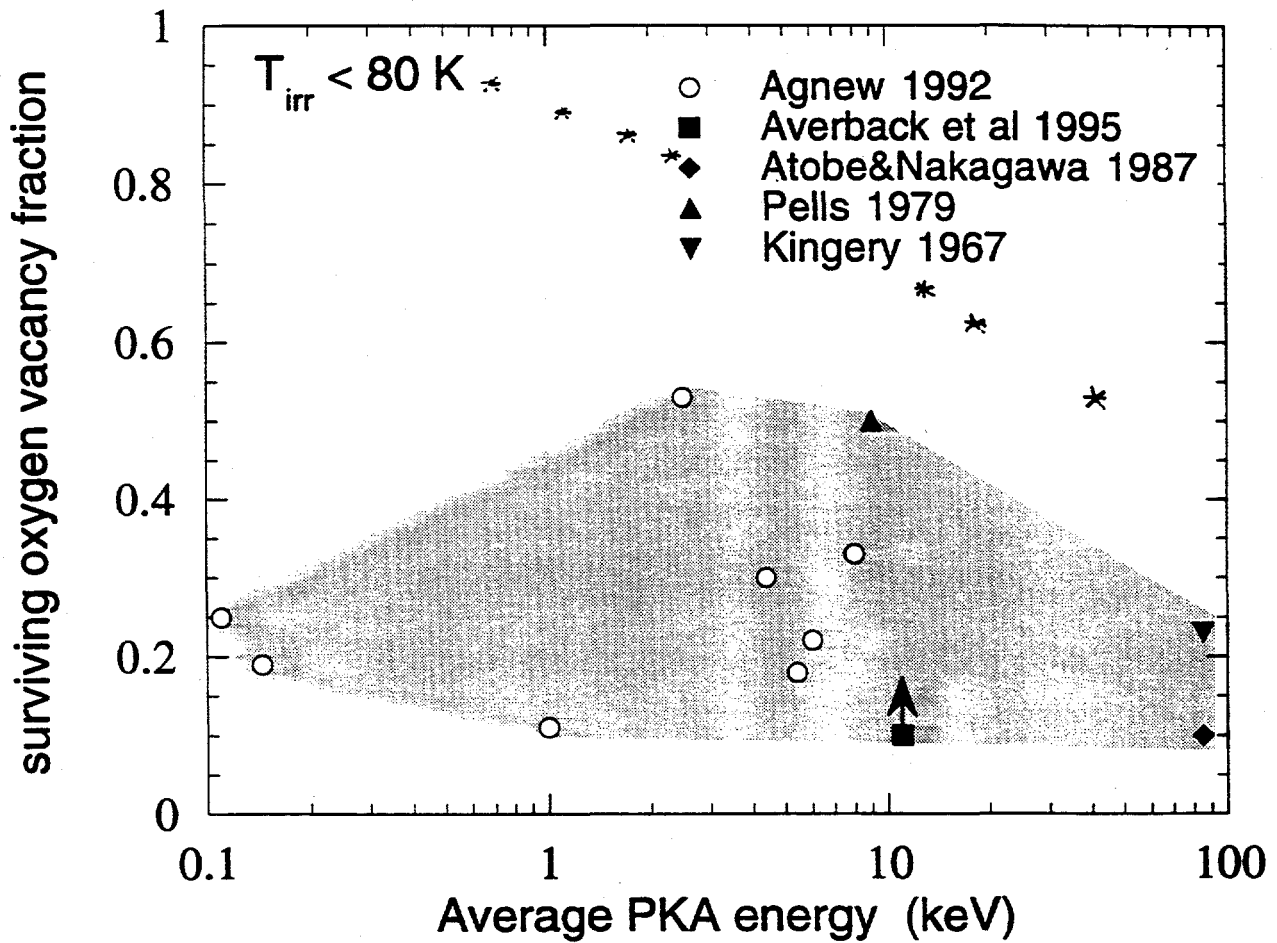


EFFECT OF ELECTRONIC TO NUCLEAR STOPPING POWER ON THE LOOP SIZE IN ION IRRADIATED CERAMICS



- Loop coarsening observed at high ENSP ratios for all 3 ceramics

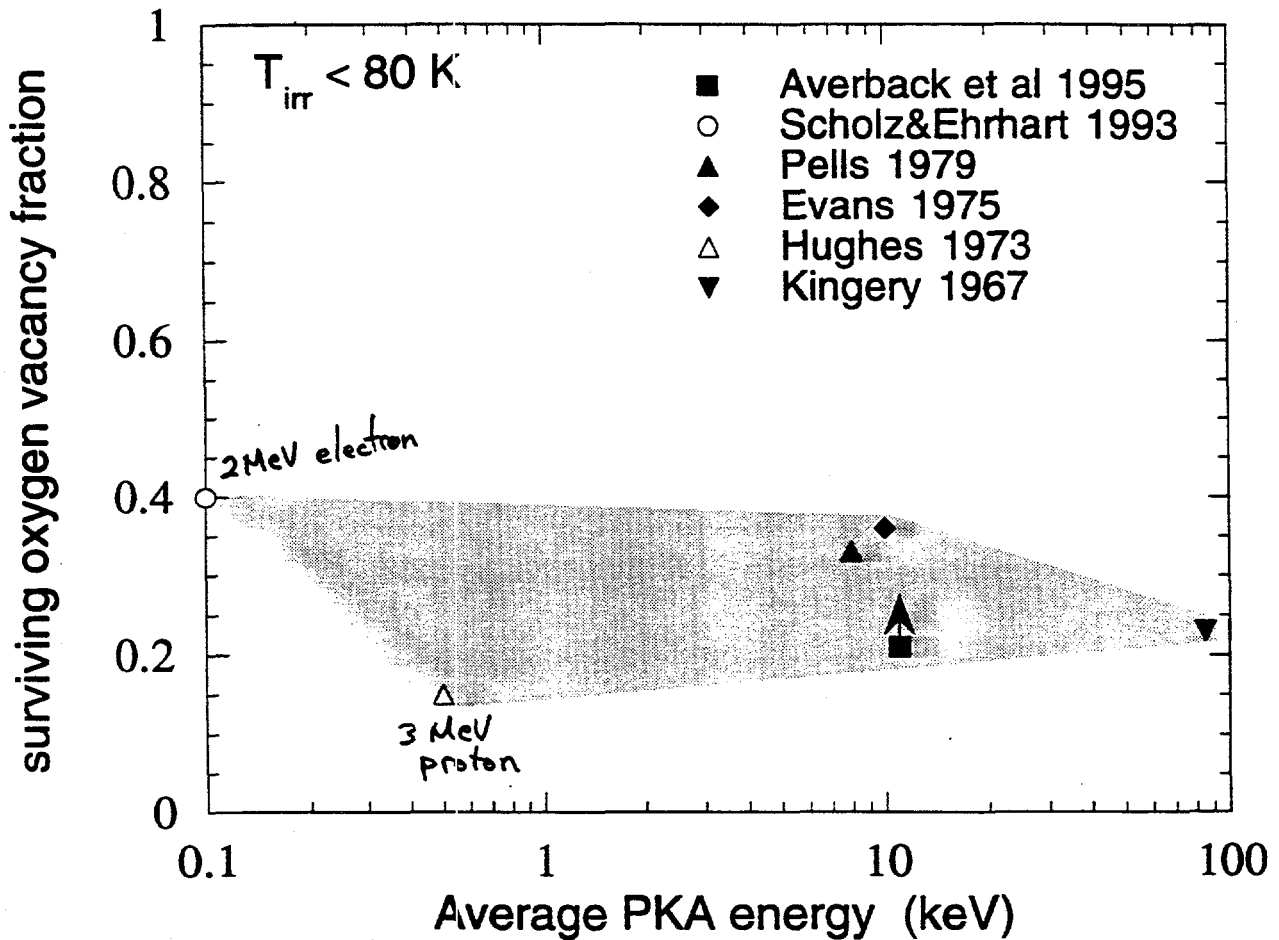
Surviving defect fraction in irradiated Al_2O_3



- No significant dependence on PKA energy
- reported values are significantly lower than for irradiated Al. (*)
 (Averbach et al 1983)

Zinkle + Kinoshita
 J. Nucl. Mater., in press
 (Davos workshop)

Surviving defect fraction in irradiated MgO



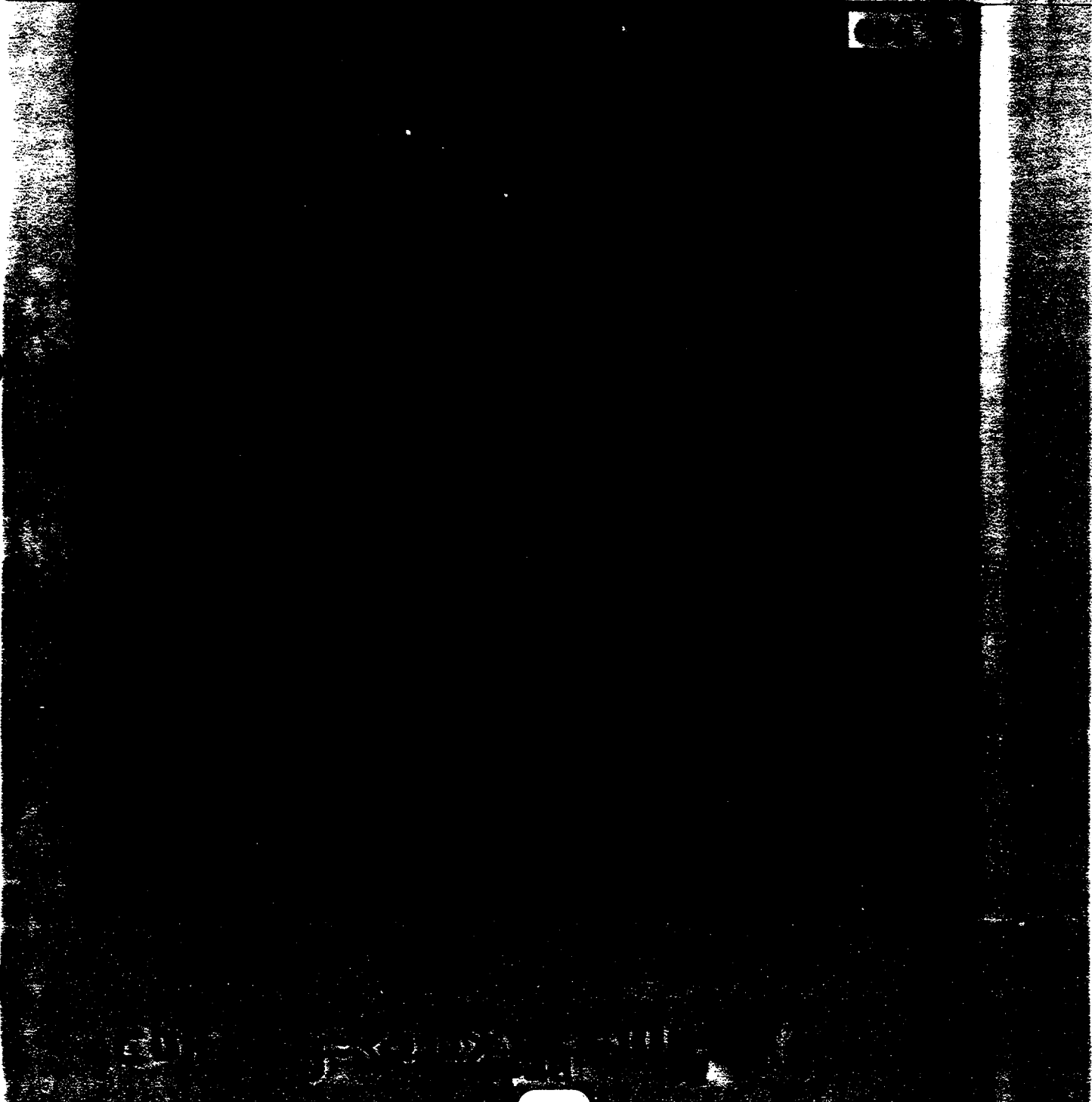
- No significant dependence on PKA energy

* possibly ionization-stimulated point defect recombination, particularly for electron and light ion (low PKA) irradiations.
energy

~17 d% Al @ peak

ORNL-PROG-1033-89

ALUMINUM CONCENTRATIONS IN SPINEL IMPLANTED WITH 5.1×10^{20} cm^{-3}



Comments on Existing Models for RIED

S.J. Zinkle (ORNL)

Y. Chen model (charge injection from electrodes):

- agrees with electron irradiation data by Zong et al.
 - "incubation dose" for RIED initiation
 - suppressed RIED for reversed electric field
- requires high dislocation density (sometimes seen, sometimes not seen)
- pronounced RIED would be expected in cyclotron and fission reactor irradiation experiments due to extended irradiation time (>10 h) with current flowing in one direction
 - however, pronounced RIED was not observed in these experiments
- role of electrode material (blocking vs. injecting) on charge injection??

● ● Comments on Existing Models for RIED (cont'd)

E. Hodgson model ($F \rightarrow F^+ \rightarrow F_2 \rightarrow \text{colloid} \rightarrow \gamma\text{-Al}_2\text{O}_3$)

- * agrees with CIEMAT electron irradiation data
- * no explanation of field reversal data by Zong et al. ??
- * why does colloid density of $\sim 10^{23}/\text{m}^3$ result in the formation of only $\sim 10^8/\text{m}^3$ optically visible defects (clusters of $\gamma\text{-Al}_2\text{O}_3$)?
- * what is the low-conductivity pathway connecting the isolated clusters of $\gamma\text{-Al}_2\text{O}_3$?
- * applicability of model to other ceramics (e.g. MgO)?

● Is RIED associated with a physical process that is unique to electron irradiation?

● Why has RIED not been observed in some electron irradiations?



Recent ceramics work

E.R.Hodgson and A. Moróño

Euratom/CIEMAT Fusion Association, Madrid, Spain

1. RIED theoretical model and basic studies on sapphire

Considerable work has been carried out on the effect of an electric field on the production and evolution of the point defects (oxygen vacancies)

The experimental work has permitted the observation of;

$F \rightarrow F^+ \rightarrow F_2 \rightarrow$ small colloids (≤ 1 nm diam)

The theoretical work has given an explanation for the role of the electric field

Oxygen displacement \rightarrow F centres

Ionization $F \rightarrow F^+ + e^-$

Electric field lifetime F^+ markedly increases \implies enhanced mobility

Aggregation $F^+ + F$ (or F^+) \rightarrow F_2 type centres

$F^+ + F_2 \rightarrow$ higher aggregates and hence colloids

Colloid production gives a satisfactory explanation for the γ alumina observation

(Colloids remove aluminium from the lattice and the oxygen interstitials increase the local oxygen content)

The combination of colloids in a local γ alumina region all within an α alumina matrix predicts the observed degradation of the activation energy.

See figure 1 and figs. 10 to 15 in talk "Evidence for Bulk RIED"

2. Surface and volume (RIED) degradation in Wesgo AL995 alumina

Many hundreds of accelerator hours have been dedicated to this material from which we have been able to establish;

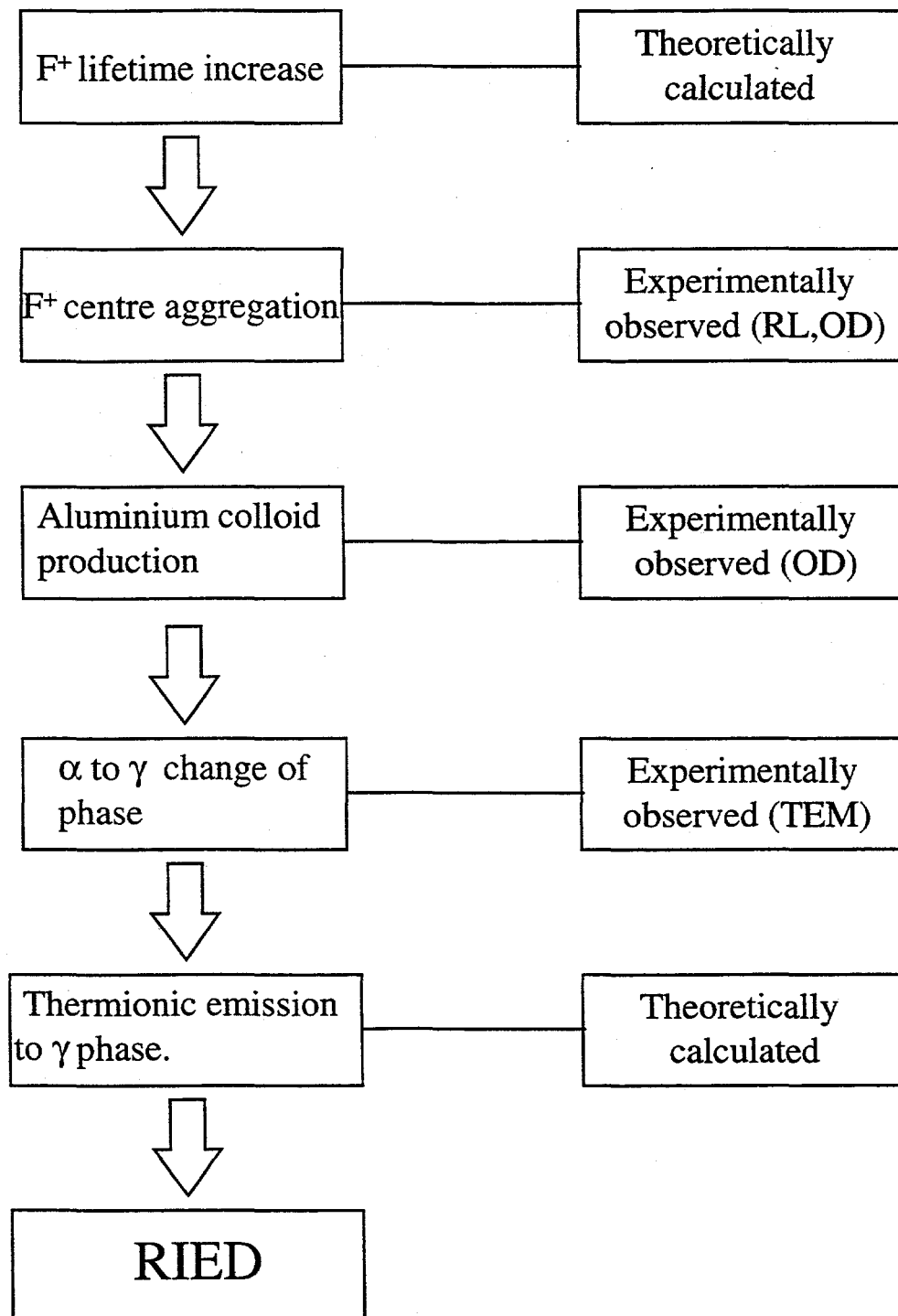
- i) Irradiation in vacuum causes severe surface degradation
- ii) Irradiation in air or He does NOT cause surface degradation
- iii) Collimation of the electron beam to irradiate only the central electrode drastically reduces the surface degradation (ie the surface degradation is radiation induced or enhanced) This explains the conflicting results of Kesternich and Möslang
See fig. 2
- iv) At 100 kV/m no volume degradation is observed
- v) At 500 kV/m no volume degradation was observed (> 200 h irradiation)
- vi) At 1 MV/m a clear volume degradation was observed BUT the process is complicated by radiation enhanced impurity segregation (electrolysis) at the -ve electrode Saturation is observed in the RIED but is completely removed by polishing off < 0.1 mm
- vii) At 1.5 MV/m (AC 50 Hz) a clear volume degradation is observed with no saturation
See figs. 3 to 6

3. Optical absorption and emission in KU1 (RF silica)

Work for the ITER diagnostics programme has looked at the Russian KU1 quartz glass material (kindly provided for the T246 task by Dorian Orlinski and colleagues)

In terms of radiation resistance to both displacement damage and radioluminescence this is the best silica material we have looked at. In particular the radioluminescence is almost limited to the Cherenkov radiation. (figs. 7 & 8)

Fundamental processes associated to RIED.



AL995
large grain size
low density alumina

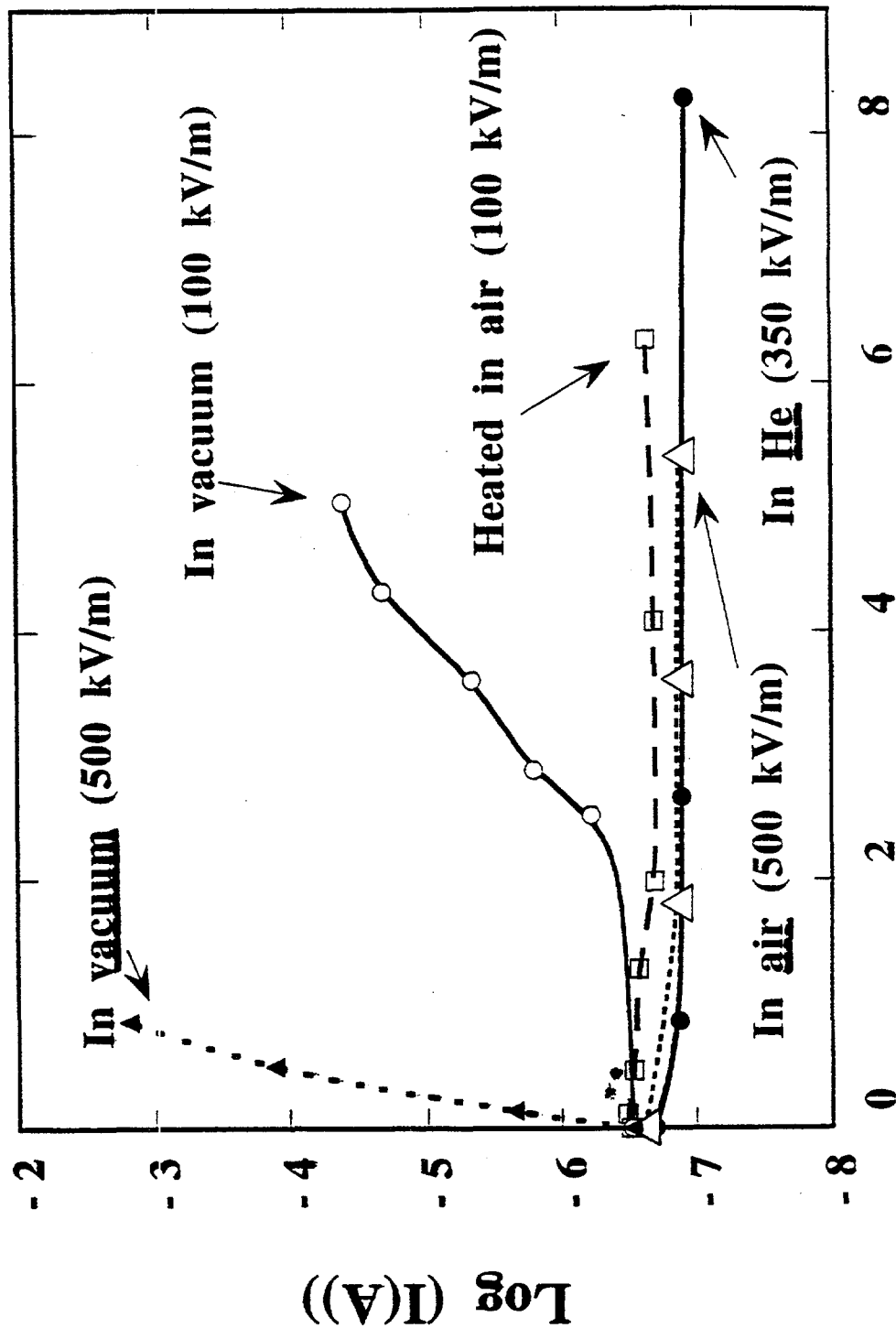


Fig. 2

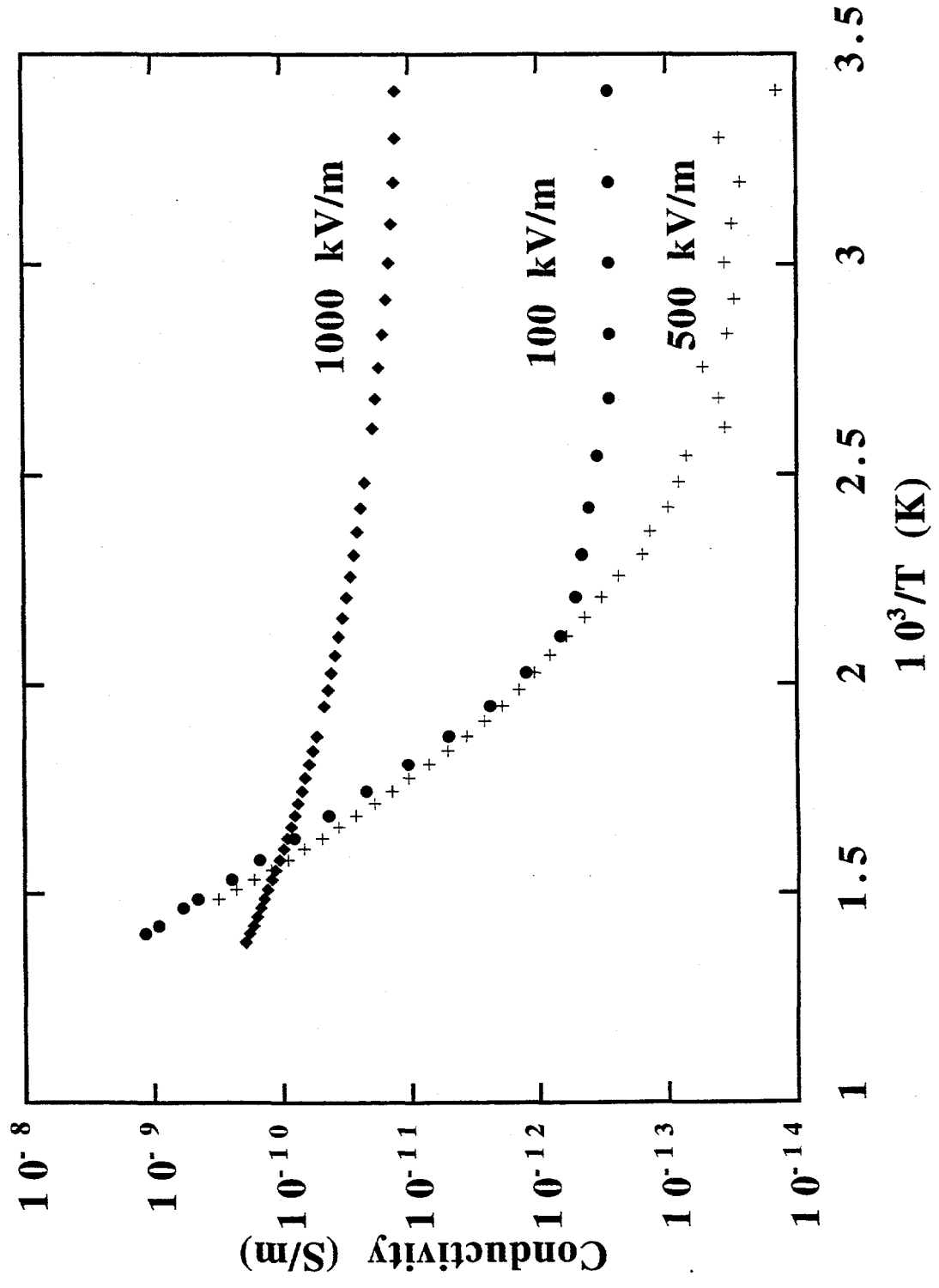
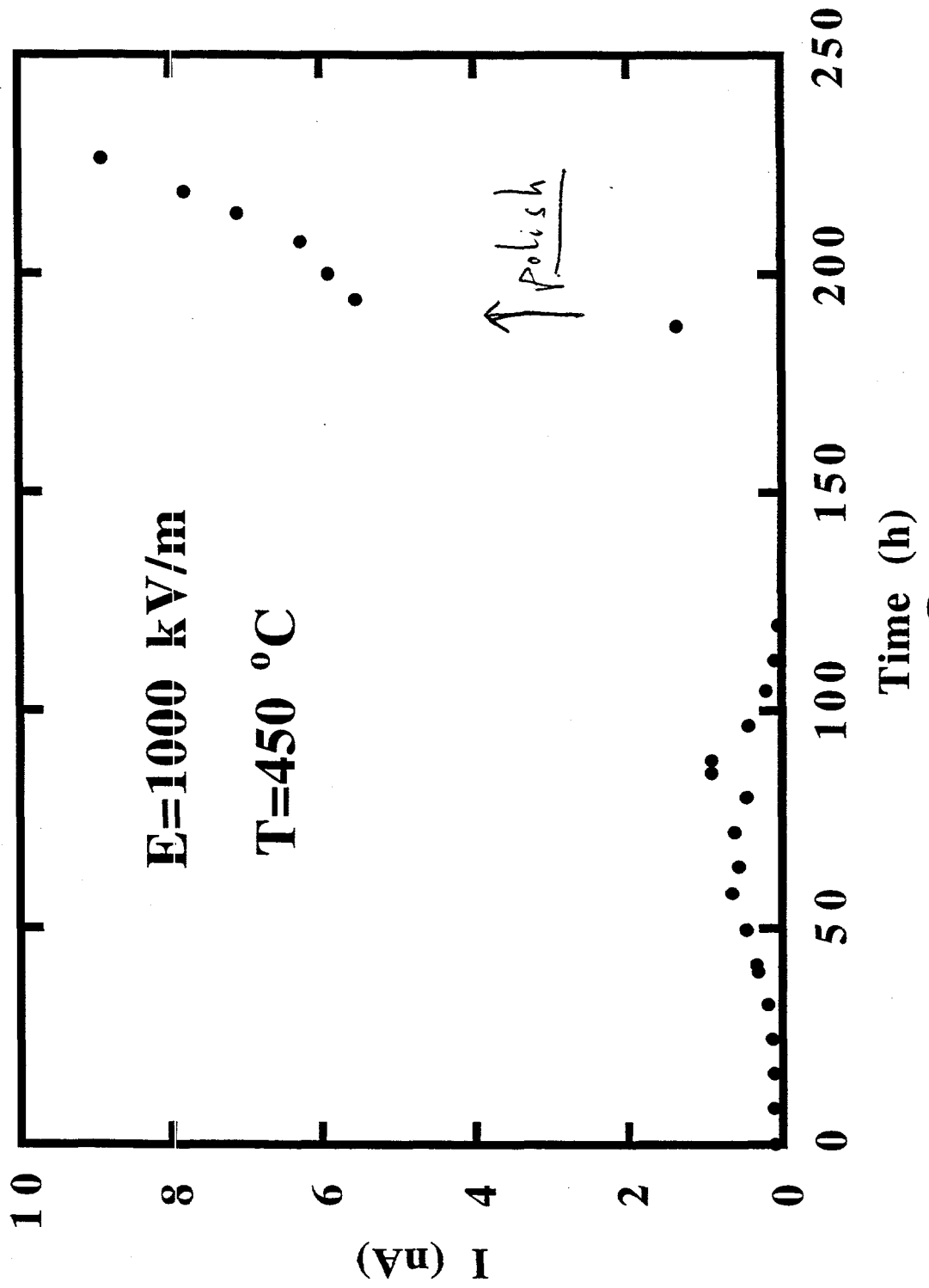
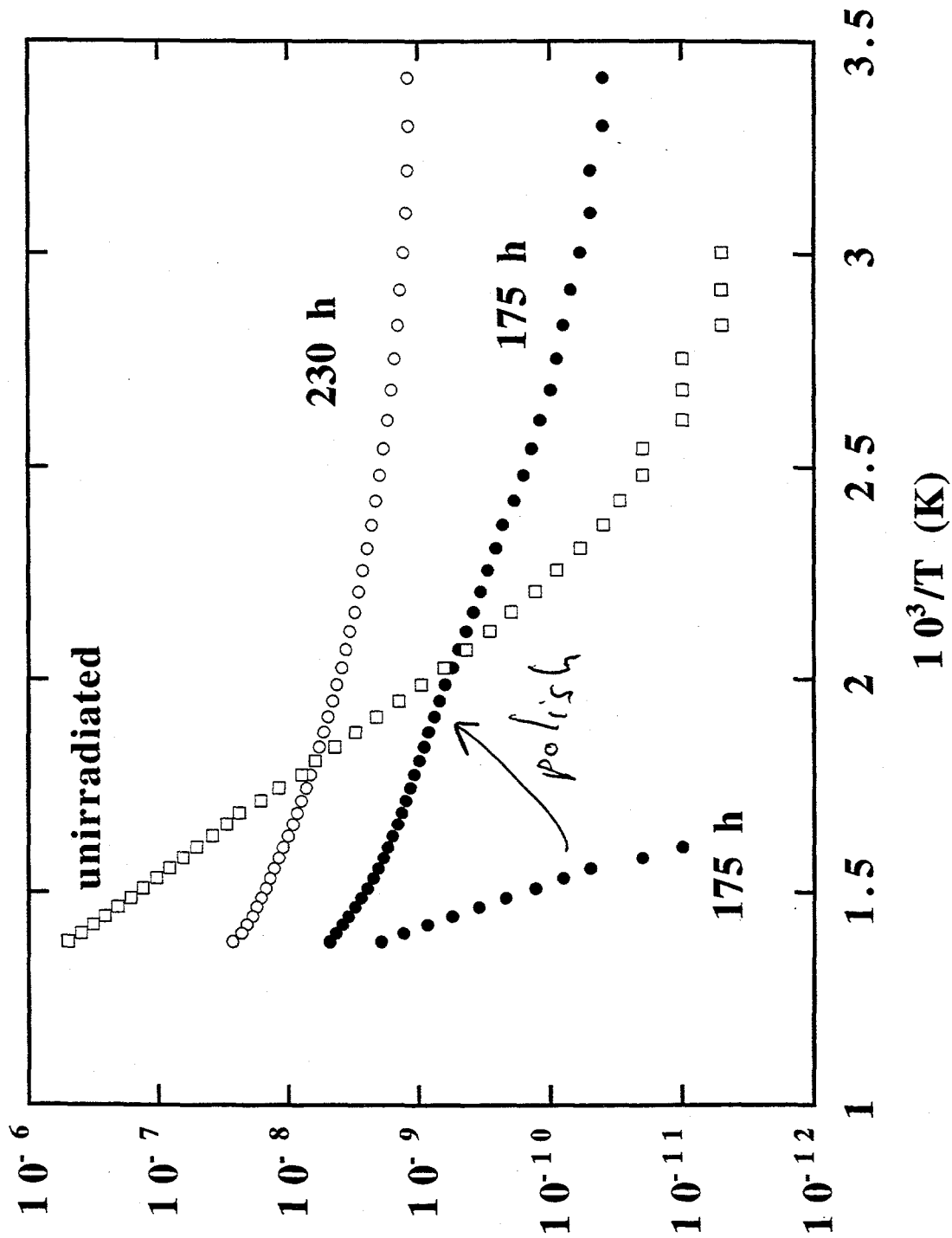


Fig. 3





I (A)

Fig. 1

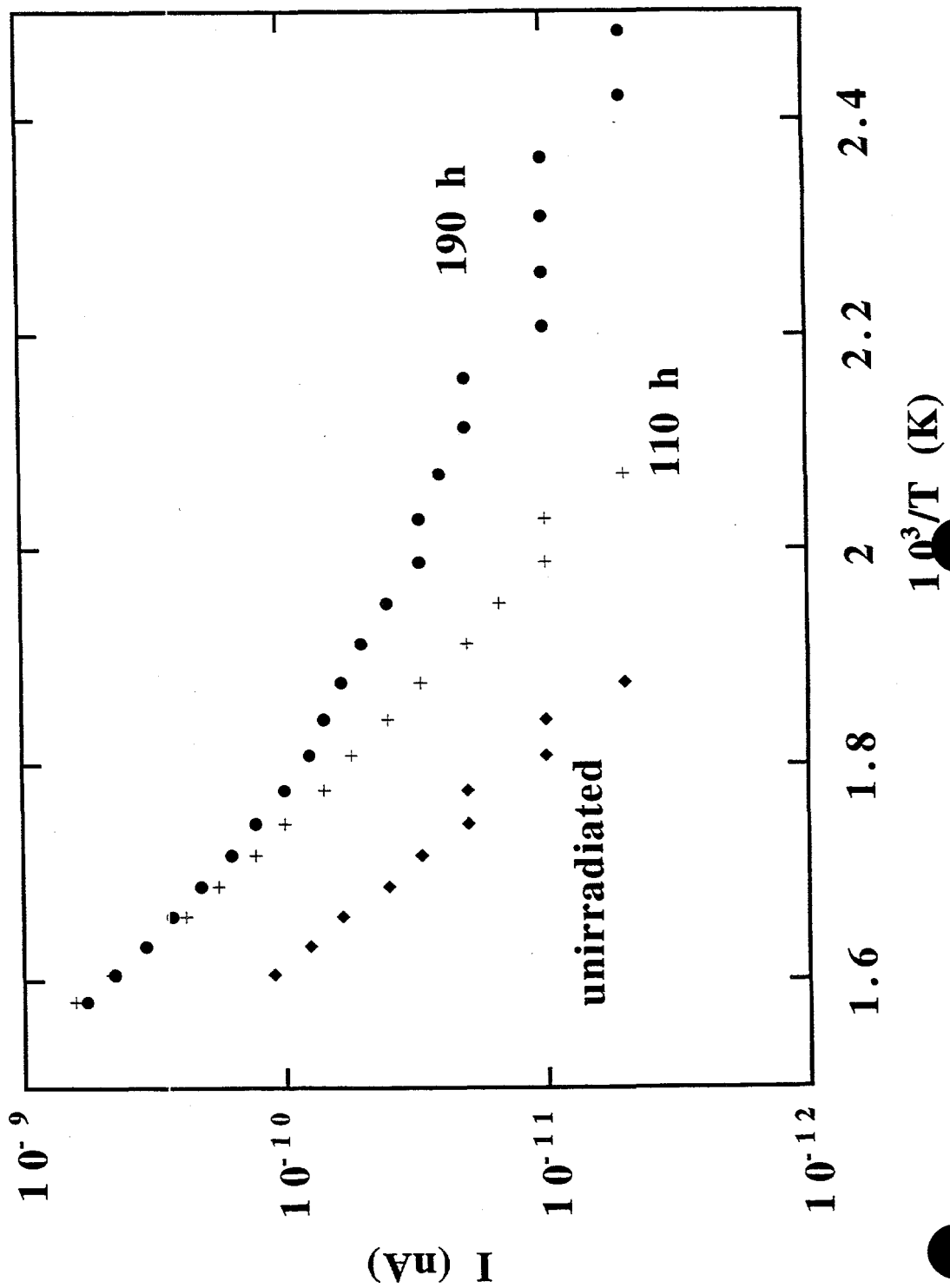


Fig. 6

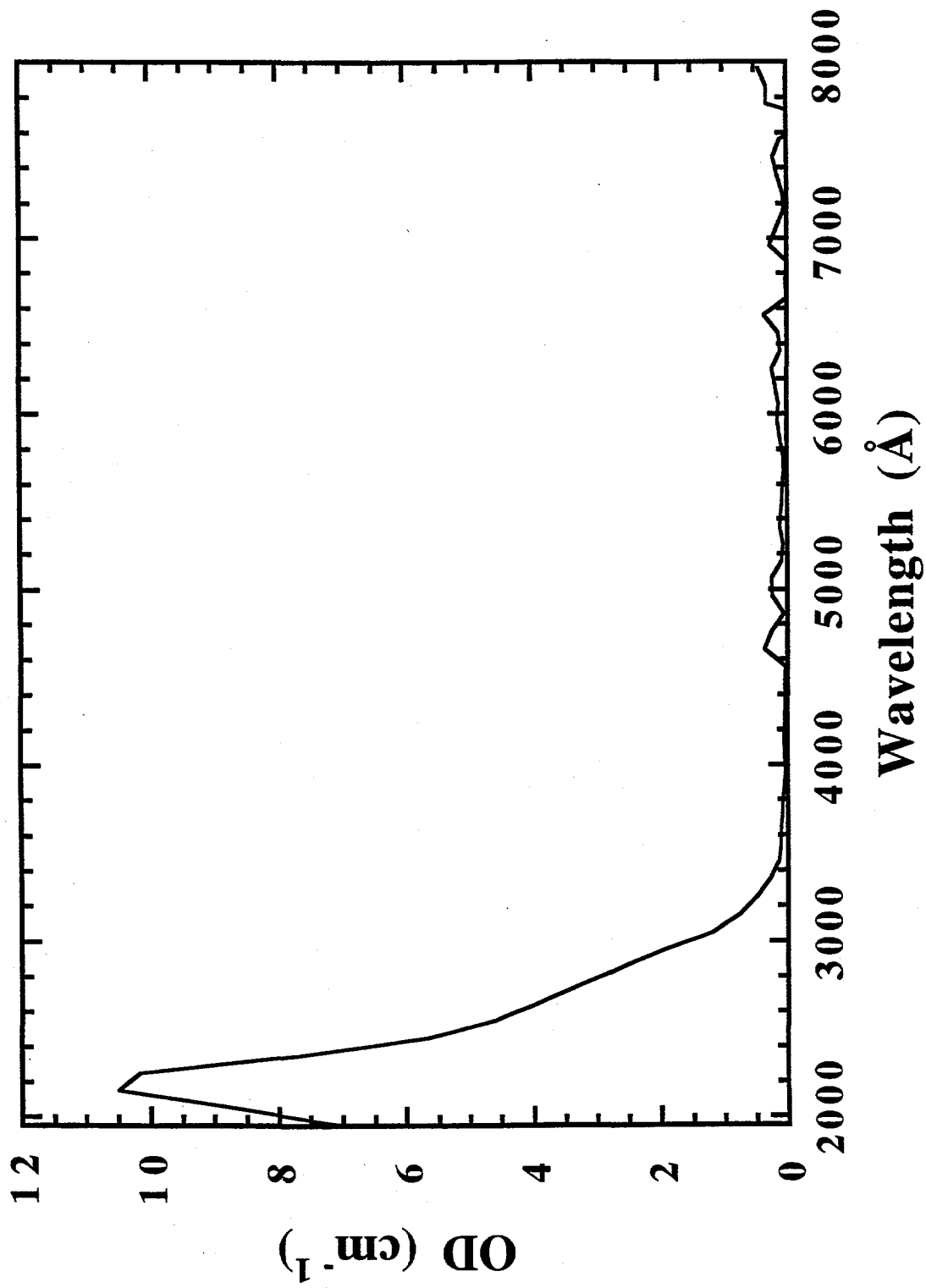
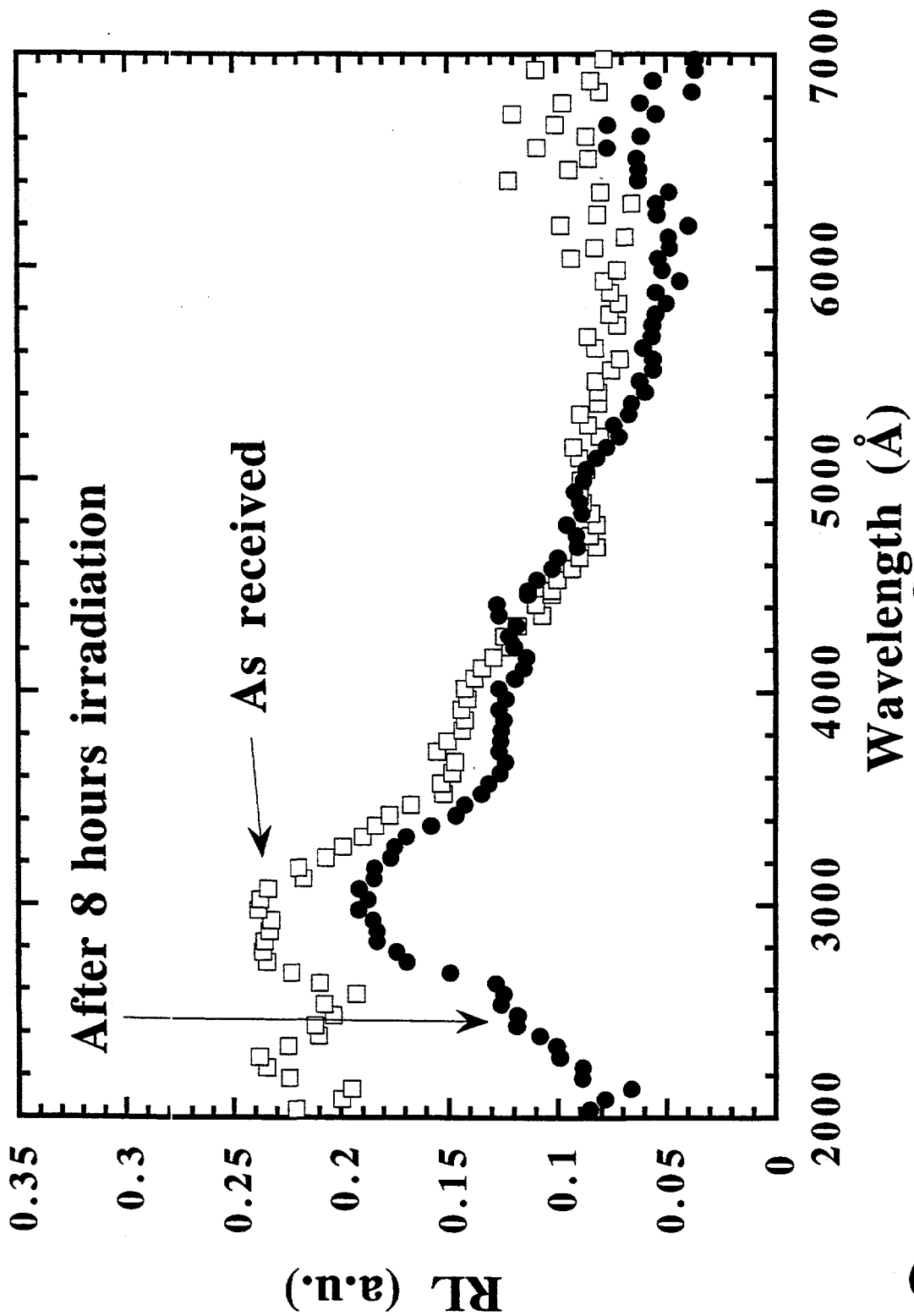


Fig. 7

r



CIEMAT Work Abstract

R. Vila

Outside RIED effect work.

1.- The major part of the time has been devoted to new equipment:

a) The optimization of the resonant cavity operating at 70-100 Mhz. The instrumentation has been improved and camera design was changed in order to increase radiation dose rate by a factor 4x, up to about 2 KGy/s.

b) Design, construction and testing of a camera for low-frequency (~0.1 kHz to 1MHz) dielectric measurements.

Both systems can measure ϵ and $\tan \delta$ in the 2MeV electron accelerator. Only Si sample showed a very high in-beam effect. Alumina, Diamond and BeO will be measured again at the new dose rate.

2.- Basic research:

More work has been done in several commercial aluminas. We enlarged the non-irradiated alumina dielectric database (see for example data for Kyocera A473).

Reducing and oxidizing heat treatments have been done in order to obtain more information about the role of impurities in dielectric loss.

For example, iron doping does not seem to change high frequency properties but, under reducing conditions (1550°C in Ar atmosphere), an increase of H.F loss was observed.

By contrary, Vitox sample did not show any variation under several heat treatments.

3.- Silicon: A neutron-irradiated sample (10^{-5} dpa) has been measured as a function of frequency. As in the case of electron irradiation, a decrease of loss was observed, due to the formation of recombination centers that reduces conductivity.

4.- Diamond: We show the $\tan \delta$ vs freq curve for a neutron irradiated sample (up to 10^{-5} dpa). Although at RF., $\tan \delta$ values are in the range 10^{-3} - 10^{-2} , they rapidly fall to near 10^{-5} at 145 GHz (as measured by R. Heidinger). Taking into account that material quality is improving every day and the radiation-resistant behaviour observed up to now, we think that it is the most promising candidate for ECH heating.

Workshop on Ceramic

Insulators for Fusion

Energy Applications

USA- 1997

Outline

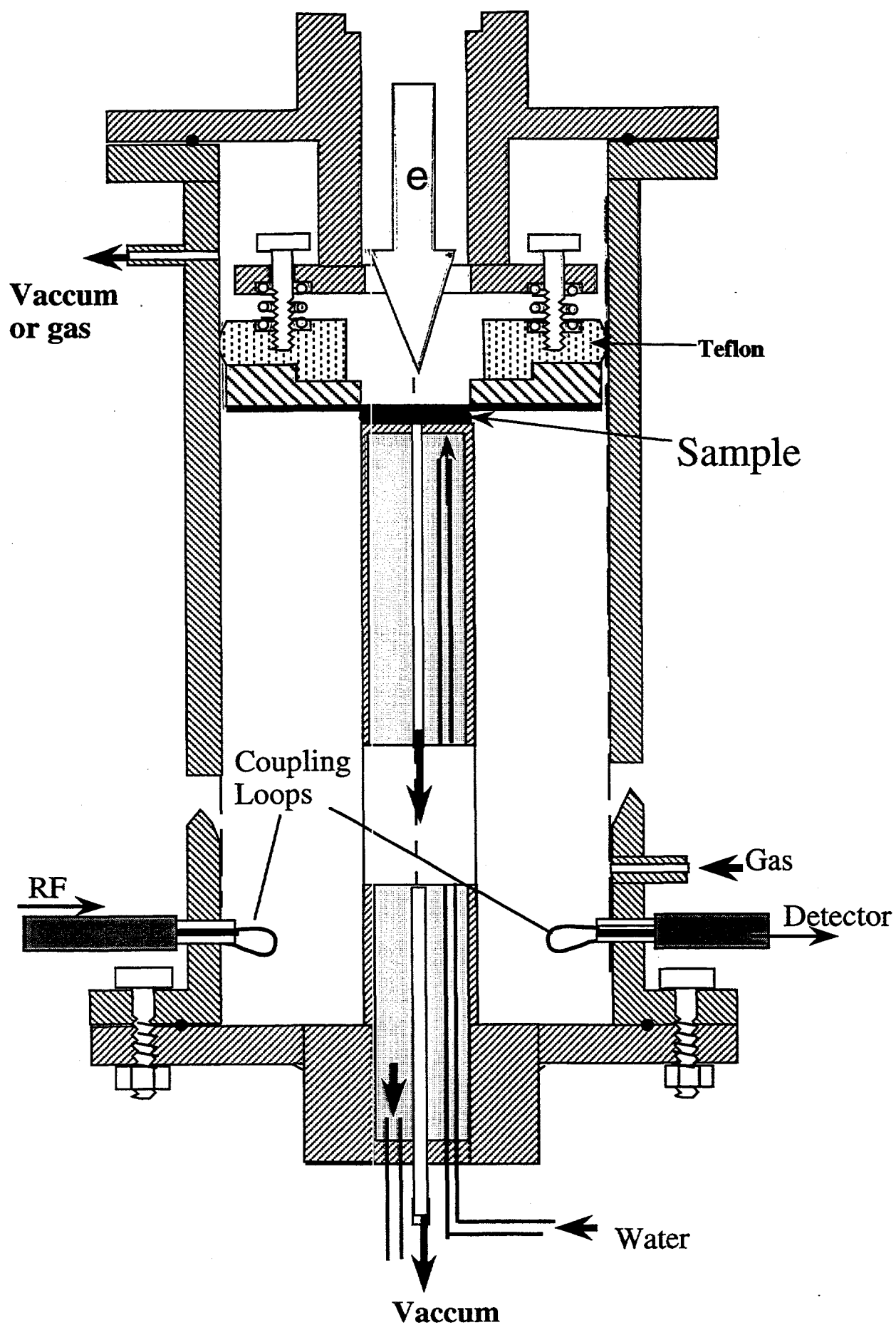
- **New Dielectric Measurement Techniques.**
- **Basic Research.**
- **Silicon.**
- **Diamond.**

1. New Experimental Techniques

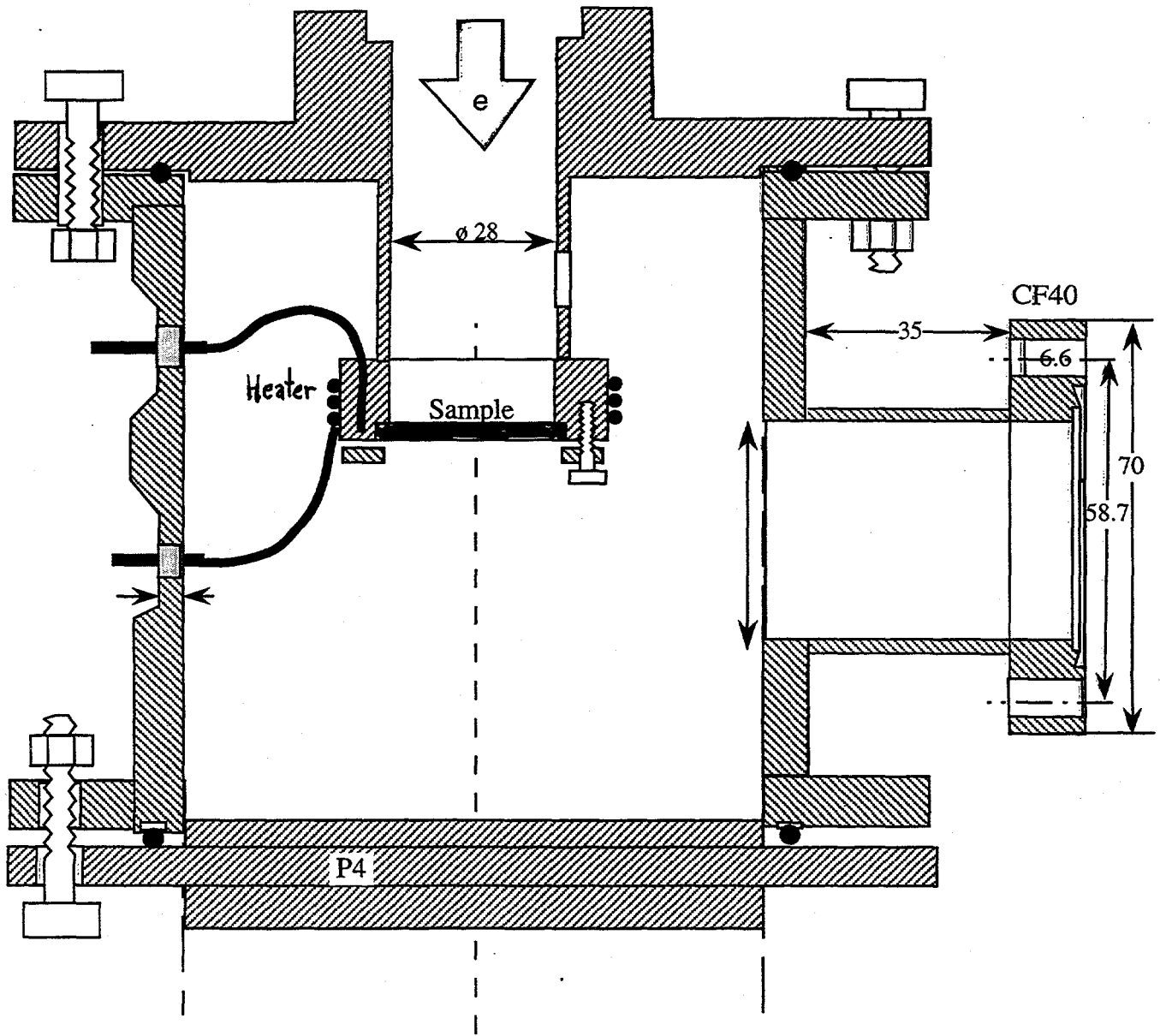
- 1.1 Coaxial Resonant Cavity
 - The resonant cavity operating at about 70-100 MHz is now fully operating . We can measure ϵ and $\text{Tan } \delta$ under electron irradiation in the 2MeV VDG accelerator.
 - Design improvements have been made on order to increase the dose rate x4 up to 2KGy/s aprox .
 - Measured:
 - » Aluminas
 - » Sapphire
 - » Diamond
 - » Silicon

- 1.2. Low Frequency Camera
 - Design, construction and testing of a camera with the following characteristics:
 - » ϵ and $\text{Tan } \delta$ from ~0.1 KHz to 1 MHz.
 - » Under electron irradiation
 - » From RT to about 300°C.

100 MHz Camera



Low Frequency Van de Graaff Camera



2. Basic Research.

- We continue to study a large set of aluminas with two purposes:
 - a) Provide a reliable database of dielectric properties of commercial aluminas for different applications
 - b) To discover the origin of the high losses found in some of them. Focussed on the effect of common impurities.

Thermal redox treatments and correlation of loss with impurities have been done

Results:

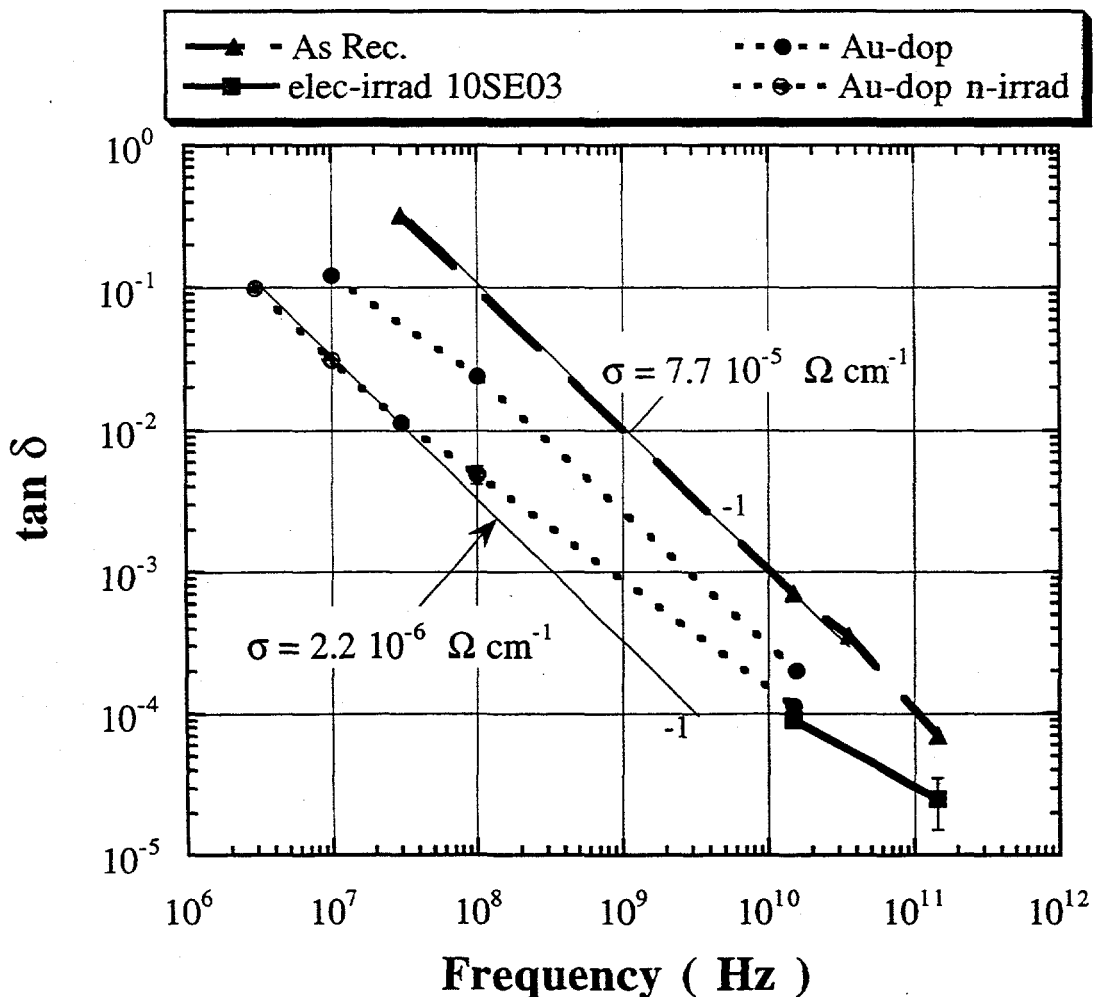
- Mg : has been found responsible for the $\text{Tan } \delta$ peak at about 1GHz. (No changes after several heat treatments)
- Fe : No effect at H.F in as-grown samples
 - » After reducing treatment (1550°C in Ar) a dielectric loss appears at about 100Mhz.

3. Silicon

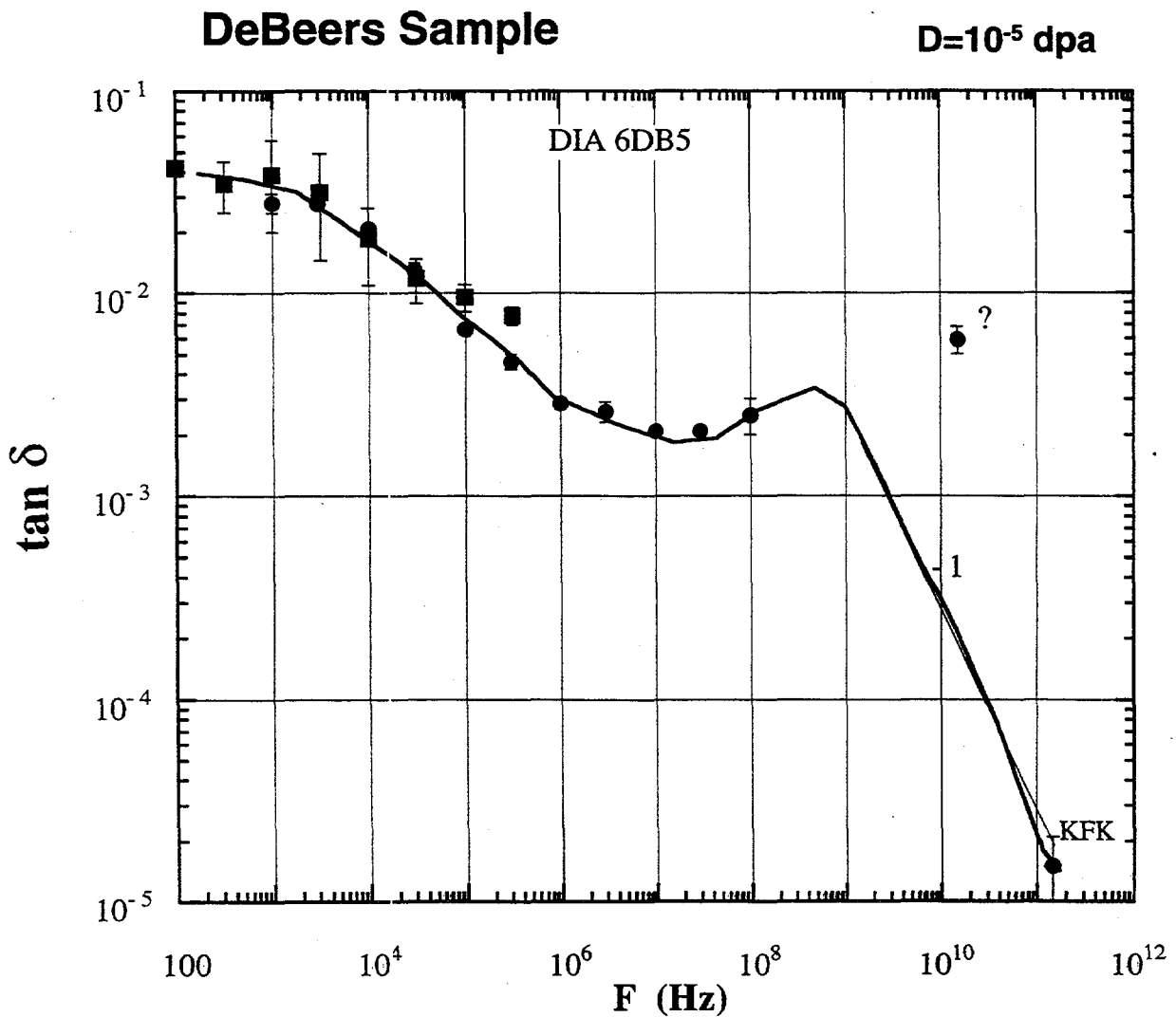
- We continue to study different Si samples to study the decreases in loss induced by some defects (recombination centers in electron irradiated and gold-doped samples)

New Results:

– Neutron Irradiated sample: $\sim 10^{-5}$ dpa



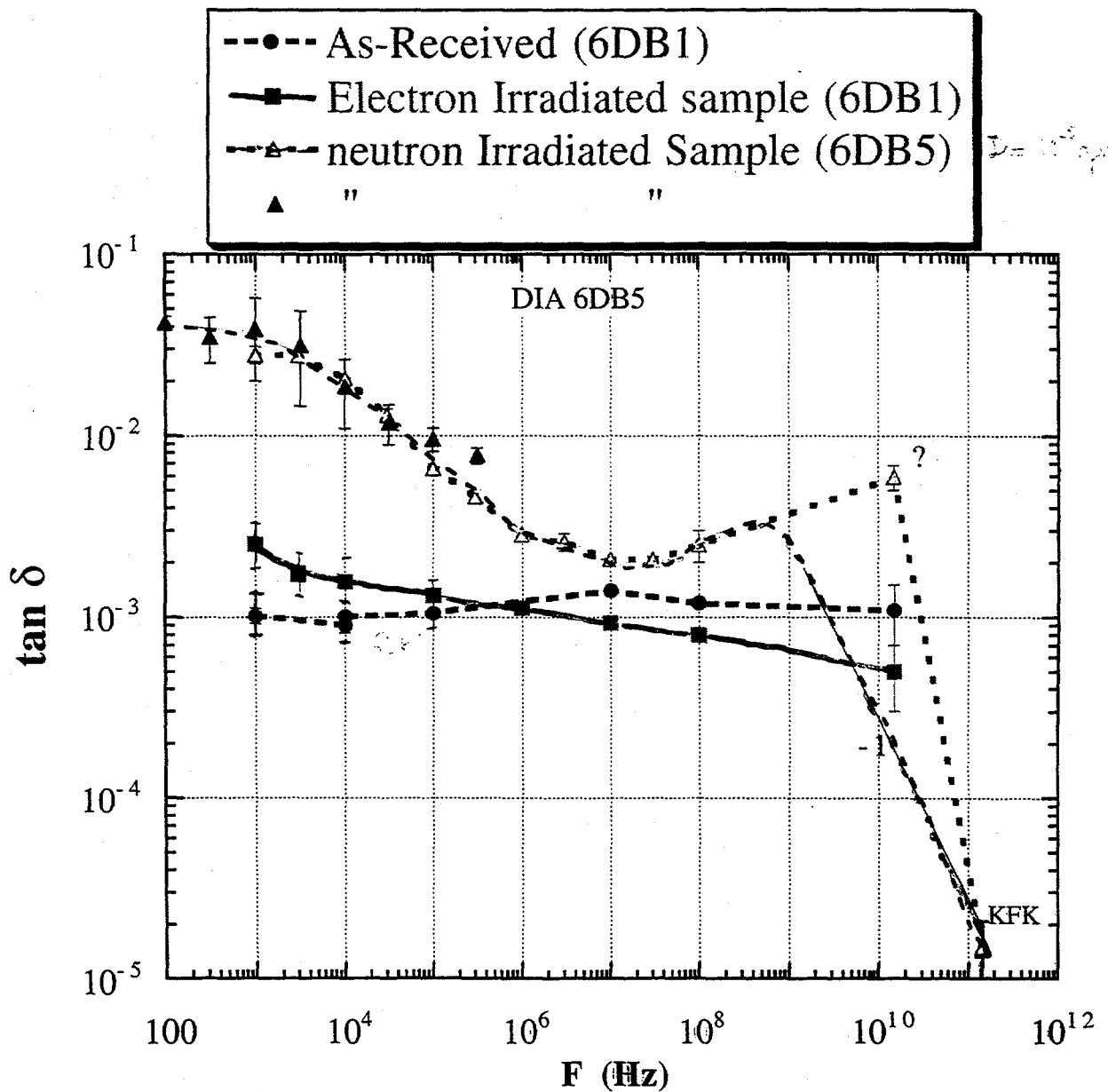
Diamond Neutron Irradiated



➔ **Very promising for high frequency applications**

KFK: Measured by Dr. R. Heidinger

Commercial CVD Diamonds





Effects of Triple Beam Irradiation with H, He and O-ions on Damage Structures in Al₂O₃

K. Noda and Y. Katano

Department of Materials Science and Engineering,
Japan Atomic Energy Research Institute,
Tokai-mura, Ibaraki-ken, 319-11 Japan

IEA Workshop on Radiation Effects in Ceramic Insulators

Omni Netherland Plaza Hotel, Cincinnati, OH, USA
May 7-8, 1997

The radiation-induced microstructural changes have been investigated by cross sectional transmission electron microscopy (XTEM) for single crystal Al₂O₃ irradiated to dose level in the range 0.1 to 8.4 dpa at the damage peak with triple ion beams of "triple A" mode (i.e., 0.25MeV H⁺, 0.6MeV He⁺ and 2.4MeV O²⁺) and "triple B" mode (i.e., 0.33MeV H⁺, 0.45MeV He⁺ and 1.3MeV O⁺) at 923K.

In the specimen irradiated with "triple A" mode, cavities with average diameter of 13 nm were observed in the narrow region of depths from 1.2 to 1.7 μ m. The maximum cavity density of $1.7 \times 10^{23}/\text{m}^3$ was attained at depth of about 1.5 μ m and the swelling at the depth was estimated to be about 0.1%. The swelling was larger than that of the specimen irradiated with "triple B mode".

Optical absorption spectroscopy for this specimen exhibited significant increase in intensity of absorption bands due to F and F⁺ centers, which indicated production of oxygen vacancies by the irradiation.

The extent of distribution of cavities formed with "triple A" mode was narrower than that in the region where He⁺ and O⁺ ions or H⁺ ions were implanted in the sample irradiated with "triple B" mode. Cavities formed in the region implanted with H⁺ ions in the sample irradiated with "triple B" mode were found to be inhomogeneously distributed in the vicinity of dislocation loops. These cavities, which resulted in 0.07% swelling at the peak of the number of implanted H⁺ ions, were considered to be bubbles containing H atoms. Implanted H atoms can enhance the cavity growth, although displacement damage due to a H⁺ ion is smaller than that by a He⁺ ion or an O⁺ ion. Consequently, ratio between the swelling and displacement damage introduced was 10 to 150 times as large as those in the region irradiated with the same projected range by triple ion beam ("triple A" mode) and in the region where He⁺ and O⁺ ions were simultaneously implanted in "triple B" mode.

**EFFECTS OF TRIPLE BEAMS IRRADIATION WITH H, He AND O- IONS ON
DAMAGE STRUCTURES IN Al₂O₃**

by

K. NODA

&

Y. KATANO

*Department of Material Science and Engineering,
Japan Atomic Energy Research Institute,
Tokai-mura, Ibaraki 319-11, JAPAN*

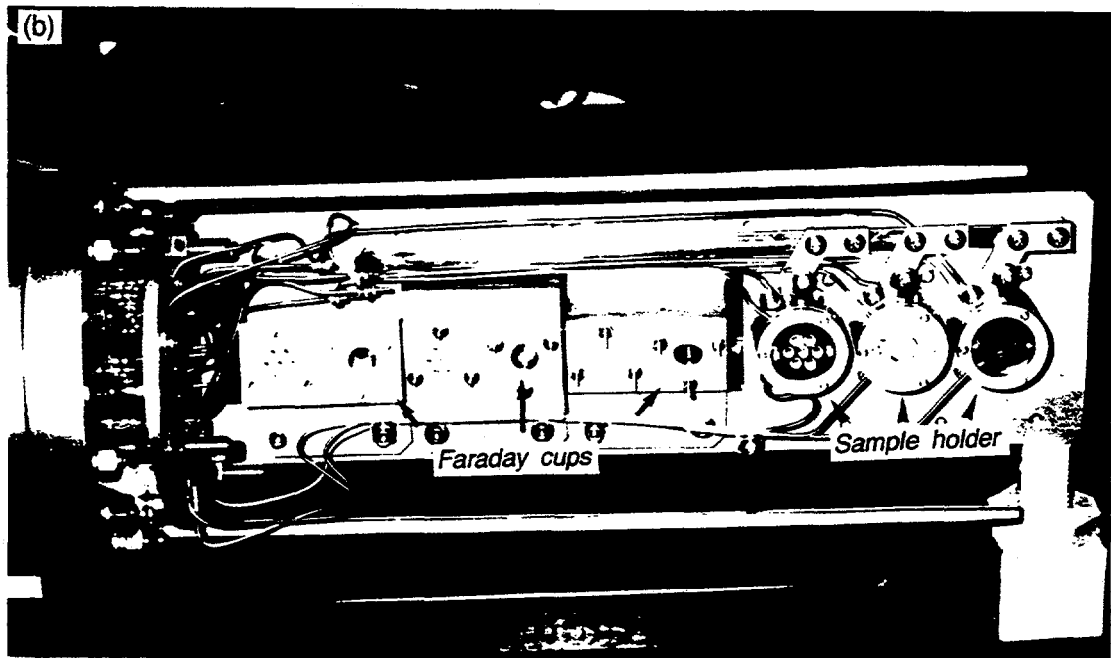
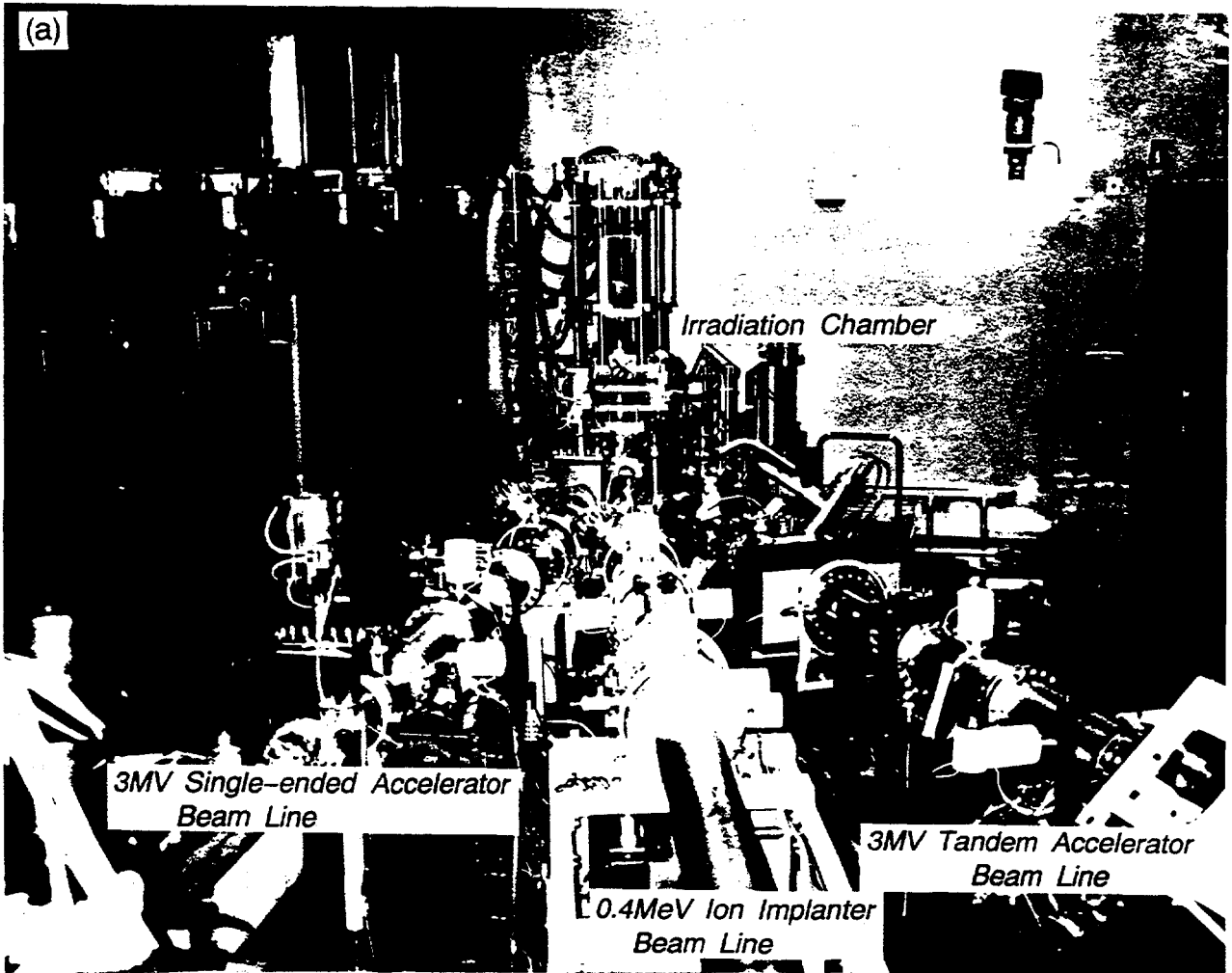
**Cincinnati, USA
May 4 -7, 1997**

Objective:

Cross-sectional transmission electron microscopy(XTEM) is utilized to study microstructural evolution in single crystalline Al₂O₃ irradiated with triple beams (H⁺, He⁺ and O²⁺ ions) to elucidate the effects of transmuteds such as H and He on damage structure in Al₂O₃ for fusion reactor application.

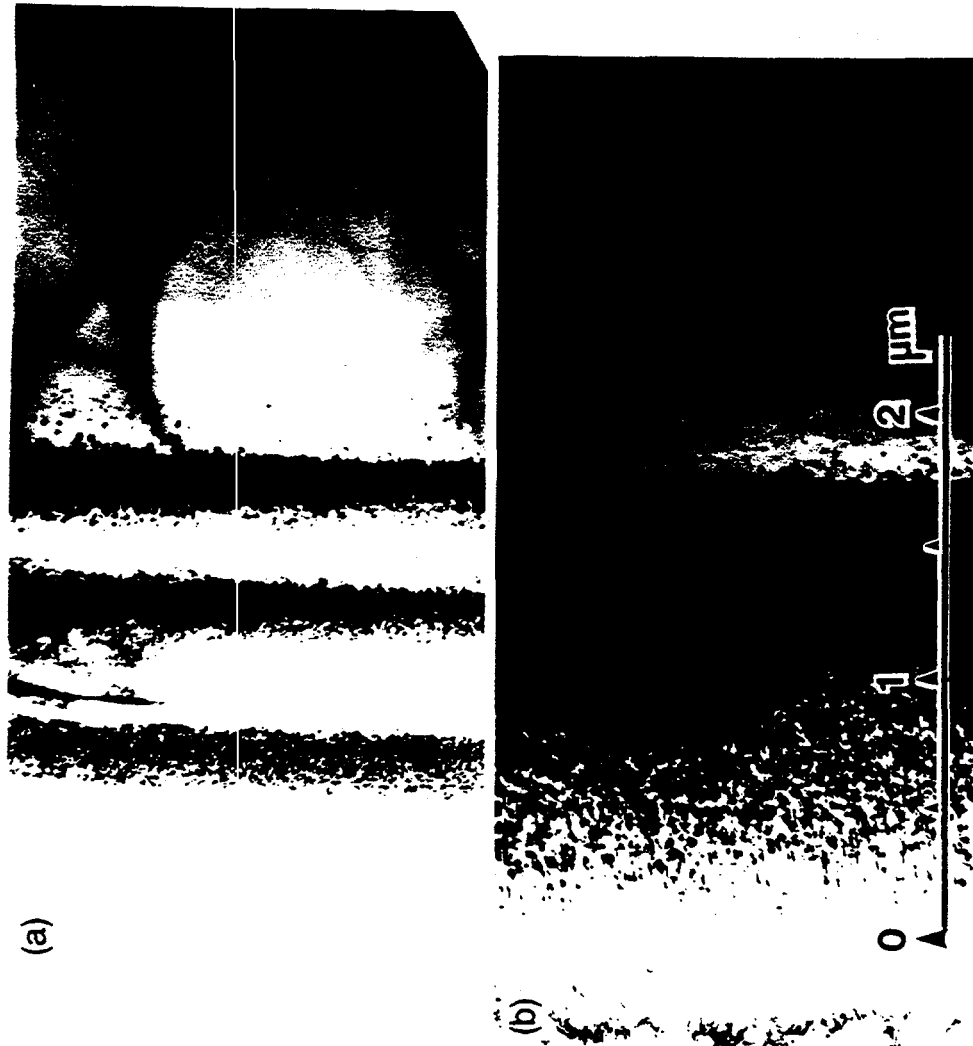
JAERI, Tokai

"Triple ion beams irradiation facility" of JAERI



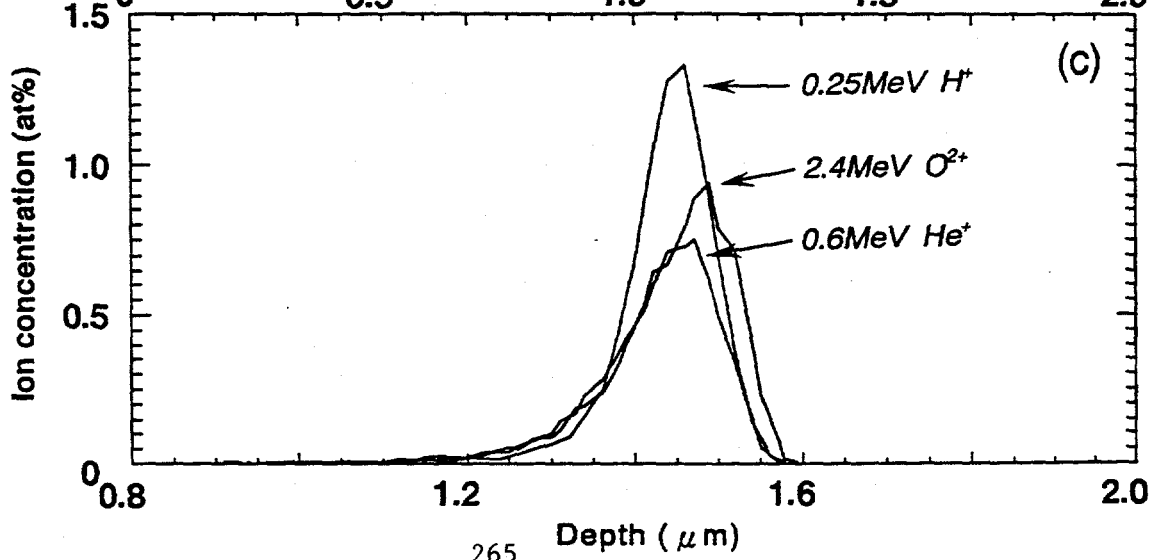
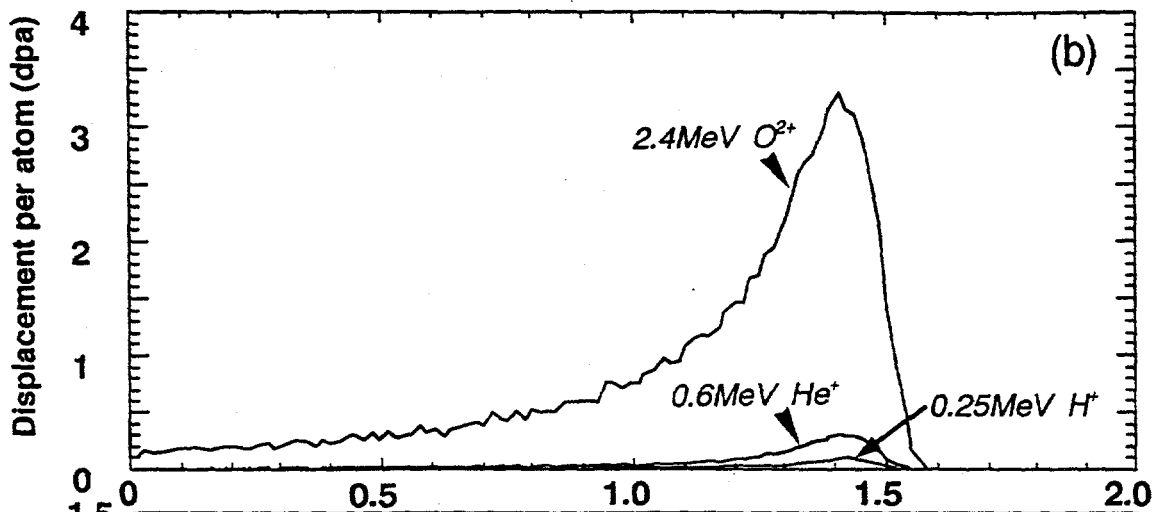
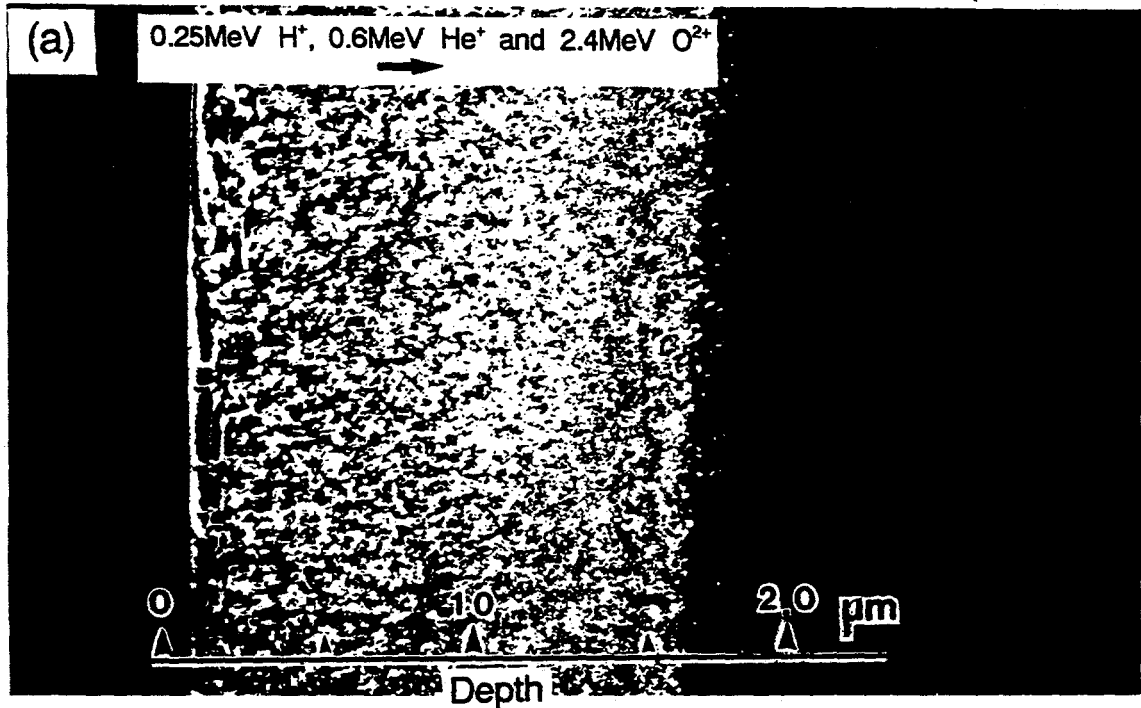
JAERI, Tokai

Comparison of the depth-dependent microstructure of Al_2O_3 irradiated with O^+ , He^+ and H^+ -ions at $650^\circ C$ to a fluence of 0.9 to 5×10^{20} ion/ m^2 . The particle flux was about 3×10^{16} ion/ $m^2 \cdot s$.

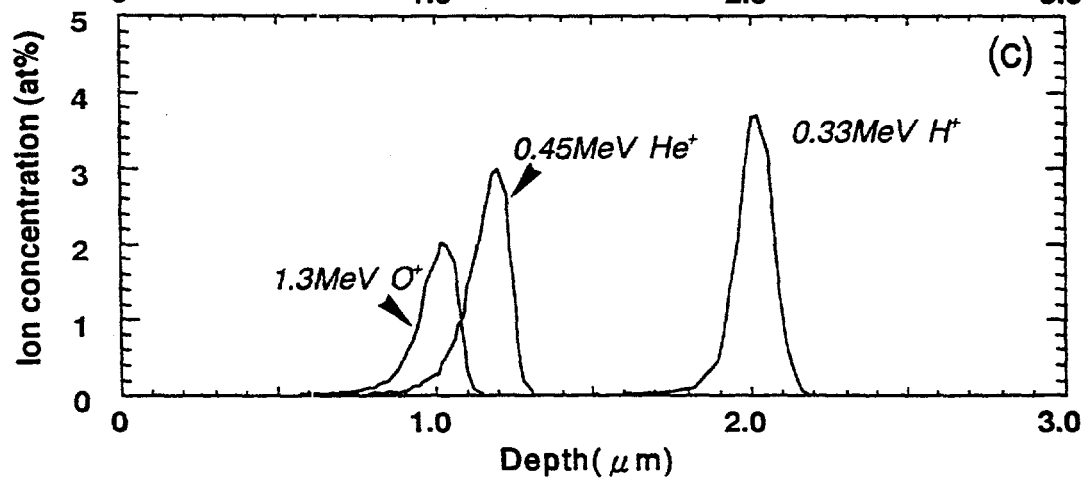
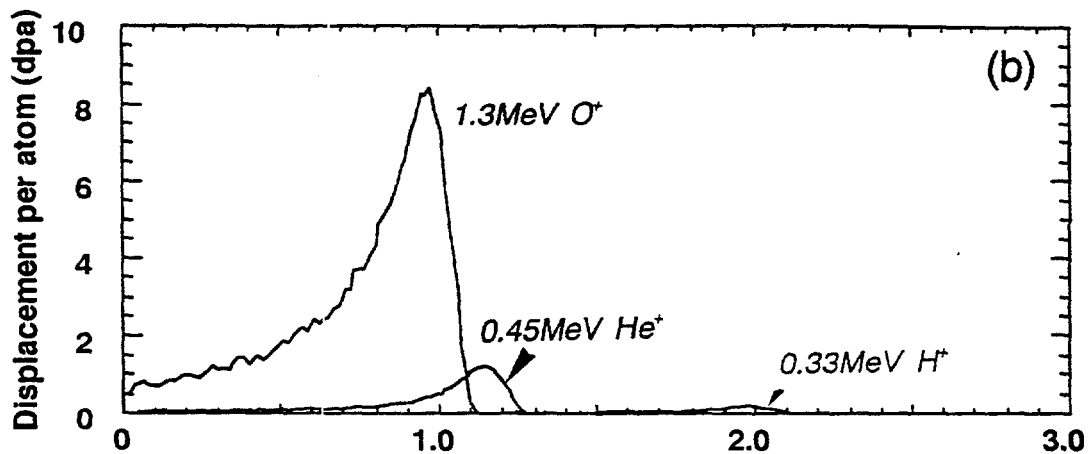
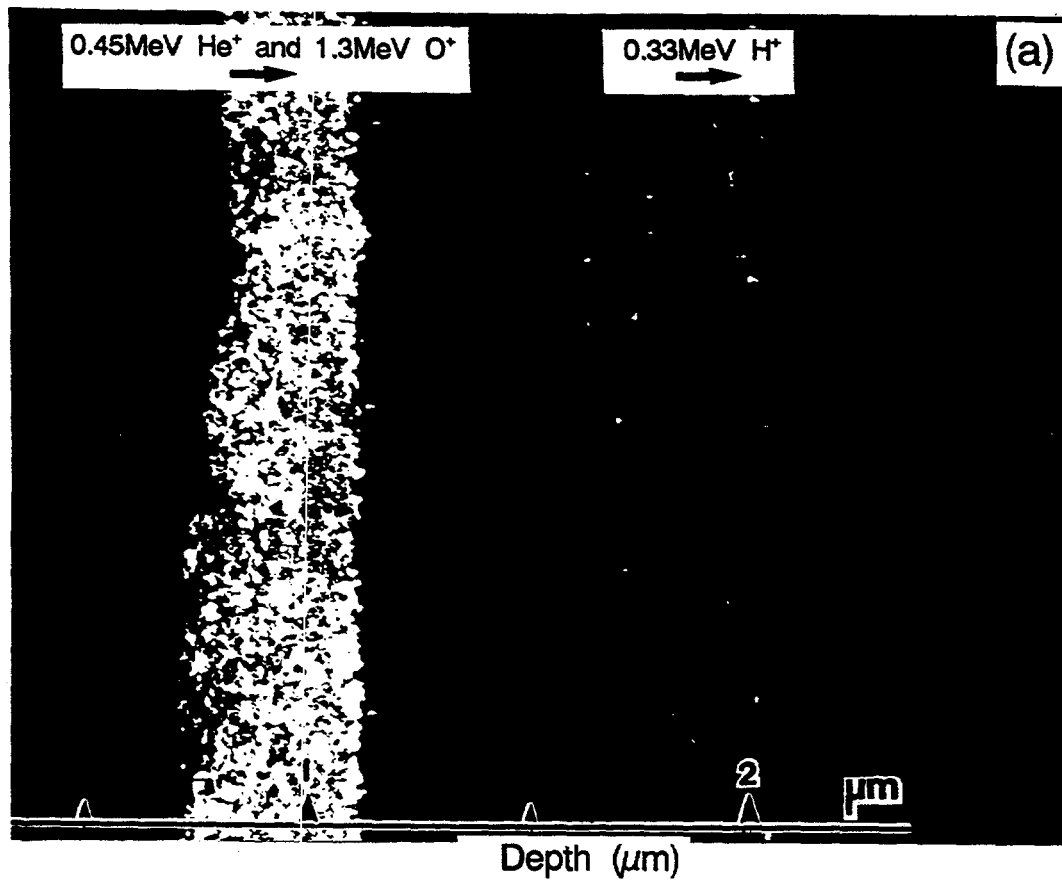


(a) Single ion beams irradiation used 0.8MeV O^+ , 0.6MeV He^+ and 0.3MeV H^+ ions.
(b) Triple ion beams irradiation used 2.4MeV O^{2+} , 0.6MeV He^+ and 0.25MeV H^+ ions.

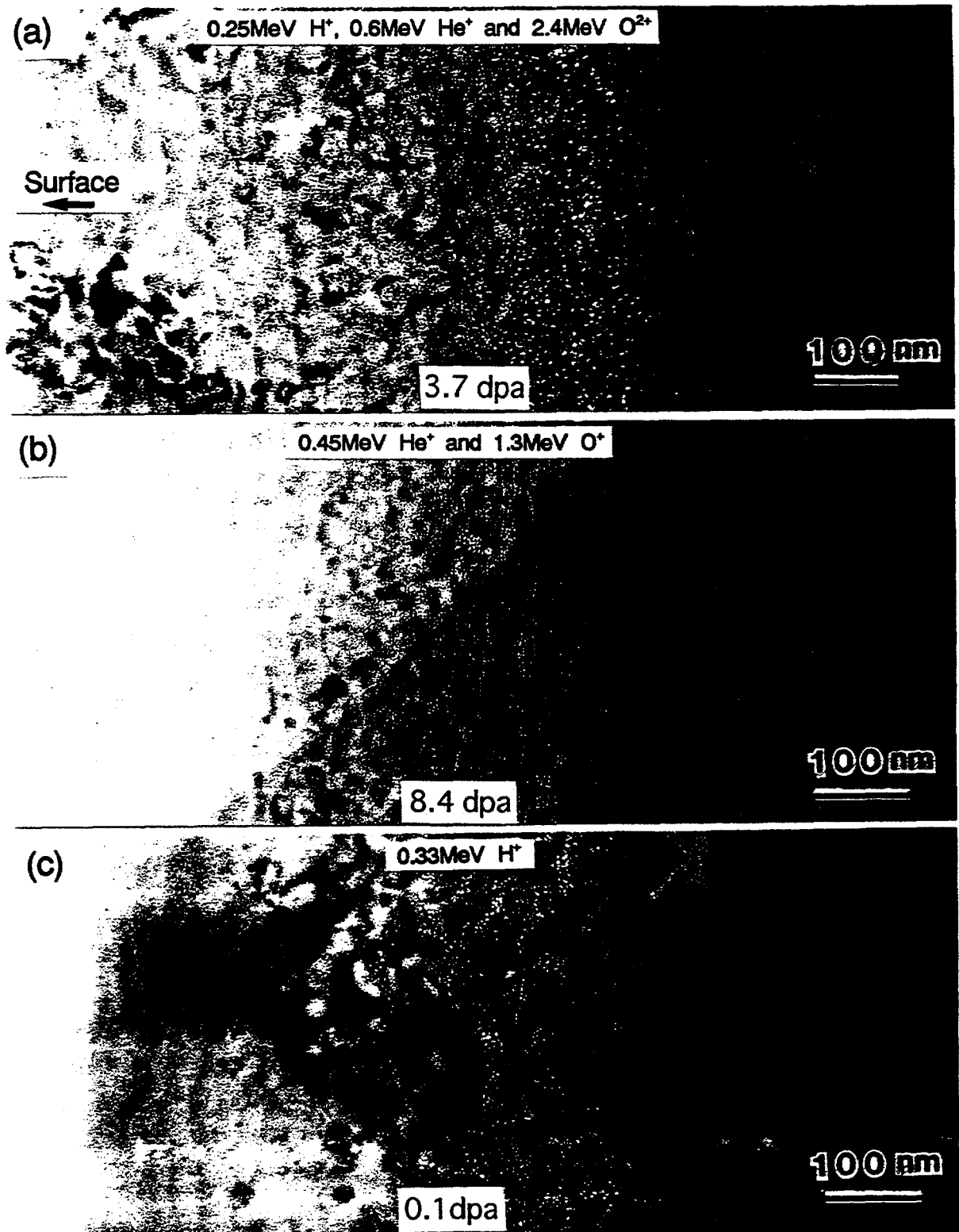
Depth-dependent microstructure in Al_2O_3 irradiated with Triple A (a) and depth profiles calculated by TRIM89 (b), (c)



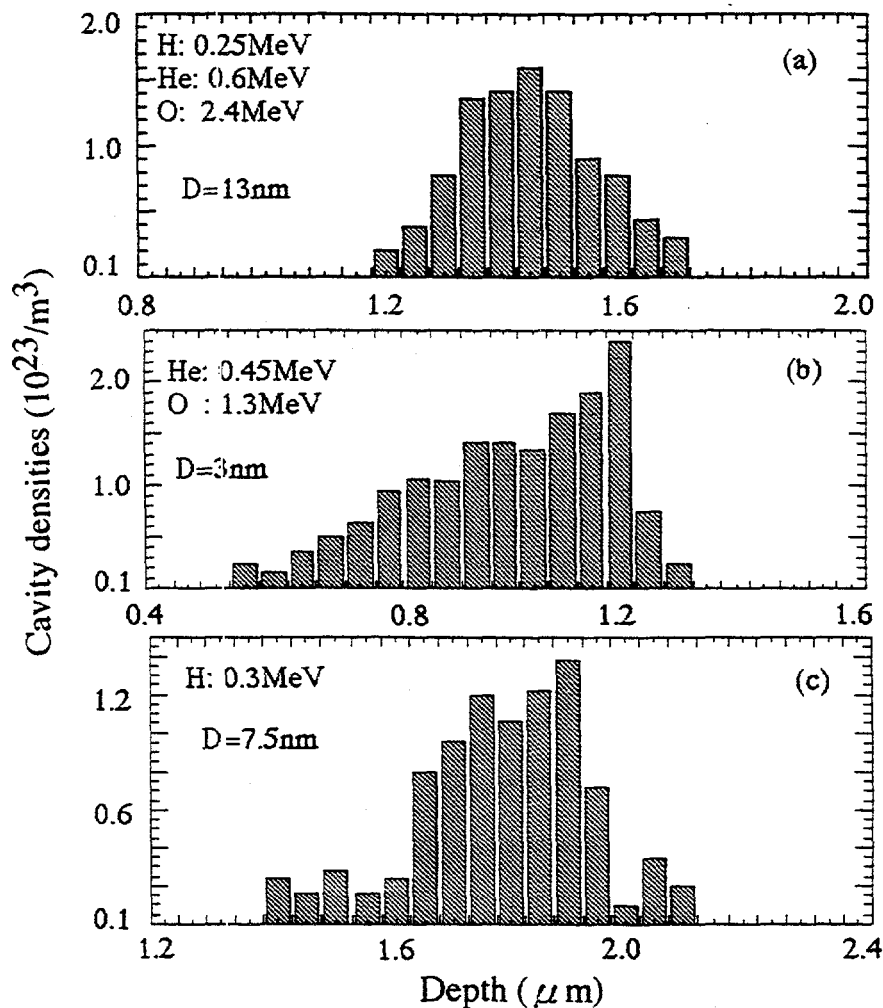
Depth-dependent microstructure in Al_2O_3 irradiated with Triple B (a) and depth profiles calculated by TRIM89 (b), (c)



Comparison of the cavity formed of Al_2O_3 irradiated with (a) "Triple A" and (b), (c) "Triple B" at 923K (0.4Tm)



Comparison of the cavity density depth profiles in Al_2O_3 irradiated at 923K with (a) "Triple A" mode (H^+ , He^+ and O^{2+}), (b) "Triple B" mode (He^+ and O^+ ions) and (c) H^+ ion beams

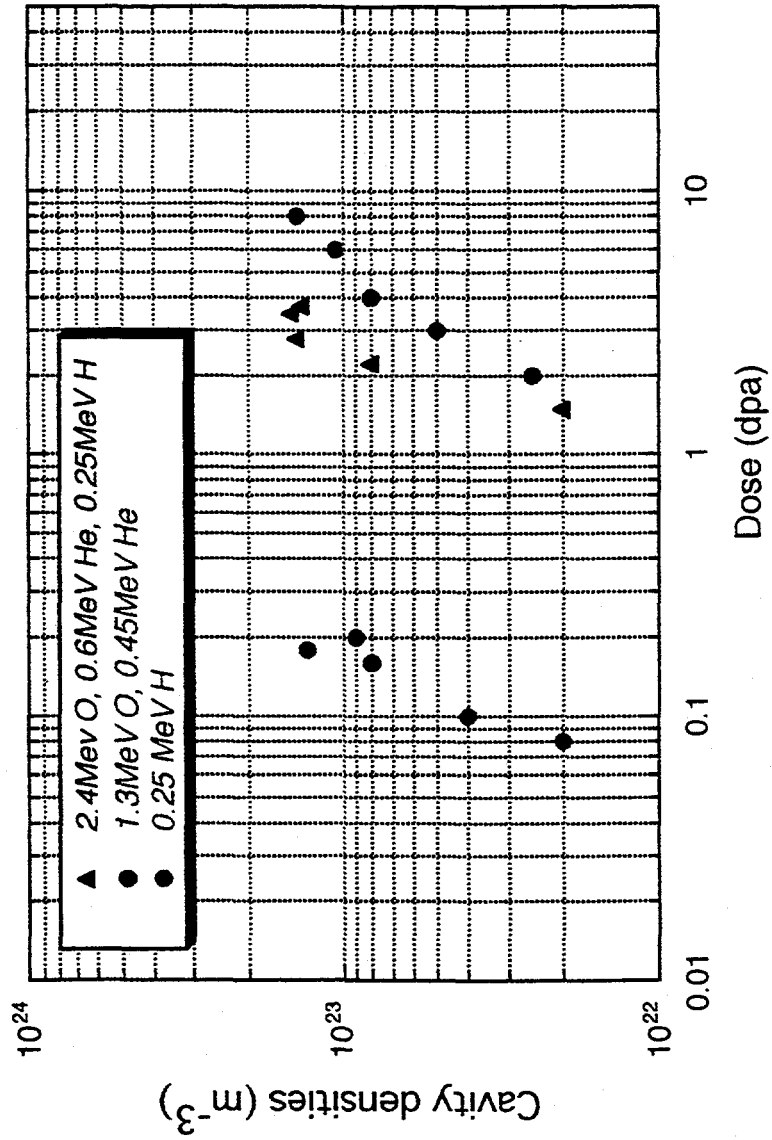


(D is average diameter of cavity)

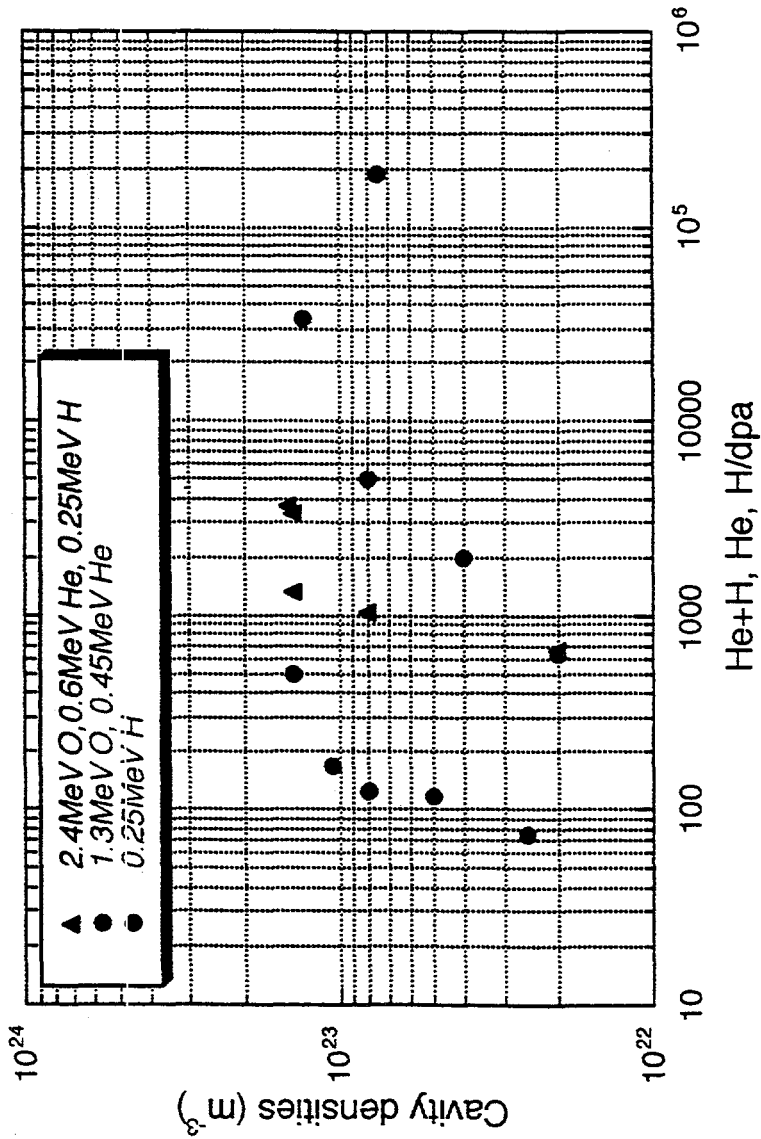
The extent of distribution of cavities formed with "Triple A" mode was narrower than that in the region where He^+ and O^+ ions or H^+ -ions were implanted in the sample irradiation with "Triple B" mode.

These suggest that implanted H atoms play an important role in evolution of cavities for the triple-beam irradiation.

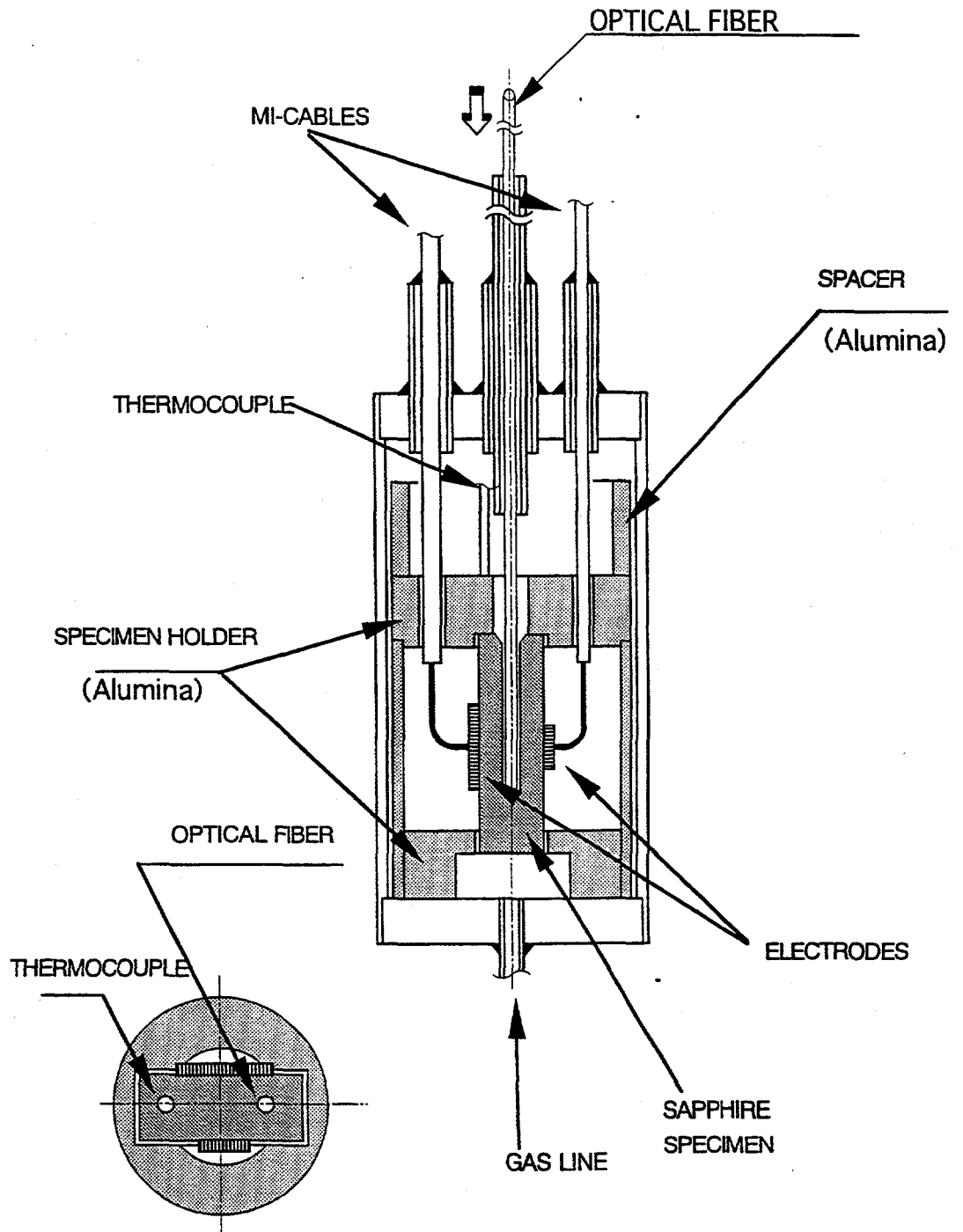
Dose dependent cavity density in the Al_2O_3 irradiated at 923K



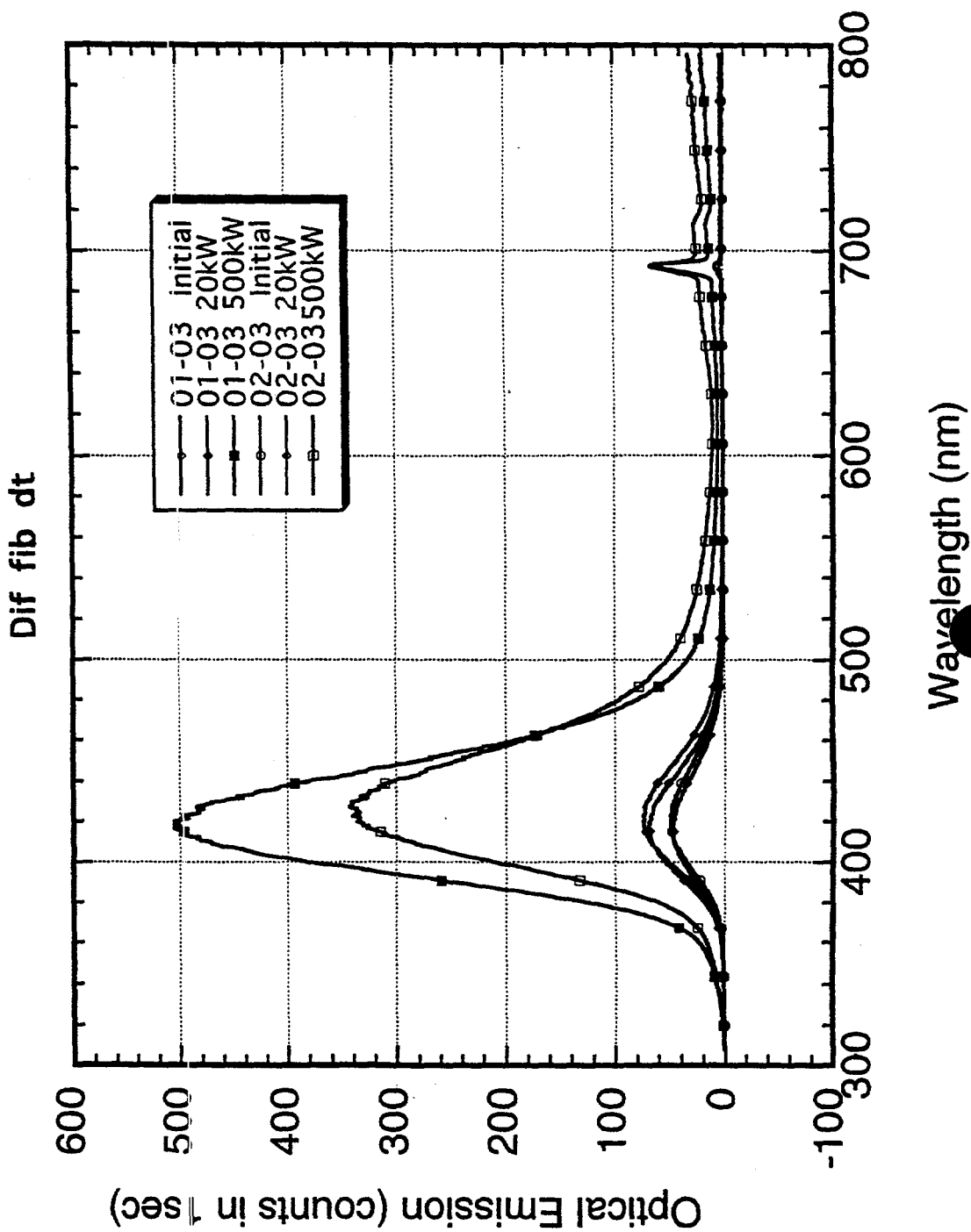
*He+H, He, H/dpa dependent cavity density in the Al₂O₃
irradiated at 923K*



structure of subcapsule



comparison of P1 peaks from Spec. No.1 and 2 at low reactor powers



Recent ORNL Research on Ceramic Insulators

- (1) Analysis of in-situ data and PIE of HFIR TRIST-ER1 experiment (Monbusho/DOE JUPITER collaboration)
- (2) Thermal conductivity measurements on Al_2O_3 , $MgAl_2O_4$, AlN , and Si_3N_4 after irradiation at 60 and 300°C to doses of 0.001 to 0.1 dpa (also limited studies at ~1 to 2 dpa)
- (3) Limited ion irradiation studies (microstructure of Al_2O_3 , $MgAl_2O_4$, and Si_3N_4)
 - role of irradiation spectrum (ionizing irradiation)
 - H, He cavity nucleation (H has strong effect)
- (4) Loss tangent (~100 MHz), flexure strength, and thermal conductivity of Al_2O_3 , AlN , Si_3N_4 , $MgAl_2O_4$, and Sialon after HFIR irradiation to 0.2 dpa (2×10^{20} n/cm², $E > 0.1$ MeV) at 200°C (SBIR Phase II program)
- (5) R&D (concept verification) and planning for in-situ thermal conductivity experiment in HFIR (JAERI/DOE collaboration)



EXTERNAL DISTRIBUTION

1. T. Bazilevskaya
2. Y. Chen
3. V. M. Chernov
4. K. Ehrlich
5. E. H. Farnum
6. A. Hasegawa
7. R. Heidinger
- 8-10. E. Hodgson (3)
11. W. Kesternich
12. C. Kinoshita
13. A. Kohyama
14. A. Möslang
15. C. Namba
16. K. Noda
17. J. Y. Park
18. G. P. Pells
19. K. Shiiyama
- 20-22. T. Shikama (3)
23. F. Tavassoli
24. T. Terai
26. R. Vila
26. D. P. White
27. F. W. Wiffen
28. S. Yamamoto
29. T. Yano
30. K. Young

INTERNAL DISTRIBUTION

31. E. E. Bloom
32. L. L. Snead
- 33-37. S. J. Zinkle (5)
- 38-39. Central Research Library (2)
40. Document Reference Library
- 41-42. Laboratory Records Department (2)
43. Laboratory Records, ORNL-RC